

高活性・高選択的新規ホスホジエステラーゼ 2A 阻害薬

TAK-915 およびバックアップ化合物の創薬研究

2018 年

味上 達

本学位論文は、下記の原著論文を基に作成され、東北大学大学院薬学研究科に提出されたものである。

1. Discovery of an Orally Bioavailable, Brain-Penetrating, In Vivo Active Phosphodiesterase 2A Inhibitor Lead Series for the Treatment of Cognitive Disorders. *J. Med. Chem.* **2017**, *60*, 7658–7676.
2. Discovery of Clinical Candidate *N*-((1*S*)-1-(3-Fluoro-4-(trifluoromethoxy)phenyl)-2-methoxyethyl)-7-methoxy-2-oxo-2,3-dihydro pyrido[2,3-*b*]pyrazine-4(1*H*)-carboxamide (TAK-915): A Highly Potent, Selective, and Brain-Penetrating Phosphodiesterase 2A Inhibitor for the Treatment of Cognitive Disorders. *J. Med. Chem.* **2017**, *60*, 7677–7702.
3. Discovery of a Novel Series of Pyrazolo[1,5-*a*]pyrimidine-Based Phosphodiesterase 2A Inhibitors Structurally Different from *N*-((1*S*)-1-(3-Fluoro-4-(trifluoromethoxy)phenyl)-2-methoxyethyl)-7-methoxy-2-oxo-2,3-dihydro pyrido[2,3-*b*]pyrazine-4(1*H*)-carboxamide (TAK-915), for the Treatment of Cognitive Disorders. *Chem. Pharm. Bull.* **2017**, *65*, 1058–1077.

目次

略号表

序論	1
----	---

本論

第 1 章 PDE2A 選択的阻害活性を有するリード化合物の創製	
第 1 節 ヒット化合物の同定とリード化合物創出を指向した薬物設計戦略	13
第 2 節 生物活性と構造活性相関	15
第 3 節 化合物 10a と PDE2A の X 線共結晶構造解析	23
第 4 節 化合物 10a の in vitro および薬物動態プロファイル	26
第 5 節 化合物 10a の in vivo 薬理評価	28
第 6 節 化合物の合成	30
第 7 節 結語	36
第 2 章 高活性・高選択性・高い中枢移行性を示す PDE2A 阻害薬の創製：臨床候補化合物 TAK-915 の創出	
第 1 節 研究背景	37
第 2 節 X 線共結晶構造情報に基づいた薬物設計戦略	38
第 3 節 新規母核の探索に向けた薬物設計戦略：戦略 1	39
第 4 節 生物活性と構造活性相関：戦略 1	41
第 5 節 化合物 32 の光学分割と in vitro 活性および PDE ファミリー選択性	44
第 6 節 <i>p</i> -トリフルオロメトキシフェニル部位の最適化：戦略 2	46
第 7 節 分岐エチル側鎖の変換：戦略 3	49
第 8 節 新規母核への置換基導入：戦略 4	50

第 9 節	化合物 39f およびその周辺誘導体の光学分割と光学活性体の <i>in vitro</i> 評価	52
第 10 節	化合物 42a の薬物動態プロファイル	55
第 11 節	化合物 42a と PDE2A の X 線共結晶構造解析	57
第 12 節	化合物 42a の <i>in vivo</i> 薬理評価	59
第 13 節	化合物 42a の既存抗精神病薬で見られる副作用に対する評価	63
第 14 節	化合物の合成	65
第 15 節	結語	78
第 3 章	既存ケモタイプに特徴的な部分構造のハイブリッド化による新規 TAK-915 バックアップ化合物の創製	
第 1 節	研究背景および新規リード化合物の創出	79
第 2 節	薬物設計戦略	81
第 3 節	ピラゾロ[1,5- <i>a</i>]ピリミジン環 5 位への置換基導入と構造活性相関	84
第 4 節	ピラゾロ[1,5- <i>a</i>]ピリミジン環 5, 6 位への置換基導入と構造活性相関	89
第 5 節	化合物 122b と PDE2A の X 線共結晶構造解析	92
第 6 節	化合物 122b の薬物動態プロファイル	94
第 7 節	化合物 122b の <i>in vivo</i> 薬理評価	95
第 8 節	化合物の合成	99
第 9 節	結語	105
総括		106
謝辞		111
実験の部		113

第 1 章に関する実験	115
第 2 章に関する実験	140
第 3 章に関する実験	209
引用文献	235
論文目録	249

略号表

Ac	acetyl
AcOH	acetic acid
ADME-Tox	absorption, distribution, metabolism, excretion, and toxicity
ADU	Affective Disorders Unit
APCI	atmospheric pressure chemical ionization
AUC	area under the concentration-time curve
BBB	blood brain barrier
Bn	benzyl
Boc	<i>tert</i> -butoxycarbonyl
BSA	bovine serum albumin
Bu	butyl
CaCl ₂	calcium chloride
cAMP	3',5'-cyclic adenosine monophosphate
CDCl ₃	deuterated chloroform
cGMP	3',5'-cyclic guanosine monophosphate
CH ₂ Cl ₂	dichloromethane
CH ₃ CN	acetonitrile
CL	clearance
C _{max}	maximum drug concentration
compd	compound
COPD	chronic obstructive pulmonary disease
<i>c</i> -Pr	cyclopropyl
dba	dibenzylideneacetone
DBU	1,8-diazabicyclo[5.4.0]undec-7-ene

DDCL	Drug Discovery Chemistry Laboratories
DIEA	<i>N,N</i> -diisopropylethylamine
DMA	<i>N,N</i> -dimethylacetamide
DME	1,2-dimethoxyethane
DMF	<i>N,N</i> -dimethylformamide
DMSO	dimethyl sulfoxide
DPPA	diphenylphosphoryl azide
dppf	1,1'-bis(diphenylphosphino)ferrocene
DTT	dithiothreitol
EDCI	1-ethyl-3-(3-dimethylaminopropyl)carbodiimide
EDTA	ethylenediaminetetraacetic acid
ee	enantiomeric excess
EGTA	ethylene glycol tetraacetic acid
EHNA	<i>erythro</i> -9-(2-hydroxy-3-nonyl)adenine
ER	efflux ratio
ESI	electrospray ionization
Et	ethyl
EtMgBr	ethylmagnesium bromide
Et ₃ N	triethylamine
Et ₂ O	diethyl ether
EtOAc	ethyl acetate
EtOH	ethanol
<i>F</i>	bioavailability
Fcx	frontal cortex
GCDC	glycochenodeoxycholate

GDP	guanosine diphosphate
<i>gem</i>	geminal
Gln	glutamine
Gly	glycine
GPCR	G protein-coupled receptor
GTP	guanosine triphosphate
HATU	1-(bis(dimethylamino)methylene)-1 <i>H</i> -1,2,3-triazolo[4,5- <i>b</i>]pyridinium-3-oxid hexafluorophosphate
HBA	hydrogen bond acceptor
HBD	hydrogen bond donor
HCl	hydrogen chloride
HIP	hippocampus
His	histidine
HLM	human liver microsomes
HMBC	heteronuclear multiple bond correlation
HOBt	1-hydroxybenzotriazole
HOSA	hydroxylamine- <i>O</i> -sulfonic acid
HPLC	high-performance liquid chromatography
HTS	high throughput screening
IBMX	3-isobutyl-1-methylxanthine
IC ₅₀	50% inhibitory concentration
Ile	isoleucine
<i>i</i> -Pr	isopropyl
<i>i</i> -Pr ₂ O	diisopropyl ether
iv	intravenous

KHMDA	potassium hexamethyldisilazide
K_p	brain-to-plasma ratio
LC-MS	liquid chromatography-mass spectrometry
LC-MS/MS	liquid chromatography tandem mass spectrometry
LE	ligand efficiency
Leu	leucine
LipE	lipophilic efficiency
<i>m</i> -CPBA	<i>m</i> -chloroperoxybenzoic acid
MDR1	multidrug resistance protein 1
Me	methyl
MeMgBr	methylmagnesium bromide
MeOH	methanol
Met	methionine
MgCl ₂	magnesium chloride
MgSO ₄	magnesium sulfate
MK-801	(5 <i>R</i> ,10 <i>S</i>)-(+)-5-methyl-10,11-dihydro-5 <i>H</i> -dibenzo[<i>a,d</i>]cyclohepten-5,10-imine
MLM	mouse liver microsomes
MRT	mean residence time
Ms	methanesulfonyl
MW	molecular weight
NaCl	sodium chloride
NADP ⁺	nicotinamide adenine dinucleotide phosphate, oxidized form
NADPH	nicotinamide adenine dinucleotide phosphate, reduced form
NaHCO ₃	sodium hydrogen carbonate

NaOH	sodium hydroxide
Na ₂ SO ₄	sodium sulfate
NBS	<i>N</i> -bromosuccinimide
ND	not determined
NDI	novelty discrimination index
NH ₃	ammonia
NMDA	<i>N</i> -methyl-D-aspartic acid
NMR	nuclear magnetic resonance
NO	nitric oxide
NOE	nuclear Overhauser effect
NOR	novel object recognition
NOS	nitric oxide synthase
NT	not tested
NTA	nitrilotriacetic acid
PAH	pulmonary arterial hypertension
PD	pharmacodynamic
PDB	protein data bank
Pd/C	palladium on carbon
PDE	phosphodiesterase
PFC	prefrontal cortex
P-gp	P-glycoprotein
Ph	phenyl
Phe	phenylalanine
PKA	protein kinase A
PKG	protein kinase G

po	per os
POC	proof of concept
POCl ₃	phosphoryl chloride
Pr	propyl
RHS	right-hand side
RLM	rat liver microsomes
rt	room temperature
SAR	structure-activity relationship
SEC	size-exclusion chromatography
SEM	(2-(trimethylsilyl)ethoxy)methyl
S.E.M.	standard error of mean
Ser	serine
SPA	scintillation proximity assay
STR	striatum
TBS	tris-buffered saline
TEA	triethylamine
TEV	tobacco etch virus
TFA	trifluoroacetic acid
THF	tetrahydrofuran
TLC	thin layer chromatography
T_{\max}	time to maximum value
TPSA	topological polar surface area
Tyr	tyrosine
$V_{d_{ss}}$	volume of distribution
WHO	World Health Organization

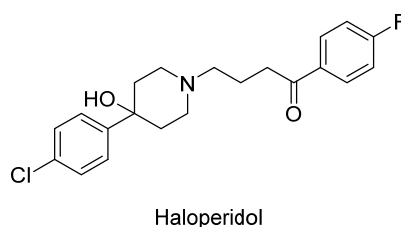
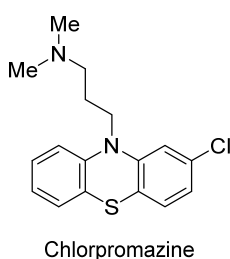
序論

統合失調症は、主に思春期から青年期の人生早期に発症し、幻覚妄想や思考・感情・意欲・認知機能などに重い障害をきたす精神疾患である。その有病者数は、全世界で 2100 万人以上 (WHO, 2017 年)¹、本邦において約 79.5 万人 (厚生労働省, 2008 年)² と推定されており、世界人口のおよそ 1% が罹患する頻度の高い疾患といえる³。その症状は、(1) 幻覚、幻聴、妄想、思考の混乱、異常行動などを特徴とする「陽性症状」、(2) 感情・意欲の減退、引きこもり、無関心などに代表される「陰性症状」、(3) 記憶力・理解力・注意力・情報処理能力や問題解決能力などの低下を伴う「認知機能障害」の大きく分けて 3 つに分類される。陽性症状は一般に発症直後の急性期に認められ、陰性症状および認知機能障害は陽性症状に遅れて消耗期に現れる。これらの症状は初回発症時に寛解しても、その後再発して増悪することが多く、再燃・再発の経過を辿り慢性化することによって長期間にわたり患者やその家族に多大な苦しみや経済的負担を強いている。また、本疾患にかかる医療費、適切な生活支援、就労支援、労働力減少等による経済的損失は極めて大きいとされ、それゆえ統合失調症の予防および治療法の開発はわが国のみならず世界各国において喫緊の課題となっている^{4,5}。

統合失調症の薬物療法に用いられる抗精神病薬は、主に第一世代抗精神病薬 (定型抗精神病薬: 例えば、クロルプロマジン、ハロペリドール)^{6,7} と第二世代抗精神病薬 (非定型抗精神病薬: 例えば、オランザピン、クエチアピン、リスペリドン、アリピプラゾール)⁸⁻¹² に分類される (Figure 1)^{13,14}。第一世代抗精神病薬は中脳辺縁系のドパミン D2 受容体に拮抗的に作用し、陽性症状に対して改善効果を示す一方で、認知機能障害や陰性症状には効果が薄く、また黒質線条体や視床下部・下垂体の D2 受容体にも拮抗的に働くため、錐体外路症状、高プロラクチン血症などの副作用の発現が問題となっている^{15,16}。第二世代抗精神病薬は、第一世代抗精神病薬に比べ、弱いドパミン D2 受容体拮抗作用に加えて、セロトニン 2A 受容体拮抗作用を有する。この作用に基づく中脳辺縁系以外のドパミン系の脱抑制効果により、錐体

外路症状、高プロラクチン血症などの副作用が軽減すると考えられている^{17,18}。しかしながら、第二世代抗精神病薬は、脂質代謝異常、体重増加、過鎮静、低血圧など依然として発生頻度の高い重篤な副作用が問題となっている^{18,19}。また第一世代、第二世代抗精神病薬では、いずれも認知機能障害や陰性症状に対する十分な改善効果が認められないことから、更なる有効性と副作用軽減を実現した新規メカニズムに基づく薬剤が待望されている。

定型 (第一世代) 抗精神病薬



非定型 (第二世代) 抗精神病薬

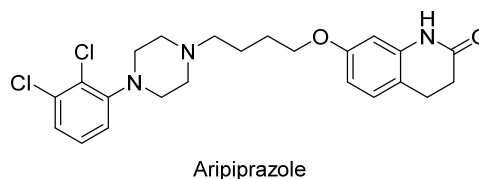
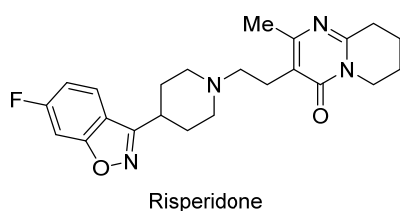
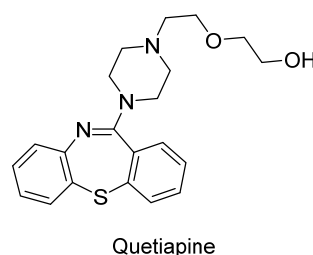
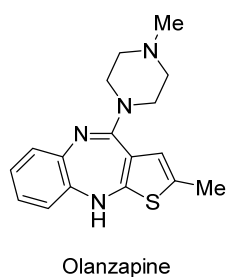


Figure 1. Structures of selected examples of currently approved typical or first-generation antipsychotics and atypical or second-generation antipsychotics.

3',5'-環状アデノシンーリン酸 (3',5'-cyclic adenosine monophosphate, cAMP) および 3',5'-環状グアノシンーリン酸 (3',5'-cyclic guanosine monophosphate, cGMP) は、細胞内セカンドメッセンジャーとして幅広く生体内のシグナル制御に関与している分子であり、生物の恒常性

において重要な役割を果たしている。これらは、それぞれアデニル酸シクラーゼ²⁰あるいはグアニル酸シクラーゼ²¹が活性化することによって産生される。アデニル酸シクラーゼの活性化は、Gs タンパク質^{注1)}と共役する受容体にホルモンや神経伝達物質などの生理活性物質が結合することで引き起こされる。一方、グアニル酸シクラーゼは一酸化窒素合成酵素 (nitric oxide synthase, NOS) によって産生される一酸化窒素 (nitric oxide, NO) により活性化される。生成した cAMP および cGMP はそれぞれタンパク質リン酸化酵素 A (protein kinase A, PKA) あるいはタンパク質リン酸化酵素 G (protein kinase G, PKG) といった cAMP あるいは cGMP 依存性タンパク質リン酸化酵素の活性化を経て細胞内シグナルが伝達された後、標的遺伝子の転写活性化によって様々な生理作用を示す。

ホスホジエステラーゼ (phosphodiesterase, PDE) は cAMP や cGMP といった環状ヌクレオチドの 3'-リン酸エステル結合部位の加水分解を選択的に触媒し、それぞれ不活性な 5'-AMP あるいは 5'-GMP に変換する酵素である (Figure 2)²²。これまでに 21 種類の遺伝子がクローニングされ、組織あるいは細胞における局在性、酵素化学的性質、アミノ酸配列の相同性および触媒活性の制御機構などに基づいて、PDE1 から PDE11 まで 11 種類のファミリーに分類されている。それぞれのファミリーにはアミノ酸配列の相同性の高い 1 から 4 つのアイソザイムが存在する。また基質特異性に基づいて²³、PDE ファミリーは 3 つのカテゴリー: (1) cAMP のみを基質とする PDE (PDE4, PDE7, および PDE8), (2) cGMP のみを基

注1) G タンパク質は α , β および γ サブユニットから成るヘテロ三量体タンパク質であり、7 回膜貫通型受容体 (G タンパク質共役型受容体 (G protein-coupled receptor, GPCR)) に共役するタンパク質である。 α サブユニットの機能および遺伝子の相違により、Gs, Gi, Gq, Gt などのサブファミリーに分類される。アゴニストが GPCR に結合すると α サブユニットに結合しているグアノシン二リン酸 (guanosine diphosphate, GDP) とグアノシン三リン酸 (guanosine triphosphate, GTP) の交換反応が起こり、GTP 結合型 α サブユニットと β , γ サブユニットに解離する。これらのサブユニットは、それぞれ標的タンパク質や酵素を活性化し、シグナルを下流へと伝達する。 α サブユニットが Gs タンパク質の場合、GPCR の活性化を経て遊離した GTP 結合型 α サブユニットがアデニル酸シクラーゼと結合することで活性化を引き起こし cAMP が産生される。

質とする PDE (PDE5, PDE6, および PDE9), (3) cAMP および cGMP の両方を基質とする二重基質 PDE (PDE1, PDE2, PDE3, PDE10, および PDE11) に分類される。

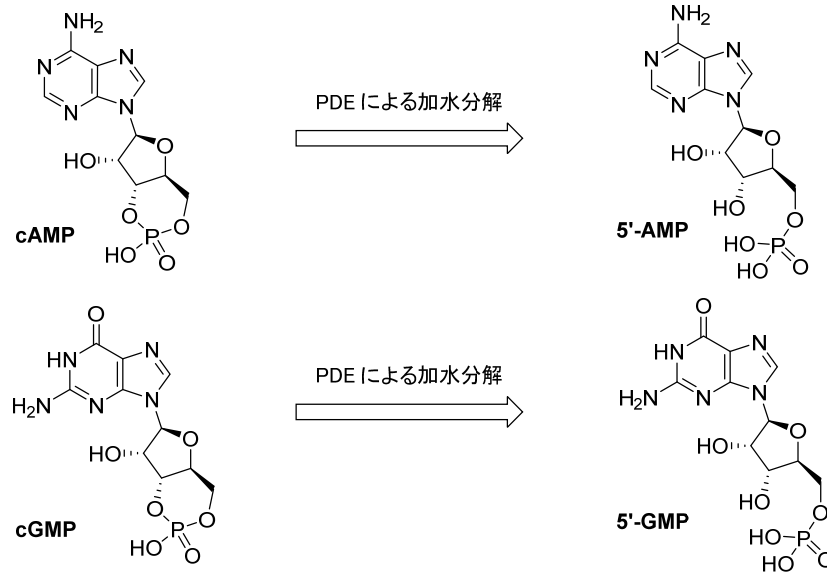
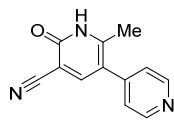


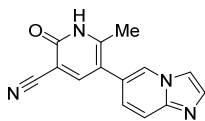
Figure 2. Hydrolysis of cyclic nucleotide substrates by PDEs.

これまでに PDE3-5 を標的とする PDE 阻害剤が、急性心不全、慢性閉塞性肺疾患 (chronic obstructive pulmonary disease, COPD), 男性性機能障害や肺動脈性肺高血圧症 (pulmonary arterial hypertension, PAH) などの治療薬として上市され、臨床応用が進められている (Figure 3)²⁴. 上述のように末梢を標的とする PDE 阻害剤が臨床で大きな成功を収めているのに加え、いくつかの PDE ファミリーは脳部位特異的に発現していることから、近年 PDE は中枢神経系の様々な疾患に対する有望な創薬標的としても大きな注目を集めている

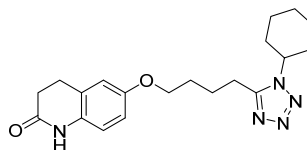
PDE3 阻害剂



Milrinone

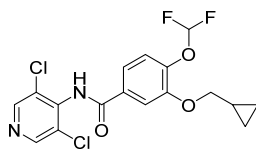


Olprinone

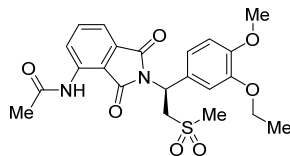


Cilostazol

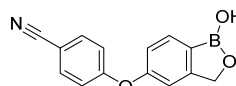
PDE4 阻害剂



Roflumilast

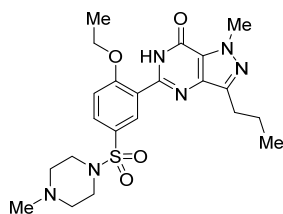


Apremilast

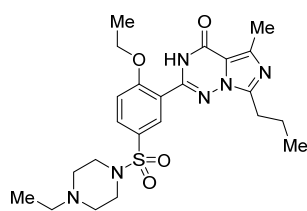


Crisaborole

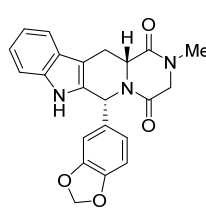
PDE5 阻害剂



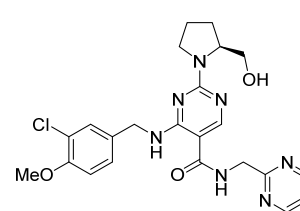
Sildenafil



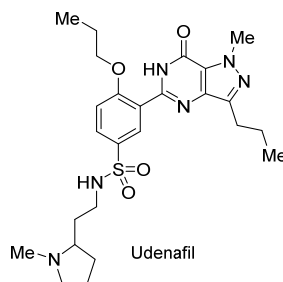
Vardenafil



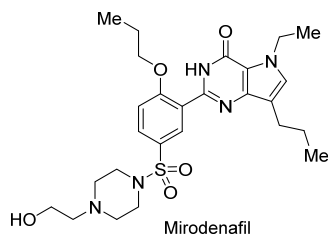
Tadalafil



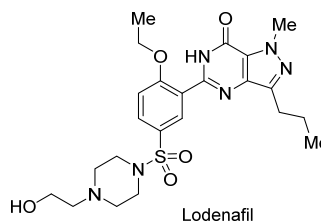
Avanafil



Udenafil



Mirodenafil



Lodenafil

Figure 3. Structures of selected examples of currently approved PDE inhibitors. Of these, the PDE3 inhibitors milrinone, olprinone, and cilostazol have been approved for the short-term treatment of congestive heart failure²⁵ and the treatment of intermittent claudication,²⁶ respectively. The PDE4 inhibitor roflumilast has entered the market as an oral treatment for reducing the risk of exacerbations in patients with chronic obstructive pulmonary disease (COPD), who also have chronic bronchitis.²⁷⁻²⁹ Another PDE4 inhibitors apremilast and crisaborole have been approved for the treatment of psoriasis and psoriatic arthritis,³⁰ and the treatment of atopic dermatitis,³¹ respectively. The PDE5 inhibitors sildenafil, tadalafil, vardenafil, avanafil, udenafil, mirodenafil, and lodenafil are now marketed for the treatment of erectile dysfunction.^{24,32} Sildenafil and tadalafil have also been approved as treatments for pulmonary arterial hypertension (PAH),³³ moreover, the latter has also been used clinically for the treatment of benign prostatic hyperplasia.³⁴

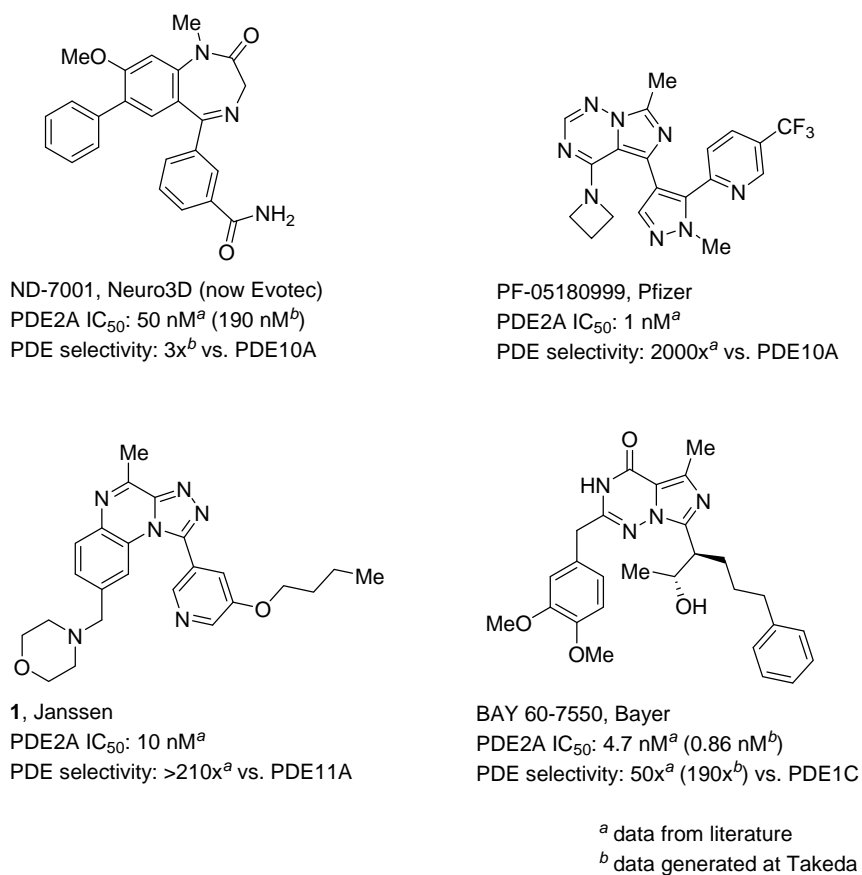
PDE2A は cAMP および cGMP の両基質を加水分解する二重基質酵素である。また、PDE2A は脳部位に高発現しており、中でも学習および記憶形成に重要な領域である前頭皮質、海馬、線条体、扁桃体に多く存在しているのに対し、末梢領域での発現は脳部位に比べて少ないことが報告されている^{39,40}。したがって脳部位を標的とする場合、PDE2A を阻害することによる末梢部位への薬理的影響は少ないことが期待でき、副作用軽減の観点から魅力的な発現分布と考えられる^{24,41,42}。また、環状ヌクレオチドを介したシグナル伝達に関する前臨床研究において、細胞内 cAMP および cGMP 濃度の上昇によって、シナプス伝達および長期増強 (long-term potentiation) の増大を引き起こすことが報告されている^{43,44}。また、cGMP および cAMP はそれぞれ短期記憶および長期記憶の形成に重要な役割を果たしていることが知られている⁴⁵。これらの結果から、PDE2A 阻害薬は学習・記憶に関連する脳部位での細胞内 cAMP あるいは cGMP 濃度を高め神経回路を活性化することによって、精神疾患や神経変性疾患における認知機能障害を改善する治療薬になる可能性が期待されている。一方で、PDE には上述のように 11 種類のファミリーが存在し、それぞれに特異的な組織発現や細胞内局在、そして基質特異性を示すことから、各種 PDE は生体内の様々な細胞内シグナル伝達において重要な生理的役割を果たしていることが知られている。したがって、PDE 阻害薬の臨床開発において、PDE 選択性の確保は、標的とする PDE の薬理学的特性を明らかにし、他の PDE 阻害に基づく副作用を回避・軽減するという観点から極めて重要といえる。

これまでに PDE2A 阻害薬の探索は複数の製薬企業で活発に行われてきており、数多くの関連特許ならびに論文が報告されている (Figure 4)⁴⁶⁻⁵⁴。しかしながら、多くの化合物は、PDE2A に対する阻害活性、PDE ファミリー選択性、中枢移行性を含めた薬物動態など、いずれかのプロファイルで課題を有しており、当社で PDE2A 阻害薬の合成研究が開始された 2010 年までに臨床開発に至った化合物は ND-7001 のみであった⁴⁷。ND-7001 は第 I 相臨床試験まで進んだものの、社内の評価において PDE2A 阻害活性および PDE 選択性ともに不十分なプロファイル (PDE2A IC₅₀ = 190 nM, 3 倍の PDE 選択性) であったため、本化合物を用いた非臨床 POC (proof of concept) の検証は困難であった。このような状況下において、最

近 Pfizer 社より強力な PDE2A 阻害活性, 優れた PDE ファミリー選択性, 良好な中枢移行性を併せ持つ臨床候補化合物 (PF-05180999) が報告された^{51,52}. 本化合物は, 統合失調症, その後片頭痛治療薬を指向して第 I 相臨床試験が実施されたが, 2014 年に臨床開発の中止が報告されている (理由は不明). また 2014 年には Janssen 社より, 良好な PDE2A 阻害活性と PDE 選択性を有するツール化合物^{注2)}, [1,2,4]トリアゾロ[4,3-*a*]キノキサリン誘導体 **1** が報告されている^{48,49}. 一方, 2002 年に Bayer 社より世界に先駆けて特許公開された BAY-60-7550⁴⁶ は, PDE2A 阻害薬の非臨床研究における重要なツール化合物として広く用いられており, PDE2A の生理的役割の解明に大きく貢献してきた^{55,56}. しかしながら本化合物の経口吸収性, さらに中枢移行性は極めて低いことが報告されており, これまでに報告されている *in vivo* 作用が PDE2A の阻害作用に基づくものかどうかに関しては議論の余地ある問題となっていた^{53,57}.

このような背景のもと, 著者らは, 非臨床および臨床において PDE2A が統合失調症などの認知機能障害を改善する有望な標的分子であることを実証するべく, 構造独自性が高く, 高活性・高選択性で, 高い経口吸収性および中枢移行性を示す PDE2A 阻害薬の探索研究を開始した.

注2) 創薬標的の薬理学的機能, 分子機構などの解明を目的として利用される化合物のことをいう.



^a data from literature

^b data generated at Takeda

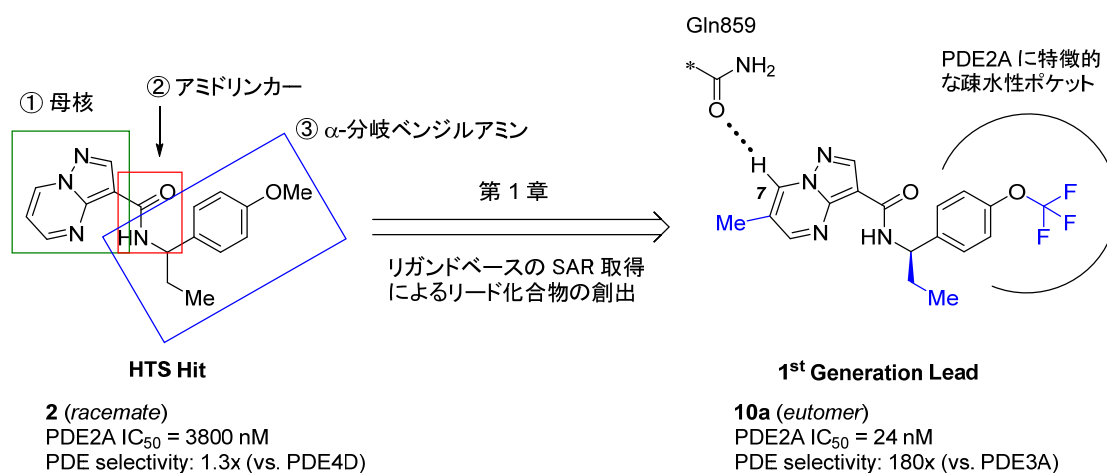
Figure 4. Representative structures and profiles of reported selective PDE2A inhibitors.

以下に各章の概要を示す。

【第 1 章】 ハイスループットスクリーニング (high through-put screening, HTS) で見出されたヒット化合物 **2** の PDE2A 阻害活性と PDE ファミリー選択性の向上を指向して, (1) ピラゾロ[1,5-*a*]ピリミジン環母核上への置換基導入, (2) アミドリンカー部位の変換, (3) α -分岐ベンジルアミン部位の変換を行った. その結果, PDE2A 阻害活性がおよそ 160 倍向上し, PDE3A 阻害と比較して 180 倍の良好な PDE2A 選択性を示すリード化合物 **10a** (IC₅₀ = 24 nM) を見出した (Scheme 1). また X 線共結晶構造解析の結果, 化合物 **10a** が PDE2A の触媒ドメインに特徴的な結合様式で結合していることを明らかにした. さらに, 本化合物のマウスへの経口投与によって脳内 cGMP 含量を有意に上昇させることを確認し, 本化合物が

in vivo 試験用ツール化合物, ならびにその後の最適化研究のリード化合物として有用であることを明らかにした. これらの詳細を第 1 章で述べる.

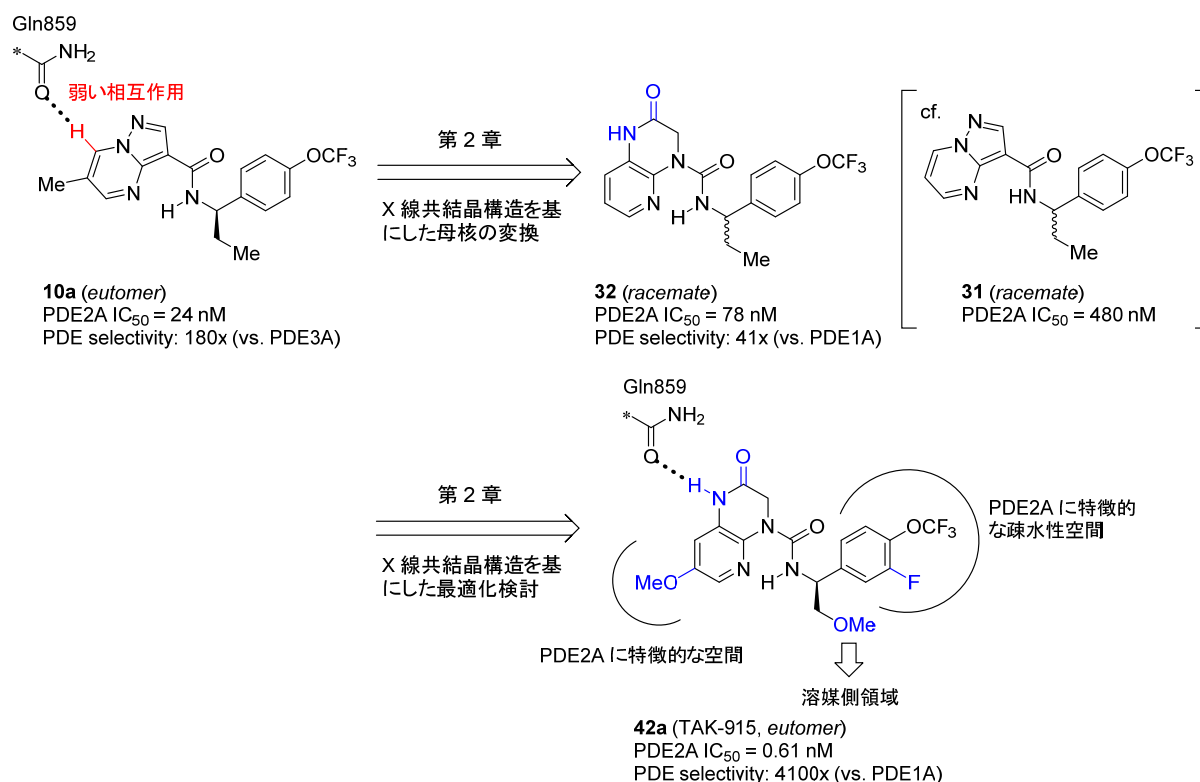
Scheme 1



【第 2 章】 本章では, 化合物 **10a** と PDE2A との X 線共結晶構造解析の情報を活用して, さらなる活性および PDE ファミリー選択性の向上とケモタイプの拡充を目指した. 第 1 章で見出した化合物 **10a** のピラゾロ[1,5-*a*]ピリミジン環は PDE ファミリー共通の基質結合部位である Gln859 と CH-O の弱い水素結合で相互作用していることが明らかになったことから, Gln859 と明確な水素結合が形成可能な新規骨格を種々設計・合成し, 活性に対する影響を検討した. その結果, 対応するピラゾロ[1,5-*a*]ピリミジン誘導体 **31** よりも PDE2A 阻害活性が約 6 倍向上した新規骨格化合物, 2-オキソ-2,3-ジヒドロピリド[2,3-*b*]ピラジン誘導体 **32** を見出すことに成功した. 続いて, 化合物 **32** を新たなリード化合物として, α-分岐ベンジルアミン部位の変換および 2-オキソ-2,3-ジヒドロピリド[2,3-*b*]ピラジン環母核上への置換基導入を中心に行い, PDE2A との新たな相互作用の獲得および PDE2A に特徴的な空間の充填により活性および PDE ファミリー選択性の向上を目指した. 同時に, 良好な中枢移行性を獲得する上で重要な物理化学的および物性パラメータを指標とした構造最適化検討を行った結果, 非常に強力な PDE2A 阻害活性 (IC₅₀ = 0.61 nM) ならびに PDE1A に対して 4100

倍の極めて高い PDE ファミリー選択性を示す化合物 **42a** を見出すことに成功した。本化合物は、ラットおよびマウスにおいて良好な経口吸収性および中枢移行性を示し、マウスにおける経口投与によって脳内 cGMP 含量を有意に上昇させた。またラットにおける新奇物体認知試験 (novel object recognition test) および受動的回避試験 (passive avoidance test) において、有意な認知機能の亢進および改善作用を示し、既存の抗精神病薬で認められる錐体外路症状・高プロラクチン血症・耐糖能異常などの副作用の懸念の少ない化合物であることを明らかにした。その後、化合物 **42a** は臨床候補化合物 (開発コード番号: **TAK-915**) として選出された。これらの詳細を第 2 章で述べる。

Scheme 2

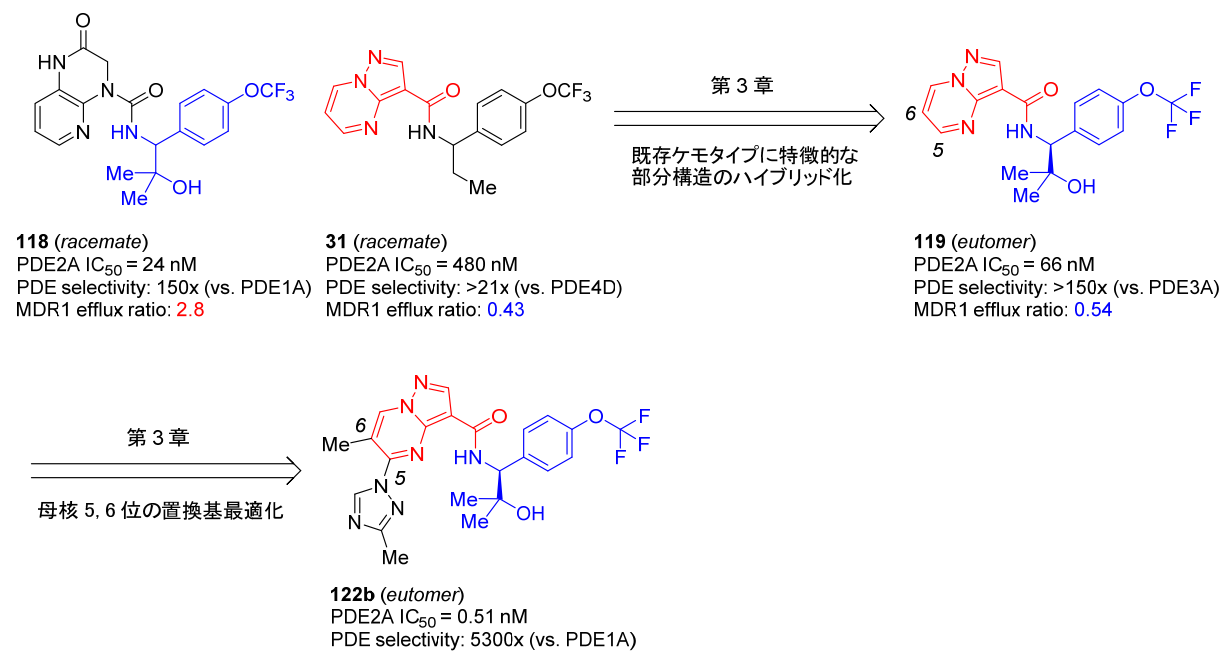


【第 3 章】 本章では、高い PDE2A 阻害活性および PDE ファミリー選択性かつ中枢移行性に優れた TAK-915 バックアップ化合物の創出を目指した。第 1 章および第 2 章の合成研究の過程で見出された化合物 **118** および **31** に特徴的な部分構造を組み合わせることで TAK-915 とは異なる構造、そして P-糖タンパク質 (P-glycoprotein, P-gp)^{注3),注4)} による排出の懸念の少ない新規リード化合物 **119** を見出すことに成功した。さらなる PDE2A 阻害活性および PDE ファミリー選択性の向上を指向して、化合物 **10a** の X 線共結晶構造解析の情報を基に化合物 **119** のピラゾロ[1,5-*a*]ピリミジン環 5 および 6 位への置換基導入を検討した結果、TAK-915 と同等の PDE2A 阻害活性 ($IC_{50} = 0.51 \text{ nM}$) と PDE ファミリー選択性 (PDE1A 阻害作用に対して 5300 倍) を示すピラゾロ[1,5-*a*]ピリミジン誘導体 **122b** を見出すことに成功した。また、この過程でピラゾロ[1,5-*a*]ピリミジン環 5 位に窒素原子で結合したヘテロ 5 員環を導入することにより、ラット *in vivo* クリアランスと *in vitro* 光毒性ポテンシャルの両プロファイルが大きく改善されることも見出した。化合物 **122b** は、ラットへの経口投与によって用量依存的かつ有意に脳内 PDE2A の占有率および cGMP 含量を上昇させるとともに、受動的回避試験において認知機能改善効果を示すことを明らかにした。これらの詳細を第 3 章で述べる。

注³⁾ P-糖タンパク質をコードする遺伝子は MDR1 (multidrug resistance protein 1) と呼ばれる。良好な中枢移行性を確保するためには、薬物を脳内から排出するトランスポーターである P-gp の基質にならないことが重要である。P-gp の基質として脳から排出されやすいか否かは、P-gp 過剰発現細胞膜を用いた膜透過性試験の結果から算出された P-gp による排出比 (P-gp or MDR1 efflux ratio) を用いて見積もる。P-gp による排出比 (B to A/A to B) は、P-gp 過剰発現細胞膜を用い、吸収方向および排出方向、それぞれの単位面積当たりの透過速度を測定し、それらの値を用いて算出する。

注⁴⁾ 上市されている中枢薬および非中枢薬で P-gp による排出比を比較した研究によると、薬物が脳に到達するためには、排出比は 2.5 未満が理想的であるとされている⁵⁸。本論文における P-gp 基質の判断基準として、排出比が 2.5 以上の場合は P-gp の基質と判定した。

Scheme 3



本論

第 1 章 PDE2A 選択的阻害活性を有するリード化合物の創製

第 1 節 ヒット化合物の同定とリード化合物創出を指向した薬物設計戦略

独自性の高い PDE2A 阻害薬を創出するに当たり、著者らは、社内化合物ライブラリーを用いた HTS を実施した結果、ピラゾロ[1,5-*a*]ピリミジン骨格を有するヒット化合物 **2** を見出した (Figure 1-1(A)). 化合物 **2** の PDE2A 阻害活性および PDE ファミリー選択性は、それぞれ 3.8 μM , 1.3 倍 (vs. PDE4D) と十分なものではなかったものの、構造活性相関 (structure activity relationship, SAR) を取得しやすいアミド構造を有していたこと、また良好な経口吸収性や中枢移行性を指向する上で重要な指標である分子量 (molecular weight, MW) や二次元極性表面積 (topological polar surface area, TPSA) 等の物性パラメータ^{注5)} が小さな値であったことから、最適化検討を推し進める上で構造変換の余地が大きく良質なヒット化合物と考えられた。さらに化合物 **2** は、ピラゾロ[1,5-*a*]ピリミジン環 4 位の窒素原子とアミド部位の NH が分子内水素結合を形成することによってそれぞれの塩基性および HBD 性がマスクされていると推察されることから、中枢薬を指向した合成展開を行う上で有利であると考えられた。上述の考察を踏まえ、著者らは、主に PDE2A 阻害活性の向上を目指し、ヒット化合物 **2** の構造変換を開始した。

本研究を開始した当初は、化合物 **2** と PDE2A タンパクとの X 線共結晶が得られていなかったことから、非選択的 PDE 阻害剤である 3-イソブチル-1-メチルキサンチン (3-isobutyl-1-methylxanthine, IBMX)⁵⁹ (Figure 1-2) と PDE2A の結晶構造を鋳型とする分子モ

注 5) 経口投与可能な低分子医薬品の分子構造に基づく物性パラメータの範囲は、リピンスキーの法則 (Lipinski's rule of 5)⁶⁰ に基づいて以下の 4 条件 (1. MW \leq 500, 2. cLog P (脂溶性指標) \leq 5, 3. 水素結合受容体 (hydrogen bond acceptor, HBA) 数 \leq 10, 4. 水素結合供与体 (hydrogen bond donor, HBD) 数 \leq 5) を満たすことが望ましいとされている。また、Hitchcock らは良好な中枢移行性の獲得には TPSA $<$ 90, $2 \leq$ clogP \leq 5, MW $<$ 500 および HBD 数 = 0 あるいは 1 で定義される範囲内で薬物設計を行うことを推奨している^{61,62}。

デリングにより結合様式の予測を試みたが、いずれもドッキングスコアが低く、信頼性のある結合様式の同定には至らなかった。そこで著者らは、構造活性相関の情報に基づくリガンドベースの合成展開を行うこととした。

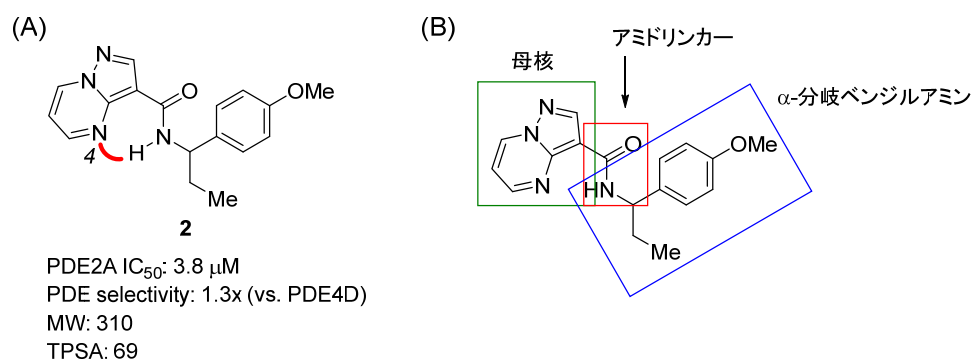


Figure 1-1. (A) Structure and profile of pyrazolo[1,5-*a*]pyrimidine hit **2** from a high-throughput screen. The presumed intramolecular hydrogen bond is indicated in red. (B) SAR approach.

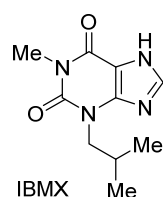


Figure 1-2. Structure of non-specific PDE inhibitor, IBMX.

まず化合物 **2** をFigure 1-1 (B) に示す 3 つのフラグメントに分け (1. 母核, 2. アミドリンカー部位, 3. α-分岐ベンジルアミン部位), Figure 1-3 で概説する合成戦略に従って各フラグメントの構造活性相関を取得した。

戦略 1 ピラゾロ[1,5-*a*]ピリミジン環への置換基導入の許容性を検証する目的で、ピラゾロ[1,5-*a*]ピリミジン環上 2, 5, 6 および 7 位にメチル基の導入を検討する。

戦略 2 アミド部位のカルボニル基および NH が PDE2A 阻害活性に与える影響を検証する。具体的には、カルボニル基の除去、その他 HBA 能のあるスルホニル基への変換、アミド NH のメチル化を検討する。

戦略 3 ピラゾロ[1,5-*a*]ピリミジン環 4 位の窒素原子とアミド部位の NH の分子内水素結合の活性発現に対する重要性を検証するために、アミド部位 NH のメチル化 (戦略 2), およびピラゾロ[1,5-*a*]ピリミジン環 4 位窒素原子の炭素原子への変換, あるいは分子内水素結合を形成していると考えられる部位で新たに環形成させた誘導体を検討する。

戦略 4 パラレル合成を活用して網羅的に α -分岐ベンジルアミン部位の変換を実施する。

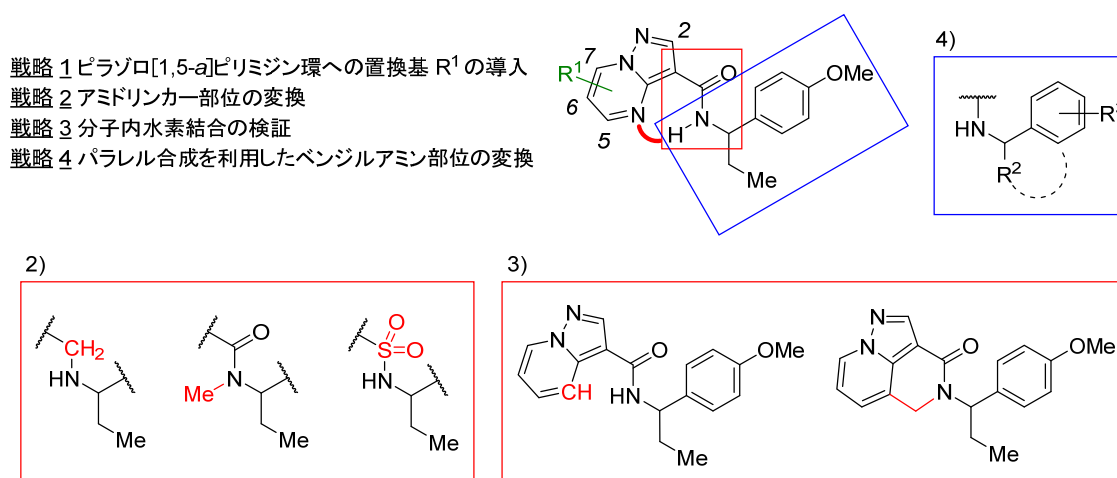


Figure 1-3. Synthetic strategies of compound 2.

第 2 節 生物活性と構造活性相関

ピラゾロ[1,5-*a*]ピリミジン環 2, 5, 6 および 7 位に置換基を導入した結果を Table 1-1 に示す。ピラゾロ[1,5-*a*]ピリミジン環 2 位にメチル基を導入 (**3a**) すると活性が大きく減弱する一方で, 5 位メチル置換体 **3b** は活性が保持することが分かった。化合物 **3a** で見られた活性の減弱は, 2 位メチル基の導入によって近傍のアミドカルボニル基との立体反発が生じ, 活性コンフォメーションに影響を及ぼしたためと考えられる。一方, 6 位メチル置換体 **3c** は無置換体 **2** と比較して約 8 倍の活性の向上が認められた。また, 5 位および 7 位の両部位にメチル基を導入したジメチル誘導体 **3d** は, 5 位メチル体 (**3b**) と比べて活性が低下する傾向が認められた。このことは, 7 位へのメチル基導入が PDE2A 阻害活性に好ましくない影響を与えていることを示唆する結果であり, 7 位周辺はメチル基を許容する程の空間

しか存在しない、あるいは脂溶性置換基を好まない親水性領域である可能性が考えられる。以上の結果を踏まえ、PDE2A 阻害活性の向上が認められた 6 位置換体について引き続き詳細な検討を行った。その結果、6 位クロロ体 (**3e**)、シクロプロピル体 (**3f**)、フェニル体 (**3g**) は 6 位メチル体 (**3c**) と比較して、いずれも活性が減弱することが明らかとなった。これらの結果は、6 位周辺がメチル基を許容できる程度の小さな空間であることを示唆するものと考えられる。以上のように、ピラゾロ[1,5-*a*]ピリミジン環上置換基の構造活性相関の結果、6 位メチル置換体 **3c** が良好なリガンド効率 (ligand efficiency, LE)^{注6)} を保持しつつ、最も強い PDE2A 阻害活性を示すことが明らかとなった。

注 6) リガンド効率は、標的タンパク質と相互作用するリガンドの非水素原子一つ当たりの Gibbs エネルギーとして定義される。分子量が異なる化合物同士の活性を比較するのに用いられる指標である。また、良質なリード化合物を選定する上で重要な指標となる。

$$\text{リガンド効率} = \Delta G / \text{水素以外の原子数} \sim -RT \ln(\text{IC}_{50}) / \text{水素以外の原子数}$$

新たに構築した環構造が分子右側鎖の α -エチルベンジルアミン部位の活性コンフォメーションに影響を及ぼしたことが原因と考えられる。

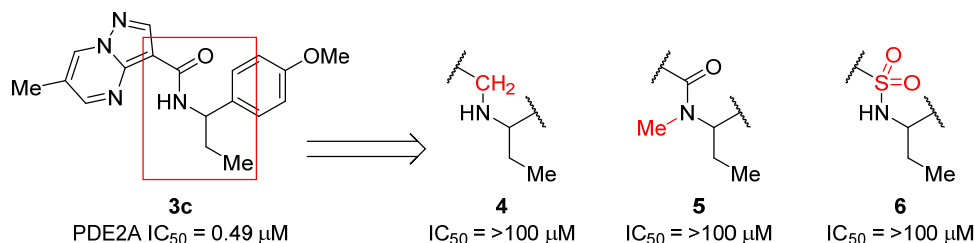


Figure 1-4. Effect of the amide linker connecting the pyrazolo[1,5-*a*]pyrimidine core and *p*-methoxyphenyl moiety on PDE2A inhibitory activity.

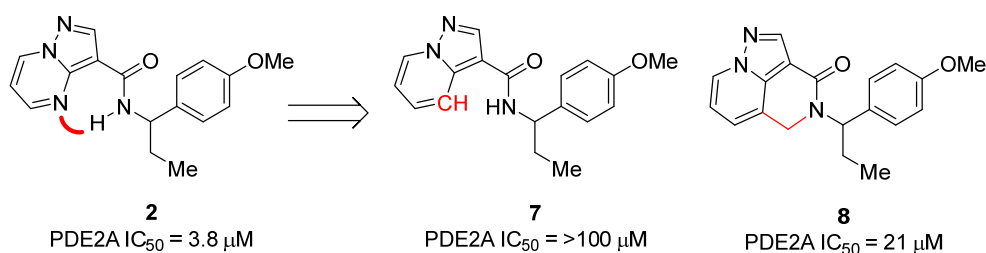


Figure 1-5. Analog designed to test the involvement of intramolecular hydrogen bonding in PDE2A inhibitory activity. The intramolecular hydrogen bond is depicted as a red arc in compound **2**.

次に著者らは、分子内水素結合の重要性を考慮して、第二級アミド構造はそのまま保持する形で右側鎖のアミンパーツの変換を行った。アミド誘導体は市販の試薬、あるいは社内化合物ライブラリーから選択した一級アミンと 6-メチルピラゾロ[1,5-*a*]ピリミジン-3-カルボン酸との平行合成を用いたアミド化反応によって合成した。代表的な誘導体の構造活性相関を Table 1-2 に示した。また、対照化合物として *p*-メトキシフェニル誘導体 **3c** の活性も Table 1-2 に掲載した。化合物 **3c** のパラ位メトキシ基を除去した無置換体 **9a** は、およそ 7 倍の活性の減弱が認められた。この結果は、パラ位メトキシ基が近傍の空間を効果的に充填している、あるいは電子供与基としてフェニル基の電子密度を高め、PDE2A タンパク

との相互作用を増強させている可能性を示唆するものと考えられる。一方、分岐アルキル側鎖のエチル基 (**9a**) をメチル基に変換した化合物 **9b** は活性が 6 倍減弱し、化合物 **3c** のエチル分岐側鎖をさらに除去した化合物 **9d** は活性が大きく低下した。さらに、化合物 **9a** の分岐エチル基末端炭素を隣接するフェニル基のオルト位で環化させたインダン誘導体 (**9c**) では 9 倍の活性の低下が認められた。これらの結果は、分岐アルキル側鎖が PDE2A 阻害活性を発現する上で重要な役割を果たしていることを示唆しており、本側鎖が PDE2A のポケットを効果的に充填するとともに、フェニル基を活性発現に有利な空間配置に誘起していると考えられる。一方、化合物 **9d** のパラ位メトキシ基をメタ位 (**9e**)、あるいはオルト位 (**9f**) に移すと活性が消失したことから、フェニル基上の置換様式も PDE2A 阻害活性に重要であることが明らかとなった。また、パラ位置換基であるメトキシ基 (**9d**) をトリフルオロメトキシ基 (**9g**) に変換すると、およそ 9 倍活性が向上した。一般に、トリフルオロメトキシフェニル構造を有する化合物は $C=C-O-CF_3$ の二面角が直交する配座が安定なのに対して、メトキシフェニル構造を有する化合物ではフェニル基、酸素原子、メチル基の炭素原子が同一平面上に位置する配座を取りやすいことが報告されている (Figure 1-6)⁶³。トリフルオロメチル基はメチル基と比べると立体的に嵩高く、隣接するフェニル基上オルト位水素原子との立体反発を生じやすいこと、またトリフルオロメチル基の電子求引効果により、対応するメチル基と比べて酸素原子からベンゼン環への共役が弱まる一方で、トリフルオロメトキシ基の酸素原子上の非共有電子対が C-F 結合の反結合性軌道に超共役し安定化することで上述の配座の違いが生じるものと考えられている⁶⁴。これらのことから、化合物 **9g** で認められた活性の向上は、メトキシ基からトリフルオロメトキシ基への変換によって PDE2A タンパクとの脂溶性相互作用が増強しただけでなく、トリフルオロメトキシフェニル基の直交型立体配座が活性コンフォメーションに類似していることによってタンパクへの結合に伴うエントロピーの損失が抑制されたことに起因していると考えられる。

Table 1-2. SAR of Representative RHS Amines

compd	R	PDE2A IC ₅₀ (μM) ^a	compd	R	PDE2A IC ₅₀ (μM) ^a
3c		0.49 (0.43–0.57)	9d		52 (39–68)
9a		3.6 (2.8–4.6)	9e		>100
9b		28 (20–39)	9f		>100
9c		49 (33–74)	9g		6.1 (3.6–10)

^a IC₅₀ values (95% confidence intervals given in parentheses) were calculated from percent inhibition data (duplicate, *n* = 1). All values were rounded to two significant digits.

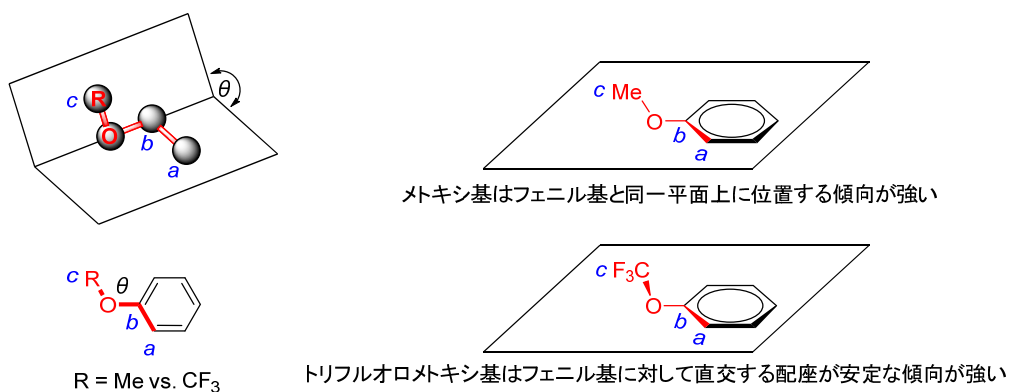
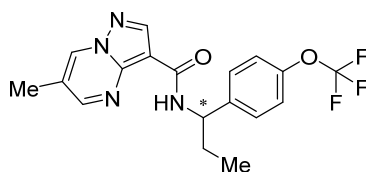


Figure 1-6. A difference in conformational preferences (dihedral angles θ of C^a–C^b–O–C^c) between the methoxyphenyl and trifluoromethoxyphenyl groups.

次に、これまで述べてきた構造活性相関研究の知見を基に、活性向上において重要な知見、すなわち、① ピラゾロ[1,5-*a*]ピリミジン環 6 位へのメチル基の導入、② 末端トリフル

オロメトキシ基への変換をそれぞれ組み合わせた化合物 (**10**) を設計し合成した結果, PDE2A 阻害活性が相加的に向上することが明らかとなった ($IC_{50} = 0.053 \mu\text{M}$). 続いて, 光学活性体の PDE2A 阻害活性および PDE ファミリー選択性に対する影響を検証するために, 化合物 **10** の光学分割を実施した. その結果, (*R*)-体 **10a** はラセミ体 **10** と比べて活性が約 2 倍向上し, (*S*)-体である **10b** は $10 \mu\text{M}$ の濃度においても活性を示さないことが明らかとなった (Table 1-3). なお, ユートマー **10a**^{注7)} の絶対立体配置は, 後述する PDE2A との X 線共結晶構造解析により決定した. また, (*R*)-体 **10a** は PDE3A に対して 180 倍, PDE10A に対して 310 倍, その他の PDE ファミリーに対しては 420 倍以上の良好な選択性プロファイルを示すことも明らかとなった (Table 1-4).

注7) エナンチオマー間で薬理活性に差がある場合, 活性の強い方をユートマー (eutomer), 弱い方をディストマー (distomer) という.

Table 1-3. In Vitro Activity Profiles of **38** and Its Enantiomers **10a** and **10b**

compd	stereo	PDE2A IC ₅₀ (μM) ^a
10	<i>rac</i>	0.053 (0.047–0.059)
10a	<i>R</i> ^b	0.024 (0.022–0.027)
10b	<i>S</i> ^b	>100

^a IC₅₀ values (95% confidence intervals given in parentheses) were calculated from percent inhibition data (duplicate, *n* = 1). All values are rounded to two significant digits. ^b Absolute configuration assigned based on the stereochemistry of the bound conformation in the crystal structure of **10a** (see Figure 1-6).

Table 1-4. In Vitro PDE Selectivity Profile of **10a**

PDE subtypes	IC ₅₀ (μM) ^a	selectivity ratio ^b
PDE1A	>10	>420
PDE2A3	0.024	–
PDE3A	4.2	180
PDE4D2	>10	>420
PDE5A1	>10	>420
PDE6AB	>10	>420
PDE7B	>10	>420
PDE8A1	>10	>420
PDE9A2	>10	>420
PDE10A2	7.4	310
PDE11A4	>10	>420

^a IC₅₀ values were calculated from percent inhibition data (duplicate, *n* = 1). All values are rounded to two significant digits. ^b Selectivity ratio (rounded to two significant digits) = PDE"X" IC₅₀/PDE2A IC₅₀.

第 3 節 化合物 **10a** と PDE2A の X 線共結晶構造解析

これまで述べてきたように、ヒット化合物 **2** を端緒化合物とした合成展開により良好な活性と PDE 選択性を示す化合物 **10a** を見出すことに成功した。本化合物の結合様式を明らかにするために、**10a** と PDE2A の X 線共結晶構造解析を実施した。その結果、Figure 1-7 (A) および 1-7 (B) に示すように、化合物 **10a** が PDE2A の触媒ドメインに結合していることが明らかとなった。また上述の構造活性相関と一致して、アミド部位の NH はピラゾロ [1,5-*a*]ピリミジン環 4 位窒素原子と分子内水素結合を形成し、活性コンフォメーションの固定化に寄与していることを確認することができた。さらに、**10a** のベンジルアミン部位の絶対立体配置は *R* 体と決定した。この X 線共結晶構造解析によって、化合物 **10a** と PDE2A との相互作用が明らかとなった。以下に特筆すべき相互作用についてまとめる。

1. ピラゾロ [1,5-*a*]ピリミジン環 7 位の水素原子は PDE ファミリー共通の基質結合部位である Gln859 と CH-O の擬似的水素結合 (C-O の距離: 3.2 Å)⁶⁵ を介して相互作用している。
2. アミドカルボニル基は Tyr655 と水分子を介した水素結合のネットワークを形成するとともに、さらにもう一つ別の水分子と水素結合を形成している。この知見は、カルボニル基を除去した場合 (化合物 **3c** → 化合物 **4**, Figure 1-4) に大幅に活性が減弱した結果と矛盾のないものといえる。
3. ピラゾロ [1,5-*a*]ピリミジン環は上に位置する Phe862, 下に位置する Ile826 とそれぞれ π - π ならびに CH- π の相互作用を形成している (Figure 1-7 (B))。
4. ピラゾロ [1,5-*a*]ピリミジン環 6 位メチル基は Leu858 側鎖とファンデアワールスの相互作用をしている。メチル基を許容しているポケットの大きさは限られており、この部位のメチル基をより大きな置換基に変換すると活性が減弱した結果と一致する (Table 1-1, **3e-3g**)。
5. 分岐エチル側鎖は Ile826, Phe830, His656, Tyr655 で囲まれた脂溶性空間を占めている。

6. *p*-トリフルオロメトキシフェニル基は PDE2A タンパクとの結合によって新たに形成された脂溶性空間を効果的に充填している。最近になって Zhu らは、この空間がこれまで報告されている他の PDE の X 線共結晶構造解析において認められず、PDE2A に特徴的な空間である可能性を報告している^{48,66}。したがって、化合物 **10** で確認された良好な PDE ファミリー選択性は、PDE2A に特徴的な本空間を利用することによってもたらされているのではないかと考えられる。また、トリフルオロメトキシ基はフェニル基に対してエネルギー的に有利な直交型の立体配座で脂溶性空間を占有していることが明らかとなった。フェニル基と同一平面上に位置する傾向の強いメトキシフェニル誘導体 **3c** と比べて、トリフルオロメトキシフェニル誘導体 **10** は脂溶性相互作用の増加に加えて、結合の際に引き起こされる構造変化 (エントロピー変化) が小さいことが約 9 倍の活性向上に繋がったと考えられる。

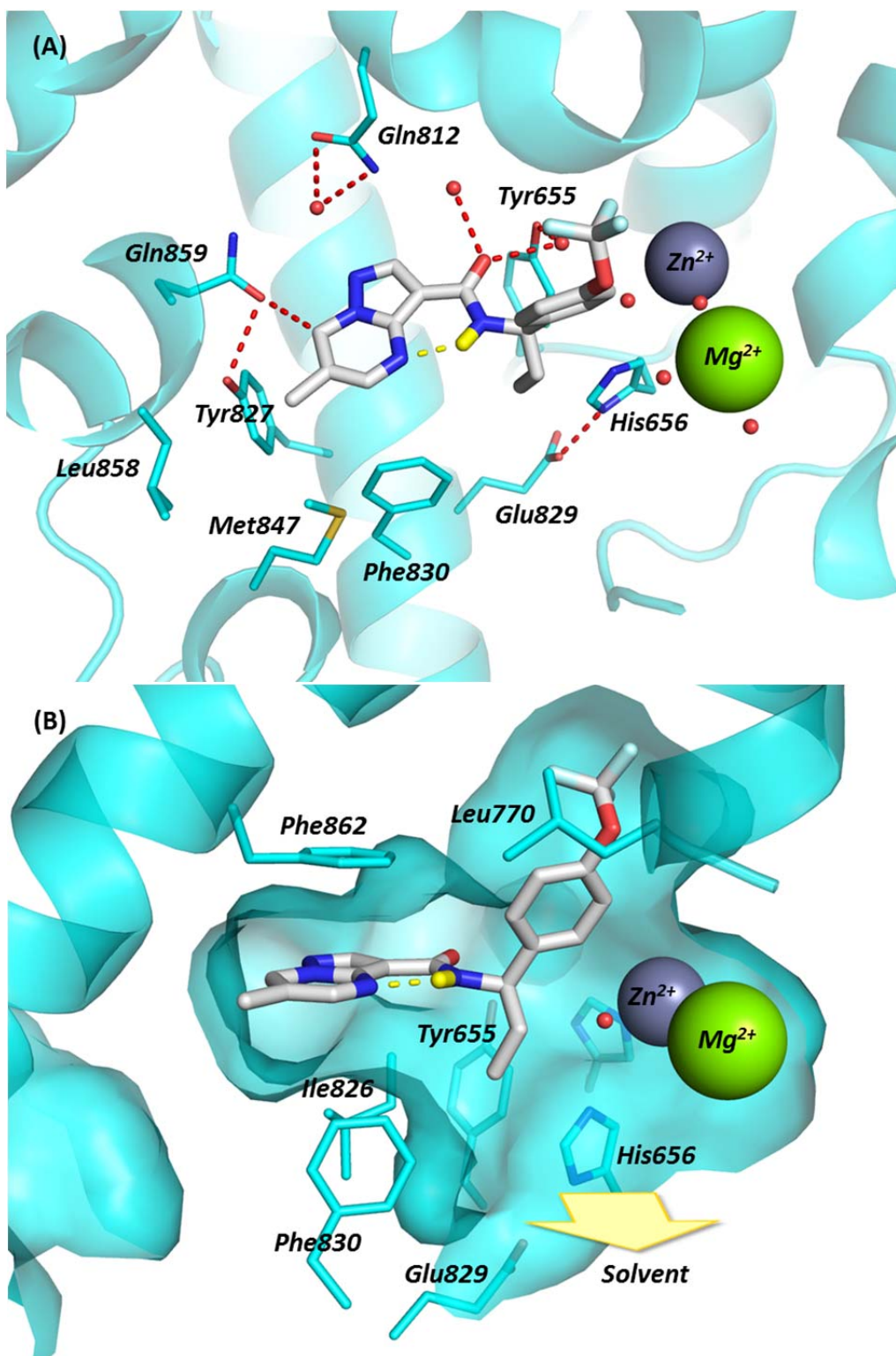


Figure 1-7. X-ray crystal structure of **10a** bound in the PDE2A catalytic site (PDB 5XKM) viewed from the top (A) and the entrance of the catalytic site (B). The key hydrogen bonding interactions of **10a** with PDE2A and the intramolecular hydrogen bond in **10a** are indicated by red and yellow dotted lines, respectively.

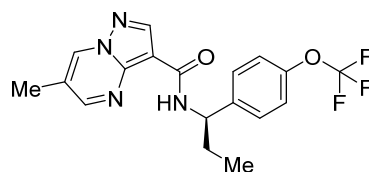
第 4 節 化合物 10a の in vitro および薬物動態プロファイル

化合物 10a の in vitro (Table 1-5) および薬物動態プロファイル (Table 1-6) を示す。化合物 10a は分子量, TPSA, リガンド効率, 脂溶性効率 (Lipophilic efficiency, LipE)^{注8)} などの点で良好な物理化学的性質^{注9)} を有していた。また, ヒト, ラット, マウスいずれの種においても良好な代謝安定性プロファイルを示し, P-gp の基質の可能性が低く (MDR1 efflux ratio = 0.43), 高い中枢移行性を示すことが期待された。本化合物をラットおよびマウスに 0.3 mg/kg の静脈内投与をしたところ, 比較的大きなクリアランス (CL_{total}) および分布容積 (V_{dss}) を示したが, 1 mg/kg の経口投与において, それぞれ 15% および 34% の生物学的利用率 (bioavailability, F) と 58.7 ng·h/mL および 132.6 ng·h/mL の血中濃度-時間曲線下総面積値 (AUC_{0-8h}) を示した。さらに, 前述の P-gp 基質性の結果と一致し, ラットおよびマウスにおける最高血中濃度到達時間 (T_{max}) 付近 (化合物投与後 2 時間 (ラット) および 1 時間 (マウス)) の脳内と血漿中の薬物濃度比 K_p はそれぞれ 2.9 と 2.6 で良好な値を示し, 血液脳関門 (blood brain barrier, BBB) を通過して脳内に移行することを確認した。以上の結果から, 化合物 10a は今後の最適化検討におけるリード化合物, また in vivo ツール化合物として有用であると考えられた。

注8) 脂溶性効率は, 生物活性と脂溶性の両方を内包する, 以下の式で定義される指標である。高活性, およびドラッグライク (drug-like) な物性を有する良質なリードおよび臨床候補化合物を選定する上で有用な指標と言われている。

$$\text{脂溶性効率, LipE} = \text{pIC}_{50} - \log D$$

注9) リード化合物の MW や TPSA などの物性パラメータは以降の最適化検討における構造変換により増加する傾向があることから, 上限とされる値 (注5 参照) よりも小さい方が望ましいと考えられている。一方, LE や LipE 値に関しては, 現在上市されている医薬品の前臨床開発段階時 (ヒットやリード化合物選出時) の各パラメータの解析結果から, リード化合物選出時の平均値はそれぞれ LE = 0.39, LipE = 3.78 であることが報告されている⁶⁷⁾。

Table 1-5. Calculated Physicochemical Properties and In Vitro Profiles for Representative Lead **10a****10a** (eutomer)

property	value
PDE2A IC ₅₀	0.024 μM
MW	378
Log <i>D</i> ^a	3.46
TPSA	69
LE ^b	0.38
LipE ^c	4.16
PDE selectivity	180-fold (vs. PDE3A)
HLM ^d	<1 μL/min/mg
RLM ^e	36 μL/min/mg
MLM ^f	27 μL/min/mg
MDR1 ratio ^g	0.43

^a Log *D* value at pH 7.4.⁶⁸ ^b LE (ligand efficiency) = $-1.37\text{LogIC}_{50}/\text{number of heavy atoms}$. ^c LipE (lipophilic efficiency) = $\text{pIC}_{50} - \text{Log } D$. ^d Metabolic stability in human liver microsomes. ^e Metabolic stability in rat liver microsomes. ^f Metabolic stability in mouse liver microsomes. ^g MDR1 efflux ratio in P-gp overexpressing cells.

Table 1-6. Pharmacokinetic Properties and *K_p* Values of **10a**^a

species	iv (0.1 mg/kg)		po (1 mg/kg)		AUC _{0-8h} ^f (ng·h/mL)	<i>F</i> ^g (%)	<i>K_p</i> ^h
	CL _{total} ^b (mL/min/kg)	<i>V</i> _{d_{ss}} ^c (mL/kg)	<i>C</i> _{max} ^d (ng/mL)	<i>T</i> _{max} ^e (h)			
rat	43.9	3953	15.9	1.7	58.7	15.4	2.9
mouse	43.2	4363	44.8	0.7	132.6	33.9	2.6

^a Rat or mouse cassette dosing at 0.1 mg/kg, iv and 1 mg/kg, po (non-fasted). Average of three rats.

^b Total clearance. ^c Volume of distribution at steady state. ^d Maximum plasma concentration. ^e Time of maximum concentration. ^f Area under the plasma concentration vs. time curve (0–8 h). ^g Oral bioavailability. ^h Brain-to-plasma ratio at 2 h in rat and 1 h in mouse.

第 5 節 化合物 **10a** の in vivo 薬理評価

PDE2A 阻害作用による薬力学マーカー (pharmacodynamic (PD) marker)^{注10)} に対する影響を検証するために、化合物 **10a** をマウスに経口投与 (10, 30, 100 mg/kg) し、PDE2A が高発現している部位 (前頭葉, 線条体, 海馬)^{39,40} における cGMP および cAMP 含量を測定した (Figure 1-8 (A) と 1-8 (B)). その結果, **10a** は上述の全ての部位における cGMP 含量を 30 mg/kg から用量依存的かつ有意に増加させた. 一方 cAMP 量については, 前頭葉のみ 100 mg/kg の用量で僅かな増加が認められた. PDE2A は cGMP および cAMP の両方を加水分解することが報告されているが, 化合物 **10a** のみならず, これまでに報告されている BAY 60-7550⁵⁵, *erythro*-9-(2-hydroxy-3-nonyl)adenine (EHNA)⁶⁹, 化合物 **1** (Figure 3)⁴⁸ などの他の PDE2A 阻害薬でも同様に cAMP よりも cGMP の濃度上昇に対してより強い効果を示す傾向が認められている. この理由は現時点で不明であるが, PDE2A は本来 cAMP よりも cGMP に対して高い親和性 (低い K_m 値) を示すこと^{70,71}, また cAMP に対してより親和性の強い PDE1, 4, 7, 8, 10 などの他の PDE ファミリーが共局在することによって, PDE2A 阻害による cAMP の分解抑制作用が相殺されている可能性が考えられる^{22,39}. 以上の結果から, PDE2A 阻害薬は, 生理的な条件下において, 主に cGMP の分解の抑制に関与していることが示唆された.

注 10) 薬物が実際に標的分子に到達して想定メカニズムに基づいた作用を示しているかどうかの指標として使われる. また, その反応に基づいて, 投与量の設定や投与スケジュールの決定などが可能である.

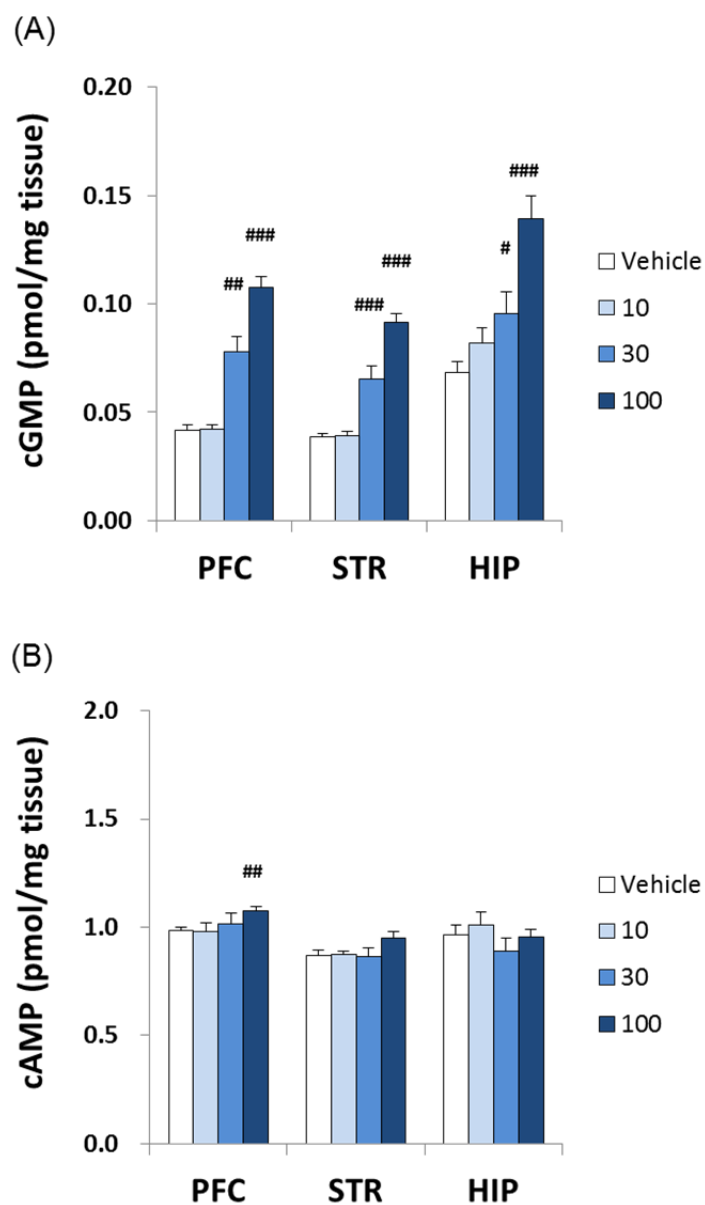
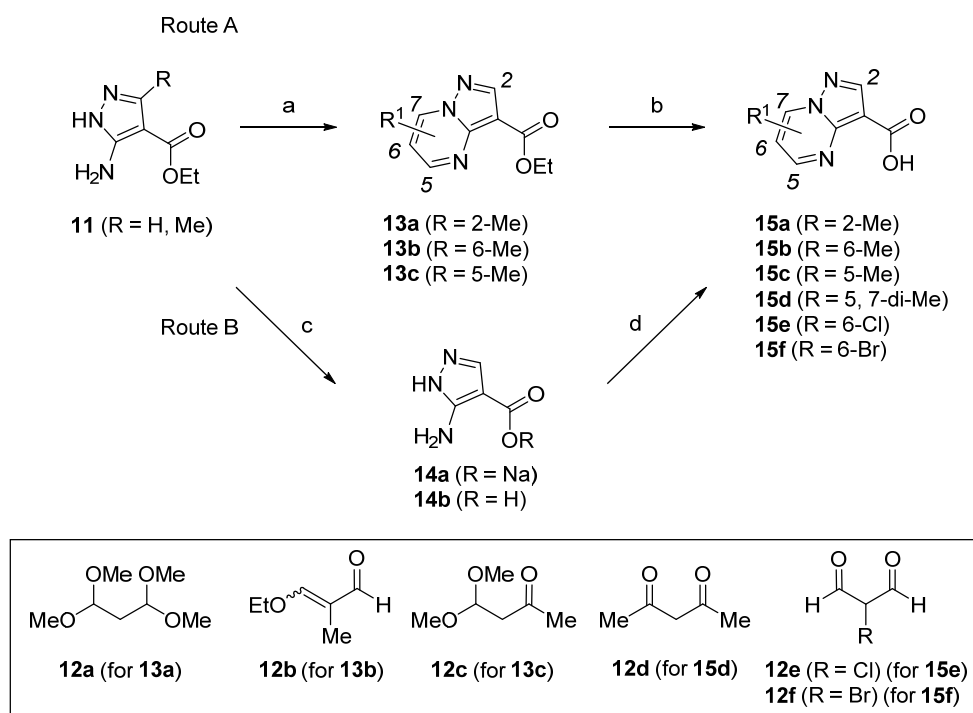


Figure 1-7. Increase in mouse brain cGMP (A) and cAMP (B) levels 30 min after oral administration of compound **10a** at 10, 30, and 100 mg/kg to ICR mice. The prefrontal cortex (PFC), striatum (STR), and hippocampus (HIP) were isolated after microwave irradiation. Data are presented as mean + SEM ($n = 7-8$); # $p < 0.025$, ## $p < 0.005$, ### $p < 0.0005$ vs vehicle by Williams' test or Shirley-Williams' test.

第 6 節 化合物の合成

置換ピラゾロ[1,5-*a*]ピリミジン-3-カルボン酸 **15** は, Scheme 1-1 に示したように, ピラゾロ[1,5-*a*]ピリミジン環の構築およびエステル部位の加水分解の 2 工程で合成された. すなわち, 酸性あるいは中性条件下, 5-アミノ-1*H*-ピラゾール **11** を種々の 1,3-ジカルボニル等価体 **12a-c** と縮合させた後, 得られたピラゾロ[1,5-*a*]ピリミジン **13a-c** をアルカリ加水分解に付すことで対応するカルボン酸 **15a-c** を得た (Route A). 一方 **15e** は, ピラゾロ[1,5-*a*]ピリミジン骨格がアルカリ加水分解の条件下で不安定であったため, 環構築の前にエステルの加水分解を実施することで合成した (Route B). また **15d,f** は, 市販のカルボン酸 **14b** を出発原料に用い, 対応する 1,3-ジカルボニル等価体 **12d,f** との縮合反応によって合成した.

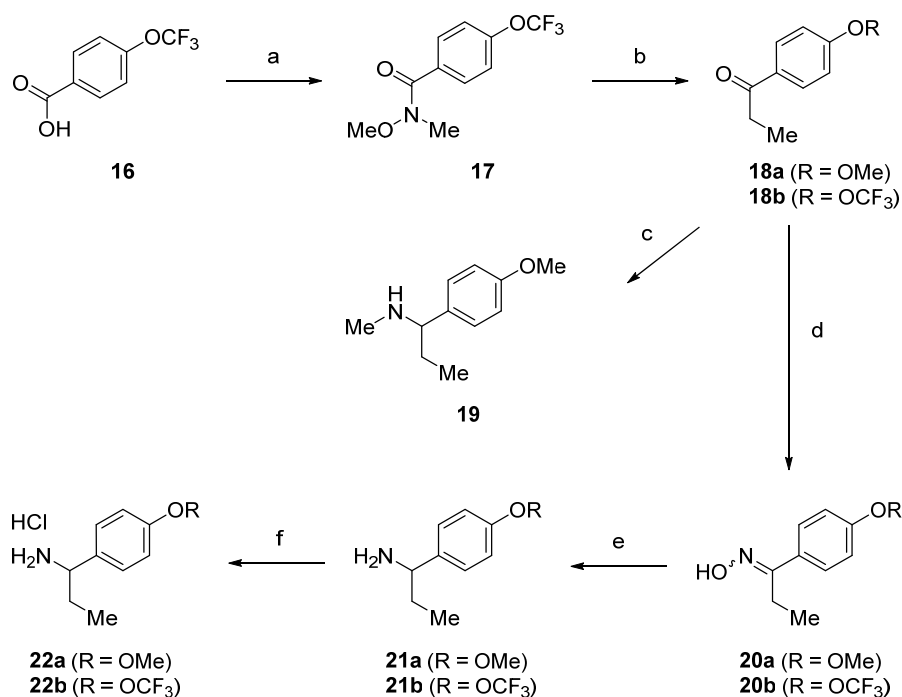
Scheme 1-1. Synthesis of Substituted Pyrazolo[1,5-*a*]pyrimidine-3-carboxylic Acids **15a-f**^a



^a Reagents and conditions: (a) **12a** or **12b**, AcOH, 70–90 °C, 0.5–16 h, 69–87% (for **13a** and **13b**); **12c**, toluene, 100 °C, 16 h, 68% (for **13c**); (b) 1 M or 2 M NaOH aq., MeOH, THF, 50–60 °C, 3 h–overnight, 80–87% (for **15a–c**); (c) 2 M NaOH aq., EtOH, reflux, 20 h, (taken on crude) (for **14a**); (d) **12d** or **12e** or **12f**, EtOH, AcOH, 80–100 °C, 1.5–2 h, 68% (for **15d**), 64% (2 steps from **11**) (for **15e**), 75% (for **15f**).

α -分岐ベンジルアミン **19**, **21a**, **21b**, **22a**, **22b** は Scheme 1-2 記載の方法で合成した. カルボン酸 **16** を Weinreb アミド **17** へ変換した後, エチルグリニャール試薬を作用させてケトン **18b** を合成した. 市販の **18a** はチタンテトライソプロポキシド共存下, メチルアミンとのイミン形成, 続く水素化ホウ素ナトリウムによる還元によって *N*-メチルベンジルアミン **19** に導いた. また, **18a,b** はヒドロキシアミン 塩酸塩を作用させてオキシム **20a,b** とし, 続いて粗生成物を水素添加の条件に付しベンジルアミン **21a,b** を合成した. ベンジルアミン **21a,b** は塩酸塩とすることで結晶化させて **22a,b** を得た.

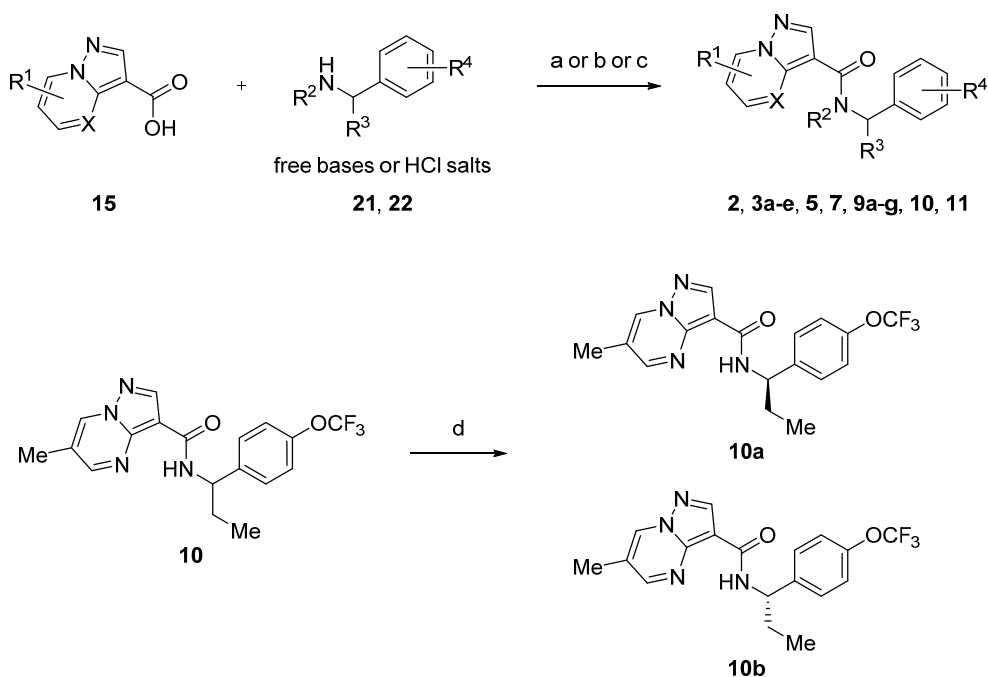
Scheme 1-2. Synthesis of RHS Benzylamine Moieties **19**, **21a**, **21b**, **22a**, and **22b**^a



^a Reagents and conditions: (a) oxalyl chloride, cat. DMF, THF, rt, 4 h, then *N,O*-dimethylhydroxylamine hydrochloride, Et₃N, DMA, rt, 16 h, 30%; (b) EtMgBr, THF, 0 °C, 2 h, 86%; (c) MeNH₂, Ti(*Oi*-Pr)₄, MeOH, rt, 5 h, then NaBH₄, rt, overnight, 25%; (d) hydroxylammonium chloride, Et₃N, EtOH, 80 °C, 3–4 h, (taken on crude); (e) H₂, 10% Pd/C, MeOH or EtOH, rt, overnight, 66–95%; (f) HCl, Et₂O, EtOAc, rt, 67–91% (2 steps from **20a,b**).

化合物 **2**, **3a-e**, **5**, **7**, **9a-g**, **10**, **11** は、市販品あるいは Scheme 1-1 で合成した置換ピラゾロ[1,5-*a*]ピリミジン-3-カルボン酸 **15** と Scheme 1-2 で合成した右骨格ベンジルアミン **21** あるいは **22** を縮合させて合成した。また、光学活性体 **10a,b** は ラセミ体 **10** の Chiralpak AD カラムを用いた光学分割により取得した (Scheme 1-3)。

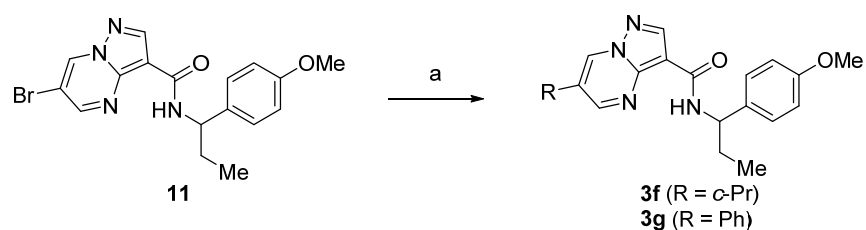
Scheme 1-3. Synthesis of Pyrazolo[1,5-*a*]pyrimidine Derivatives **2**, **3a-e**, **5**, **7**, **9a-g**, **10**, and **11**^a



^a Reagents and conditions: (a) EDCI·HCl, HOBt·H₂O, Et₃N or none, DMF, rt, 2 h–4 days, 44–98%; (b) EDCI, HOBt, DIEA, DMF, rt, overnight, 28–84%; (c) HATU, DIEA, DMF, rt, overnight, 52%; (d) Chiralpak AD, 100% EtOH.

6位シクロプロピルおよびフェニルピラゾロ[1,5-*a*]ピリミジン誘導体 **3f** および **3g** は対応するボロン酸との鈴木-宮浦クロスカップリング反応^{72,73} により合成した (Scheme 1-4).

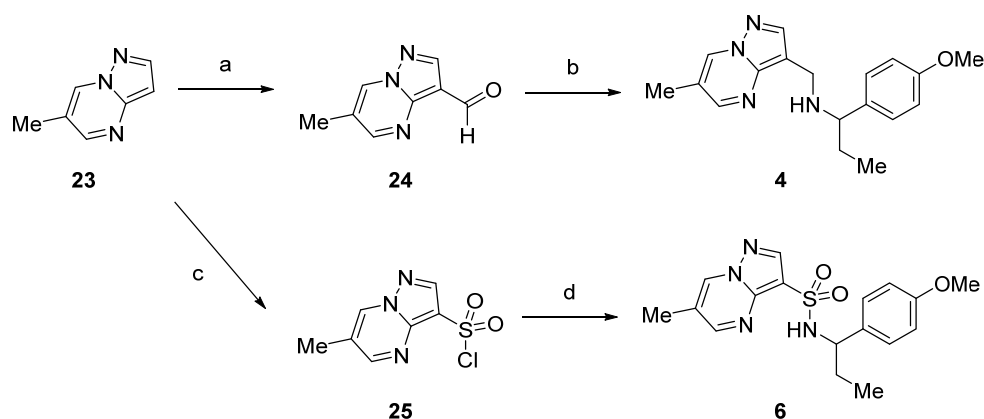
Scheme 1-4. Synthesis of Pyrazolo[1,5-*a*]pyrimidine Derivatives **3f** and **3g**^a



^a Reagents and conditions: (a) cyclopropylboronic acid, Pd(OAc)₂, Cy₃P, KO^{*t*}-Bu, toluene, 100 °C, 16 h, 10% (for **3f**); phenylboronic acid, Pd(PPh₃)₄, K₂CO₃, DME, water, 150 °C (microwave), 20 min, 77% (for **3g**).

アミドカルボニル基をメチレン基あるいはスルホンに置換した誘導体 **4** および **6** は、Vilsmeier 試薬⁷³ あるいはクロロスルホン酸を用いた 6-メチルピラゾロ[1,5-*a*]ピリミジン (**23**) への位置選択的なホルミル化あるいはクロロスルホン化によりホルミル体 **24** およびクロロスルホン体 **25** へ変換した後、ベンジルアミン **22a** との還元アミノ化反応あるいはスルホンアミド化反応により標的化合物 **4** および **6** を合成した (Scheme 1-5).

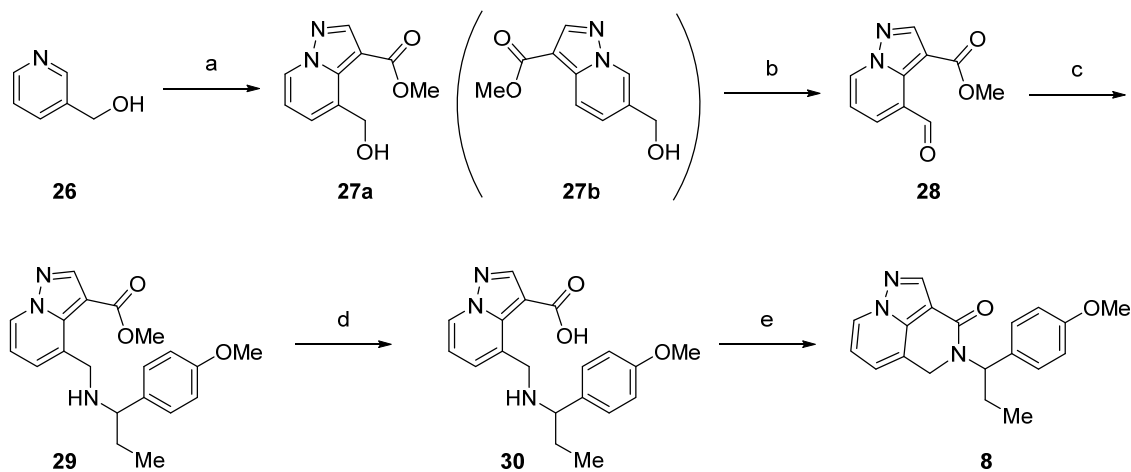
Scheme 1-5. Synthesis of Pyrazolo[1,5-*a*]pyrimidine Derivatives **4** and **6**^a



^a Reagents and conditions: (a) POCl₃, DMF, 0 °C to rt, 3 h, 82%; (b) **22a**, NaBH(OAc)₃, AcOH, Et₃N, CH₃CN, rt, overnight, 88%; (c) chlorosulfonic acid, 80 °C, 2 h, 26%; (d) **22a**, DIEA, CH₃CN, rt, overnight, 97%.

3 環性化合物 **8** は Scheme 1-6 記載の方法で合成した。ピリジン **26** を出発原料に用い、ヒドロキシアミン-*O*-スルホン酸による *N*-アミノ化反応、続くプロピオール酸メチルとの 1,3-双極子付加環化反応によって、所望のピラゾロ[1,5-*a*]ピリジン環化体 **27a** および その位置異性体 **27b** をそれぞれ 29% および 16% の収率で得た。続いて、Dess–Martin 試薬⁷⁵ による一級アルコールの酸化反応、ベンジルアミン **21a** との還元アミノ化反応、そしてエステルの加水分解によりカルボン酸 **30** に導き、最後に分子内アミド化反応を行って標的化合物 **8** を合成した。

Scheme 1-6. Synthesis of 4,5-Dihydro-3*H*-pyrazolo[4,5,1-*ij*][1,6]naphthyridin-3-one Derivative **8**^a



^a Reagents and conditions: (a) hydroxylamine-*O*-sulfonic acid, NaHCO₃, water, MeOH, 0 °C to 50 °C, 16 h, then methyl propiolate, K₂CO₃, 0 °C to rt, 2 h, 29%; (b) 1,1,1-triacetoxy-1,1-dihydro-1,2-benziodoxol-3(1*H*)-one (Dess–Martin periodinane), CH₃CN, 0 °C to rt, 2.5 h, (taken on crude); (c) **21a**, NaBH(OAc)₃, AcOH, CH₃CN, 0 °C to rt, 16 h, 79%; (d) 1 M NaOH aq., MeOH, THF, 70 °C, 2 h, 94%; (e) EDCI·HCl, HOBT·H₂O, DMF, rt, 16 h, 85%.

第 7 節 結語

以上述べてきたように、HTS ヒット化合物 **2** からのリード創出を指向した構造変換により、強い PDE2A 阻害活性および PDE ファミリー選択性を有する新規 PDE2A 阻害薬リード化合物 **10a** の創出に成功した。ヒット化合物 **2** からのリード創出の過程において、アミド部位の NH とピラゾロ[1,5-*a*]ピリミジン環 4 位窒素原子が互いに分子内水素結合を形成し、活性コンフォメーションを固定化していること、またピラゾロ[1,5-*a*]ピリミジン環 6 位へのメチル基の導入、および右末端フェニル基上の置換基変換 (*p*-メトキシ基からトリフルオロメトキシ基への変換) が PDE2A 阻害活性および PDE ファミリー選択性の向上において重要な役割を果たしていることを明らかにした。化合物 **10a** は薬物動態試験により経口吸収性および中枢移行性に優れることが示され、マウスへの経口投与において脳内 cGMP 含量の有意な増加作用を示した。これらは、**10a** が *in vivo* 経口ツール化合物および今後の最適化研究のリード化合物として有用であることを支持する結果といえる。一方で、臨床候補化合物の選択という観点においては、化合物 **10a** の *in vivo* 有効用量および PDE ファミリー選択性 (180 倍 vs. PDE3A) は不十分であり、以降の最適化検討においてさらなる PDE2A 阻害活性および PDE ファミリー選択性の改善が必要と考えられた。

第 2 章 高活性・高選択性・高い中枢移行性を示す PDE2A 阻害薬の創製：臨床候補化合物 TAK-915 の創出

第 1 節 研究背景

第 1 章では、リード化合物の取得を目指して、社内化合物ライブラリーから見出された HTS ヒット化合物 **2** を端緒とした構造変換を実施し、良好な PDE2A 阻害活性と PDE ファミリー選択性、そして薬物動態プロファイルを兼ね備えたリード化合物、ピラゾロ[1,5-*a*]ピリミジン誘導体 **10a** を見出すことに成功した。本化合物は上述の良好な *in vitro* および *in vivo* プロファイルを反映し、マウスへの経口投与によって、PDE2A が高発現している脳部位において用量依存的かつ有意な cGMP 含量の上昇作用を示した。しかしながら、本化合物の *in vivo* 有効用量 (30 mg/kg, po) における高い血中暴露量および PDE ファミリー選択性 (180 倍 vs. PDE3A) は臨床候補化合物の選択という観点から依然不十分であり、臨床において PDE2A の機能を解明し創薬標的としての有用性を検証するとともに、他の PDE やそれ以外のオフターゲットに起因する副作用を回避するためにも、さらなる PDE2A 阻害活性および PDE ファミリー選択性の向上が必要と考えられた。序論でも論じたように、11 種類の PDE ファミリーは基質特異性、発現分布、触媒活性の制御の仕方などが異なっており、それぞれが生体内の様々な組織の細胞内シグナル伝達の調節を行うことで多彩な生理作用を発揮していることが知られている。例えば、心臓や血管平滑筋などに発現する PDE1 や PDE3 の阻害は、血管拡張作用や頻脈など循環器系への影響が懸念され、^{76,77} 網膜に存在する PDE6 の阻害は、視覚異常が報告されている ⁷⁸⁻⁸⁰。したがって、PDE ファミリー選択性の確保は、副作用の回避に極めて重要と考えられる。これらの点を踏まえ、著者らは、より PDE2A 阻害活性が強く (PDE2A IC₅₀ < 5 nM)、PDE 阻害作用の選択性に優れ (>1000 倍以上)、かつ良好な中枢移行性を示す化合物の探索を進めることにした。リード化合物 **10a** の PDE2A 阻害活性および PDE ファミリー選択性向上を目指して、著者らは、PDE2A/化合物 **10a** 複合体の X 線共結晶構造情報 (Figure 1-7) に基づいた薬物設計を行った。また、設計

化合物の中核移行性を高い確率で確保するために、TPSA および HBD の数、および P-gp 基質性を指標とした合成展開を実施することとした。

第 2 節 X 線共結晶構造情報に基づいた薬物設計戦略

化合物 **10a** のさらなる PDE2A 阻害活性および PDE ファミリー選択性向上を達成するためには、PDE2A タンパクとの新たな相互作用の獲得と他の PDE ファミリーには存在しない PDE2A に特徴的な空間を利用する必要があると考えた。そこで、Figure 1-7 に示した X 線共結晶構造情報に基づいて、以下の 4 つの薬物設計戦略を立案した (Figure 2-1)。

戦略 1 第 1 章の第 3 節により、ピラゾロ[1,5-*a*]ピリミジン環 7 位の水素原子は PDE ファミリー共通の基質結合部位である Gln859 と弱い擬似的水素結合を介して相互作用していることが明らかとなった。本結果に基づき、Gln859 と明確に水素結合が形成できる新たな母核を探索し、活性の向上を図る。この骨格変換によって、活性の向上が期待できるのみならず、化合物の新規性や構造多様性を高め、最適化研究における成功確率向上に繋がること期待される。

戦略 2 *p*-トリフルオロメトキシフェニル基は、他の PDE ファミリーではこれまで存在が確認されていない PDE2A に特徴的な脂溶性空間を占有していることが分かっている。そこで、この脂溶性空間を充填する最適な置換基を導入することにより、PDE2A 阻害活性の向上と PDE ファミリー選択性の向上を同時に図る。この際、トリフルオロメトキシ基のアルコキシ酸素の必要性や適切な置換様式についても検証する。

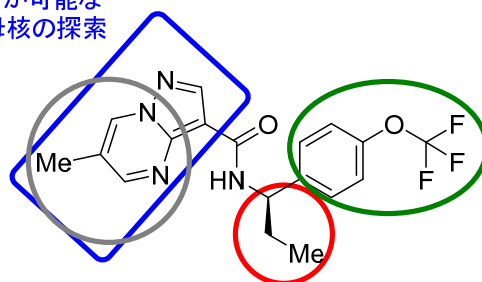
戦略 3 リガンド結合サイトのマグネシウムや亜鉛金属イオンの周辺には、極性アミノ酸残基である His656 や Glu829、さらには水分子が多く存在する。また、分岐エチル側鎖は溶媒側に面しており、この周辺は比較的大きな親水性領域と考えられた。これら His656 や Glu829 あるいは水分子との相互作用を期待し、エチル基側鎖に極性基を導入し、PDE2A 阻害活性の

向上を目指す。また、極性アミノ酸残基や水分子と相互作用するための最適な側鎖の長さを見極めることとした。

戦略 4 第 1 章・第 2 節の検討で明らかになったように、ピラゾロ[1,5-*a*]ピリミジン環 6 位へのメチル基の導入によって活性および選択性が大幅に向上した。戦略 1 で新たに見出した母核近傍の空間を効果的に充填する、あるいは PDE 間で異なるアミノ酸残基を狙い適切な位置に置換基を導入することによって、活性および PDE ファミリー選択性の向上を目指す。

戦略 1

Gln859 と明確な水素結合が可能な
ピラゾロ[1,5-*a*]ピリミジン母核の探索



戦略 2

PDE2A に特異的な脂溶性空間を
効果的に充填する置換基の探索

戦略 4

母核近傍の空間を効果的に充填する、あるいは
PDE 間で異なるアミノ酸残基を狙った置換基導入

戦略 3

金属イオン周辺に存在する水分子や His656
と相互作用可能な極性置換基の導入

Figure 2-1. Drug design strategies to improve PDE2A inhibitory activity and PDE selectivity.

第 3 節 新規母核の探索に向けた薬物設計戦略：戦略 1

化合物 **10a** のさらなる活性の向上を目指すに当たって、著者らは、**10a** のピラゾロ [1,5-*a*]ピリミジン環と Gln859 の相互作用である擬似的水素結合に着目した。一般的に CH-O の擬似的水素結合は $X-H\cdots Y$ ($X, Y = N$ or O) で表される古典的な水素結合に比べて弱い結合のため、Gln859 と古典的な水素結合を介して相互作用することができれば活性の向上が期待できると考えた。一方で、PDE2A ような cAMP と cGMP の両基質を加水分解する PDE の二重基質性を説明する分子メカニズムの一つとして「グルタミン スイッチ」が提唱されている (Figure 2-2)^{81,82}。これは、cAMP および cGMP の両基質を認識するために、PDE

ファミリー共通の基質結合部位である Gln 側鎖 (PDE2A の場合は Gln859) が自由に回転するというものである。上述の明確な水素結合による相互作用と「グルタミン スイッチ」の分子メカニズムを考慮して、Gln859 と明確な水素結合が形成可能な新規骨格を設計した (Figure 2-3)。その際、ピラゾロ[1,5-*a*]ピリミジン誘導体で認められている分子内水素結合の重要性も考慮して、アミド部位の NH と分子内水素結合が形成できるよう新規骨格の適切な位置に HBA として機能する窒素原子の導入を行った。また、P-gp による排出の懸念の少ない化合物を見出すべく、化合物設計の段階で TPSA や HBD 数などの物理化学的な指標も考慮に入れた。これまでの報告によると、P-gp による排出を抑制するためには、TPSA および HBD 数はそれぞれ $< 90 \text{ \AA}^2$ 、そして < 2 (すなわち、0 か 1) で定義される範囲内で薬物設計を行うことが推奨されている^{61,62}。分子内水素結合が認められるケモタイプでは、その結合の強さによって見かけの TPSA および HBD 数が変化すると考えられ、例えば、強固に分子内水素結合を形成する場合には、アミド部位の NH および母核の塩基性部位が完全にマスクされ、見かけの TPSA および HBD 数はそれぞれ約 20 \AA^2 と 1 つ減少すると見なすことができる⁸³。以上の考察を踏まえ、本章で論じる薬物設計は、中枢移行性を指向した 2 つの指標から定義されるケミカルスペースの範囲内 ($\text{TPSA} < 90 + 20 = 110 \text{ \AA}^2$, HBD 数 $< 2 + 1 = 3$)^{61,62,83} で実施することとした。

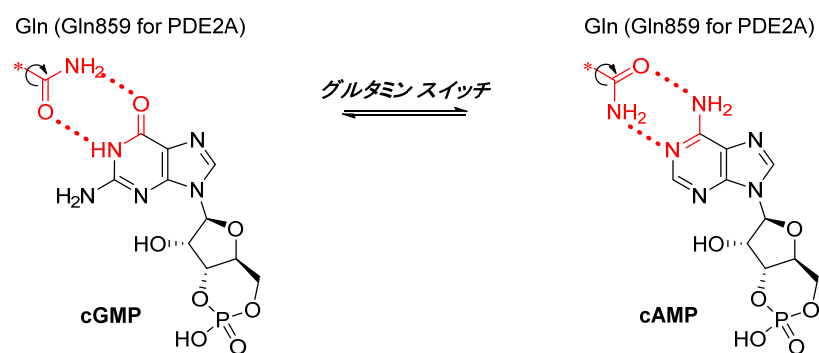


Figure 2-2. Glutamine switch mechanism proposed to explain the accommodation of both cyclic nucleotide substrates in dual-substrate PDEs.

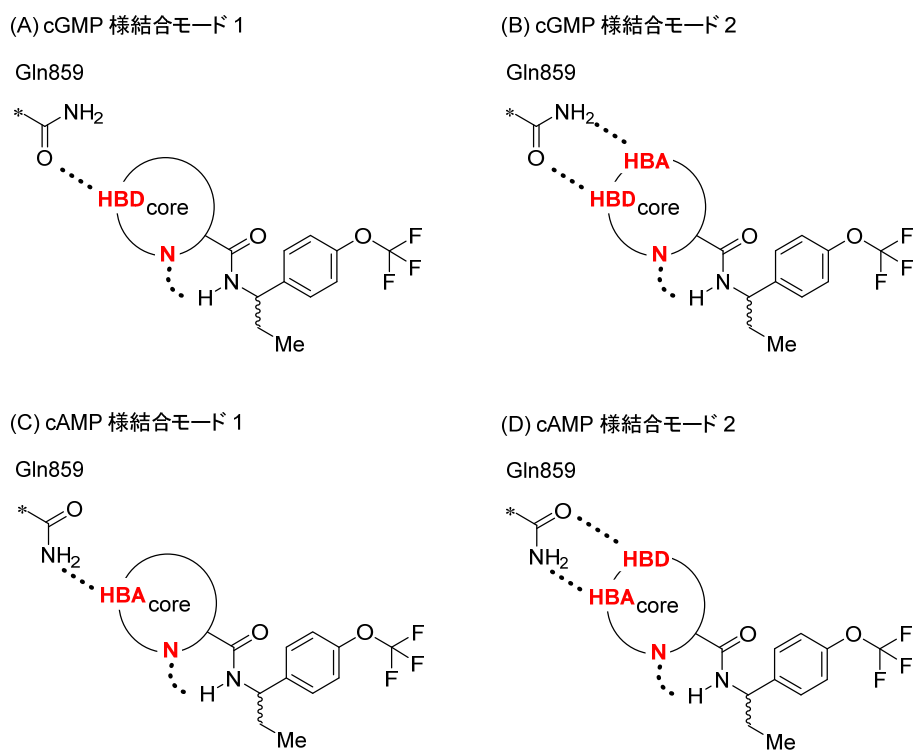


Figure 2-3. Drug design concepts (A)–(D) to identify new alternatives to the pyrazolo[1,5-*a*]pyrimidine core.

第 4 節 生物活性と構造活性相関：戦略 1

新規に設計，合成した 2 環性骨格の PDE2A 阻害活性に対する影響を Table 2-1 にまとめた。合成した全ての誘導体の TPSA は，化合物設計の段階で第 3 節で設定した 110 Å² 未満の範囲内に収まるよう考慮した。また，対照化合物としてピラゾロ[1,5-*a*]ピリミジン誘導体 **10** および **31** のデータも Table 2-1 に掲載した。Gln859 と cGMP 様の結合様式で水素結合が形成可能な 3,4-ジヒドロピリド[2,3-*b*]ピラジン-2(1*H*)-オン誘導体 **32** はピラゾロ[1,5-*a*]ピリミジン誘導体 **31** に比べ，高い PDE2A 阻害活性を示した。しかしながら，化合物 **32** の 3,4-ジヒドロピリド[2,3-*b*]ピラジン-2(1*H*)-オン環は，片方の環が飽和環になっており，ピラゾロ[1,5-*a*]ピリミジン誘導体 **31** と比べて，環上下に位置する Phe862 と Ile826 との π - π および CH- π 相互作用が減弱している可能性が考えられた。そこで，さらなる活性の向上を狙って，化合物 **32** のラクタム構造と化合物 **31** の芳香族性を併せ持つ 1,5-ナフチ

リジン-2(1*H*)-オン誘導体 **33** を設計した。その結果、期待通り **33** は誘導体 **32** よりも約 4 倍強い活性を示した。本結果は、Gln859 との相互作用のみならず、2 環性骨格の上下に位置する Phe862 および Ile826 との相互作用の両方が活性発現に重要であることを示唆するものである。一方、cAMP 様の結合様式と同様に Gln859 側鎖の $-NH_2$ との水素結合を期待したピラゾロ[1,5-*b*][1,2,4]トリアジン誘導体 **34** はピラゾロ[1,5-*a*]ピリミジン誘導体 **10** と比べて、活性が大きく減弱した。また、化合物 **33** の逆アミド構造を有するラクタム誘導体 **35** も cAMP 様の結合様式を期待したが、活性の増強には至らなかった。活性が低下した原因として、Gln859 の側鎖と相互作用が可能な適切な位置に HBA あるいは HBD を配置できていない可能性も否定できないものの、Gln859 の側鎖自体が前述の「グルタミン スイッチ」で提唱される自由な回転ができない可能性も考えられる。実際、Figure 1-6 (A) で示した化合物 **10a** の X 線共結晶構造解析では、Gln859 側鎖のカルボニル基は隣接する Tyr827 側鎖のフェノール性水酸基と水素結合を形成していることが示唆されている。したがって、化合物 **34** および **35** は、この水素結合ネットワークの切断によるエネルギー損失を上回る新たな相互作用が獲得できなかった結果、活性が低下したのではないかと推察できる。続いて、良好な活性が認められた化合物 **32** の母核上の塩基性窒素原子を CH に置換した誘導体 **36** の合成を行ったが、活性は顕著に低下した。この結果は、3,4-ジヒドロピリド[2,3-*b*]ピラジン-2(1*H*)-オン誘導体においても、ピラゾロ[1,5-*a*]ピリミジン誘導体と同様、分子内水素結合が活性発現に重要な役割を果たしていることを強く支持するものと考えられる。以上のように、Gln859 との相互作用の改善を指向した骨格変換を実施した結果、ピラゾロ[1,5-*a*]ピリミジン誘導体を上回る強い PDE2A 阻害活性を示す誘導体 **32** および **33** を見出すことに成功した。しかしながら、その後の化合物評価において、**33** は母核環構造に起因すると考えられる強い *in vitro* 光毒性ポテンシャルを示したのに加え、**32** に比べて酸性度の高いラクタム N-H のプロトンを有しているため中枢移行性が低いことも判明した。以上の結果から、化合物 **32** の 3,4-ジヒドロピリド[2,3-*b*]ピラジン-2(1*H*)-オン環を新規骨格として選択し、以降の最適化検討を実施した。

Table 2-1. In Vitro Activities of Derivatives Possessing Various Fused Bicyclic Cores

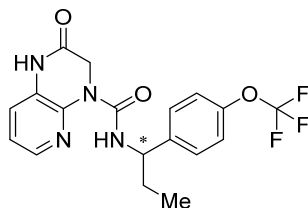
The general structure shows a fused bicyclic core (circled) attached to an amide group (-NH-). The amide nitrogen is bonded to a methyl group (-Me) and a para-substituted phenyl ring. The phenyl ring is further substituted with a trifluoromethoxy group (-OCF₃).

compd	core	anticipated binding mode ^a	PDE2A IC ₅₀ (nM) ^b	TPSA (Å ²)
10		(A)	53 (47–59)	69
31		(A)	480 (350–650)	69
32		(A) or (B)	78 (61–98)	84
33		(A) or (B)	21 (18–26)	84
34		(C)	6500 (4200–9800)	81
35		(C) or (D)	19000 (15000–24000)	84
36		(A) or (B)	70000 (40000–120000)	71

^a See Figure 2-3. ^b IC₅₀ values (95% confidence intervals given in parentheses) were calculated from percent inhibition data (duplicate, *n* = 1). All values are rounded to two significant digits.

第 5 節 化合物 **32** の光学分割と *in vitro* 活性および PDE ファミリー選択性

活性の向上が認められた化合物 **32** の光学分割を実施し、光学活性体の PDE2A 阻害活性および PDE ファミリー選択性に対する影響を検証した (Table 2-2). その結果、光学異性体 **32a** が $IC_{50} = 66 \text{ nM}$ の阻害活性を示し、もう一方の異性体 **32b** は $100 \mu\text{M}$ の濃度においても阻害活性を示さなかった. この結果は、PDE2A タンパクが厳密にリガンドの絶対立体配置を認識していること示唆していると考えられる. また **32a** は、ラセミ体 **32** と同様の選択性プロファイルを示すことが明らかとなった (PDE1A に対して 30 倍, PDE3A に対しては 64 倍, その他の PDE ファミリーに対しては 150 倍以上).

Table 2-2. In Vitro Activity Profiles of **32** and Its Enantiomers **32a** and **32b**

compd	stereo	PDE2A IC ₅₀ (nM) ^a
32	<i>rac</i>	78 (61–98)
32a	<i>eutomer</i>	66 (46–93)
32b	<i>distomer</i>	>100000

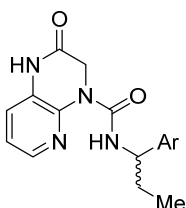
PDE subtypes	32		32a	
	IC ₅₀ (nM) ^a	selectivity ratio ^b	IC ₅₀ (nM) ^a	selectivity ratio ^b
PDE1A	3200	41	2000	30
PDE2A3	78	–	66	–
PDE3A	8100	100	4200	64
PDE4D2	>10000	>130	>10000	>150
PDE5A1	9800	130	>10000	>150
PDE6AB	>10000	>130	>10000	>150
PDE7B	>10000	>130	>10000	>150
PDE8A1	>10000	>130	>10000	>150
PDE9A2	>10000	>130	>10000	>150
PDE10A2	>10000	>130	>10000	>150
PDE11A4	>10000	>130	>10000	>150

^a IC₅₀ values were calculated from percent inhibition data (duplicate, *n* = 1). All values are rounded to two significant digits. ^b Selectivity ratio (rounded to two significant digits) = PDE"X" IC₅₀/PDE2A IC₅₀.

第 6 節 *p*-トリフルオロメトキシフェニル部位の最適化：戦略 2

さらなる PDE2A 阻害活性および PDE ファミリー選択性の改善を目的として、フェニル基上置換基の変換を実施した (Table 2-3). Figure 1-7 に示した X 線共結晶構造情報から、PDE2A サブタイプに特徴的な本空間は脂溶性側鎖で囲まれ、大きさも限られていることが示唆されていることから、コンパクトな脂溶性置換基を中心に導入の検討を行った。第 1 章のピラゾロ[1,5-*a*]ピリミジン誘導体の構造活性相関と同様に、*p*-トリフルオロメトキシ基 (**32**) をメトキシ基 (**37a**) に変換すると活性が約 8 倍減弱することが分かった。活性が大きく低下した要因として、(1) 活性コンフォメーションでは、フェニル基とパラ位置置換基が直交型の立体配座で充填していることが明らかとなっており、一般的にフェニル基と同じ平面に位置する立体配座がエネルギー的に最も有利なメトキシ基は PDE2A タンパクに結合する際に構造変化が必要となり、エントロピー損失が生じたこと⁶³、また (2) 脂溶性が低下 ($\Delta \text{Log } D = 0.83$) することによって PDE2A の脂溶性側鎖とのファンデアワールス相互作用が低下した点が挙げられる。一方、トリフルオロメトキシ基 (**32**) とは異なる 3 次元構造を有するトリフルオロメチル基 (**37b**) やシクロプロピル基 (**37c**) は **32** と同等の阻害活性を示したものの、PDE ファミリー選択性は低下する傾向が認められた。これらの結果から、置換基の 3 次元構造、あるいはフェニル基に直結したトリフルオロメトキシ基の酸素原子が PDE ファミリー選択性に重要な役割を果たしていると考えられる。また窒素原子で結合したアゼチジン誘導体 **37d** の阻害活性は約 8 倍減弱した。続いて、トリフルオロメトキシ基の最適な置換位置を検証するため、フェニル基のメタ位およびオルト位にトリフルオロメトキシ基を有する誘導体 (**37e**, **37f**) を合成したが、いずれも活性は大きく減弱した。メタ位およびオルト位近傍の空間の大きさが限られている、あるいはオルト位の置換基導入によって分岐エチル側鎖を含む近傍の置換基と立体反発が生じ、活性コンフォメーションに影響を及ぼした可能性が示唆される。次に、二置換誘導体の可能性について検証した。上述の検討により、フェニル基上のオルト位およびメタ位にはトリフルオロメトキシ基のような嵩高い置換基は許容されないことが分かっていたため、立体的に小さなフルオロ基の導入を検討した。

その結果、オルト位にフルオロ基を導入したオルト置換体 **37h** は活性が低下する傾向を示したのに対し、メタ置換体 **37g** は 42 nM の強い PDE2A 阻害活性を示すことが明らかとなった。以上の検討結果から、化合物 **32** と同等以上の PDE2A 阻害活性を示すフェニル置換体 **37b** および **37g** を見出すことができた。

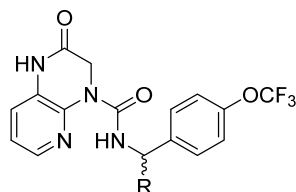
Table 2-3. SAR of the RHS Phenyl Group

compd	Ar	PDE2A IC ₅₀ (nM) ^a	PDE selectivity ^b	Log <i>D</i> ^c
32		78 (61–98)	41-fold (PDE1A)	3.61
37a		610 (480–780)	NT ^d	2.78
37b		72 (46–110)	4.2-fold (PDE1A)	3.45
37c		80 (64–100)	4.4-fold (PDE1A)	3.75
37d		500 (410–590)	NT ^d	3.13
37e		4100 (3400–4900)	NT ^d	NT
37f		8100 (5500–18000)	NT ^d	3.52
37g		42 (33–52)	15-fold (PDE1A)	3.67
37h		210 (160–290)	28-fold (PDE1A)	3.83

^a IC₅₀ values (95% confidence intervals given in parentheses) were calculated from percent inhibition data (duplicate, *n* = 1). All values are rounded to two significant digits. ^b Minimum selectivity (rounded to two significant digits) over other PDEs. The least selective PDE was given in parenthesis. ^c Log *D* values at pH 7.4. ^d Not tested.

第 7 節 分岐エチル側鎖の変換：戦略 3

リガンド結合サイトに存在するマグネシウムおよび亜鉛金属イオン周辺の極性アミノ酸残基や水分子との相互作用を目指して、分岐エチル側鎖に極性官能基の導入を検討した (Table 2-4). メトキシメチル基を有する誘導体 **38a** は PDE2A 阻害活性および PDE ファミリー選択性ともに大きく改善するとともに、この変換によって脂溶性も大きく低減 ($\Delta\text{Log } D = 0.66$) できることが明らかとなった。また、一炭素増炭したメトキシエチル誘導体 **38b** は、化合物 **32** と比べて活性は保持されたものの、PDE ファミリー選択性は低下する傾向を示した。さらに、**38a** のエーテル酸素原子をメチレン基に置換した **38c** は 10 倍以上の活性の減弱が認められた。これらの結果から、エーテル酸素原子が PDE2A タンパクと新たな相互作用を形成していることが示唆されたため、さらに他の極性官能基の導入を検討した。その結果、一級アルコール誘導体 **38d** は **32** と比較して、活性および PDE ファミリー選択性が保持するに留まったが、対応する三級アルコール誘導体 **38e** は活性および PDE 選択性共に改善することが明らかとなった。化合物 **38e** の *gem*-ジメチル基の導入によって結合周りの回転が抑制され、その結果、コンフォメーションが固定化され活性および選択性が向上したのではないかと推察した。また、極性のさらに高いスルホン誘導体 **38f** でも良好な活性と選択性を示すことが明らかとなった。これらの結果は、この位置が極性アミノ酸残基や水分子に囲まれ、溶媒側に面した親水性の空間であることと矛盾のない結果と考えられる。一方で、極性官能基の導入によって TPSA あるいは HBD 数の増加が認められている。化合物 **38d-f** は当初設定した TPSA あるいは HBD 数のいずれかの目標値 ($\text{TPSA} < 110 \text{ \AA}^2$, $\text{HBD 数} < 3$) を逸脱しており、実際のところ P-gp 基質の傾向が強いことが明らかとなった。この結果は、TPSA および HBD の数が P-gp の基質認識性を予測する上で重要な因子であり、我々が設定したこれら指標の目標値が妥当であることを支持するものといえる。以上の検討結果より、PDE2A 阻害活性と PDE ファミリー選択性の向上および脂溶性の低減を同時に実現し、さらに P-gp 基質の懸念の少ないメトキシメチル誘導体 **38a** を見出すことに成功した。本メトキシメチル基は、以降の最適化検討における分岐側鎖として選択することとした。

Table 2-4. SAR of the Branched Group at the Benzylic Position of the RHS Amine Moiety

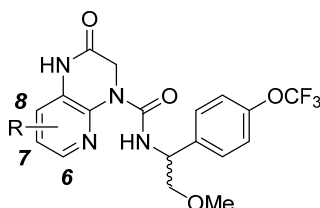
compd	R	PDE2A IC ₅₀ (nM) ^a	PDE selectivity ^b	Log <i>D</i> ^c	TPSA (Å ²)	MDR1 ^d
32	-Et	78 (61–98)	41-fold (PDE1A)	3.61	84	0.53
38a	-CH ₂ OMe	19 (15–24)	310-fold (PDE1A)	2.95	93	0.68
38b	-CH ₂ CH ₂ OMe	62 (37–100)	14-fold (PDE5)	3.09	93	0.77
38c	- <i>n</i> -Pr	250 (190–330)	NT ^e	4.05	84	0.59
38d	-CH ₂ OH	65 (35–120)	54-fold (PDE1A)	2.16	104	2.8
38e	-C(Me) ₂ OH	24 (18–33)	150-fold (PDE1A)	2.54	104	2.8
38f	-CH ₂ SO ₂ Me	29 (22–38)	220-fold (PDE1A)	1.91	118	26

^a IC₅₀ values (95% confidence intervals given in parentheses) were calculated from percent inhibition data (duplicate, *n* = 1). All values are rounded to two significant digits. ^b Minimum selectivity (rounded to two significant digits) over other PDEs. The least selective PDE was given in parenthesis. ^c Log *D* values at pH 7.4. ^d MDR1 efflux ratios in P-gp overexpressing cells. ^e Not tested.

第 8 節 新規母核への置換基導入：戦略 4

全 PDE ファミリーのアミノ酸配列の比較によって、3,4-ジヒドロピリド[2,3-*b*]ピラジン-2(1*H*)-オン環が占有すると考えられる空間近傍のアミノ酸残基 (例えば PDE2A では Tyr827, Leu858, Met847 が 3,4-ジヒドロピリド[2,3-*b*]ピラジン-2(1*H*)-オン環近傍に存在すると考えられる) には PDE ファミリー間でいくつかの違いがあることが報告されている^{84,85}. このようなアミノ酸残基の違いによって結合部位の形状・サイズ・極性に違いが生じ、各 PDE ファミリーに特徴的な空間が形成されていると考えられることから、3,4-ジヒドロピリド[2,3-*b*]ピラジン-2(1*H*)-オン環への置換基導入は PDE2A 阻害活性および選択性を改善する上で有用なアプローチと考えた. 実際に、第 1 章の第 2 節 (Table 1-1 参照) で述べたように、ピラゾロ[1,5-*a*]ピリミジン環にメチル基を導入することで活性および選択性の両面で大

幅な改善が認められている。これらの知見を基に、阻害活性および選択性の向上を目的とした 3,4-ジヒドロピリド[2,3-*b*]ピラジン-2(1*H*)-オン環上の置換基探索を行った (Table 2-5)。6 位 (**39a**) および 8 位 (**39c**) にメチル基を導入すると、共に活性が減弱する傾向を示したのに対し、7 位メチル置換体 **39b** は 2 倍の活性向上に加え、1100 倍の優れた PDE ファミリー選択性を示すことが明らかとなった。これらの結果を受けて、以後 3,4-ジヒドロピリド[2,3-*b*]ピラジン-2(1*H*)-オン環 7 位への置換基導入を詳細に検討することとした。メチル基よりも脂溶性が高く、かつ嵩高いシクロプロピル基 (**39d**) を導入すると、PDE2A 阻害活性および選択性の向上が認められた。一方、メチル基と同程度の原子サイズを有し、電子求引性基のクロロ基 (**39e**) を導入すると、活性・選択性共に悪化する傾向を示した。本結果は、クロロ基の導入によって母核の電子密度が低下し、上下に位置する Phe862/Ile826 との π - π および CH- π 相互作用が減弱したためと推察された。以上のことから、7 位への置換基導入は受容体ポケットの充填と母核の電子密度の調節という 2 つの効果によって活性発現に寄与している可能性が示唆された。一方で、化合物 **39b** および **39d** などの 7 位アルキル誘導体は数 nM オーダーの強い阻害活性と優れた選択性を示したものの、高い脂溶性に懸念が持たれた。一般的に脂溶性の高い分子は、非特異的相互作用に基づく毒性発現のリスクが高くなることが報告されている⁸⁶⁻⁸⁸。そこで、脂溶性の増加が小さなアルコキシ基の導入を検討した結果、7 位メトキシ誘導体 **39f** は、対応するシクロプロピル誘導体 **39d** と同等の活性と 2 倍以上改善した PDE ファミリー選択性を示すことが分かった。しかしながら、さらに嵩高いイソプロポキシ誘導体 **39g** は、大幅な活性の低下が認められた。以上の検討を経て見出された化合物 **39f** は、一般の中枢薬と比べると高い TPSA (102 Å²) を有しているにも関わらず、P-gp の排出比は問題のない良好な値を示した。前節と同様に、分子内水素結合による HBA および HBD の極性官能基の遮蔽効果が良好な P-gp プロファイルに寄与していると考えられる。

Table 2-5. SAR of Substitutions at the 3,4-Dihydropyrido[2,3-*b*]pyrazin-2(1*H*)-one Core

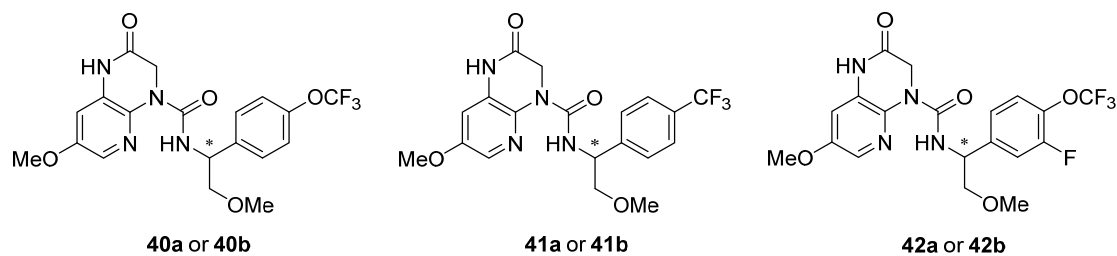
compd	R	PDE2A IC ₅₀ (nM) ^a	PDE selectivity ^b	Log <i>D</i> ^c	TPSA (Å ²)	MDR1 ^d
38a	H	19 (15–24)	310-fold (PDE1A)	2.95	93	0.68
39a	6-Me	40 (31–52)	50-fold (PDE1A)	3.38	93	0.63
39b	7-Me	8.7 (7.6–10)	1100-fold (PDE5)	3.35	93	1.0
39c	8-Me	85 (67–110)	NT ^e	3.16	93	0.74
39d	7- <i>c</i> -Pr	3.5 (3.0–4.1)	1300-fold (PDE3A)	3.85	93	1.0
39e	7-Cl	33 (30–36)	210-fold (PDE5)	3.74	93	0.58
39f	7-MeO	2.8 (2.6–3.1)	2700-fold (PDE5)	3.20	102	1.3
39g	7- <i>i</i> PrO	77 (66–90)	NT ^e	3.94	102	1.1

^a IC₅₀ values (95% confidence intervals given in parentheses) were calculated from percent inhibition data (duplicate, *n* = 1). All values are rounded to two significant digits. ^b Minimum selectivity (rounded to two significant digits) over other PDEs. The least selective PDE was given in parenthesis. ^c Log *D* values at pH 7.4. ^d MDR1 efflux ratios in P-gp overexpressing cells. ^e Not tested.

第 9 節 化合物 **39f** およびその周辺誘導体の光学分割と光学活性体の *in vitro* 評価

化合物 **39f** は目標 (PDE2A 阻害活性 IC₅₀ < 5 nM, PDE selectivity > 1000 倍) とする強力な PDE2A 阻害活性と優れた選択性を示したことから光学分割を実施した。また、化合物 **39f** の *p*-トリフルオロメトキシフェニル基部位を、第 7 節の検討で見出した **37b** および **37g** の右末端フェニル基部位に変換した誘導体も同時に合成し、光学分割を実施した。各光学活性体の PDE2A 阻害活性, PDE ファミリー選択性およびその他 *in vitro* プロファイルを Table 2-6 に示した。光学分割体 **40a**, **41a**, **42a** は、それぞれ対応するもう片方の光学活性体よりも PDE2A に対して高い結合阻害活性を示した。化合物 **40a** は強力な阻害活性 (IC₅₀ = 1.6 nM) および PDE ファミリー選択性 (PDE1A に対して 3300 倍) を示したのに対し、化合物 **41a** は期待した活性 (IC₅₀ = 7.2 nM) および選択性 (PDE1A に対して 83 倍) を示さな

かった。一方、化合物 **42a** は合成した中で最も良好な活性 ($IC_{50} = 0.61 \text{ nM}$) および PDE ファミリー選択性 (PDE1A に対して 4100 倍、各 PDE ファミリーに対する IC_{50} 値は Table 2-7 参照) を示すことが明らかとなった。また、酵素・G タンパク質共役型受容体 (G protein-coupled receptor, GPCR)・核内受容体・イオンチャンネル・トランスポーターを含む合計 96 種類のオフターゲット選択性試験 (Eurofins Panlabs 社) の結果、化合物 **42a** は下記 6 種類のターゲットを除く 90 種類のターゲットに対して、極めて高い選択性を有することが判明した。一方、 $10 \mu\text{M}$ の濃度において 50% 以上の阻害活性を示した 6 種類のターゲット (アセチルコリンエステラーゼ: 99%, 5-リポキシゲナーゼ: 70%, CB1 カンナビノイド受容体: 60%, PDE5: 59%, L 型カルシウムチャンネル: 54%, 血液凝固因子 Xa ペプチダーゼ: 51%) のうち、最も強い阻害活性を示したアセチルコリンエステラーゼに関して社内で精査試験を実施したところ、 IC_{50} 値にして $3.9 \mu\text{M}$ の酵素阻害活性を示した。以上のことから、化合物 **42a** は各種の PDE ファミリー (4100 倍以上) のみならず、他の広範なターゲットに対しても極めて高い選択性 (6400 倍以上) を有する PDE2A 阻害薬であることが明らかとなった。

Table 2-6. In Vitro Profiles and Physicochemical Properties of Analogs **40a–b**, **41a–b**, **42a–b**^a

compd	stereo	PDE2A IC ₅₀ (nM) ^b	PDE selectivity ^c	Log <i>D</i> ^d	TPSA (Å ²)	MDR1 ^e
40a	<i>R</i>	1.6 (1.4–1.9)	3300-fold (PDE1A)	3.19	102	1.5
40b	<i>S</i>	39000 (28000–54000)	–	–	–	–
41a	ND ^f	7.2 (6.4–8.0)	83-fold (PDE1A)	3.03	93	0.79
41b	ND ^f	21000 (10000–42000)	–	–	–	–
42a	<i>R</i>	0.61 (0.53–0.70)	4100-fold (PDE1A)	3.32	102	0.87
42b	<i>S</i>	910 (720–1200)	–	–	–	–

^a Racemic compounds were chirally separated and each enantiomer was profiled. The absolute configurations of **40b** and **42a** were determined as *S* and *R*, respectively, via single crystal X-ray analysis of the corresponding RHS benzylamine precursors (see the Experimental Section). ^b IC₅₀ values (95% confidence intervals given in parentheses) were calculated from percent inhibition data (duplicate, *n* = 1). All values are rounded to two significant digits. ^c Minimum selectivity (rounded to two significant digits) over other PDEs. The least selective PDE was given in parenthesis. ^d Log *D* values at pH 7.4. ^e MDR1 efflux ratios in P-gp overexpressing cells. ^f Not determined.

Table 2-7. PDE Selectivity Profile of **42a**

PDE subtypes	IC ₅₀ (nM) ^a	selectivity ratio ^b
PDE1A	2497	4100
PDE2A3	0.61	–
PDE3A	>30000	>49000
PDE4D2	14882	24000
PDE5A1	>30000	>49000
PDE6AB	>30000	>49000
PDE7B	>30000	>49000
PDE8A1	>30000	>49000
PDE9A2	>30000	>49000
PDE10A2	>30000	>49000
PDE11A4	>30000	>49000

^a IC₅₀ values were calculated from percent inhibition data (duplicate, *n* = 1). All values are rounded to two significant digits. ^b Selectivity ratio (rounded to two significant digits) = PDE"X" IC₅₀/PDE2A IC₅₀.

第 10 節 化合物 **42a** の薬物動態プロファイル

化合物 **42a** のラットおよびマウス薬物動態試験の結果を Table 2-8 に示す。化合物 **42a** はラットおよびマウスの肝ミクロソームにおいては比較的高いクリアランスを示し、ヒト肝ミクロソームにおいては低いクリアランス値を示した。化合物 **42a** をラットおよびマウスに 0.3 mg/kg の静脈内投与をしたところ、ラットにおいて比較的大きなクリアランスおよび分布容積を示したが、1 mg/kg の経口投与においては、それぞれ 57% および 56% の良好な生物学的利用率と 242.5 ng·h/mL および 1076.8 ng·h/mL の血中濃度-時間曲線下総面積値を示した。さらに、ラットおよびマウスにおける最高血中濃度到達時間付近 (化合物投与後 2 時間) の脳内と血漿中の薬物濃度比 K_p はそれぞれ 1.01 と 0.91 で、高い TPSA を示したにも関わらず、良好な中枢移行性を示した。この結果は、先の P-gp 過剰発現細胞膜を用いた膜透過性試験で P-gp の排出比 (0.87) が低かったことと矛盾のない結果である。

Table 2-8. PK Parameters and K_p Values of **42a** in Rat and Mouse^a

	rat	mouse	human
Metabolic stability ^b ($\mu\text{L}/\text{min}/\text{mg}$)	84	73	33
CL_{total} ^c ($\text{mL}/\text{min}/\text{kg}$)	39.3	8.6	–
$V_{\text{d}_{\text{ss}}}$ ^d (mL/kg)	3429	1602	–
C_{max} ^e (ng/mL)	64.2	201.0	–
T_{max} ^f (h)	1.7	1.7	–
$\text{AUC}_{0-8\text{h}}$ ^g ($\text{ng}\cdot\text{h}/\text{mL}$)	242.5	1076.8	–
F^{h} (%)	56.7	55.6	–
K_p ⁱ	1.01	0.91	–

^a Cassette dosing at 0.1 mg/kg, iv and 1 mg/kg, po (non-fasted). Average of three rats or mice.

^b Metabolic stability was determined by incubation with liver microsomes. ^c Total clearance.

^d Volume of distribution at steady state. ^e Maximum plasma concentration. ^f Time of maximum concentration. ^g Area under the plasma concentration vs time curve (0–8 h). ^h Oral bioavailability.

ⁱ Brain-to-plasma ratio at 2 h after oral administration of **42a** at a dose of 10 mg/kg.

第 11 節 化合物 **42a** と PDE2A の X 線共結晶構造解析

化合物 **42a** と PDE2A との X 線共結晶構造を Figure 2-4 に示す. 本結晶構造解析により, 化合物 **42a** が化合物 **10a** と同様の結合様式で PDE2A の触媒ドメインに結合していることが示された. また 3,4-ジヒドロピリド[2,3-*b*]ピラジン-2(1*H*)-オン環のラクタム NH は予想通り, cGMP 様の結合様式で Gln859 側鎖のカルボニル基と水素結合を形成し, 一方で母核は上下の Phe862 と Phe830/Ile826 と π - π および CH- π の相互作用を介して安定化していることが分かった. また, 母核 7 位のメトキシ基は活性および PDE ファミリー選択性に対して, 以下の 2 つの重要な役割をしていると推察している. 1 つ目は, 電子供与性基として母核の電子密度を高め, Phe862 や Phe830/Ile826 との π - π および CH- π の相互作用を増強していると考えられる. 2 つ目は, 7 位メトキシ基が近傍の Tyr827, Leu858, Met847 で囲まれた小さな脂溶性空間を効果的に充填し活性向上に寄与していると考えられる. また PDE2A ポケットでは, メトキシ基が伸びる方向に脂溶性の Leu858 側鎖が存在するため効果的なファンデアワールス相互作用が形成されるのに対し, PDE1A ポケットでは, Leu858 に対応するアミノ酸残基がより極性の高い Ser416 であるため効果的な相互作用が獲得できず, その結果 PDE1A との選択性が向上したと考えられる. さらに ウレア部位のカルボニル基は, 化合物 **10a** のアミドカルボニル基と同様に, Tyr655 の水酸基と水分子を介した水素結合ネットワークを形成すると同時に, 別の水分子とも水素結合を形成していることが明らかとなった. 一方, ウレアの NH は予想通り母核上の窒素原子と分子内水素結合を形成していることも明らかとなった. また, 分岐メトキシメチル基は紙面下側の溶媒側方向 (Figure 2-4 (B)) を向いているにも関わらず, 予想した水分子や近傍のアミノ酸残基との明確な相互作用は確認できなかった. しかしながら, 興味深いことに, メトキシメチル側鎖の酸素原子はウレア NH と前述の分子内水素結合とは別の新たな分子内水素結合の形成に関与していることが明らかとなった. 化合物 **42a** は上述の 2 つの分子内水素結合を介してコンフォメーションを強固に安定化することによって, PDE2A タンパクと効果的に相互作用していると考えられる.

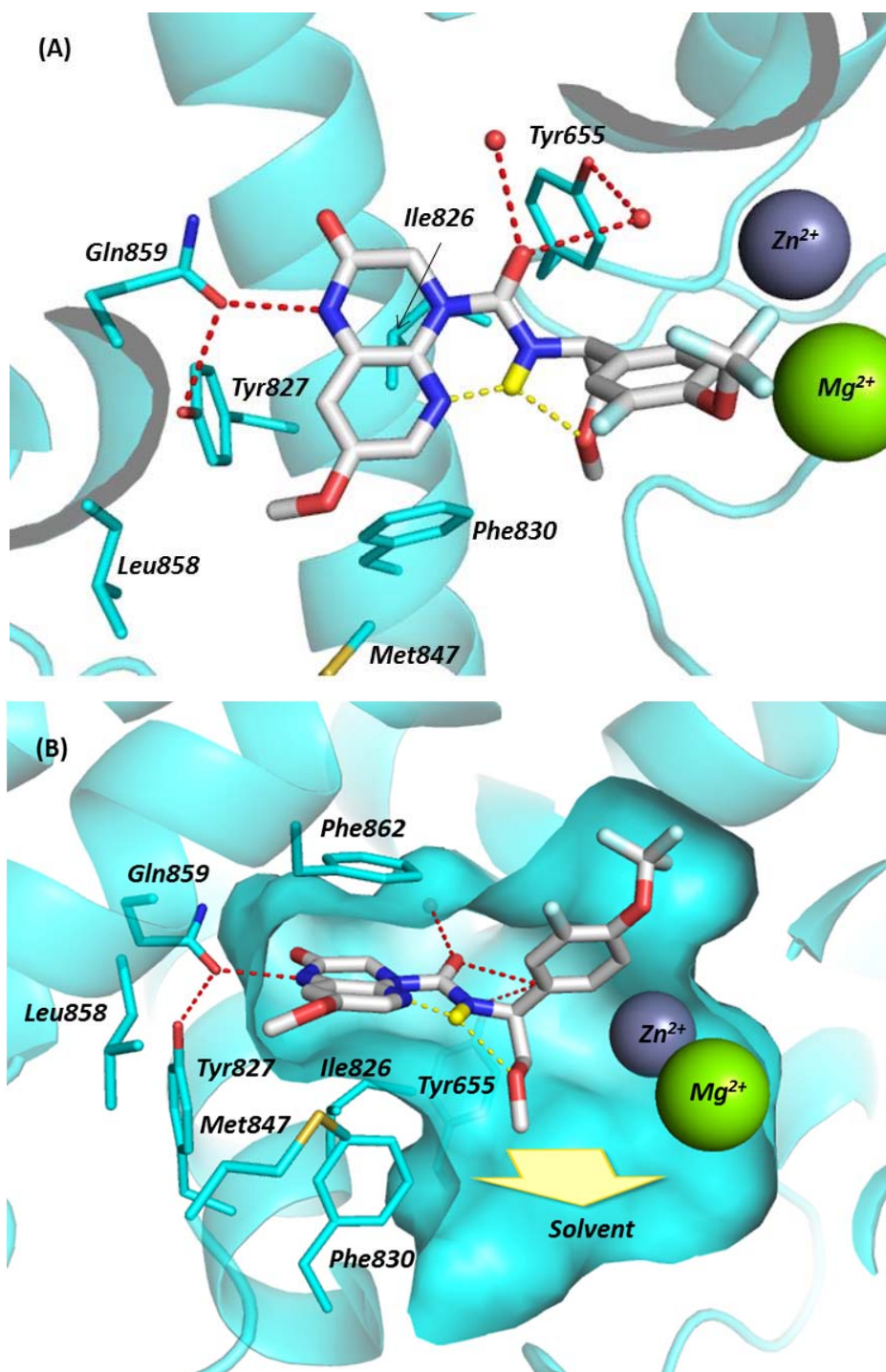


Figure 2-4. X-ray crystal structure of **42a** bound in the PDE2A catalytic site (PDB 5VP0) viewed from the top (A) and the entrance of the catalytic site (B). The key hydrogen bonding interactions of **42a** with PDE2A and the intramolecular hydrogen bond in **42a** are indicated by red and yellow dotted lines, respectively.

第 12 節 化合物 42a の in vivo 薬理評価

化合物 42a の PDE2A 阻害作用による PD マーカーに対する影響を確認するために、化合物 42a をマウスに経口投与し、前頭葉、線条体ならびに海馬の cGMP および cAMP 含量を測定した。その結果、化合物 42a は用量依存的に各脳部位の cGMP 含量を増加させ、特に海馬においては、1 mg/kg の用量から有意な変化を示した (Figure 2-5 (A))。一方 cAMP に関しては、前頭葉において 10 mg/kg の高用量でのみ有意な増加を示したが、その増加量は限定的であった。また、その他の脳部位においては cAMP に対して影響を及ぼさなかった (Figure 2-5 (B))。これらの結果は、化合物 10a ならびに既存の PDE2A 阻害薬を用いた知見とよく一致した^{48,55,69}。さらに、化合物 42a による認知機能亢進作用を検証するために、ラットを用いた新奇物体認知試験を実施した⁸⁹。新奇物体認知試験は獲得試行と保持試行で構成されており、獲得試行において 2 つの同一物体を探索させた後、一定時間経過後の保持試行において、片方の物体を新規な物体に置き換えて動物の探索行動の変化を見る試験である。動物は獲得試行と保持試行の間隔が短いとき、新奇性のある物体により長い探索行動を示し、その嗜好性は時間の間隔を広げていくことにより消失する。このことから、新奇物体認知試験の行動変化は、獲得試行時の物体への記憶を反映していると考えられている。化合物 42a をラットに経口投与し、2 時間後に 3 分間の獲得試行を行い、さらに獲得試行から 48 時間後、3 分間の保持試行を行った。ここでは、獲得試行および保持試行の物体への探索時間、ならびに保持試行の新奇物体選択率 ($NDI = \text{novel object interaction} / \text{total interaction} \times 100$) を算出した。化合物 42a の経口投与は、すべての用量 (0.01, 0.1 ならびに 1 mg/kg) において獲得試行の探索時間に影響を及ぼさなかった (Figure 2-6 (A))。獲得試行から 48 時間後、対照群の新奇物体と既知物体への探索時間が同程度となり、物体への記憶が低下することを確認した (Figure 2-6 (B))。一方、獲得試行前に化合物 42a を投与した薬物群は、0.1 mg/kg の用量から新奇物体への探索時間の有意な増加が認められた。また、1 mg/kg の用量で、新奇物体選択率 (NDI) において有意な変化が認められた (Figure 2-6 (C))。これらのことから、化合物 42a が脳内の cGMP 含量の増加を介し、認知機能の亢進作用を示すことが示唆された。続いて、統合失調症モデル動物を用いた

in vivo 薬効試験を実施した。NMDA (*N*-methyl-D-aspartic acid) 受容体拮抗薬のフェンサイクリジンやケタミンが統合失調症様の症状を惹起することから、NMDA 受容体機能低下が統合失調症の病態に関与している可能性が示唆されている。この仮説に基づき、NMDA 受容体拮抗薬である MK-801 ((*5R,10S*)-(+)-5-methyl-10,11-dihydro-5*H*-dibenzo[*a,d*]cyclohepten-5,10-imine) により惹起された認知機能障害モデル^{90,91}を用いて、化合物 **42a** のラットにおける受動的回避試験を実施した (Figure 2-7)⁹²。この試験は、ラットが暗室に進入した際に電気刺激を与えることにより、暗室への進入と痛みを伴う恐怖を関連付けて記憶させる試験である。正常なラットは、暗室に侵入すると電気刺激により痛みが与えられることを記憶しているため明室に留まる傾向を示す一方で、MK-801 を投与したラットでは認知機能の低下により暗室に進入する傾向が強くなる。実際に MK-801 (0.1 mg/kg) をラットに皮下投与すると、対照群 (control group) に対して認知機能の障害作用が認められた (Figure 2-7, 対照群 vs. 溶媒投与群 (vehicle group))。一方、化合物 **42a** の経口投与 (3 および 10 mg/kg) により、MK-801 により惹起された認知機能障害を有意に改善することが明らかとなった (Figure 2-7 (B), (C))。以上のことから、PDE2A 阻害薬である化合物 **42a** は NMDA 受容体機能低下による記憶障害を改善することが明らかとなった。

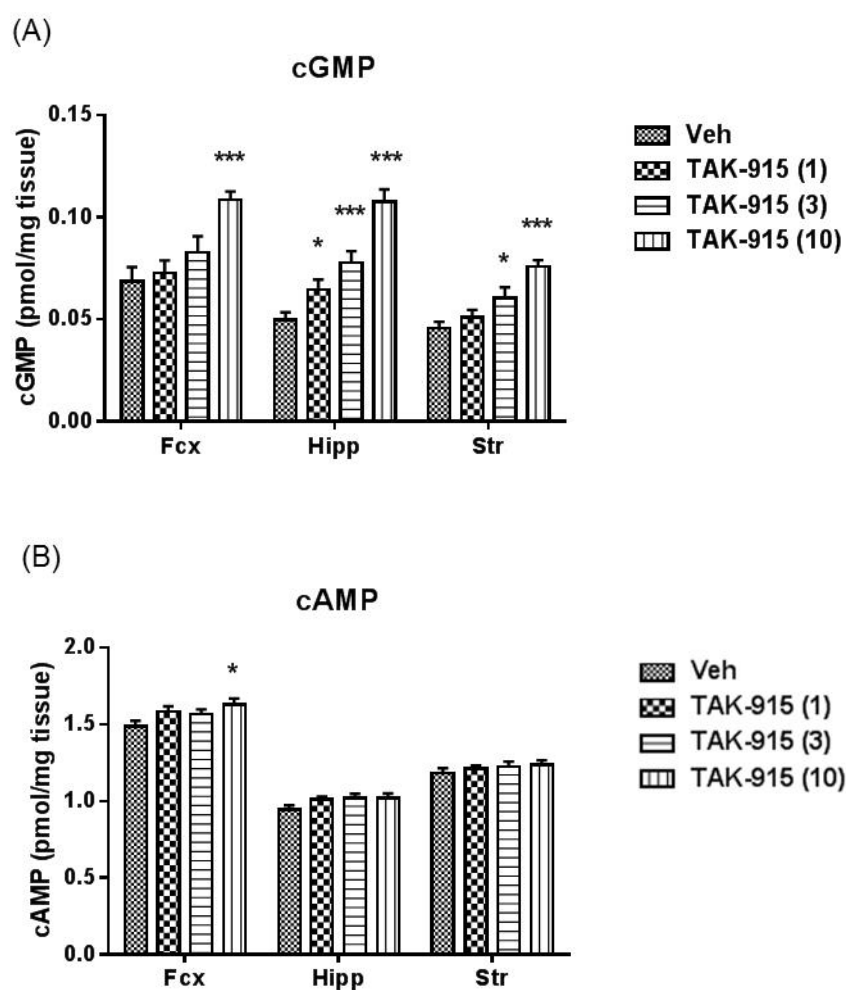


Figure 2-5. Effects of compound **42a** on cyclic nucleotides in mouse brain. cGMP (A) and cAMP (B) levels 1 h after oral administration of compound **42a** (1 mg/kg, 3 mg/kg, and 10 mg/kg) were measured in the mouse frontal cortex (Fcx), hippocampus (Hipp), and striatum (Str). Data are presented as mean \pm SEM ($n = 18$); * $p < 0.05$, *** $p < 0.001$, vs. vehicle by Shirley–Williams’ test.

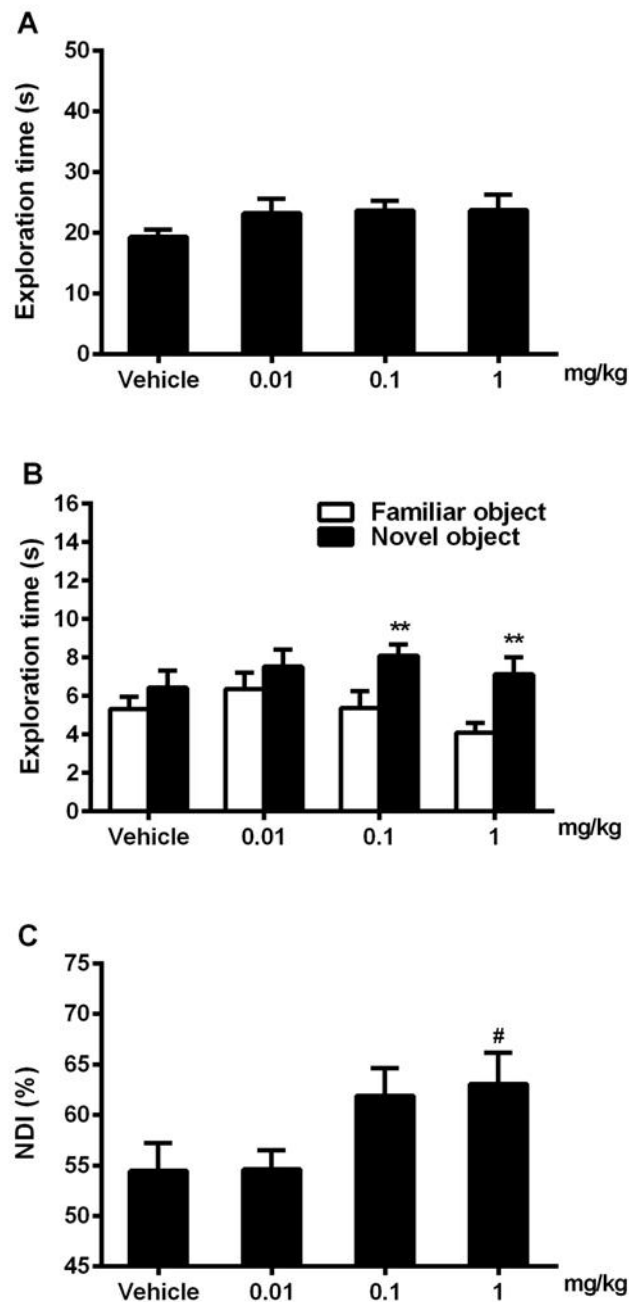


Figure 2-6. Effects of **42a** on a novel object recognition task in rats. Vehicle or **42a** (0.01, 0.1, and 1 mg/kg) was orally administered 2 h prior to the acquisition trials. Exploration times in the acquisition trial (A) and the retention trial (performed 48 h after the acquisition trial) (B) were scored. Novelty discrimination index (NDI) (C) in the retention trial was calculated as: novel object interaction time/total interaction time \times 100 (%). Data are presented as the mean \pm S.E.M., $n = 9$ for 1 mg/kg, $n = 10$ for the other groups; ** $p \leq 0.01$ vs familiar object by paired t-test, # $p \leq 0.025$ vs vehicle by one-tailed Williams' test.

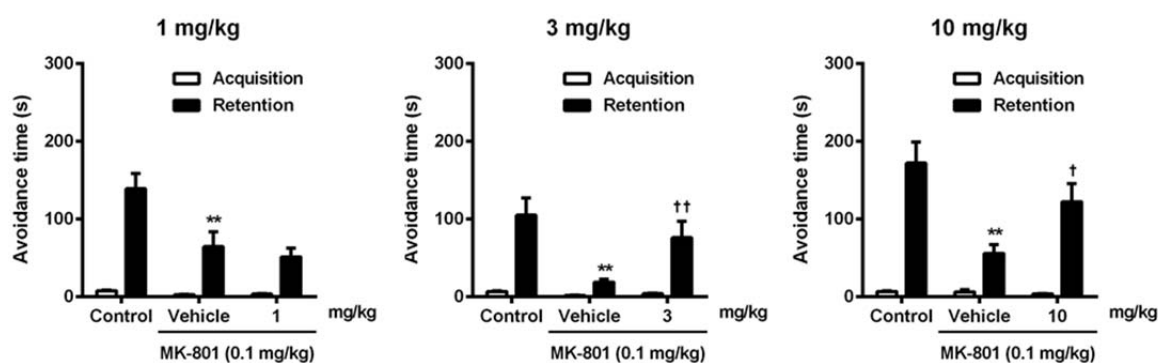


Figure 2-7. Effects of compound **42a** on MK-801-induced episodic memory deficits assessed by the passive avoidance task in rats. Vehicle or compound **42a** (1, 3, and 10 mg/kg) was orally administered 2 h before the s.c. administration of saline or MK-801. Thirty minutes after the s.c. administration of saline or MK-801 (0.1 mg/kg), the rat was placed on the illuminated chamber. The latency to cross over into the dark chamber was recorded for up to a maximum of 300 s. The retention test was carried out 24 h after the acquisition trial. Data (latency to cross over into the dark compartment on the retention trial) are expressed as mean \pm S.E.M., $n = 20$, ** $p \leq 0.01$ (versus control by Wilcoxon's test), $^{\#}p \leq 0.01$ (versus vehicle + MK-801 by Wilcoxon's test).

第 13 節 化合物 **42a** の既存抗精神病薬で見られる副作用に対する評価⁹²

序論で論じたように既存の抗精神病薬で認められる重大かつ代表的な副作用として、ドパミン D2 受容体遮断作用による錐体外路症状や高プロラクチン血症、セロトニン 2A 受容体やヒスタミン H1 受容体遮断作用による体重増加や耐糖能異常が知られている^{15,16,18,19}。そこで、化合物 **42a** のこれら副作用に対する影響をラットを用いて検証した。錐体外路症状を評価する指標として、不自然な姿勢を長時間持続する症状として知られているカタレプシー (catalepsy) 反応を測定した (Figure 2-8)。また、高プロラクチン血症および体重増加に繋がる摂食亢進の指標として、それぞれ血漿中のプロラクチン濃度 (Figure 2-9 (A)) およびグルコース濃度 (Figure 2-9 (B)) を測定した。その結果、非定型抗精神病薬であるオランザピンが 10 mg/kg の用量でカタレプシー反応を示したのに対して、化合物 **42a** は 100 mg/kg の用量においても全くカタレプシー反応の傾向を示さなかった。さらに、本化合物は同じ 100 mg/kg の用量で血漿中プロラクチン濃度およびグルコース濃度に対しても全く影響を及ぼさないことが明らかとなった。以上のことから、化合物 **42a** は既存の抗精神病薬で認められ

る副作用に悪影響を及ぼさない認知機能改善作用を有する新規な統合失調症治療薬になる可能性が示唆される。

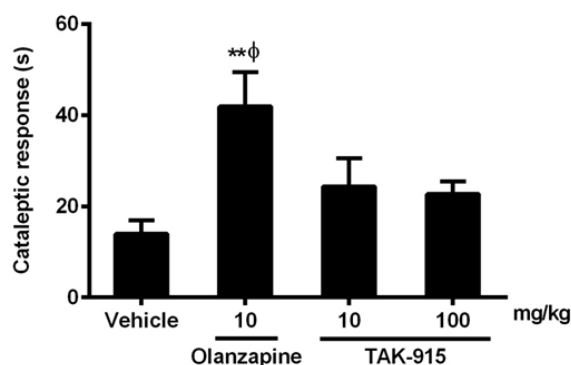


Figure 2-8. Effects of **42a** on cataleptic response in rats. Duration of cataleptic response was measured using the bar test 2 h after the administration of **42a** (10 or 100 mg/kg, po) and olanzapine (10 mg/kg, po). Data are expressed as mean + S.E.M., $n = 8$ for each group, $**p \leq 0.01$ (versus vehicle by Student's t -test). †Occurrence of animals in a cataleptic position for more than 90 s.

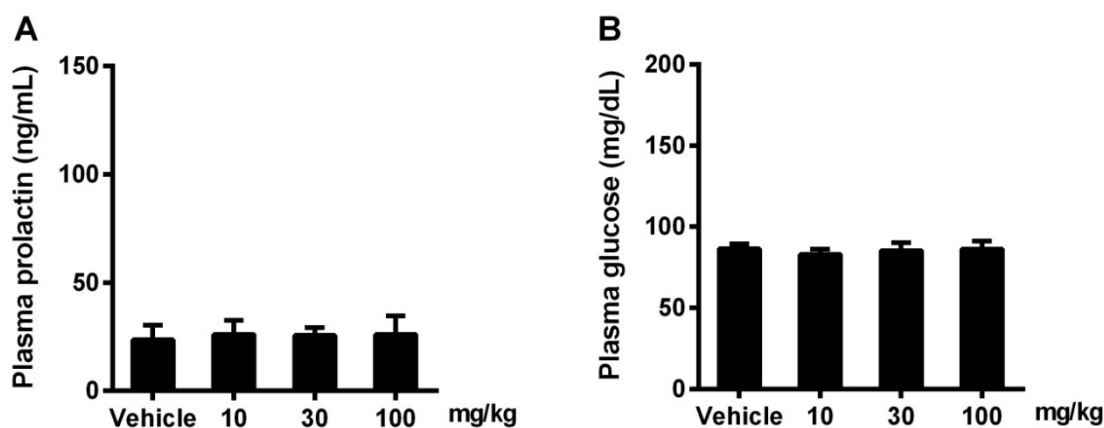
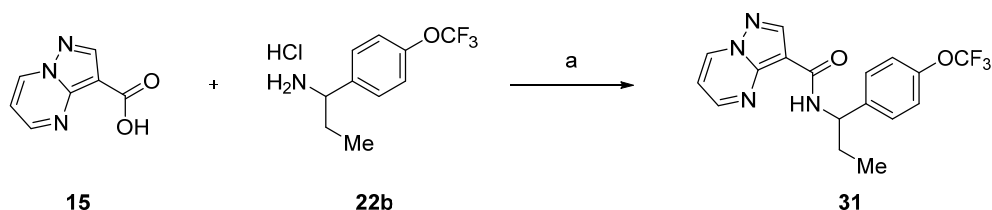


Figure 2-9. Effects of **42a** on plasma prolactin and glucose levels in rats. Blood samples were collected from the tail vein 2 h after the administration of **42a** (10, 30, or 100 mg/kg, po). (A) The plasma prolactin concentration was determined by enzyme immunoassay kits. (B) The plasma glucose concentration was determined by colorimetric detection using a chemical analyzer. Data are expressed as mean + S.E.M., $n = 5$ per each group.

第 14 節 化合物の合成

ピラゾロ[1,5-*a*]ピリミジン誘導体 **31** は市販の **15** とベンジルアミン **22b** の縮合反応により合成した (Scheme 2-1).

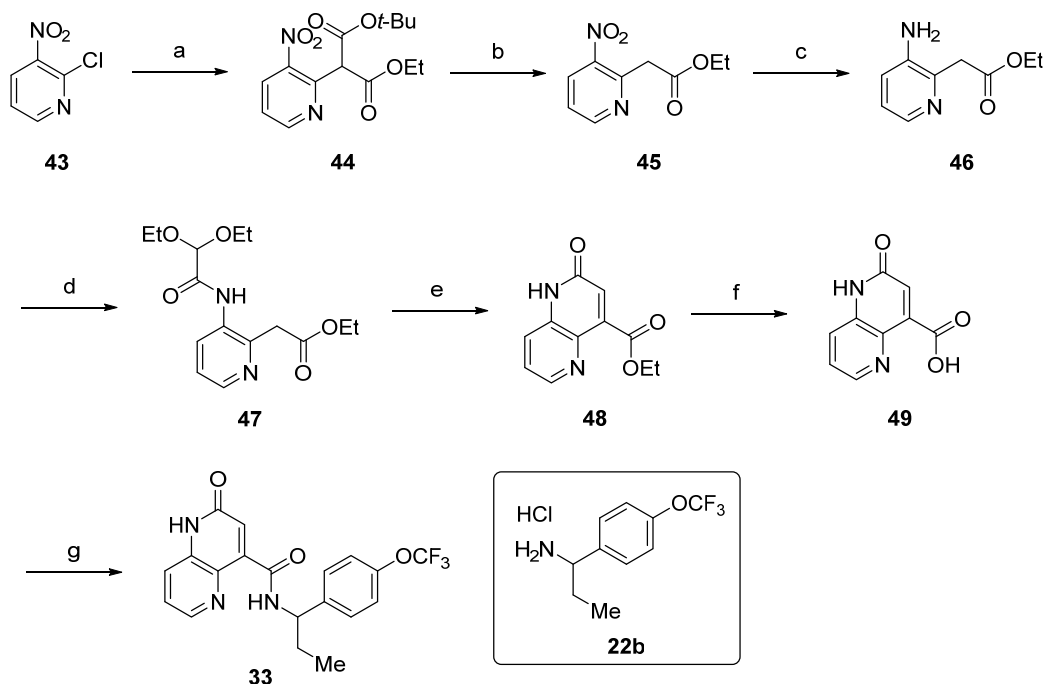
Scheme 2-1. Synthesis of Pyrazolo[1,5-*a*]pyrimidine Derivative **31**^a



^a Reagents and conditions: (a) EDCI·HCl, HOBT·H₂O, Et₃N, DMF, rt, overnight, 83%.

1,5-ナフチリジン-2(1*H*)-オン誘導体 **33** は Scheme 2-2 記載の方法で合成した. 2-クロロ-3-ニトロピリジン (**43**) に塩基性条件下, 非対称マロン酸ジエステルを求核剤として作用させてジエステル付加体 **44** とした後, TFA 条件下, *tert*-ブチルエステルの加水分解と脱炭酸を行ってエチルエステル **45** を合成した. 続いて, ニトロ基の還元と 2,2-ジエトキシ酢酸との縮合反応によって, アセタール **47** を 4 工程 53% の収率で合成した. 得られた **48** のアセタール部位を酸性条件下, ホルミル基へ変換した後, ピペリジン共存下, トルエン中加熱還流することで, 環化およびその後の脱水反応が一挙に進行し, 所望の 1,5-ナフチリジン-2(1*H*)-オン環化体 **48** を得ることができた. 最後に, **48** のアルカリ加水分解, 続く右骨格のベンジルアミン **22b** との縮合反応により標的化合物 **33** を合成した.

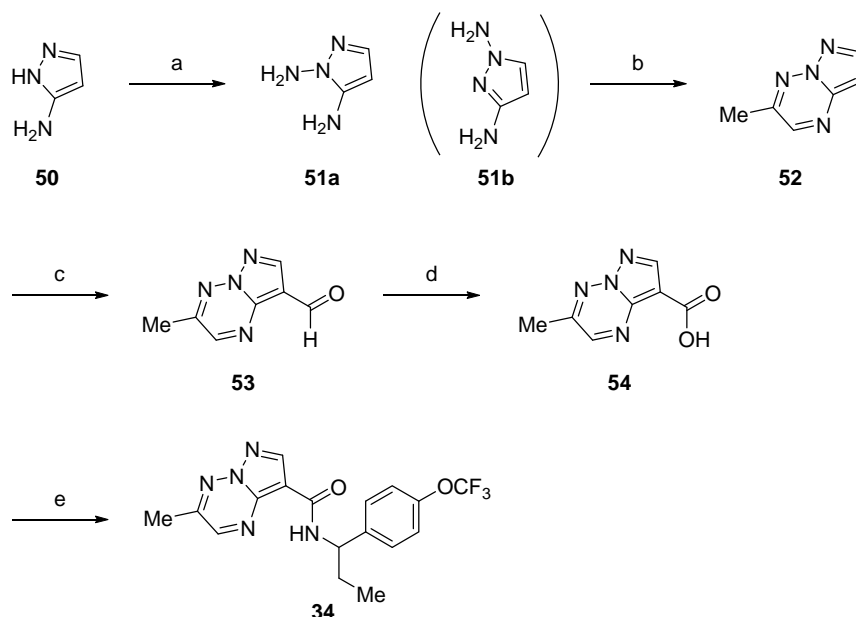
Scheme 2-2. Synthesis of 1,5-Naphthyridin-2(1*H*)-one Derivative **33**^a



^a Reagents and conditions: (a) *tert*-butyl ethyl malonate, *KOtert*-Bu, THF, 60 °C to reflux, 3 h, (taken on crude); (b) TFA, CH₂Cl₂, rt, overnight, (taken on crude); (c) H₂, 10% Pd/C, EtOH, 50 psi, rt, overnight, (taken on crude); (d) 2,2-diethoxylacetic acid, HATU, DIEA, DMF, rt, overnight, 53% (4 steps from **43**); (e) TFA, H₂O, cat. I₂, 50 °C, overnight, then piperidine, toluene, reflux, 6 h, 26%; (f) 2 M NaOH aq., EtOH, rt, 2 h, 87%; (g) **22b**, HATU, DIEA, DMF, rt, 2.5 h, 46%.

ピラゾロ[1,5-*b*][1,2,4]トリアジン **34** は Scheme 2-3 記載の方法に従って合成した。3-アミノピラゾール (**50**) に対してヒドロキシアミン-*O*-スルホン酸 (HOSA) を作用させることで位置異性体 **51b** を含む *N*-アミノ化体 **51a** を得た。位置異性体混合物はシリカゲルカラム精製により分離し、その後 NOE 実験によりそれぞれの構造を決定した。次に、**51a** を酸性条件下、1,3-ジカルボニル等価体である 2-オキソ-プロピオンアルデヒドとの縮合反応に付すことによって 3-メチルピラゾロ[1,5-*b*][1,2,4]トリアジン (**52**) を得た。続いて、Vilsmeier 試薬⁷³ による **52** の位置選択的なホルミル化、続く Pinnick 酸化⁹³ によりカルボン酸 **54** へ導き、最後にベンジルアミン **22b** とのアミド化反応によって標的化合物 **34** を合成した。

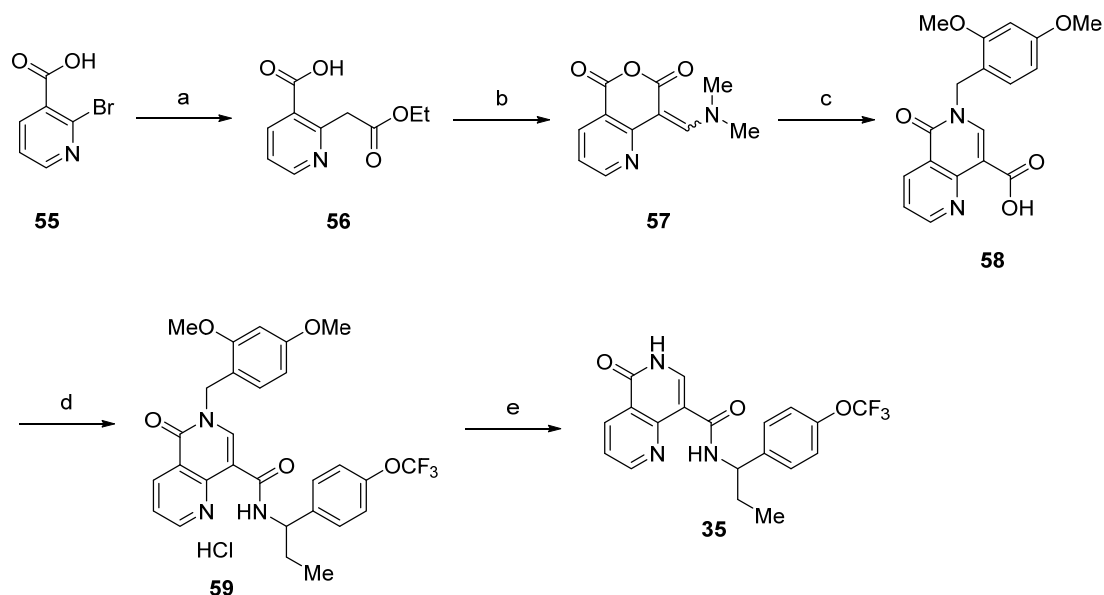
Scheme 2-3. Synthesis of 3-Methylpyrazolo[1,5-*b*][1,2,4]triazine Derivative **34**^a



^a Reagents and conditions: (a) HOSA, KOH, DMF, 0 °C to 15 °C, 2 h, 17%; (b) 2-oxo-propionaldehyde, concd HCl, H₂O, 60 °C to reflux, 1 h, 37%; (c) POCl₃, DMF, 0 °C to 40 °C, 16 h, 28%; (d) NaClO₂, NaH₂PO₄, 2-methyl-2-butene, *tert*-BuOH, H₂O, 30 °C, 16 h, (taken on crude); (e) **22b**, EDCI, HOBt, Et₃N, DMF, 10–15 °C, 16 h, 3% (2 steps from **53**).

1,6-ナフチリジン-5(6*H*)-オン誘導体 **35** の合成は Scheme 2-4 記載の方法で合成した. 2-ブロモピリジン-3-カルボン酸 (**55**) に対する銅 (II) 触媒を用いたアセト酢酸エチルの付加と脱アセチル化によって **56** に導き, 続いて Vilsmeier 試薬⁷⁴ を作用させることで環化体 **57** を合成した. 得られた **57** に 2,4-ジメトキシベンジルアミンを反応させることでカルボン酸無水物への求核置換反応と続く環の再構築反応が進行し, 1,6-ナフチリジン-5(6*H*)-オン誘導体 **58** を得た. 次にベンジルアミン **22b** との縮合と TFA 条件下, 2,4-ジメトキシベンジル基の脱保護を行い標的化合物 **35** を合成した.

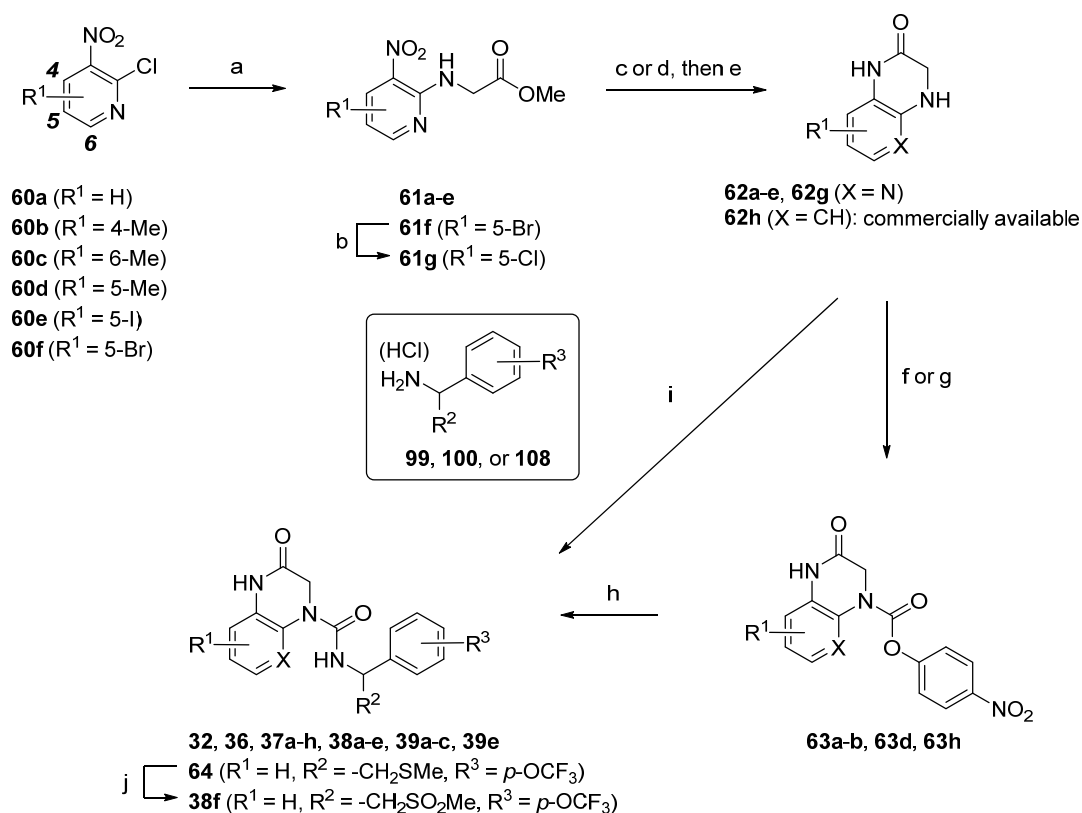
Scheme 2-4. Synthesis of 1,6-Naphthyridin-5(6*H*)-one Derivative **35**^a



^a Reagents and conditions: (a) ethyl acetoacetate, Na, EtOH, Cu(OAc)₂, reflux, 16 h, 54%; (b) POCl₃, DMF, 0 °C to 5 °C, 2 h, (taken on crude); (c) 2,4-dimethoxybenzylamine, Et₃N, DMF, 5 °C, 16 h, 26% (2 steps from **56**); (d) amine **22b**, EDCI, HOBT, Et₃N, DMF, 5 °C to 40 °C, 32 h; (e) TFA, reflux, 16 h, 12% in 2 steps from **58**.

3,4-ジヒドロピリド[2,3-*b*]ピラジン-2(1*H*)-オン誘導体 **32**, **36**, **37a-h**, **38a-e**, **39a-c**, **39e** の合成を Scheme 2-5 に示す。2-クロロ-3-ニトロピリジン誘導体 **60a-f** にトリエチルアミン共存下、メチルグリシンを求核剤として作用させることで 2 位置換アミノピリジン **61a-f** を得た。また、5-ブロモピリジン **61f** はマイクロウェーブ照射下、塩化銅 (I) を作用させることによって対応するクロロ体 **61g** へ導いた。得られたニトロ体 **61a-e**, **g** をパラジウムあるいは白金を用いた水素添加により還元し、続いてエタノール中加熱することで 3,4-ジヒドロピリド[2,3-*b*]ピラジン-2(1*H*)-オン環 **62a-e** および **62g** を構築した。標的化合物 **32**, **36**, **37a-h**, **38a-e**, **39a-c**, **39e** は 3,4-ジヒドロピリド[2,3-*b*]ピラジン-2(1*H*)-オン環 **62** をクロロギ酸 4-ニトロフェニル、あるいはトリホスゲンと反応させた後、トリエチルアミン共存下、ベンジルアミン **22a**, **22b**, **99**, **100**, **108** を作用させて合成した。また、スルホン誘導体 **38f** はスルフィド **64** を *m*-クロロペルオキシ安息香酸 (*m*-CPBA) で酸化して合成した。

Scheme 2-5. Synthesis of 3,4-Dihydropyrido[2,3-*b*]pyrazin-2(1*H*)-one Derivatives **32**, **36**, **37a-h**, **38a-e**, **39a-c**, and **39e**^a

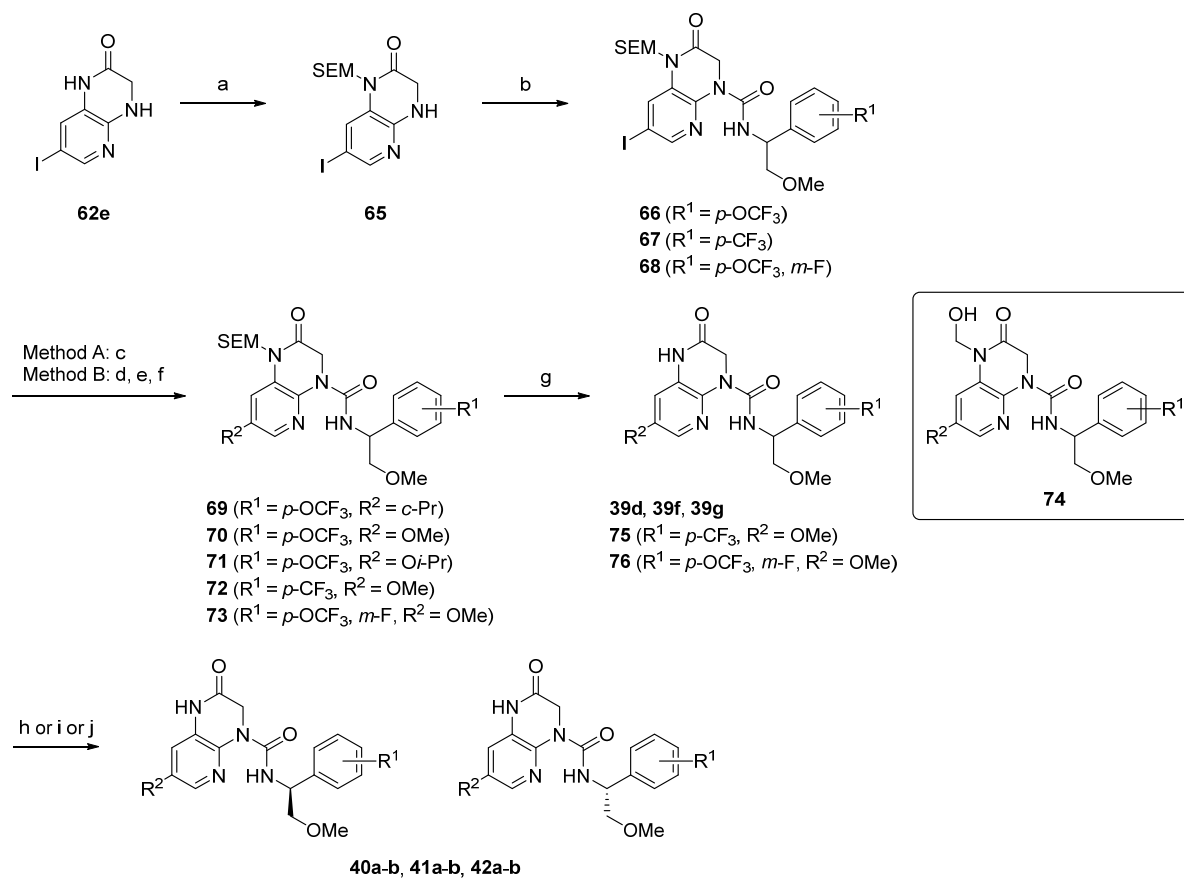


^a Reagents and conditions: (a) methyl glycinate hydrochloride, Et₃N, DMF or EtOH, rt–90 °C, 3–16 h, 31%–quant.; (b) CuCl, NMP, 150 °C (microwave), 2.5 h, 64%; (c) H₂ (balloon pressure), 10% Pd/C, EtOH, rt, 16 h or overnight, (taken on crude) (for **62a-d**); (d) H₂ (balloon pressure), 5% Pt/C, THF, rt, 2–16 h, (taken on crude) (for **62e** and **62g**); (e) EtOH, reflux, 5–16 h, 58–99%; (f) 4-nitrophenyl chloroformate, pyridine, DMA, rt–80 °C, 16–24 h, 70–81% (for **63a**, **63d**, and **63h**); (g) 4-nitrophenyl chloroformate, DIEA, THF, 0 °C to rt, 1 h, 51% (for **63b**); (h) RHS benzylamine **22b**, **99**, **100**, or **108**, Et₃N, DMF, rt–80 °C, 1–16 h, 23–96%; (i) triphosgene, THF, 40 °C, 1–5 h, then RHS benzylamine **22a**, **99**, or **100**, Et₃N, THF, rt–60 °C, 16 h–overnight, 3–95%; (j) *m*-CPBA, EtOAc, rt, overnight, 66%.

3,4-ジヒドロピリド[2,3-*b*]ピラジン-2(1*H*)-オン環 7 位の置換基 R² の変換を行うにあたり、Scheme 2-5 の合成法では置換基導入を合成初期段階で行わなければならない、種々の 7 位置換誘導体を効率的に合成するには適さないと考えた。そこで著者らは、誘導体合成の後期段階で置換基導入が可能な効率的な新規合成法の開発を目指して検討を行った (Scheme 2-6)。ラクタム **62e** のプロトン性ドナーを (2-(トリスメチルシリル)エトキシ)メチル (SEM)

基で保護した後、トリホスゲンを用いて SEM 保護体 **65** とベンジルアミン **99**, あるいは **100** の縮合反応によってウレア体 **66-68** に導いた。母核 7 位置換基の変換 (誘導体 **69-73**) は以下の 2 通りの方法で行った。すなわち, 7 位シクロプロピル誘導体 **69** はヨウ素体 **66** と対応するボロン酸との鈴木-宮浦クロスカップリング反応により良好な収率で合成した。一方, 7 位アルコキシ誘導体 **70-73** は, ヨウ素体 **66** とピナコールジボランを用いた宮浦-石山ホウ素化反応⁹⁴により対応するボロン酸エステル体とした後, 炭素-ホウ素結合の酸化的開裂によるヒドロキシ基への変換, 続くフェノール性水酸基のアルキル化により目的の 7 位アルコキシ体を合成した。得られた **69-73** に TFA と水の混合物を作用させて SEM 基の脱保護を試みたが, 全ての誘導体において, 所望の脱保護体と共に脱保護の過程で生成するヒドロキシメチル中間体 **74** が残存することが判明した。ヘミアミナール **74** の分解を促進するため, TFA を留去した後, アンモニア/メタノール溶液を作用させることで脱保護体 **39d, f, g, 75, 76** を良好な収率で得ることができた。光学活性体 **40a-b, 41a-b, 42a-b** は, ラセミ体 **39f, 75, 76** の光学分割によって取得した。

Scheme 2-6. Synthesis of 3,4-Dihydropyrido[2,3-*b*]pyrazin-2(1*H*)-one Derivatives **39d**, **39f–g**, **40a–b**, **41a–b**, and **42a–b**^a

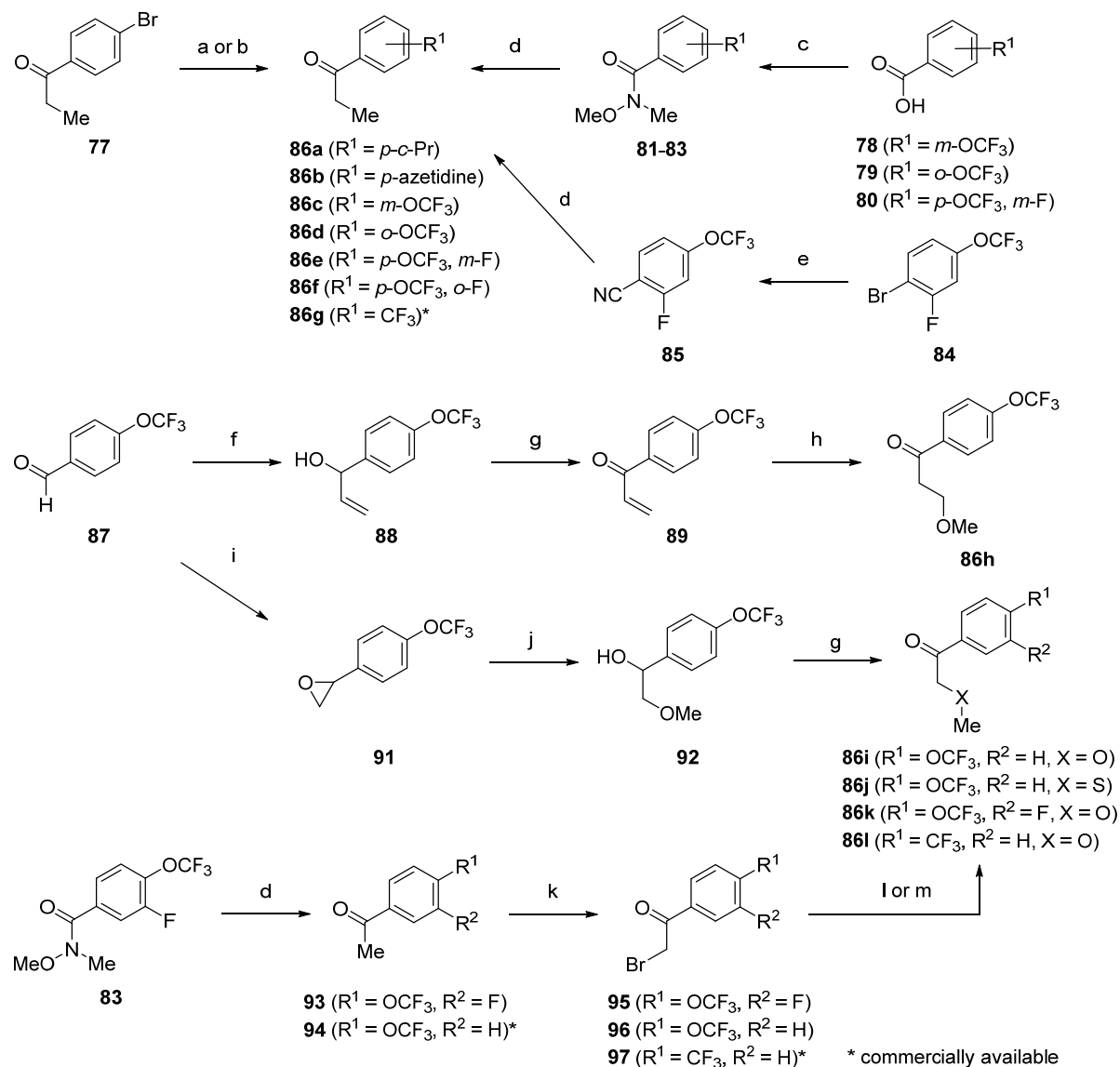


^a Reagents and conditions: (a) KHMDS, DMF, DMSO, 0 °C, 20 min, then SEMCl, rt, 3 h, 38%; (b) triphosgene, THF, 40 °C, 1–5 h, then RHS benzylamines **99** or **100**, Et₃N, THF, rt–60 °C, 16 h–overnight, 64–95%; (c) cyclopropylboronic acid, Pd(OAc)₂, Cy₃P, K₃PO₄, toluene, 100 °C, overnight, 73%; (d) B₂pin₂, PdCl₂(dppf), KOAc, DMF, 80 °C, overnight, (taken on crude); (e) 2 M NaOH aq., THF, 0 °C, 30 min, then 35–36% H₂O₂ aq., rt, 1.5–2 h, 80–97% (2 steps from **66–68**); (f) R²I, K₂CO₃, DMF, rt–70 °C, overnight, 60–82%; (g) TFA, H₂O, rt, 1–3.5 h, then NH₃, MeOH, rt, 10 min–2 h, 67–93%; (h) Chiralpak IA, CO₂/MeOH = 43:7 (for **40a** and **40b**); (i) Chiralpak AD, hexane/EtOH = 3:2 (for **41a** and **41b**); (j) Chiralpak AD, hexane/EtOH = 43:7 (for **42a** and **42b**).

右骨格の α -分岐ベンジルアミン合成に必要な共通中間体 **86** は Scheme 2-7 記載の方法で合成した。ケトン **86a** あるいは **86b** はそれぞれブロモベンゼン **77** とシクロプロピルボロン酸を用いた鈴木–宮浦クロスカップリング反応^{72,73}、あるいはアゼチジンとの Buchwald アミノ化反応⁹⁵ により合成した。ケトン **86c–e** は対応する安息香酸 **78–80** を出

発原料に用い、Weinreb アミドへの変換と続くエチルグリニャール試薬との反応によって合成した。またケトン **86f** はブロモベンゼン **84** とパラジウム触媒を用いたシアン化亜鉛とのカップリング反応によりシアノ体 **85** とした後、エチルグリニャール試薬と反応させて合成した。一方、ケトン **86h** は、アルデヒド **87** へのビニルグリニャール試薬の求核付加反応で得られた二級アルコール **88** を Dess–Martin 試薬⁷⁵ で酸化した後、パラジウム触媒を用いたメタノールの α,β -不飽和ケトン **89** への付加反応⁹⁶ によって合成した。**86i** はアルデヒド **90** を Corey–Chaykovsky 反応⁹⁷ によりエポキシ体 **91** へ変換した後、ナトリウムメトキシドによるエポキシの開環および得られた二級アルコールの Dess–Martin 酸化⁷⁵ により合成した。また **86j-1** は、**83** のメチルグリニャール試薬との反応によって合成したアセトフェノン **93** あるいは市販の **94** のカルボニル基 α 位の臭素化、続く炭酸銀(I) およびフッ化ホウ素を用いたメタノールの求核置換⁹⁸、あるいはナトリウムチオメトキシドによる求核置換反応によって合成した。

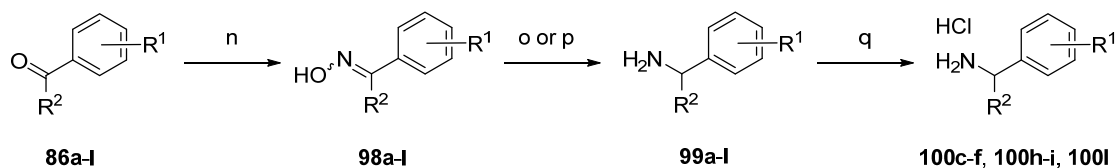
Scheme 2-7. Synthesis of Common Ketone Intermediates **86** for RHS Benzylamine Moieties^a



^a Reagents and conditions: (a) cyclopropylboronic acid, $\text{PdCl}_2(\text{dppf})$, K_3PO_4 , DME, H_2O , 85°C , 20 h, 78% (for **86a**); (b) azetidine, $\text{Pd}_2(\text{dba})_3$, Xantphos, $\text{NaO}t\text{-Bu}$, toluene, 85°C , 20 h, 73% (for **86b**); (c) *N,O*-dimethylhydroxylamine hydrochloride, EDCI or EDCI·HCl, HOBt or HOBt· H_2O , Et_3N , DMF, 0°C –rt, 16 h, 86–96%; (d) EtMgBr , Et_2O , THF, 0°C to rt, 16 h–3 days, 69–96%; (e) ZnCN_2 , $\text{Pd}_2(\text{dba})_3$, dppf, DMF, 100°C , overnight, 43%; (f) vinylmagnesium bromide, THF, 0°C , 2 h, 60%; (g) 1,1,1-triacetoxy-1,1-dihydro-1,2-benziodoxol-3(1*H*)-one (Dess–Martin periodinane), CH_3CN , 0°C or rt, 1–1.5 h, 67–97%; (h) $\text{PdCl}_2(\text{CH}_3\text{CN})_2$, MeOH, CH_2Cl_2 , 0°C to rt, 50%; (i) $(\text{CH}_3)_3\text{SOI}$, NaH, DMSO, THF, rt, 1 h, 45%; (j) NaOMe, DMF, 60°C , 2 h, 65%; (k) Br_2 , AcOH, 50°C , 1 or 3 h, 82%; (l) MeOH, Ag_2CO_3 , $\text{BF}_3\cdot\text{OEt}_2$, $50\text{--}60^\circ\text{C}$, 2.5 h–overnight, 80–90%; (m) NaSMe, THF, 0°C to rt, 2 h, 86%.

Scheme 2-7 で得られた **86** は ヒドロキシアミンとのオキシム形成反応, 続いて金属触媒を用いた接触還元を付すことによってベンジルアミン **99** へ導いた. アミン **99** は塩酸塩とすることで結晶化させて **100c-f, 100h-i, 100l** とした (Scheme 2-8).

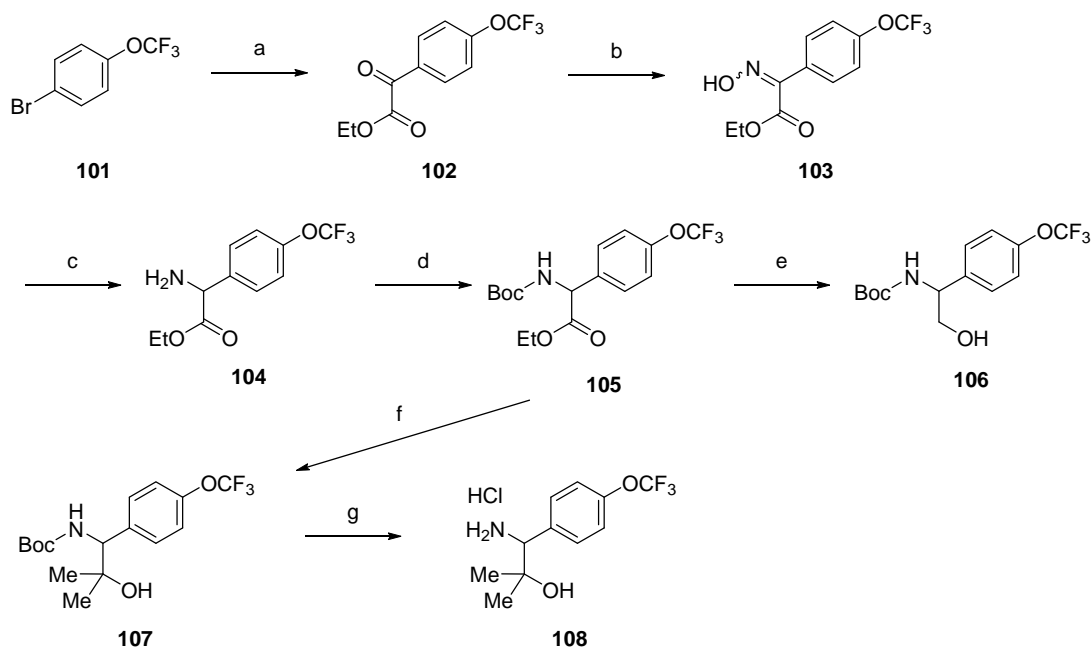
Scheme 2-8. Synthesis of RHS Benzylamine Moieties **99** and **100** from Ketones **86**^a



^a Reagents and conditions: (n) hydroxylammonium chloride, Et₃N, EtOH, rt–80 °C, 3–72 h, (taken on crude); (o) H₂, 10% Pd/C or Raney Ni or 20% Pd(OH)₂/C, EtOH or MeOH, rt, 4 h–overnight, (taken on crude); (p) BH₃·THF, reflux, 20 h or overnight, (taken on crude); (q) HCl, EtOAc, rt.

アルコール分岐側鎖を有するベンジルアミン **108** は Scheme 2-9 記載の方法に従って合成した. ブロモベンゼン **101** に対して *n*-ブチルリチウムを作用させてハロゲン–リチウム交換を行った後, 求電子補足剤として 2-クロロ-2-オキシ酢酸エチルを作用させることで α -ケトエステル **102** を得た. 次に, 定法に従い, オキシムへの変換, 続くパラジウム/炭素を用いた接触還元によりベンジルアミン **104** を合成した. さらにアミノ基を Boc で保護 (**105**) した後, エステルを水素化アルミニウムリチウムで還元して一級アルコール **106** を合成した. また, **105** はメチルグリニャール試薬を反応させることで三級アルコール **107** へ導き, 最後に塩酸/酢酸エチル溶液にて脱 Boc 化することで塩酸塩 **108** を得た.

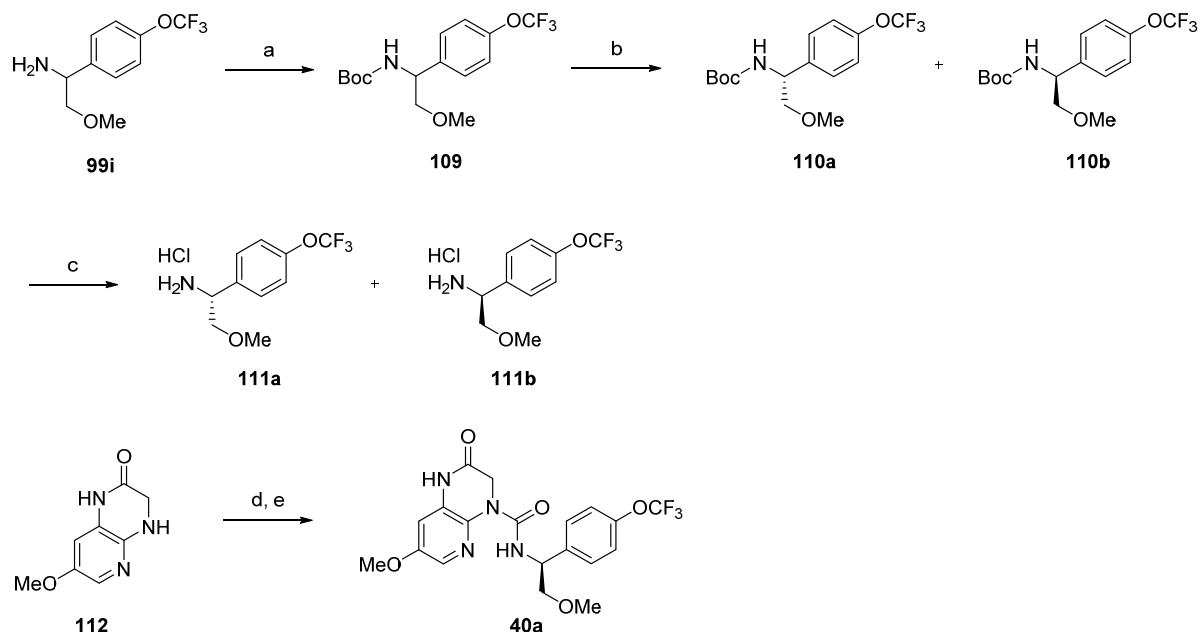
Scheme 2-9. Synthesis of RHS Benzylamine Moiety **108**^a



^a Reagents and conditions: (a) *n*-BuLi, THF, $-78\text{ }^{\circ}\text{C}$, 50 min, then ethyl 2-chloro-2-oxoacetate, $-78\text{ }^{\circ}\text{C}$ to rt, overnight, 23%; (b) hydroxylammonium chloride, Et_3N , EtOH, $80\text{ }^{\circ}\text{C}$, overnight, 27%; (c) H_2 , 10% Pd/C, EtOH, rt, overnight, 86%; (d) Boc_2O , THF, rt, 2 days, (taken on crude); (e) LAH, THF, $0\text{ }^{\circ}\text{C}$, 30 min, 62%; (f) MeMgBr , THF, $0\text{ }^{\circ}\text{C}$, 2 h, 41%; (g) HCl, EtOAc, rt, 84%.

化合物 **40a** の別ルートによる合成法を Scheme 2-10 に示す. Scheme 2-8 で合成したベンジルアミン **99i** のアミノ基を Boc 基 で保護し, 得られた **109** を Chiralpak IC カラムを用いて光学分割することにより, 光学活性体 **110a** および **110b** を得た. これらに, 塩酸/酢酸エチル溶液を加えて脱 Boc 化することでベンジルアミン **111a** および **111b** をそれぞれ塩酸塩の固体として得た. なお, **111b** のベンジル位の絶対立体配置は, **111a** の単結晶 X 線構造解析結果に基づいて *S* 体と決定した. また, 標的化合物 **40a** は 3,4-ジヒドロピリド [2,3-*b*]ピラジン-2(1*H*)-オン環 **112** とベンジルアミン **111b** のクロロギ酸 4-ニトロフェニルを用いたウレア化反応により合成した.

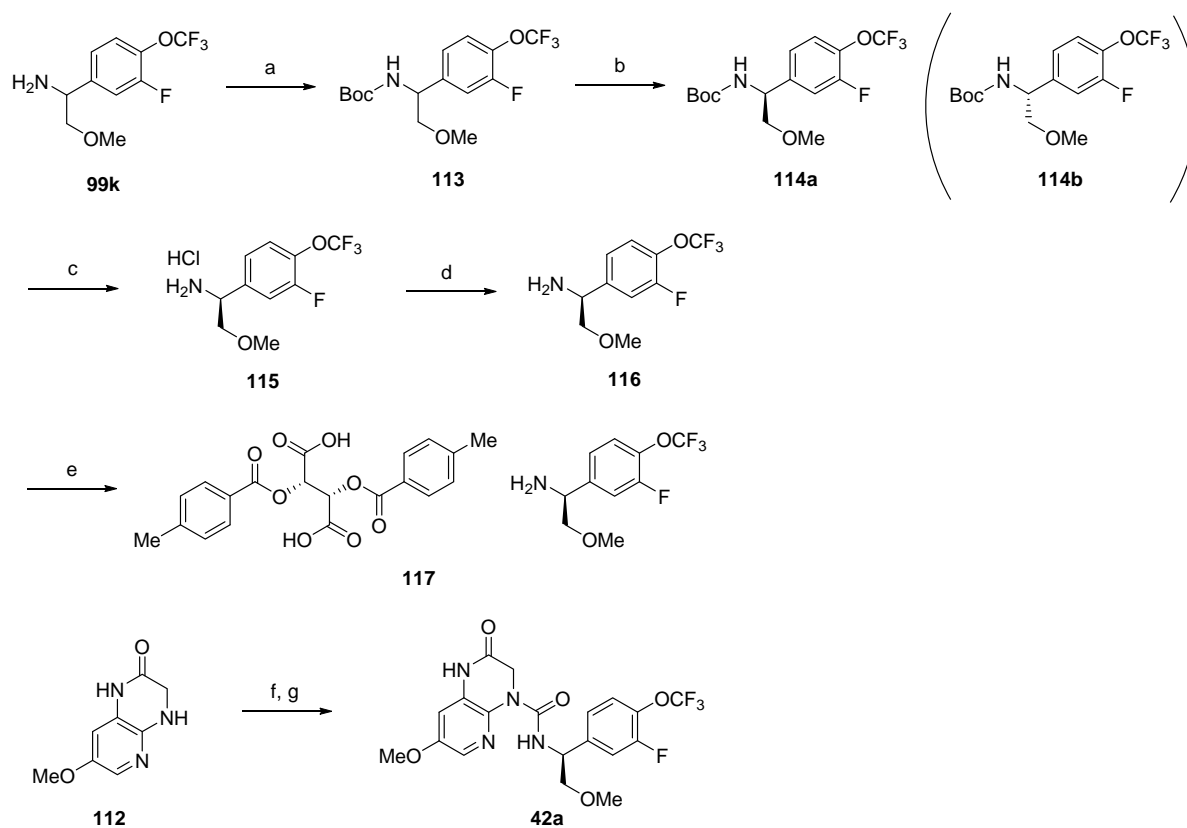
Scheme 2-10. Alternative Synthetic Route for **40a**^a



^a Reagents and conditions: (a) Boc_2O , Et_3N , THF, rt, 20 h, 82%; (b) Chiralpak IC, hexane/EtOH, = 93:7; (c) HCl, EtOAc, rt, 1 h, 96%; (d) 4-nitrophenyl chloroformate, DIEA, THF, rt, 24 h, (taken on crude); (e) amine **111b**, Et_3N , DMF, rt, 24 h, 52% (2 steps from **112**).

化合物 **42a** の別ルートによる合成法を Scheme 2-11 に示す. Scheme 2-8 で合成した分岐ベンジルアミン **99k** のアミノ基を Boc で保護し, 得られた **113** を Chiralpak AD カラムを用いて光学分割することにより, 光学活性体 **114a** および **114b** を得た. 続いて, **114a** に塩酸/酢酸エチル溶液を加えて脱 Boc 化することでベンジルアミン **115** を塩酸塩の固体として得た. ベンジルアミンの絶対立体配置を決定する上で良質な単結晶を取得するべく, 塩酸塩 **115** を一旦脱塩 (**116**) し, 新たに (+)-ジ-(*p*-トルオイル)-D-酒石酸塩 **117** を調製した. 本結晶の X 線構造解析により, ベンジル位の絶対立体配置は *S* 体と決定した. また, 標的化合物 **42a** は 3,4-ジヒドロピリド[2,3-*b*]ピラジン-2(1*H*)-オン **112** とベンジルアミン **117** のクロロギ酸 4-ニトロフェニルを用いたウレア化反応により合成した.

Scheme 2-11. Alternative Synthetic Route for **42a** and Synthesis of (+)-Di-(*p*-toluoyl)-D-tartaric Acid Salt **117** Suitable for X-ray Crystallography^a



^a Reagents and conditions: (a) Boc₂O, Et₃N, THF, rt, 16 h, 79%; (b) Chiralpak AD, hexane/EtOH, = 19:1; (c) HCl, EtOAc, rt, 3 h, 95%; (d) NaHCO₃, H₂O, quant.; (e) (2*S*,3*S*)-(+)-di-(*p*-toluoyl)-D-tartaric acid, EtOH, H₂O, 50 °C, overnight; (f) 4-nitrophenyl chloroformate, DIEA, THF, rt, 3 h, 88%; (g) amine **115**, DIEA, DMF, rt, 16 h, 63%.

第 15 節 結語

リード化合物 **10a** の PDE2A 阻害活性と PDE ファミリー選択性のさらなる向上を目指して、**10a** と PDE2A の X 線共結晶構造解析情報を基に、以下の 4 つの薬物設計戦略を考案した。

戦略 1 Gln859 と明確な水素結合の形成

戦略 2 PDE2A に特徴的な脂溶性空間を占有する *p*-トリフルオロメトキシフェニル基の置換基最適化

戦略 3 近傍の水分子や極性アミノ酸残基との相互作用を指向したエチル基側鎖の最適化

戦略 4 母核への置換基導入と最適化

また、良好な中枢移行性化合物を得るために、脳移行性を予測する上で重要な 2 つの物理化学的パラメータ ($TPSA < 110 \text{ \AA}^2$, $HBD < 3$) の目標値を分子内水素結合を考慮して設定し、化合物設計の指標とした。上述の戦略に基づいた構造最適化検討を行うことで、 $IC_{50} = 0.61 \text{ nM}$ の強力な PDE2A 阻害活性と PDE1A 阻害と比較して 4100 倍以上の優れた PDE2 選択性および良好な中枢移行性を併せ持つ新規 3,4-ジヒドロピリド[2,3-*b*]ピラジン-2(1*H*)-オン誘導体 **42a** を見出すことに成功した。化合物 **42a** はマウスの脳内 cGMP 含量を用量依存的に増加させ、ラットを用いた新奇物体認知試験およびマウスを用いた受動的回避試験において有意な認知機能の亢進および改善作用を示した。一方、既存の抗精神病薬で認められる副作用に関する評価試験において、化合物 **42a** は良好な安全性プロファイルを有することが明らかとなった。また、各種動物を用いた安全性試験の結果、危惧すべき毒性所見が認められず十分な毒性マージンが確保されたことから、化合物 **42a** (開発コード: TAK-915) を臨床試験の候補化合物として選出した。

第 3 章 既存ケモタイプに特徴的な部分構造のハイブリッド化による新規 TAK-915 バックアップ化合物の創製

第 1 節 研究背景および新規リード化合物の創出

これまでに著者らは、第 1 章にて HTS によりピラゾロ[1,5-*a*]ピリミジン環を母核とするヒット化合物 **2** を端緒化合物として新規 PDE2A 阻害剤の探索研究を行い、母核への置換基導入、 α -エチルベンジルアミン部位の変換および光学分割を行い、PDE2A 阻害活性および PDE ファミリー選択性の向上したリード化合物 **10a** を見出した (Figure 3-1). さらに第 2 章にて、リード化合物 **10a** の X 線共結晶構造解析の情報を基に構造最適化検討を実施した結果、非常に強力な PDE2A 阻害活性と 4100 倍以上の優れた PDE ファミリー選択性を示す臨床候補化合物 **42a** (TAK-915) を見出した (Figure 3-1). **42a** は経口投与によって脳内 cGMP 含量を用量依存的かつ有意に増加させ、また種々の統合失調症動物モデルにおいて有効性を示した. 本化合物はその後、統合失調症治療薬として臨床入りを果たすに至ったが、化合物探索段階においては **42a** の安全性への影響も不明瞭であったことから、不測の事態に備えてバックアップ化合物の準備が必要と考えられた.

42a の発見に至る過程において、著者らは、化合物 **118** に代表されるように、**42a** とは構造の異なる α -分岐ベンジルアミン骨格を見出していた (Figure 3-2). 化合物 **118** は **42a** と同様のエーテル側鎖を有する **38a** と比べて、同等の PDE2A 阻害活性および PDE ファミリー選択性を有していたものの、P-gp による排出が強く (排出比 = 2.8)、これら一連の誘導体は中枢移行性の面で課題があった. **42a** と **118** は、両化合物共にほぼ同じ TPSA (102 \AA^2 vs. 104 \AA^2) を有しているにも関わらず、前者は P-gp 基質の懸念がなく良好な中枢移行性が確認されている. 前章の第 3 節で論じたように、HBD の数は P-gp 基質プロファイルおよび中枢移行性に大きな影響を与える重要な因子であることが報告されており^{61,62}, **42a** と **118** の P-gp 基質プロファイルの違いは HBD 数の違い (**42a**: 2 HBDs vs. **118**: 3 HBDs) に起因していることが示唆された. 一方で、第 1 章の研究過程で見出されたピラゾロ[1,5-*a*]ピリミジ

ン誘導体 **31** は、この時点において母核およびベンジルアミン部位が最適化されていないため PDE2A 阻害活性は不十分であったものの、理想的な TPSA (69 \AA^2) および HBD 数 (一つ) を反映して良好な P-gp プロファイル (排出比 = 0.43) と中枢移行性を示した。これらの結果を基に、著者らは、**118** の母核である 3,4-ジヒドロピリド[2,3-*b*]ピラジン-2(1*H*)-オン環を HBD 数の 1 つ少ないピラゾロ[1,5-*a*]ピリミジン環に変換し、分子全体の HBD 数を前章で設定した 2 つまで低減したハイブリッド化合物 **119** を設計し、P-gp 基質の懸念のない新規リード化合物の取得を目指した。その結果、ハイブリッド化合物 **119** は、 $IC_{50} = 66 \text{ nM}$ の良好な PDE2A 阻害活性と 150 倍以上の PDE ファミリー選択性を示し、かつ期待通り P-gp 基質性が低いことが明らかとなった。以上の検討結果を基に、著者らは、**119** を新規リード化合物として位置付け、置換基変換を中心とした構造最適化研究を開始した。

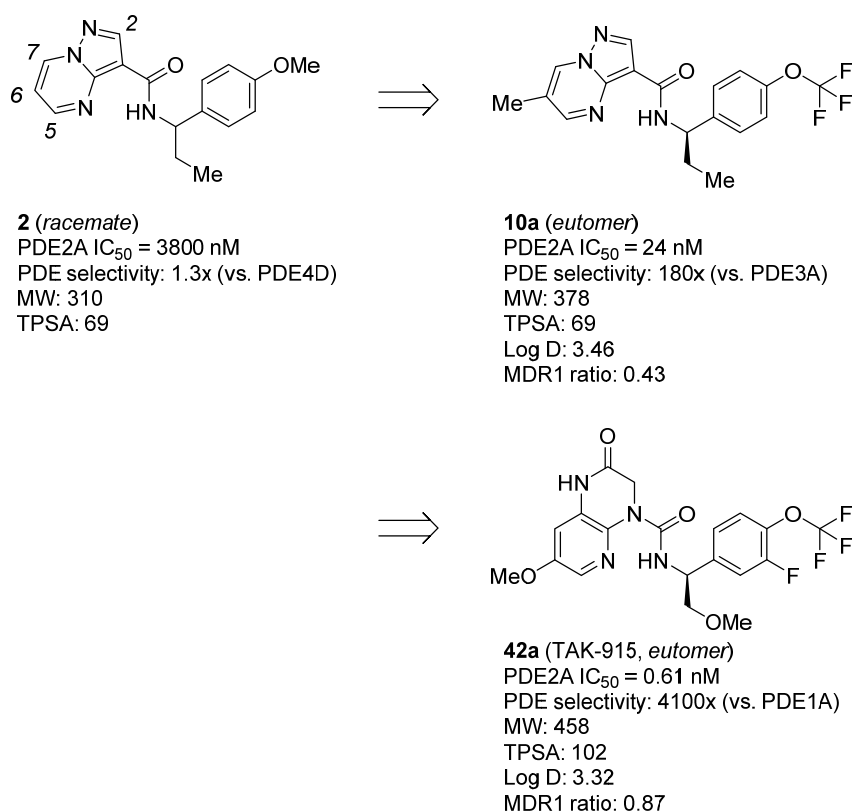


Figure 3-1. Transition from high-throughput screening hit **2** to clinical candidate **42a**.

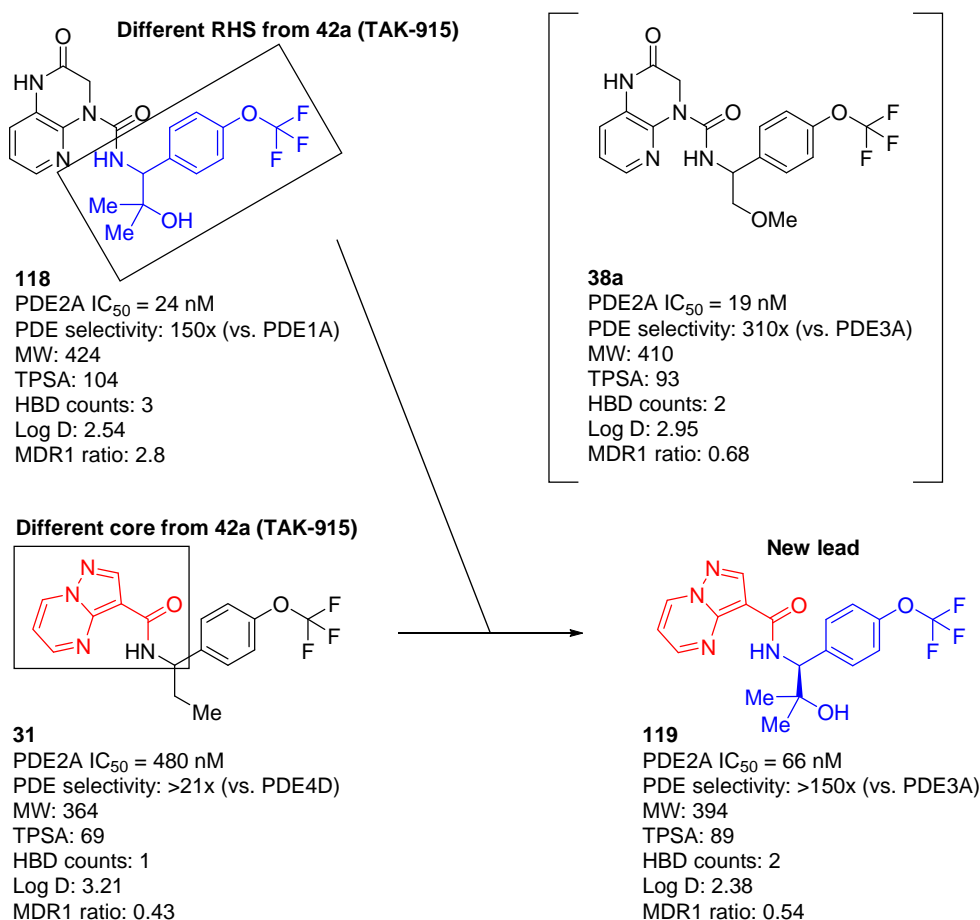


Figure 3-2. Origin of a novel PDE2A lead compound **119**.

第 2 節 薬物設計戦略

第 1 章の第 3 節 (Table 1-1) で論じたように、化合物 **2** のピラゾロ[1,5-*a*]ピリミジン環上へのメチル基導入の検討において、6 位メチル置換体は無置換体と比べて活性が約 10 倍向上した。一方、5 位メチル置換体は活性が保持したのに対し、2 位あるいは 7 位メチル置換体は活性が減弱する傾向を示した。これらの知見を基に、化合物 **119** のピラゾロ[1,5-*a*]ピリミジン環 6 位にメチル基を導入 (**120**) したところ、期待した通り、約 13 倍の活性向上が認められた (Figure 3-3)。化合物 **10a** と PDE2A との複合体 X 線結晶構造解析の結果から、母核 5 位置換基の方向には溶媒領域に至るまでの比較的大きな空間の存在が明らかとなっており (Figure 3-4)、5 位置換基として種々の置換基が許容される可能性が示唆されて

いる。また、この知見は前述の Table 1-1 で 5 位メチル基が許容された結果とよく一致した。以上の考察を踏まえ、リード化合物 **119** のさらなる活性の向上を指向して、5 位置換基の最適化 (Figure 3-5 の R¹)、ならびに 6 位メチル基の導入 (Figure 3-5 の R²) を検討することとした。この際、誘導体合成の効率を優先し、まずは 5 位置換基の最適化検討を実施し、その後、6 位メチル基との組み合わせ検討を行うこととした。

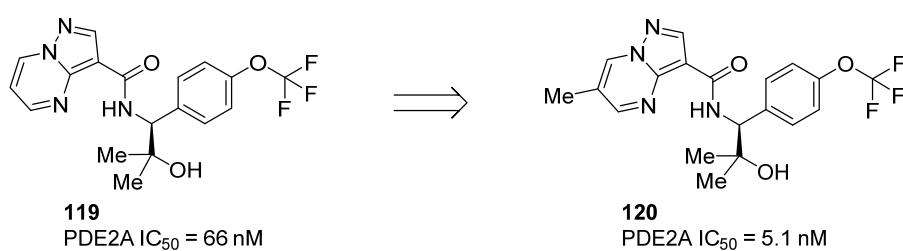


Figure 3-3. Effect of a 6-methyl substitution on PDE2A inhibitory activity.

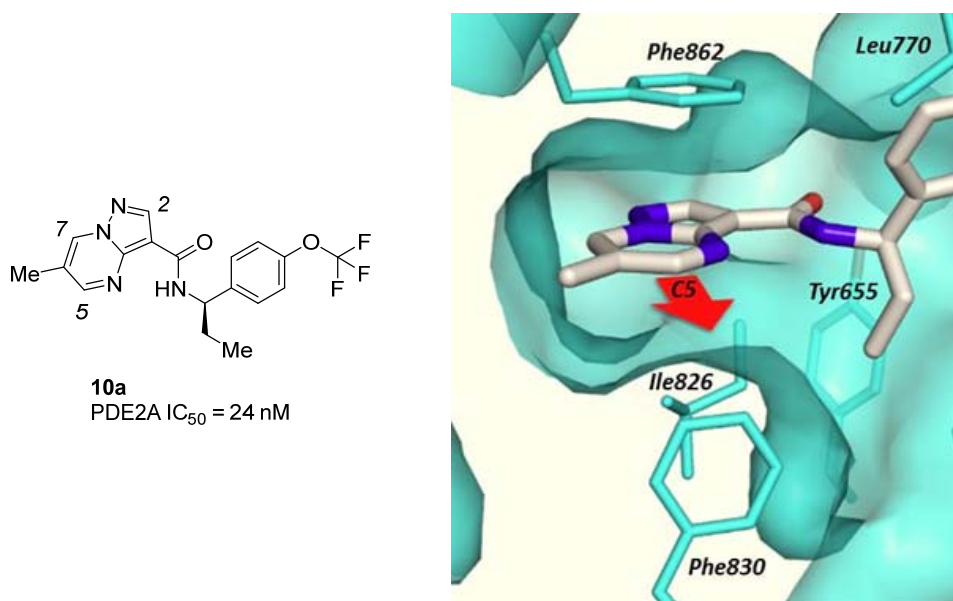


Figure 3-4. X-ray crystal structure of **10a** bound in the PDE2A catalytic site (PDB 5XKM).

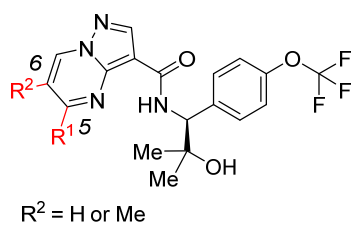


Figure 3-5. Drug design strategies to further increase potency and PDE selectivity.

第 3 節 ピラゾロ[1,5-*a*]ピリミジン環 5 位への置換基導入と構造活性相関

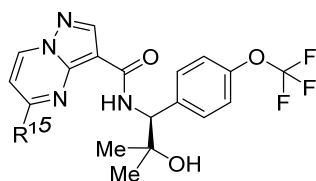
ピラゾロ[1,5-*a*]ピリミジン環 5 位に炭素結合型置換基^{注 11)}を導入した結果を Table 3-1 に示す。また、対照化合物として化合物 **119** のプロファイルも Table 3-1 上段に掲載した。ピラゾロ[1,5-*a*]ピリミジン環 5 位置換基の許容性を検証するために、メチル基よりも嵩高い脂肪族置換基の導入を検討した。その結果、イソプロピル誘導体 **121a** は、無置換体 **119** と比べて活性に大きな変化は認められなかったのに対して、さらに嵩高く、脂溶性の低減したテトラヒドロ-2*H*-ピラニル誘導体 **121b** は **119** と比べて活性がおおよそ 6 倍増強する傾向が認められた。しかしながら、**121b** は P-gp 基質の傾向が強く、さらに高い *in vivo* クリアランスを示すことが明らかとなった。化合物 **121b** で見られた脂肪族ヘテロ環の問題点を克服するべく、次に芳香族ヘテロ環の導入を検討した。その結果、2-ピリジル基 (**121c**) の導入によって、PDE2A 阻害活性および PDE ファミリー選択性のみならず、P-gp 基質プロファイルおよび *in vivo* クリアランスも大幅に改善することが分かった。さらに、3- および 4-ピリジン誘導体 **121d** および **121e** は、2-ピリジン誘導体 **121c** と同様に、活性・選択性および P-gp 基質性の点で好ましいプロファイルを保持したが、*in vivo* クリアランスは悪化の傾向を示した。クリアランスの悪化は、ピリジン環上のメチル基、あるいはピリジン塩基性窒素の酸化代謝に起因するものと考えられた。そこで、メチルピリジン誘導体の代謝安定性の改善を指向して、メチル基の代謝をフッ素原子の導入により抑制し、同時に窒素原子の塩基性を低減したピラゾール環へ変換したジフルオロメチルピラゾール誘導体 **121f** を設計し、合成したところ、予想通り *in vivo* クリアランスが大幅に改善し、活性・選択性および P-gp 基質性も 2-ピリジル誘導体 **121c** と同等の良好なプロファイルを保持することが分かった。しかしながら、一連の炭素結合型芳香族ヘテロ環誘導体 **121c-f** は、全ての化合物において非常に強

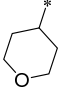
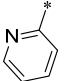
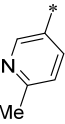
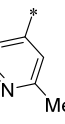
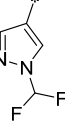
注 11) 導入する置換基として、ピラゾロ[1,5-*a*]ピリミジン環 5 位炭素原子に直接炭素原子、あるいは窒素原子が結合する置換基を、それぞれ「炭素結合型置換基」、 「窒素結合型置換基」と称する。

い *in vitro* 光毒性ポテンシャル^{注 12)} を示すことが明らかとなった。光毒性は、薬剤性光線過敏症の一つであり、体内に化合物が投与された後、光照射（紫外線や可視光）が加わることで丘疹、紅斑、水泡、蕁麻疹などの症状を引き起こす毒性所見である。光毒性を有する化合物は、日焼け止めクリームやサングラス、全身を覆う衣類を着用するなど、日光への露出を避けなければならない。臨床での使用が制限される可能性があるため、前臨床研究において光毒性ポテンシャルのない化合物の探索が求められる^{99,100}。そこで著者らは、化合物 **121c-f** で認められた *in vitro* 光毒性ポテンシャルの軽減を目指した。上述の検討において、ピラゾール誘導体 **121f** は *in vitro* 光毒性を除く他のプロファイルで良好であったことから、引き続き芳香族ヘテロ 5 員環、特に窒素結合型置換基の導入を検討することとした。その結果、窒素結合型ピラゾール誘導体 **121g** は **121f** と比べて、活性および選択性が 2-3 倍低下したものの、P-gp 基質性および *in vivo* クリアランスは良好な値を示した。さらに特筆すべき点として、化合物 **121g** の光毒性ポテンシャルが大幅に改善することが明らかとなった。詳細は不明であるが、5 位置換基の結合様式によって、*in vitro* 光毒性の原因骨格と考えられる 5 位置換基を含むピラゾロ[1,5-*a*]ピリミジン環の電子状態に変化が生じ、その結果、*in vitro* 光毒性ポテンシャルの軽減に繋がったのではないかと推察している。続いて、ピラゾール類縁体としてメチルイミダゾール誘導体 **121h** を合成したところ、本化合物は強力な活性と良好な PDE ファミリー選択性および *in vitro* 光毒性ポテンシャルを示した反面、強い P-gp 基質であることが明らかとなった。イミダゾール環の強い塩基性その原因と考えられたことから、以下の 2 通りの方法にて塩基性低減の可能性を検討した。一つ目のアプローチとして、イミダゾール環上に電子求引基であるトリフルオロメチル基の導入を試みた (**121i**)。二つ目のアプローチとして、イミダゾール環にさらにもう一つの窒素原子を導入することにより塩基性の非局在化を図った (**121j**, **121k**)。その結果、**121i-k** のいずれの化合物も良好な *in vitro*

注 12) 光照射下および非照射下での化合物に暴露した細胞生存率の相対的な減少により *in vitro* 光毒性ポテンシャルを評価する。

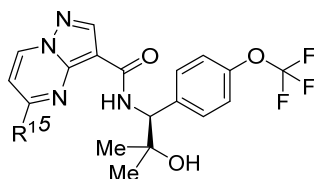
光毒性プロファイルおよび *in vivo* クリアランスを示し、さらに P-gp 基質性も大幅に改善することが明らかとなったが、PDE2A 阻害活性および PDE ファミリー選択性は大きく減弱する傾向を示した。

Table 3-1. Profiles of Pyrazolo[1,5-*a*]pyrimidine Derivatives with Substitutions at the 5-Position

compd	R ¹	PDE2A IC ₅₀ (nM) ^a	PDE selectivity ^b	MDR1 ^c	rat in vivo CL (mL/h/kg) ^d	phototox (%) ^e	Log <i>D</i> ^f
119	H	66 (41–110)	>150-fold	0.54	632	–0.1	2.38
121a	<i>i</i> -Pr	34 (24–49)	190-fold	0.48	NT ^g	–9.2	3.30
121b		10 (5.2–19)	NT ^g	3.6	4142	–6.6	2.82
121c		1.2 (0.80–1.8)	2700-fold	0.52	381	102.1	3.48
121d		0.98 (0.61–1.6)	3800-fold	0.80	2361	78.9	3.38
121e		0.77 (0.44–1.4)	1400-fold	0.80	4350	108.7	3.22
121f		1.7 (1.2–2.5)	1300-fold	1.2	558	102.1	3.14

^a IC₅₀ values (95% confidence intervals given in parentheses) were calculated from percent inhibition data (duplicate, *n* = 1). All values are rounded off to two significant digits. ^b Minimum selectivity (rounded off to two significant digits) over other PDEs. ^c MDR1 efflux ratios in P-gp overexpressing cells. ^d Plasma clearance calculated following 0.1 mg/kg, iv cassette dosing in rats (non-fasted). ^e Values (%) represent the difference between viability of cells exposed to 50 μM of the test compound in the absence of UV irradiation and that in the presence of UV irradiation, where cell viability was measured by intracellular ATP content (%) at 50 μM relative to vehicle control. A larger value is interpreted as a higher risk of phototoxicity. ^f Log *D* values at pH 7.4. ^g Not tested. ^h Precipitates observed.

Table 3-1 (continued). Profiles of Pyrazolo[1,5-*a*]pyrimidine Derivatives with Substitutions at the 5-Position

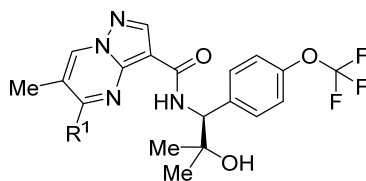


compd	R ¹	PDE2A IC ₅₀ (nM) ^a	PDE selectivity ^b	MDR1 ^c	rat in vivo CL (mL/h/kg) ^d	phototox (%) ^e	Log <i>D</i> ^f
119	H	66 (41–110)	>150-fold	0.54	632	–0.1	2.38
121g		5.4 (3.4–8.7)	630-fold	0.54	353	11.0	3.29
121h		1.2 (0.94–1.6)	1900-fold	5.2	NT ^g	–1.0	3.08
121i		7.1 (4.6–11)	230-fold	2.1	637	11.8	3.42
121j		5.4 (3.5–8.3)	690-fold	0.73	476	7.5 ^h	3.12
121k		11 (8.8–14)	610-fold	0.90	779	3.8	3.15

^a IC₅₀ values (95% confidence intervals given in parentheses) were calculated from percent inhibition data (duplicate, *n* = 1). All values are rounded off to two significant digits. ^b Minimum selectivity (rounded off to two significant digits) over other PDEs. ^c MDR1 efflux ratios in P-gp overexpressing cells. ^d Plasma clearance calculated following 0.1 mg/kg, iv cassette dosing in rats (non-fasted). ^e Values (%) represent the difference between viability of cells exposed to 50 μM of the test compound in the absence of UV irradiation and that in the presence of UV irradiation, where cell viability was measured by intracellular ATP content (%) at 50 μM relative to vehicle control. A larger value is interpreted as a higher risk of phototoxicity. ^f Log *D* values at pH 7.4. ^g Not tested. ^h Precipitates observed.

第 4 節 ピラゾロ[1,5-*a*]ピリミジン環 5,6 位への置換基導入と構造活性相関

前節において見出した化合物 **121j** および **121k** は P-gp 基質性, in vivo クリアランス, および in vitro 光毒性ポテンシャルのいずれも良好なプロファイルを有していたものの, 活性および選択性に改善の余地が残されていた. 第 1 章の第 2 節で論じたピラゾロ[1,5-*a*]ピリミジン環上への置換基の構造活性相関から, 6 位メチル体は PDE2A 阻害活性および PDE ファミリー選択性を大きく改善することが明らかとなっており, この知見を **121j** および **121k** の両化合物に適応することとした. その結果, **122a** および **122b** は共に 100 pM オーダーの非常に強い PDE2A 阻害活性と 5000 倍を超える PDE ファミリー選択性 (Table 3-2, 詳細は Table 3-3 参照) を示し, その他のプロファイルも 6 位メチル基の導入によって悪化の傾向は認められなかった. 化合物 **122a** は in vitro 光毒性ポテンシャルを評価した 50 μ M の濃度において析出物が観察されており, それゆえ, 過小評価の可能性は否めないが, 少なくとも析出物が認められていない 25 μ M の濃度においては, 炭素結合型誘導体 **121c-f** のいずれの化合物と比較しても, 化合物 **122a** の in vitro 光毒性ポテンシャルは顕著に軽減されていることが明らかとなった. 一方, 化合物 **122a** と **122b** の溶解度を測定したところ (Table 3-4), 化合物 **122a** は酸性および中性のどちらの条件下においても溶解度が非常に低いことが明らかとなった. 化合物 **122a** の低溶解性は, Table 3-2 の in vitro 光毒性評価において析出物が確認されていたこととも矛盾のない結果であり, この後の薬理評価および毒性試験での経口吸収性に課題を残した. 一方で, 化合物 **122b** は評価したいずれの条件下においても良好な溶解性を示した. さらに, **122b** の PDE2A 阻害活性, PDE ファミリー選択性, その他種々のプロファイルを勘案して, 本化合物をこれ以降の精査化合物として選定することとした.

Table 3-2. Profiles of Di-substituted Pyrazolo[1,5-*a*]pyrimidine Derivatives

compd	R ¹	PDE2A IC ₅₀ (nM) ^a	PDE selectivity ^b	MDR1 ^c	rat in vivo CL (mL/h/kg) ^d	phototox (%) ^e	Log <i>D</i> ^f
120	H	5.1 (4.3–6.1)	1600-fold	0.53	2743	4.2	2.66
122a		0.31 (0.27–0.35)	5800-fold	1.2	940	13.0 ^g	3.24
122b		0.51 (0.46–0.58)	5300-fold	1.0	1169	3.7	3.42

^a IC₅₀ values (95% confidence intervals given in parentheses) were calculated by nonlinear regression analysis of percent inhibition data (*n* = 2). All values are rounded off to two significant digits.

^b Minimum selectivity (rounded off to two significant digits) over other PDEs. ^c MDR1 efflux ratios in P-gp overexpressing cells. ^d Plasma clearance calculated following 0.1 mg/kg, iv cassette dosing in rats (non-fasted). ^e Values (%) represent the difference between viability of cells exposed to 50 μM of the test compound in the absence of UV irradiation and that in the presence of UV irradiation, where cell viability was measured by intracellular ATP content (%) at 50 μM relative to vehicle control. A larger value is interpreted as a higher risk of phototoxicity. ^f Log *D* values at pH 7.4. ^g Precipitates observed.

Table 3-3. Inhibitory Activities of **122a** and **122b** against Human PDEs^a

PDE subtypes	122a		122b	
	IC ₅₀ (nM) ^a	selectivity ratio ^b	IC ₅₀ (nM) ^a	selectivity ratio ^b
PDE1A	3300	11000	2700	5300
PDE2A3	0.31	–	0.51	–
PDE3A	>10000	>32000	>10000	>20000
PDE4D2	3300	11000	9400	18000
PDE5A1	8800	28000	9100	18000
PDE6AB	1800	5800	8000	16000
PDE7B	>10000	>32000	>10000	>20000
PDE8A1	>10000	>32000	>10000	>20000
PDE9A2	>10000	>32000	>10000	>20000
PDE10A2	1700	5500	3100	6100
PDE11A4	3000	9700	>10000	>20000

^a IC₅₀ values (nM) were calculated by nonlinear regression analysis of percent inhibition data (*n* = 2). All values are rounded off to two significant digits.

Table 3-4. Thermodynamic Solubility of Compound **122a** and **122b**

compd	thermodynamic solubility (µg/mL)			crystallinity (%)
	pH 1.2	pH 6.8	pH 6.8 + GCDC ^a	
122a	0.45	0.32	16	89
122b	7	4.1	140	83

^a Solubility in a pH 6.8 solution containing sodium glycochenodeoxycholate (GCDC). This is considered as simulated intestinal fluid (pH 6.8) in the presence of bile acid.

第 5 節 化合物 **122b** と PDE2A の X 線共結晶構造解析

化合物 **122b** と PDE2A との X 線共結晶構造および化合物 **10a** と PDE2A との X 線共結晶構造をそれぞれ Figure 3-6 (A) および 3-6 (B) に示す。結晶構造解析の結果、化合物 **122b** は第 1 章で見出したリード化合物 **10a** と同様に、以下の 1-5 に示す相互作用を保持していることが明らかとなった。

1. ピラゾロ[1,5-*a*]ピリミジン環 7 位の水素原子は Gln859 と CH-O の擬似的水素結合を介して相互作用している。
2. ピラゾロ[1,5-*a*]ピリミジン環は上下の Phe862 および Ile826 とそれぞれ π - π ならびに CH- π の相互作用により安定化している。
3. ピラゾロ[1,5-*a*]ピリミジン環 6 位メチル基は Tyr827, Leu858, Ile826 で囲まれた脂溶性空間とファンデアワールス相互作用を形成している。
4. アミドカルボニル基は Tyr655 と水分子を介した水素結合のネットワーク、さらにもう一つ別の水分子と水素結合を形成している (Figure 3-6 (A) には未記載。詳細は Figure 1-7 参照)。
5. *p*-トリフルオロメトキシフェニル基は PDE2A タンパクとの結合によって新たに形成された PDE2A に特異的な脂溶性空間を効果的に充填している。

これら 5 つの相互作用に加え、**122b** は PDE2A タンパクと以下の新たな相互作用を獲得していることが分かった。

6. ピラゾロ[1,5-*a*]ピリミジン環 5 位のトリアゾール環は上下にある Ile866 と Met847 に挟まれる空間を効果的に充填し、ファンデアワールス相互作用をしている。また、トリアゾール環は Leu858 の主鎖カルボニル基と水を介して水素結合を形成している。
7. 分岐側鎖の三級アルコール部位はアミド部位の NH と分子内水素結合を形成するとともに、*gem*-ジメチル基による結合軸周りの回転抑制効果によって活性コンフォメーションの固定化に寄与している。

以上のように、化合物 **122b** はリード化合物 **10a** と同様、Gln859 との相互作用は TAK-915 と比べて弱いことが予想されるものの、上述の PDE2A 特異的な新たな相互作用を獲得することによって TAK-915 と同等の強力な PDE2A 阻害活性および 5300 倍以上の優れた PDE ファミリー選択性を示していると考えられる。

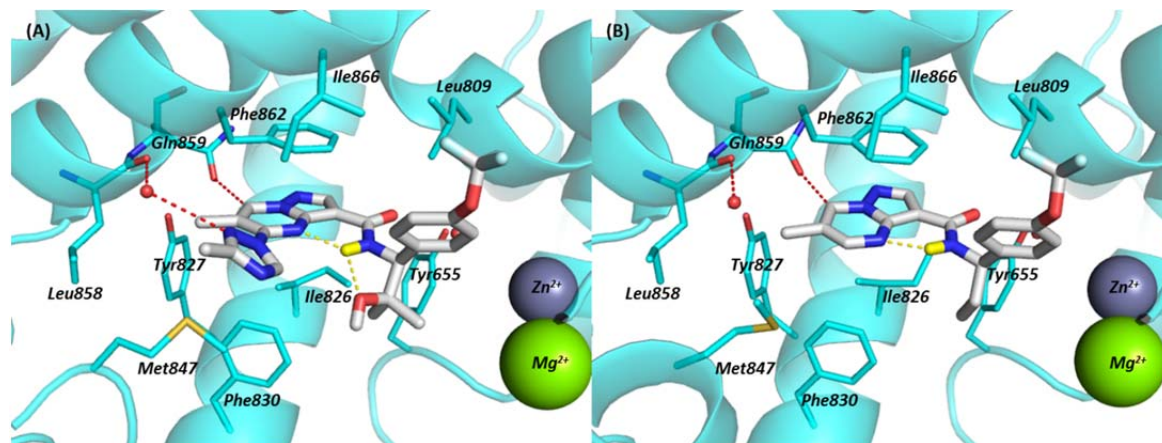


Figure 3-6. (A) X-ray crystal structure of **122b** bound in the PDE2A catalytic site (PDB 5VP1) and (B) X-ray crystal structure of **10a** bound in the PDE2A catalytic site (PDB 5XKM). The intramolecular hydrogen bonds are indicated by yellow dotted lines.

第 6 節 化合物 **122b** の薬物動態プロファイル

化合物 **122b** のラットおよびマウスにおける薬物動態試験の結果を Table 3-5 に示す。化合物 **122b** をラットおよびマウスに 0.3 mg/kg の静脈内投与をしたところ、共に良好なクリアランスおよび分布容積を示し、1 mg/kg 経口投与においては、それぞれ 31% および 48% の良好な生物学的利用率と 272.8 ng·h/mL および 628.6 ng·h/mL の血中濃度-時間曲線下総面積値を示した。さらに、ラットの最高血中濃度到達時間における脳内と血漿中の薬物濃度比 K_p は 0.32 で、高い TPSA (114 Å²) を示したにも関わらず、比較的良好な中枢移行性を示すことが明らかとなった。

Table 3-5. PK Parameters and K_p Values of Compound **122b** in Rat and Mouse^a

	rat	mouse
CL_{total}^b (mL/h/kg)	1169	768
Vd_{ss}^c (mL/kg)	2329	1337
C_{max}^d (ng/mL)	58.1	181.0
T_{max}^e (h)	2.0	0.7
AUC_{0-8h}^f (ng·h/mL)	272.8	628.6
F^g (%)	31.2	48.2
K_p^h	0.32	—

^a Cassette dosing at 0.1 mg/kg, iv and 1 mg/kg, po (non-fasted), in an average of 3 rats or mice. ^b Total clearance. ^c Volume of distribution at steady state. ^d Maximum plasma concentration. ^e Time of maximum concentration. ^f Area under the plasma concentration vs time curve (0–8 h). ^g Oral bioavailability. ^h Brain-to-plasma ratio at 2 h after oral administration of **122b** at a dose of 10 mg/kg.

第 7 節 化合物 **122b** の in vivo 薬理評価

精査化合物 **122b** が標的分子に直接作用しているかどうか (target engagement) を検証するために、化合物 **122b** の PDE2A 酵素に対する結合占有率を算出した。結果を Figure 3-7 に示す。化合物 **122b** を経口投与することによって、本化合物が線条体部位に発現する PDE2A に用量依存的に結合していることが明らかとなった。このとき、ED₅₀ (50% 占有率のときの用量) は 3.9 mg/kg であった。また、化合物 **122b** の PD マーカーに対する影響を確認するために、前頭葉、線条体ならびに海馬の cAMP および cGMP 含量を測定した (Figure 3-8)。これまでの知見と同様に^{48,55,69}、化合物 **122b** は上記の脳部位において用量依存的に cGMP 含量を増加させ、3 mg/kg の用量から有意な変化が認められた。一方、化合物 **122b** はこれまでの結果と同様に、cAMP 含量に有意な影響を及ぼさなかった。前述の用量-占有率相関の結果 (Figure 3-7) から、3 mg/kg の用量における PDE2A 酵素占有率は ~37% であることから、動物モデルにおいても本占有率を超える用量にて薬理作用を発揮することが期待される。そこで、脳内 cGMP 含量の増加が認められた 3 mg/kg の投与量で認知機能障害モデルを用いたラット受動的回避試験を実施した (Figure 3-9)。その結果、MK-801 (0.1 mg/kg) の皮下投与によって誘発された認知機能障害作用が、化合物 **122b** の経口投与 (3 mg/kg) により有意に改善することが確認できた。以上のことから、化合物 **122b** は第 2 章で見出した TAK-915 と同等の PD マーカーに対する作用および薬理作用を示すことが明らかとなった。

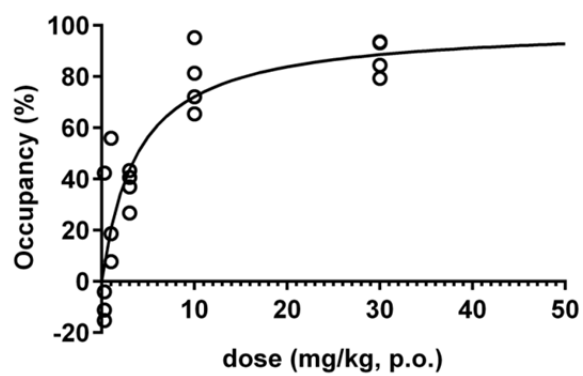


Figure 3-7. In vivo PDE2A target occupancy in the striatum measured 2 h after oral administration of **122b** in rats.

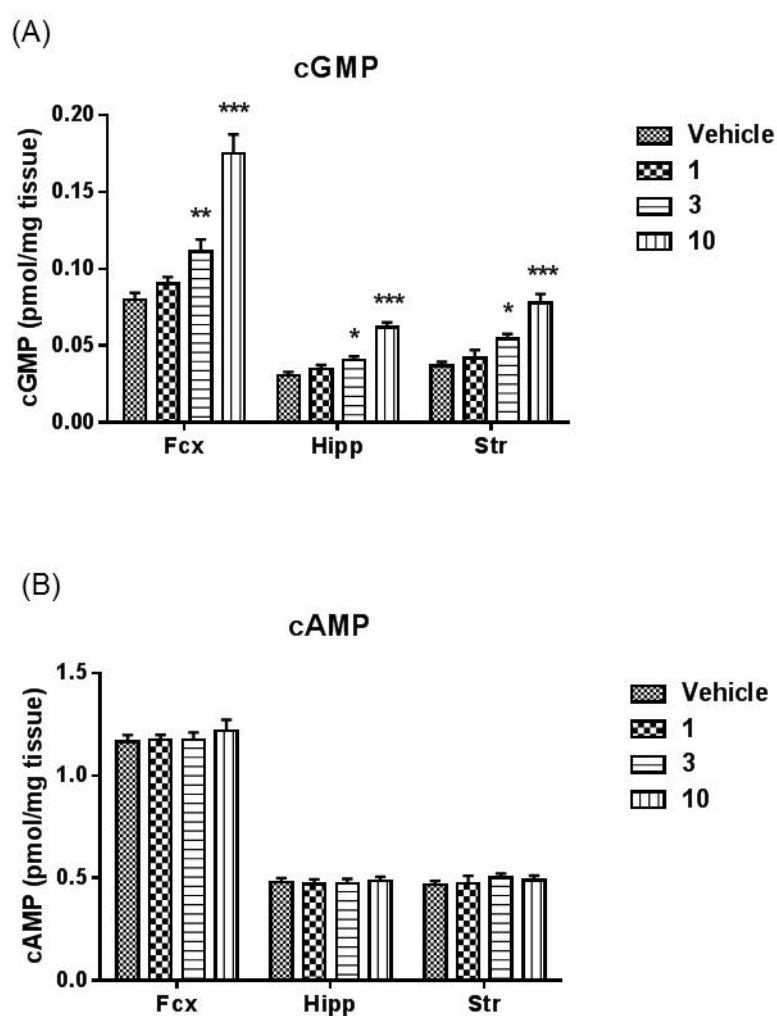


Figure 3-8. Effects of compound **122b** on cyclic nucleotides in rat brain. cGMP (A) and cAMP (B) levels 2 h after oral administration of compound **122b** (1 mg/kg, 3 mg/kg, and 10 mg/kg) were measured in the rat frontal cortex (Fcx), hippocampus (Hipp), and striatum (Str). Data are presented as mean \pm SEM ($n = 9$); * $p < 0.025$, ** $p < 0.005$, *** $p < 0.0005$, vs. vehicle by Shirley–Williams' test.

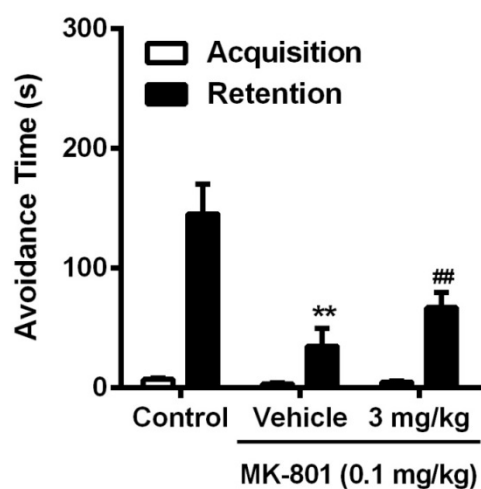
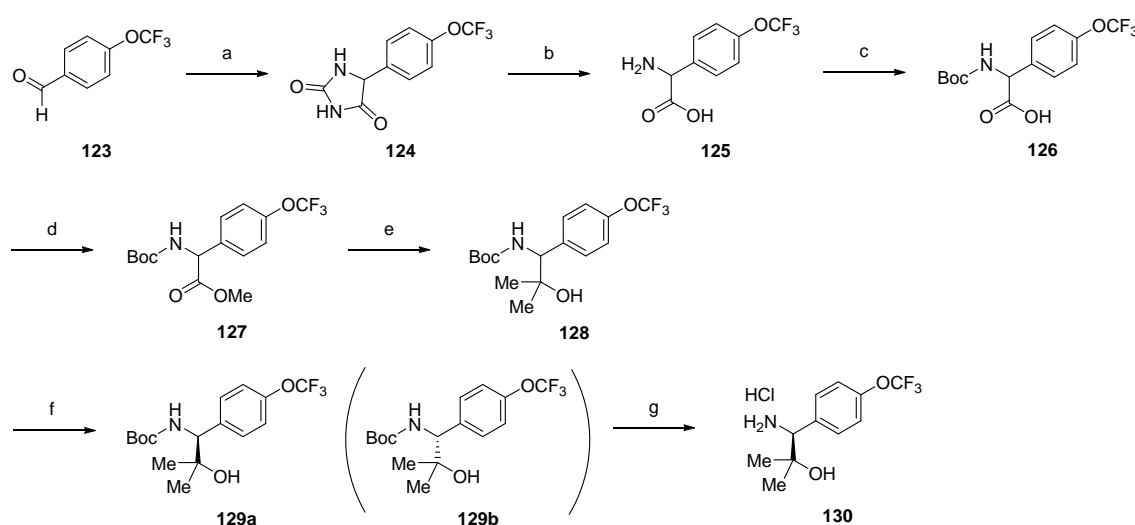


Figure 3-9. Effects of compound **122b** on MK-801-induced episodic memory deficits assessed by the passive avoidance task in rats. Vehicle or compound **122b** (3 mg/kg) was orally administered 90 min before the s.c. administration of saline or MK-801. Thirty minutes after the s.c. administration of saline or MK-801 (0.1 mg/kg), the rat was placed on the illuminated chamber. The latency to cross over into the dark chamber was recorded for up to a maximum of 300 s. The retention test was carried out 24 h after the acquisition trial. Data (latency to cross over into the dark compartment on the retention trial) are expressed as mean \pm SEM, $n = 20$, ** $p \leq 0.01$ (versus control by Wilcoxon's test), ## $p \leq 0.01$ (versus vehicle + MK-801 by Wilcoxon's test).

第 8 節 化合物の合成

三級アルコール側鎖を有するベンジルアミン **130** は Scheme 3-1 記載の方法で合成した。ベンズアルデヒド **123** は Bucherer–Bergs 反応¹⁰¹ により対応するヒダントイン **124** へ導いた後、アルカリ加水分解によりアミノ酸 **125** を合成した。**125** のアミノ基を Schotten–Baumann の条件下、Boc 基で保護し、続いてカルボン酸 **126** をメチル化することによってメチルエステル **127** に変換した。得られた **127** をメチルグリニャール試薬と反応させて三級アルコール **128** とした後、Chiralpak AD を用いた光学分割により光学活性体 **129a** および **129b** を取得した。続いて、所望の絶対配置 (決定法は後述 (Scheme 3-5)) を有する光学活性体 **129a** を塩酸/酢酸エチルで脱 Boc 化することによってベンジルアミン **130** を塩酸塩として得た。

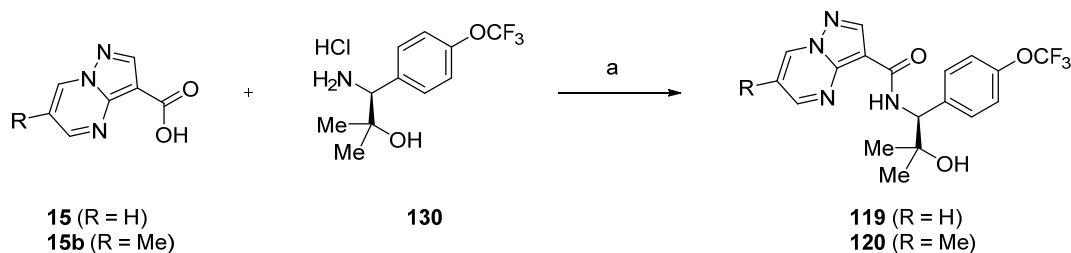
Scheme 3-1. Synthesis of RHS Benzylamine Moiety **130**^a



^a Reagents and conditions: (a) KCN, $(\text{NH}_4)_2\text{CO}_3$, EtOH, H_2O , 50 °C to 60 °C, 3 h, (taken on crude); (b) KOH, water, 90 °C, 3 days, (taken on crude); (c) Boc_2O , 2 M NaOH aq., THF, rt, overnight, (taken on crude); (d) MeI, K_2CO_3 , DMF, rt, 2 h, 46% (4 steps from **123**); (e) MeMgBr, THF, 0 °C, 1 h, 76%; (f) Chiralpak AD, hexane/EtOH = 95:5; (g) HCl, EtOAc, rt, 1.5 h, 84%.

化合物 **119** と **120** は市販の原料 **15** および **15b** (Scheme 1-1 参照) とベンジルアミン塩酸塩 **130** とのアミド化反応によって合成した (Scheme 3-2).

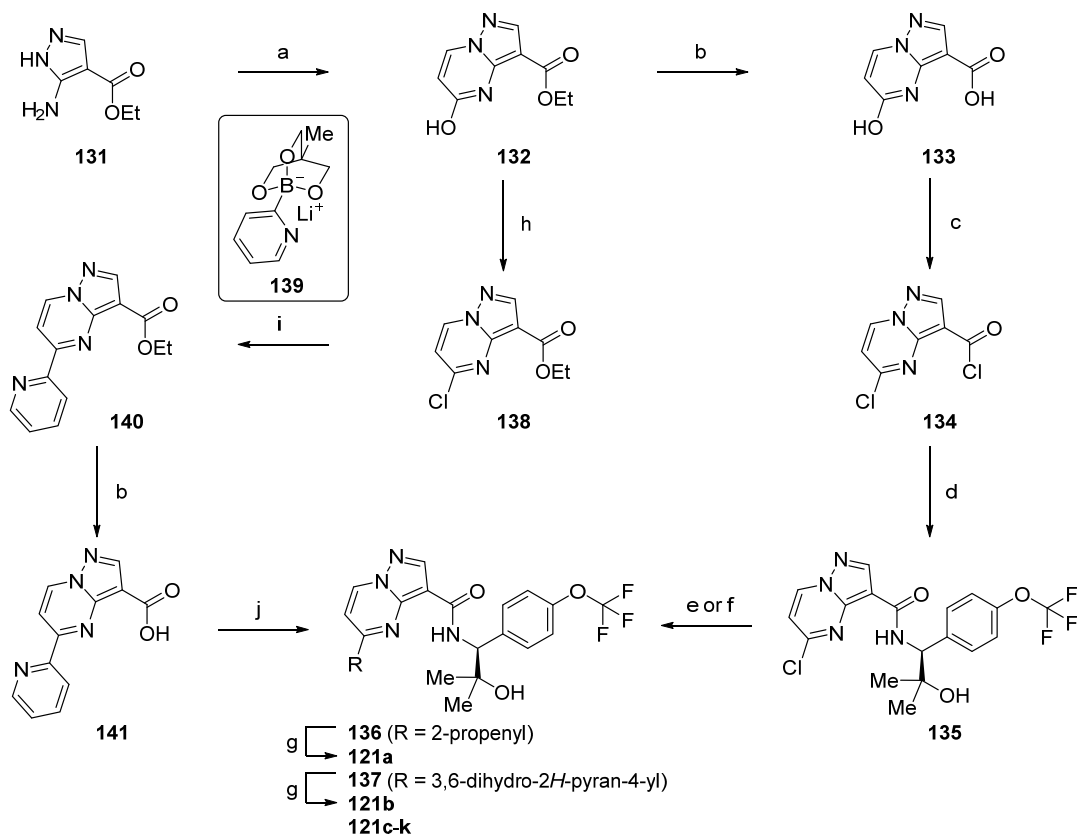
Scheme 3-2. Synthesis of Pyrazolo[1,5-*a*]pyrimidine Derivatives **119** and **120**^a



^a Reagents and conditions: (a) EDCI·HCl, HOBt·H₂O, Et₃N, DMF, rt, overnight, 41–87%.

5 位置換ピラゾロ[1,5-*a*]ピリミジン誘導体 **121a–k** は Scheme 3-3 記載の方法で合成した。ピラゾロ[1,5-*a*]ピリミジン **132** は塩基性条件下、5-アミノ-1*H*-ピラゾール **131** と 3-エトキシアクリル酸エチルとの縮合反応により合成した。次に、エステル **132** をアルカリ加水分解によりカルボン酸 **133** とした後、オキシ塩化リン (POCl₃) を加えて 130 °C で加熱することによってビスクロロ体 **134** を得た。続いて、右骨格のベンジルアミン **130** を作用させることで鍵中間体の 5-クロロピラゾロ[1,5-*a*]ピリミジン誘導体 **135** を合成した。ピラゾロ[1,5-*a*]ピリミジン環 5 位への置換基導入は鈴木–宮浦クロスカップリング反応,^{72,73} あるいは対応するアゾール環との求核置換反応を用いて行い、標的化合物 **121d–k** へ導いた。またカップリング体 **136** および **137** は、引き続きパラジウム/炭素を用いた接触還元で付し、オレフィン還元体 **121a** および **121b** を得た。一方、2-ピリミジン誘導体 **121c** については、上述の 5-クロロピラゾロ[1,5-*a*]ピリミジン誘導体 **135** を基質とする鈴木–宮浦クロスカップリング反応が進行しなかったため、別ルートでの合成を検討した。**135** に含まれるアミドや三級アルコール部位などの極性官能基がカップリング反応に悪影響を及ぼしている可能性が考えられたため、ベンジルアミン部位の導入前のヒドロキシ体 **132** から誘導した 5-クロロピラゾロ[1,5-*a*]ピリミジン誘導体 **138** と 2-ピリジルトリオールボレート塩 **139** を銅触媒存在下、無水溶媒中、80 °C で加熱することで 87% の良好な収率で所望のカップリング体 **140** を得ることができた¹⁰²。最後に、エステル体 **140** はアルカリ加水分解に次ぐベンジルアミン **130** との縮合反応によって標的化合物 **121c** へ導いた。

Scheme 3-3. Synthesis of 5-Substituted Pyrazolo[1,5-*a*]pyrimidine Derivatives **121a-k**^a

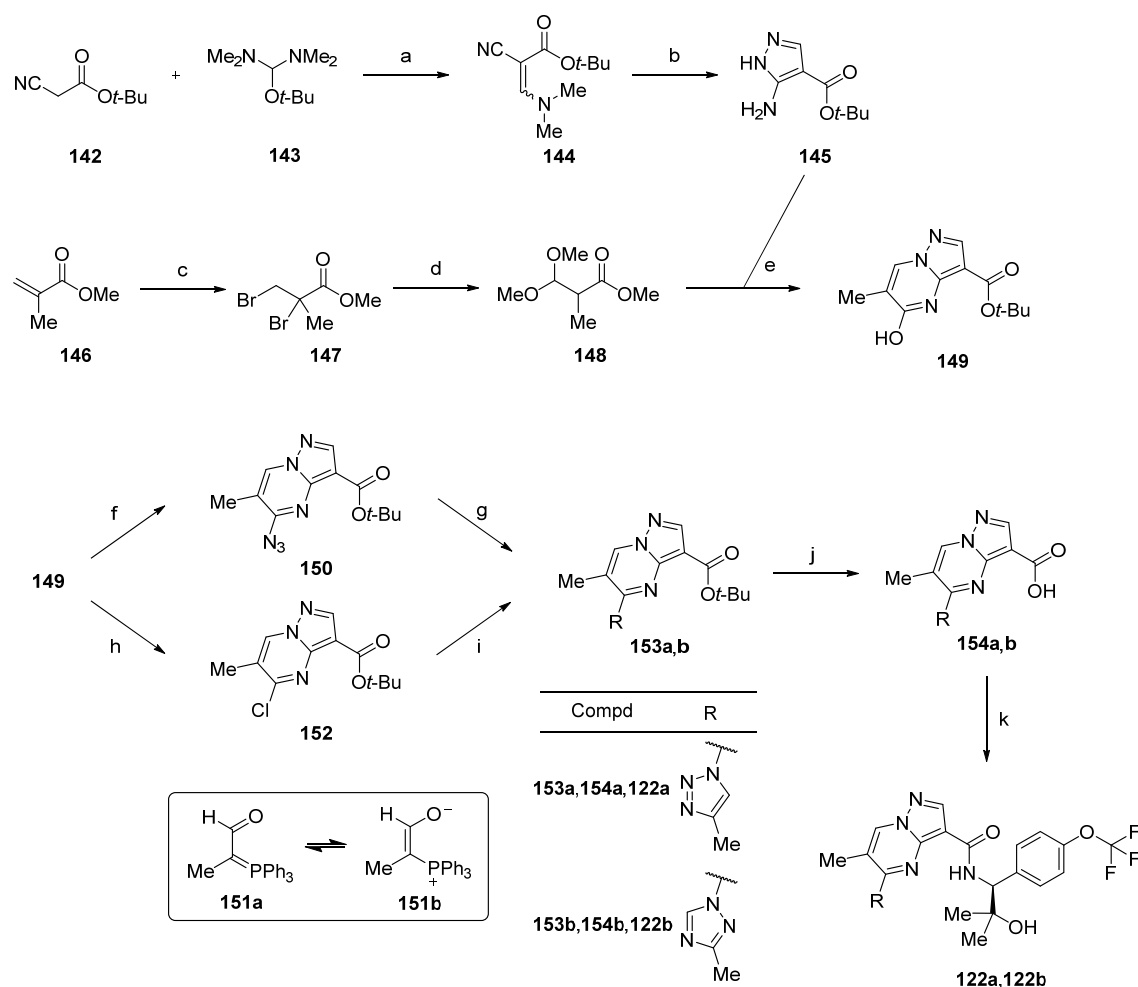


^a Reagents and conditions: (a) ethyl 3-ethoxyacrylate (cis- and trans-mixture), Cs₂CO₃, DMF, 100 °C, 2 h, 91%; (b) NaOH aq., THF, EtOH, 50–60 °C, 2 h–overnight, 75–98%; (c) POCl₃, DIEA, 130 °C, 4 h, 74%; (d) RHS benzylamine **130**, DIEA, CH₃CN, 0 °C to rt, 16 h, 77%; (e) alkyl or arylboronic acid pinacolester, (Amphos)₂PdCl₂, K₂CO₃, toluene, H₂O, 120–150 °C (microwave), 25 min–2.5 h, 63–78%; (f)azole, K₂CO₃, DMF, 80–90 °C, 30 min–2 h, 7–74%; (g) H₂, 5% Pd/C–ethylenediamine complex, MeOH, rt, 16 h, 83–98%; (h) POCl₃, 100 °C, 16 h, 61%; (i) lithium 4-methyl-1-pyridin-2-yl-2,6,7-trioxa-1-borabicyclo[2.2.2]octan-1-uide **139**, Pd(OAc)₂, Ph₃P, CuI, DMF, 80 °C, 2 h, 87%; (j) RHS benzylamine **130**, HATU, DIEA, DMF, rt, 12 h, 84%.

5,6-ジ置換ピラゾロ[1,5-*a*]ピリミジン誘導体 **122a** および **122b** の合成を Scheme 3-4 に示す. アミノピラゾール **145** は 2-シアノ酢酸 *tert*-ブチル (**142**) と *tert*-ブトキシビス(ジメチルアミノ)メタン (**143**) との縮合反応, 続くヒドラジンとのピラゾール環構築反応の 2 工程, 64% の収率で合成した. 得られた **145** は 1,3-ジカルボニル等価体 **148** との縮合反応によって, ピラゾロ[1,5-*a*]ピリミジン環 **149** へ導いた. なお, **148** はメタクリル酸メチル (**146**)

のオレフィン部位の臭素化とナトリウムメトキシド/メタノール溶液との反応によって合成した。また、化合物 **149** の 5 位ヒドロキシ基を DBU 共存下、ジフェニルリン酸アジドを用いてアジド体 **150** に変換した後、 α -ホルミルエチリデントリフェニルホスホラン (**151a**) の互変異性体 **151b** との 1,3-双極子付加環化とトリフェニルホスフィンオキシドの脱離を伴うトリアゾール環構築反応によって 1,2,3-トリアゾール体 **153a** を合成した^{103,104}。一方で、**149** を四塩化炭素およびトリフェニルホスフィンを用いた Appel 型反応¹⁰⁵ に付しクロロ体 **152** とした後、塩基性条件下、3-メチル-1*H*-1,2,4-トリアゾールの芳香族求核置換反応により 1,2,4-トリアゾール体 **153b** を位置選択的に得た。**153a,b** は酸性条件下での *tert*-ブチルエステルの加水分解、その後のベンジルアミン **130** とのアミド化反応によって標的化合物 **122a,b** を得た。

Scheme 3-4. Synthesis of 6-Methyl-5-Substituted Pyrazolo[1,5-*a*]pyrimidine Derivatives **122a** and **122b**^a

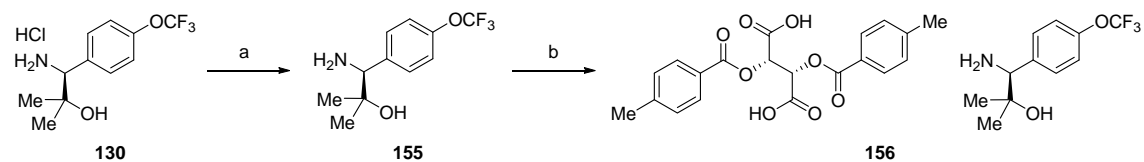


^a Reagents and conditions: (a) neat, rt, 30 min, (taken on crude); (b) $\text{NH}_2\text{NH}_2 \cdot \text{H}_2\text{O}$, MeOH, 70 °C, overnight, 64%; (c) Br_2 , EtOAc, rt, 16 h, (taken on crude); (d) NaOMe, MeOH, 70 °C, 3 h, (taken on crude); (e) Cs_2CO_3 , DMF, 100 °C, 16 h, 84%; (f) DPPA, DBU, THF, 60 °C, 5 h, 74%; (g) **151**, toluene, 80 °C, 3 h, then MgCl_2 , 60 °C, 2 h, 97%; (h) CCl_4 , PPh_3 , 1,2-dichloroethane, 75–85 °C, 4.5 h, 88%; (i) 3-methyl-1*H*-1,2,4-triazole, K_2CO_3 , DMF, 60 °C, 2 h, 69%; (j) MsOH, CH_3CN , rt–60 °C, 5.5 h–overnight, 85–91%; (k) RHS benzylamine **130**, EDCI·HCl, $\text{HOBt} \cdot \text{H}_2\text{O}$, Et_3N , DMF, rt, 2 h–overnight, 75–82%.

ベンジルアミン **130** の絶対立体配置を決定するために、塩酸塩 **130** を中和によりフリー一体 **155** とした後, (+)-ジ-(*p*-トルオイル)-D-酒石酸との新たな塩形成によって **156** を結晶と

して取得した (Scheme 3-5). **156** の単結晶 X 線構造解析の結果、ベンジル位の絶対立体配置は *S* 体と決定した.

Scheme 3-5. Synthesis of (+)-Di-(*p*-toluoyl)-D-tartaric Acid Salt **156** of **155** Suitable for X-ray Crystallography^a



^a Reagents and conditions: (a) NaHCO₃, H₂O; (b) (2*S*,3*S*)-(+)-di-(*p*-toluoyl)-D-tartaric acid, EtOH, H₂O, 50 °C, overnight.

第 9 節 結語

第 1 章および第 2 章の合成研究の過程で見出した誘導体 **118** および **31** の化合物特性に着目し、それぞれの部分骨格を組み合わせた化合物 **119** を設計・合成した結果、TAK-915 とは構造的に異なり、かつ PDE2A 阻害活性、PDE ファミリー選択性および P-gp プロファイルの優れた新規リードケモタイプを見出すことに成功した。また、新たに見出したリード化合物を端緒化合物として、X 線共結晶構造情報に基づき、ピラゾロ[1,5-*a*]ピリミジン環 5 位および 6 位の置換基探索を行った結果、TAK-915 と同等の強力な阻害活性 ($IC_{50} = 0.51$ nM) と優れた PDE ファミリー選択性 (5300 倍 vs. PDE1A) および *in vitro* プロファイルを示す化合物 **122b** を見出すことに成功した。また、炭素結合型芳香族ヘテロ環をピラゾロ[1,5-*a*]ピリミジン環 5 位に導入することで認められた強い *in vitro* 光毒性ポテンシャルは、ピラゾール環やトリアゾール環などの窒素結合型芳香族ヘテロ 5 員環に変換することで劇的に改善されることを明らかにした。さらに化合物 **122b** は、ラットへの経口投与によって、線条体における PDE2A 酵素への占有率を用量依存的に増加させ、占有率の増加に伴いラット脳内 cGMP 含量も用量依存的に上昇させることが明らかとなった。また統合失調症の認知機能障害を反映するモデルとされる受動的回避試験においても、脳内 cGMP 含量を有意に上昇させた用量にて有意な認知機能改善効果を示した。以上のように、化合物 **122b** は TAK-915 の構造とは異なり、かつ良好な ADME-Tox (absorption, distribution, metabolism, excretion, and toxicity) および薬理プロファイルを示したことから、TAK-915 のバックアップ化合物として相応しい候補化合物であると考えられる。

総括

統合失調症は、陽性症状・陰性症状・認知機能障害の 3 つの症状を特徴とする重度の精神疾患である。既存の抗精神病薬は主症状のうち陽性症状の軽減には一定の治療効果が確認されている一方で、陰性症状や認知機能障害に対する効果は限定的で、かつ重篤な副作用の問題点も指摘されていることから、これらの課題を改善する次世代統合失調症治療薬の開発が強く求められている。このような背景のもと、近年、既存の抗精神病薬とは作用機序が異なる新規認知機能改善薬として PDE2A 阻害薬が注目を集め、複数の製薬企業から低分子化合物が報告されている。しかしながら、いずれの化合物も主活性・PDE 選択性・薬物動態あるいは中枢移行性などに課題を有しており、PDE2A が統合失調症の認知機能を改善する有望な標的分子であるかどうかはこれまで不明であった。そこで著者らは、非臨床および臨床において PDE2A の認知機能改善薬としての有用性を実証するべく、構造独自性が高く、経口投与可能で、良好な中枢移行性を示す安全かつ高選択的な PDE2A 阻害薬の探索研究を実施した。その結果、3,4-ジヒドロピリド[2,3-*b*]ピラジン-2(1*H*)-オン環を基本骨格とした臨床候補化合物 **42a** (TAK-915) を見出すことに成功した。さらに、TAK-915 の開発過程における不測の事態に備えるためにバックアップ化合物の探索研究に着手し、TAK-915 とは構造が異なり、かつ TAK-915 と同等の PDE2A 阻害活性・PDE 選択性および *in vivo* 活性を有する化合物 **122b** を見出すことに成功した。臨床候補化合物 TAK-915 に代表される選択的 PDE2A 阻害薬は、MK-801 により惹起された認知機能障害モデルにおいて認知機能の改善作用を示すとともに、既存薬に特徴的な錐体外路症状・高プロラクチン血症・耐糖能異常などの副作用やその他懸念すべき毒性所見を認めなかったことから、統合失調症のアンメットニーズを満たす新しい認知機能改善薬として期待される。

本研究で得られた知見を以下にまとめる。これらの知見は、PDE2A 阻害剤の研究のみならず、相同性の高い他の PDE 阻害剤や中枢薬を指向した薬剤の研究にも応用できる有用なものと考えられる。

1. HTS ヒット化合物 **2** を端緒化合物とした合成展開において、ピラゾロ[1,5-*a*]ピリミジン環上への置換基の導入、右骨格ベンジルアミン部位の最適化検討およびベンジルアミン側鎖部位の光学分割により、良好な PDE2A 阻害活性 ($IC_{50} = 24 \text{ nM}$) および PDE ファミリー選択性 (180 倍 vs. PDE3A) を有し、経口投与において脳内 cGMP 含量の増加を示すリード化合物 **10a** を見出した。
2. 化合物 **10a** の X 線共結晶構造解析の結果、特徴的な結合様式が明らかとなった。中でも、*p*-トリフルオロメトキシフェニル基は PDE2A に特徴的な脂溶性空間を最安定構造に近い配座で効果的に占有していること、ピラゾロ[1,5-*a*]ピリミジン環 7 位水素原子は PDE ファミリー共通の基質結合部位である Gln859 と CH-O の擬似的水素結合を介して相互作用していること、アミド NH とピラゾロ[1,5-*a*]ピリミジン環 4 位窒素原子が強い分子内水素結合を形成することで活性コンフォメーションを安定化し、強い PDE2A 阻害活性の発現に寄与していることを明らかにした。本化合物の結合様式は、さらなる活性および選択性の向上を指向した最適化研究の薬物設計において、重要な知見を与えた。
3. 化合物 **10a** のピラゾロ[1,5-*a*]ピリミジン骨格を Gln859 と明確な水素結合が形成可能な縮合環へ骨格変換することで、PDE2A 阻害活性の向上した新規 3,4-ジヒドロピリド[2,3-*b*]ピラジン-2(1*H*)-オン誘導体 **32** を見出した。
4. 化合物 **32** の右末端フェニル基上置換基の最適化において、種々置換基導入の構造活性相関を明らかにし、中でも *p*-トリフルオロメトキシ基の隣の位置にフッ素原子を導入することで PDE2A 阻害活性がおおよそ 2 倍向上した化合物 **37h** を見出した。
5. リガンド結合サイトに存在する金属イオン周辺の極性アミノ酸残基や水分子との新たな相互作用を指向した化合物 **32** の分岐エチル側鎖への極性基導入を通じて、4 倍強力な

PDE2A 阻害活性 ($IC_{50} = 19 \text{ nM}$) と 310 倍の良好な PDE ファミリー選択性, かつ顕著に脂溶性が低減 ($\Delta\text{Log } D = 0.66$) した化合物 **38a** を見出した.

6. 化合物 **38a** の 3,4-ジヒドロピリド[2,3-*b*]ピラジン-2(1*H*)-オン環上への置換基導入を通じて, 各部位の構造活性相関を明らかにするとともに, 7 位メトキシ基 (**39f**) が PDE2A 阻害活性および PDE ファミリー選択性の両面において, 顕著な改善効果 ($IC_{50} = 2.8 \text{ nM}$, 2700 倍の選択性 vs. PDE5) を示すことを明らかにした. 各 PDE 間でアミノ酸残基の異なる空間領域を狙った構造変換が PDE2A 阻害活性および選択性向上を図る上で有効な戦略の一つであることを例示することができた.
7. 上記 3-6 で得られた知見を組み合わせ, その後分岐側鎖部位の光学分割を行うことにより, 強力な PDE2A 阻害活性 ($IC_{50} = 0.61 \text{ nM}$) と優れた PDE ファミリー選択性 (4100 倍以上) およびオフターゲット選択性 (6400 倍以上 vs. 96 種類のオフターゲット) を示し, 中枢移行性の良好な化合物 **42a** を見出した. 本化合物は 経口投与の結果, マウス脳内の cGMP 含量を用量依存的に増加させるとともに, 種々の薬効モデル動物において認知機能改善効果を示した. また, 既存の抗精神病薬に特徴的な副作用の評価および各種動物を用いた安全性試験の結果, 危惧すべき毒性所見が認められず十分な毒性マージンが確保されたことから, 化合物 **42a** (開発コード: TAK-915) を臨床試験の候補化合物として選出した.
8. 上記 3-7 の化合物探索において, 我々が設定した分子内水素結合を考慮した TPSA および HBD 数の基準 ($\text{TPSA} < 110 \text{ \AA}^2$, HBD 数 < 3) が良好な中枢移行性を示す化合物を獲得する上で妥当な指標であることを実証することができた.

9. 化合物 **118** および **31** に代表される既存ケモタイプの構造特性を理解し、それぞれの部分構造を組み合わせることで、**118** の高い P-gp 基質プロファイルおよび **31** の弱い阻害活性の双方の問題点を同時に克服し、TAK-915 とは構造の異なる新規リード化合物 **119** を見出すことに成功した。
10. 化合物 **10a** の X 線共結晶構造解析の情報に基づいてピラゾロ[1,5-*a*]ピリミジン誘導体 **119** の母核 5 および 6 位の最適化研究を行った結果、非常に強力な PDE2A 阻害活性と PDE1A に対して 5300 倍の PDE ファミリー選択性を示す **122b** を見出した。
11. 炭素結合型芳香族ヘテロ環を 5 位置換基として導入することで認められた強い *in vitro* 光毒性ポテンシャルは、**122b** の置換基に代表される窒素結合型芳香族ヘテロ 5 員環に置換することで劇的に改善されることを明らかにした。 π 共役系を短くする一般的な光毒性回避の戦略とは異なる本知見は、今後の創薬研究において有用であると考えられる。
12. 化合物 **122b** の X 線共結晶構造解析の結果、本化合物は第 1 章で見出したリード化合物 **10a** と同様の相互作用に加えて、5 位トリアゾール環の上下に位置する Ile866/Met847 とのファンデアワールス相互作用と Leu858 主鎖カルボニル基との水を介した水素結合を新たに獲得するとともに、分岐側鎖の三級アルコール部位酸素原子とアミド NH との分子内水素結合、さらには *gem*-ジメチル基による立体配座の固定化によって強い PDE2A 阻害活性と高い PDE ファミリー選択性が発現していることを明らかにした。
13. 化合物 **122b** のラットへの経口投与によって、ラット脳内 cGMP 含量が用量依存的かつ有意に上昇するとともに、受動的回避試験においても、脳内 cGMP 含量を有意に上昇させた用量にて有意な認知機能改善効果を示すことを見出した。また化合物評価を通じて、

化合物 **122b** が TAK-915 とは構造が異なり、良好な ADME-Tox および薬理プロファイルを示す有望なバックアップ化合物候補であることを実証することができた。

謝辞

本論文の発表および作成にあたり、終始ご懇切なるご指導とご鞭撻を賜りました東北大学大学院薬学研究科教授 岩渕好治先生に深く感謝いたします。また、本論文の審査にあたり、ご指導ならびにご助言を賜りました東北大学大学院薬学研究科教授 土井隆行先生、ならびに東北大学大学院薬学研究科教授 徳山英利先生に厚く御礼申し上げます。

本研究の機会を与えてくださいました、武田薬品工業株式会社 ニューロサイエンス創薬ユニット ユニット長 Ceri Davis 博士、ニューロサイエンス創薬ユニット ドラッグディスカバリーケミストリー研究所 (Drug Discovery Chemistry Laboratories; DDCL) 所長 一川隆史博士に深謝申し上げます。

本研究は終始、ニューロサイエンス創薬ユニット DDCL リサーチマネージャー 谷口孝彦博士のご指導の下行われたものであり、ここに厚く御礼申し上げます。

本研究を遂行するにあたり、有益なご助言とご指導を頂きました元医薬研究本部化学研究所所長 内川 治博士および元中枢疾患創薬ユニットリサーチマネージャー 黒板孝信博士に深謝致します。

化合物の合成や分子設計において多大なご協力と有益なご助言を頂きました元医薬研究本部化学研究所主席研究員 福本正司博士、ニューロサイエンス創薬ユニット主任研究員 中村信二博士、元中枢疾患創薬ユニット研究員 芦沢朋子博士、ニューロサイエンス創薬ユニット DDCL リサーチマネージャー 野村泉博士、アクセリード研究本部化学主席研究員 川崎昌紀博士、ニューロサイエンス創薬ユニット研究員 佐々木茂和博士、ニューロサイエンス創薬ユニット主任研究員 池田周平博士、リサーチセントラルオフィスストラテジー & オペレーショングループ主席部員 根来伸行博士、アクセリード研究本部化学主席研究員 浅野恭臣博士、アクセリード研究本部化学主任研究員 宇治川治博士、アクセリード研究本部化学主任研究員 沖英幸氏、アクセリード研究本部化学主任研究員 小久保裕功博士、武

田カリフォルニア研究員 Isaac D. Hoffman 氏, 武田カリフォルニア主任研究員 Hua Zou 博士に深謝致します.

本研究の薬理試験をご担当頂きましたニューロサイエンス創薬ユニット アフェクティブディスオーダーズ ユニット (Affective Disorders Unit; ADU) リサーチマネージャー 岩下弘樹博士, ニューロサイエンス創薬ユニット研究員 今田はるか氏, ニューロサイエンス創薬ユニット主任研究員 中島政人氏, ニューロサイエンス創薬ユニット主任研究員 井藤勇輝氏, ニューロサイエンス創薬ユニット主任研究員 白石絵理氏, アクセリード研究本部統合生物主任研究員 鈴木敬子氏に深謝致します.

本研究の化合物スクリーニングをご担当頂きましたニューロサイエンス創薬ユニット主任研究員 中島康祐博士, 武田ボストン主任研究員 内山紀子氏に深謝致します.

本研究の薬物動態試験をご担当頂きました薬物安全性研究所主席研究員 上口尚美氏, 元薬物動態研究所研究員 日浦悠斗氏, 薬物動態研究所主任研究員 宮本真紀氏に深謝致します.

最後に, 本論文の作成に際して, 終始温かく応援していただいた妻 味上 Chawalrat, 父 味上祥, 母 味上秋子に心から感謝致します.

実験の部

All solvents and reagents were obtained from commercial sources and were used as received. Microwave-assisted reactions were carried out in a single-mode reactor, Biotage Initiator 2.0 or 2.5 microwave synthesizer. Yields were not optimized. All reactions were monitored by thin layer chromatography (TLC) analysis on Merck Kieselgel 60 F254 plates or Fuji Silysia NH plates, or LC–MS (liquid chromatography–mass spectrometry) analysis. LC–MS analysis was performed on a Shimadzu liquid chromatography–mass spectrometer system operating in atmospheric pressure chemical ionization (APCI) (+ or –) or electrospray ionization (ESI) (+ or –) mode. Analytes were eluted using a linear gradient with a mobile phase of water/acetonitrile containing 0.05% TFA or 5 mM ammonium acetate and detected at 220 nm. Column chromatography was carried out on silica gel ((Merck Kieselgel 60, 70–230 mesh, Merck) or (Chromatorex NH-DM 1020, 100–200 mesh, Fuji Silysia Chemical, Ltd.)), or on prepacked Purif-Pack columns (SI or NH, particle size: 60 μm , Fuji Silysia Chemical, Ltd.). Analytical HPLC was performed using a Corona Charged Aerosol Detector or photo diode array detector with a Capcell Pak C18AQ (3.0 mm ID \times 50 mm L, Shiseido, Japan) or L-column2 ODS (2.0 mm ID \times 30 mm L, CERI, Japan) column at a temperature of 50 $^{\circ}\text{C}$ and a flow rate of 0.5 mL/min. Mobile phases A and B under neutral conditions were a mixture of 50 mmol/L ammonium acetate, water, and acetonitrile (1:8:1, v/v/v) and a mixture of 50 mmol/L ammonium acetate and acetonitrile (1:9, v/v), respectively. The ratio of mobile phase B was increased linearly from 5% to 95% over 3 min, and then maintained at 95% over the next 1 min. Mobile phases A and B under acidic conditions were a mixture of 0.2% formic acid in 10 mmol/L ammonium formate and 0.2% formic acid in acetonitrile, respectively. The ratio of mobile phase B was increased linearly from 14% to 86% over 3 min, and then maintained at 86% over the next 1 min. All final test compounds were purified to >95% chemical purity as measured by analytical HPLC. Elemental analyses were carried out by Takeda Analytical Laboratories, and all results were within $\pm 0.4\%$ of the theoretical

values. Melting points were determined on a BÜCHI B-545 melting point apparatus or a DSC1 system (Mettler-Toledo International Inc., Greifensee, Switzerland) and are uncorrected. Optical rotation was determined by a Jasco P-2300 polarimeter. Specific rotations $[\alpha]_{20}^D$ are given in $\text{deg dL g}^{-1} \text{mm}^{-1}$. Proton (^1H) and carbon (^{13}C) nuclear magnetic resonance (NMR) spectra were recorded on a Varian Mercury-300 (300 MHz), Bruker DPX300 (300 MHz), or Bruker Avance II⁺ 600 (600 MHz) instrument. All ^1H and ^{13}C NMR spectra were consistent with the proposed structures. All proton and carbon shifts are given in parts per million (ppm) downfield from tetramethylsilane (δ) as the internal standard in deuterated solvent, and coupling constants (J) are in hertz (Hz). NMR data are reported as follows: chemical shift, integration, multiplicity (s, singlet; d, doublet; t, triplet; q, quartet; quint, quintet; m, multiplet; dd, doublet of doublets; td, triplet of doublets; ddd, doublet of doublet of doublets; and brs, broad singlet), and coupling constants. Very broad peaks for protons of, for example, hydroxyl and amino groups are not always indicated.

第 1 章に関する実験

N-(1-(4-Methoxyphenyl)propyl)pyrazolo[1,5-*a*]pyrimidine-3-carboxamide (**2**). To a solution of pyrazolo[1,5-*a*]pyrimidine-3-carboxylic acid (**15**) (50 mg, 0.31 mmol) in DMF (2 mL) were added EDCI (71 mg, 0.37 mmol), HOBt (49 mg, 0.37 mmol), and DIEA (79 mg, 0.61 mmol). Then **21a** (55 mg, 0.34 mmol) was added. After stirred at rt overnight, the reaction mixture was diluted with EtOAc and washed with saturated aqueous NaHCO₃ and saturated aqueous NaCl. The organic layer was dried over anhydrous Na₂SO₄ and concentrated in vacuo. The residue was purified by preparative TLC (petroleum ether/ethyl acetate, 1:1) to give **2** (50 mg, 0.16 mmol, 52%) as a colorless oil. ¹H NMR (400 MHz, CDCl₃) δ 0.97 (3H, t, *J* = 7.6 Hz), 1.92–2.00 (2H, m), 3.78 (3H, s), 5.12–5.14 (1H, m), 6.87 (2H, d, *J* = 8.8 Hz), 6.97–6.99 (1H, m), 7.33 (2H, d, *J* = 8.8 Hz), 8.19–8.21 (1H, m), 8.63–8.66 (2H, m), 8.76–8.78 (1H, m). MS (ESI/APCI) mass calculated for [M + H]⁺ (C₁₇H₁₉N₄O₂) requires *m/z* 311.14, found *m/z* 311.1. HPLC purity: 99.3%.

N-(1-(4-Methoxyphenyl)propyl)-2-methylpyrazolo[1,5-*a*]pyrimidine-3-carboxamide (**3a**). To a mixture of **15a** (128 mg, 0.720 mmol), **22a** (160 mg, 0.793 mmol) and Et₃N (0.151 mL, 1.08 mmol) in DMF (5 mL) were added HOBt·H₂O (133 mg, 0.868 mmol) and EDCI·HCl (166 mg, 0.866 mmol). The mixture was stirred at rt for 5 h and then poured into NaHCO₃ aqueous solution, extracted with EtOAc, washed with water, dried over anhydrous Na₂SO₄ and concentrated in vacuo. The residue was purified by column chromatography (silica gel, hexane/ethyl acetate, 2:3 to 0:100) to afford **3a** (171 mg, 0.528 mmol, 73%) as a colorless oil. ¹H NMR (300 MHz, DMSO-*d*₆) δ 0.89 (3H, t, *J* = 7.4 Hz), 1.75–1.91 (2H, m), 2.62 (3H, s), 3.73 (3H, s), 4.88–5.03 (1H, m), 6.85–6.95 (2H, m), 7.21 (1H, dd, *J* = 6.8, 4.2 Hz), 7.25–7.34 (2H, m), 8.43 (1H, d, *J* = 8.3 Hz), 8.78 (1H, dd, *J* = 4.2, 1.5 Hz), 9.20 (1H, dd, *J* = 7.0, 1.7 Hz). MS (ESI/APCI) mass calculated for [M + H]⁺ (C₁₈H₂₁N₄O₂) requires *m/z* 325.2, found *m/z* 325.3. HPLC purity: 100%.

N-(1-(4-Methoxyphenyl)propyl)-5-methylpyrazolo[1,5-*a*]pyrimidine-3-carboxamide (**3b**). To a mixture of **15c** (98.1 mg, 0.554 mmol), **22a** (123 mg, 0.610 mmol), and Et₃N (0.116 mL, 0.832 mmol)

in DMF (5 mL) were added HOBt·H₂O (102 mg, 0.666 mmol) and EDCI·HCl (127 mg, 0.662 mmol). The mixture was stirred at rt for 5 h and then poured into NaHCO₃ aqueous solution, extracted with EtOAc, washed with water, dried over anhydrous Na₂SO₄ and concentrated in vacuo. The residue was purified by column chromatography (silica gel, hexane/ethyl acetate, 1:1 to 0:100). The product was crystallized from hexane/ethyl acetate (5:1) to afford **3b** (109 mg, 0.335 mmol, 61%) as a white solid. ¹H NMR (300 MHz, DMSO-*d*₆) δ 0.88 (3H, t, *J* = 7.4 Hz), 1.73–1.96 (2H, m), 2.67 (3H, s), 3.73 (3H, s), 4.95 (1H, q, *J* = 7.2 Hz), 6.87–6.96 (2H, m), 7.16 (1H, d, *J* = 6.8 Hz), 7.26–7.34 (2H, m), 8.40 (1H, d, *J* = 8.3 Hz), 8.46 (1H, s), 9.15 (1H, d, *J* = 7.2 Hz). MS (ESI/APCI) mass calculated for [M + H]⁺ (C₁₈H₂₁N₄O₂) requires *m/z* 325.2, found *m/z* 325.3. HPLC purity: 100%. mp 89 °C.

N-(1-(4-Methoxyphenyl)propyl)-6-methylpyrazolo[1,5-*a*]pyrimidine-3-carboxamide (**3c**). The title compound was prepared in 84% yield as a yellow oil from **15b** and **21a** using the procedure analogous to that described for the synthesis of **2**. ¹H NMR (400 MHz, CDCl₃) δ 0.97 (3H, t, *J* = 7.6 Hz), 1.92–1.97 (2H, m), 2.44 (3H, s), 3.78 (3H, s), 5.11–5.13 (1H, m), 6.87 (2H, d, *J* = 8.8 Hz), 7.32 (2H, d, *J* = 8.8 Hz), 8.16 (1H, d, *J* = 8.0 Hz), 8.51 (1H, d, *J* = 2.0 Hz), 8.55 (1H, d, *J* = 1.2 Hz), 8.58 (1H, s). MS (ESI/APCI) mass calculated for [M + H]⁺ (C₁₈H₂₁N₄O₂) requires *m/z* 325.2, found *m/z* 325.2. HPLC purity: 99.9%.

N-(1-(4-Methoxyphenyl)propyl)-5,7-dimethylpyrazolo[1,5-*a*]pyrimidine-3-carboxamide (**3d**). The title compound was prepared in 53% yield as a white solid from **15d** and **22a** using the procedure analogous to that described for the synthesis of **3b**. ¹H NMR (300 MHz, DMSO-*d*₆) δ 0.82–0.94 (3H, m), 1.75–1.94 (2H, m), 2.63 (3H, s), 2.74 (3H, d, *J* = 0.8 Hz), 3.73 (3H, s), 4.88–5.03 (1H, m), 6.87–6.96 (2H, m), 7.13 (1H, d, *J* = 0.8 Hz), 7.24–7.36 (2H, m), 8.42–8.56 (2H, m). MS (ESI/APCI) mass calculated for [M + H]⁺ (C₁₉H₂₃N₄O₂) requires *m/z* 339.2, found *m/z* 339.2. HPLC purity: 100%. mp 129 °C.

6-Chloro-*N*-(1-(4-methoxyphenyl)propyl)pyrazolo[1,5-*a*]pyrimidine-3-carboxamide (**3e**). To a mixture of **15e** (200 mg, 1.01 mmol) and **21a** (176 mg, 1.06 mmol) in DMF (8 mL) were added

HOBt·H₂O (186 mg, 1.21 mmol) and EDCI·HCl (233 mg, 1.21 mmol). The mixture was stirred for 2 h and then poured into NaHCO₃ aqueous solution. The mixture was extracted with EtOAc, washed with water, dried over anhydrous Na₂SO₄ and concentrated in vacuo. The residue was purified by column chromatography (basic silica gel, hexane/ethyl acetate, 19:1 to 2:3) to afford **3e** (234 mg, 0.678 mmol, 67%) as a white solid after crystallization from hexane/ethyl acetate (5:1). ¹H NMR (300 MHz, DMSO-*d*₆) δ 0.89 (3H, t, *J* = 7.3 Hz), 1.73–1.93 (2H, m), 3.73 (3H, s), 4.96 (1H, q, *J* = 7.3 Hz), 6.82–6.95 (2H, m), 7.23–7.34 (2H, m), 8.08 (1H, d, *J* = 8.7 Hz), 8.59 (1H, s), 8.91 (1H, d, *J* = 2.3 Hz), 9.75 (1H, d, *J* = 2.3 Hz). MS (ESI/APCI) mass calculated for [M + H]⁺ (C₁₇H₁₈ClN₄O₂) requires *m/z* 345.1, found *m/z* 345.2. HPLC purity: 100%. mp 102 °C. Anal. Calcd for C₁₇H₁₇ClN₄O₂: C, 59.22; H, 4.97; N, 16.25. Found: C, 59.26; H, 4.98; N, 16.10.

6-Cyclopropyl-N-(1-(4-methoxyphenyl)propyl)pyrazolo[1,5-a]pyrimidine-3-carboxamide (3f). To a mixture of **11** (150 mg, 0.385 mmol), cyclopropylboronic acid (49.7 mg, 0.579 mmol) and potassium *tert*-butoxide (143 mg, 1.27 mmol) in toluene (5 mL) were added Pd(OAc)₂ (4.3 mg, 0.02 mmol) and tricyclohexylphosphine (10.8 mg, 0.04 mmol). The mixture was stirred at 100 °C for 16 h under Ar and then poured into water. The mixture was extracted with EtOAc, dried over anhydrous Na₂SO₄ and concentrated in vacuo. The residue was purified by column chromatography (silica gel, hexane/ethyl acetate, 19:1 to 1:4) to afford **3f** (13.9 mg, 0.040 mmol, 10%) as a pale yellow oil. ¹H NMR (300 MHz, CDCl₃) δ 0.74–0.84 (2H, m), 0.97 (3H, t, *J* = 7.4 Hz), 1.07–1.18 (2H, m), 1.84–2.07 (3H, m), 3.78 (3H, s), 5.12 (1H, q, *J* = 7.6 Hz), 6.81–6.92 (2H, m), 7.28–7.37 (2H, m), 8.17 (1H, d, *J* = 8.3 Hz), 8.47 (1H, d, *J* = 1.9 Hz), 8.52 (1H, d, *J* = 1.9 Hz), 8.58 (1H, s). MS (ESI/APCI) mass calculated for [M + H]⁺ (C₂₀H₂₃N₄O₂) requires *m/z* 351.2, found *m/z* 351.2. HPLC purity: 95.6%.

N-(1-(4-Methoxyphenyl)propyl)-6-phenylpyrazolo[1,5-a]pyrimidine-3-carboxamide (3g). Into a microwave vial equipped with a magnetic stirrer were added **11** (120 mg, 0.308 mmol), phenylboronic acid (41.3 mg, 0.339 mmol), DME (3 mL), and water (1.5 mL), followed by Pd(Ph₃P)₄ (17.8 mg, 0.02 mmol). The reaction vial was flushed with nitrogen, sealed, and heated by microwave irradiation at

150 °C for 20 min. The mixture was poured into water and extracted with EtOAc. The combined organic phases were dried over anhydrous Na₂SO₄ and concentrated in vacuo. The residue was purified by column chromatography (silica gel, hexane/ethyl acetate, 19:1 to 2:3) to afford **3g** (92 mg, 0.239 mmol, 77%) as a pale yellow solid after crystallization from hexane/ethyl acetate (5:1). ¹H NMR (300 MHz, DMSO-*d*₆) δ 0.91 (3H, t, *J* = 7.2 Hz), 1.77–1.96 (2H, m), 3.73 (3H, s), 4.99 (1H, q, *J* = 7.3 Hz), 6.84–6.98 (2H, m), 7.24–7.38 (2H, m), 7.41–7.62 (3H, m), 7.84–7.97 (2H, m), 8.22 (1H, d, *J* = 8.3 Hz), 8.60 (1H, s), 9.24 (1H, d, *J* = 1.9 Hz), 9.68 (1H, d, *J* = 2.3 Hz). MS (ESI/APCI) mass calculated for [M + H]⁺ (C₂₃H₂₃N₄O₂) requires *m/z* 387.2, found *m/z* 387.1. HPLC purity: 100%. mp 145 °C. Anal. Calcd for C₂₃H₂₂N₄O₂·0.1H₂O: C, 71.15; H, 5.76; N, 14.43. Found: C, 71.15; H, 5.84; N, 14.15.

1-(4-Methoxyphenyl)-N-((6-methylpyrazolo[1,5-a]pyrimidin-3-yl)methyl)propan-1-amine (4). To a mixture of **24** (100 mg, 0.621 mmol), **22a** (188 mg, 0.932 mmol), acetic acid (0.107 mL, 1.86 mmol), and Et₃N (0.104 mL, 0.746 mmol) in CH₃CN (5 mL) at rt was added sodium triacetoxyborohydride (263 mg, 1.24 mmol). The mixture was stirred at rt overnight. The mixture was quenched with saturated aqueous NaHCO₃ at rt and extracted with EtOAc. The organic layer was washed with water and saturated aqueous NaCl, dried over anhydrous MgSO₄, and concentrated in vacuo. The residue was purified by column chromatography (basic silica gel, hexane/ethyl acetate, 9:1 to 1:1) to give **4** (169 mg, 0.544 mmol, 88%) as a pale yellow oil. ¹H NMR (300 MHz, CDCl₃) δ 0.77 (3H, t, *J* = 7.6 Hz), 1.52–1.79 (2H, m), 2.36 (3H, d, *J* = 0.8 Hz), 3.52 (1H, dd, *J* = 7.9, 5.7 Hz), 3.73–3.96 (5H, m), 6.89 (2H, d, *J* = 8.7 Hz), 7.19–7.31 (2H, m), 7.91 (1H, s), 8.31 (1H, d, *J* = 2.3 Hz), 8.41 (1H, dd, *J* = 2.3, 1.1 Hz). MS (ESI/APCI) mass calculated for [M + H]⁺ (C₁₈H₂₃N₄O₂) requires *m/z* 311.2, found *m/z* 311.2 [M + H]⁺. HPLC purity: 100%.

N-(1-(4-Methoxyphenyl)propyl)-N,6-dimethylpyrazolo[1,5-a]pyrimidine-3-carboxamide (5). To a mixture of **15b** (70 mg, 0.40 mmol) and **19** (78 mg, 0.44 mmol) in DMF (5 mL) was added HATU (225 mg, 0.592 mmol), followed by DIEA (102 mg, 0.791 mmol). The mixture was stirred at rt

overnight, and then diluted with EtOAc and washed with saturated aqueous NaHCO₃ and saturated aqueous NaCl. The organic layer was dried over anhydrous Na₂SO₄ and concentrated in vacuo. The residue was purified by preparative TLC (petroleum ether/ethyl acetate, 1:1) to give **5** (70 mg, yield 52%) as a yellow oil. ¹H NMR (400 MHz, DMSO-*d*₆) δ 0.91–0.94 (3H, m), 1.92–2.02 (2H, m), 2.34 (3H, s), 2.67–2.72 (3H, m), 3.74 (3H, s), 6.92 (2H, d, *J* = 8.4 Hz), 7.28–7.32 (2H, brs), 8.32 (1H, s), 8.60 (1H, d, *J* = 2.0 Hz), 9.04–9.05 (1H, m). MS (ESI/APCI) mass calculated for [M + H]⁺ (C₁₉H₂₃N₄O₂) requires *m/z* 339.2, found *m/z* 339.2 [M + H]⁺. HPLC purity: 100%.

***N*-(1-(4-Methoxyphenyl)propyl)-6-methylpyrazolo[1,5-*a*]pyrimidine-3-sulfonamide (6)**. To a mixture of **25** (70.2 mg, 0.303 mmol) and **22a** (67.0 mg, 0.33 mmol) in CH₃CN (5 mL) at rt was added DIEA (0.127 mL, 0.741 mmol). The mixture was stirred at rt overnight. The mixture was quenched with water and extracted with EtOAc. The organic layer was washed with water and saturated aqueous NaCl, dried over anhydrous MgSO₄, and concentrated in vacuo. The residue was purified by column chromatography (silica gel, hexane/ethyl acetate, 9:1 to 1:3) to give **6** (106 mg, 0.294 mmol, 97%) as a white solid. ¹H NMR (300 MHz, CDCl₃) δ 0.82 (3H, t, *J* = 7.4 Hz), 1.52–2.00 (2H, m), 2.40 (3H, d, *J* = 0.8 Hz), 3.67 (3H, s), 4.15 (1H, q, *J* = 7.9 Hz), 5.25 (1H, d, *J* = 8.3 Hz), 6.32–6.55 (2H, m), 6.66–6.88 (2H, m), 8.18 (1H, s), 8.30–8.57 (2H, m). MS (ESI/APCI) mass calculated for [M – H][–] (C₁₇H₁₉N₄O₃S) requires *m/z* 359.1, found *m/z* 359.0. HPLC purity: 100%. mp 136 °C. Anal. Calcd for C₁₇H₂₀N₄O₃S: C, 56.65; H, 5.59; N, 15.54. Found: C, 56.71; H, 5.70; N, 15.28.

***N*-(1-(4-Methoxyphenyl)propyl)pyrazolo[1,5-*a*]pyridine-3-carboxamide (7)**. The title compound was prepared in 44% yield as a white solid from pyrazolo[1,5-*a*]pyridine-3-carboxylic acid (**15**) and **21a** using the procedure analogous to that described for the synthesis of **3e**. ¹H NMR (300 MHz, CDCl₃) δ 0.96 (3H, t, *J* = 7.4 Hz), 1.79–2.14 (2H, m), 3.80 (3H, s), 5.07 (1H, q, *J* = 7.6 Hz), 5.97 (1H, d, *J* = 7.9 Hz), 6.80–6.99 (3H, m), 7.28–7.40 (3H, m), 8.12 (1H, s), 8.30 (1H, d, *J* = 9.1 Hz), 8.47 (1H, d, *J* = 6.8 Hz). MS (ESI/APCI) mass calculated for [M + H]⁺ (C₁₈H₂₀N₃O₂) requires *m/z* 310.2, found *m/z* 310.1

[M + H]⁺. HPLC purity: 99.2%. mp 105 °C. Anal. Calcd for C₁₈H₁₉N₃O₂: C, 69.88; H, 6.19; N, 13.58. Found: C, 69.77; H, 6.18; N, 13.50.

4-(1-(4-Methoxyphenyl)propyl)-4,5-dihydro-3H-pyrazolo[4,5,1-ij][1,6]naphthyridin-3-one (8). To a solution of **30** (664 mg, 1.96 mmol) in DMF (20 mL) was added EDCI·HCl (413 mg, 2.15 mmol), followed by HOBt·H₂O (330 mg, 2.15 mmol). The mixture was stirred at rt for 16 h and then poured into water. The mixture was extracted with EtOAc, washed with water and saturated aqueous NaCl, dried over anhydrous Na₂SO₄, and concentrated in vacuo. The residue was purified by column chromatography (silica gel, hexane/ethyl acetate, 19:1 to 0:100) to afford **8** (535 mg, 1.67 mmol, 85%) as a white solid after crystallization from hexane/ethyl acetate (4:1). ¹H NMR (300 MHz, DMSO-*d*₆) δ 0.90 (3H, t, *J* = 7.4 Hz), 1.91–2.16 (2H, m), 3.73 (3H, s), 4.33 (1H, d, *J* = 18.6 Hz), 4.83 (1H, d, *J* = 18.6 Hz), 5.84–5.96 (1H, m), 6.86–6.96 (2H, m), 6.96–7.05 (1H, m), 7.13–7.21 (1H, m), 7.24–7.32 (2H, m), 8.27 (1H, s), 8.63 (1H, d, *J* = 6.8 Hz). MS (ESI/APCI) mass calculated for [M + H]⁺ (C₁₉H₂₀N₃O₂) requires *m/z* 322.2, found *m/z* 322.1. HPLC purity: 100%. mp 137 °C. Anal. Calcd for C₁₉H₁₉N₃O₂: C, 71.01; H, 5.96; N, 13.08. Found: C, 70.89; H, 6.01; N, 12.88.

6-Methyl-N-(1-phenylpropyl)pyrazolo[1,5-a]pyrimidine-3-carboxamide (9a). The title compound was prepared in 28% yield as a white solid from **15b** and 1-phenylpropan-1-amine using the procedure analogous to that described for the synthesis of **2**. ¹H NMR (400 MHz, CDCl₃) δ 0.99 (3H, t, *J* = 7.6 Hz), 1.93–2.00 (2H, m), 2.44 (3H, s), 5.16–5.22 (1H, m), 7.21–7.25 (1H, m), 7.31–7.35 (2H, m), 7.39–7.40 (2H, m), 8.23 (1H, d, *J* = 8.0 Hz), 8.53 (1H, d, *J* = 2.0 Hz), 8.56 (1H, s), 8.58 (1H, s). MS (ESI/APCI) mass calculated for [M + H]⁺ (C₁₇H₁₉N₄O) requires *m/z* 295.2, found *m/z* 295.1. HPLC purity: 100%. mp 116 °C.

6-Methyl-N-(1-phenylethyl)pyrazolo[1,5-a]pyrimidine-3-carboxamide (9b). The title compound was prepared in 84% yield as a white solid from **15b** and 1-phenylethanamine using the procedure analogous to that described for the synthesis of **3e**, except that silica gel was employed in place of basic silica gel in a column chromatographic separation. ¹H NMR (300 MHz, DMSO-*d*₆) δ 1.52 (3H, d,

$J = 7.2$ Hz), 2.38 (3H, d, $J = 0.8$ Hz), 5.15–5.28 (1H, m), 7.21–7.45 (5H, m), 8.21 (1H, d, $J = 8.0$ Hz), 8.49 (1H, s), 8.75 (1H, d, $J = 2.3$ Hz), 9.15–9.21 (1H, m). MS (ESI/APCI) mass calculated for $[M + H]^+$ ($C_{16}H_{17}N_4O$) requires m/z 281.1, found m/z 281.2. HPLC purity: 99.6%. mp 112 °C.

N-(2,3-Dihydro-1H-inden-1-yl)-6-methylpyrazolo[1,5-a]pyrimidine-3-carboxamide (9c). The title compound was prepared in 69% yield as a white solid from **15b** and 2,3-dihydro-1H-inden-1-amine using the procedure analogous to that described for the synthesis of **3e**, except that silica gel was employed in place of basic silica gel in a column chromatographic separation. 1H NMR (300 MHz, DMSO- d_6) δ 1.80–1.97 (1H, m), 2.35 (3H, d, $J = 0.8$ Hz), 2.51–2.64 (1H, m), 2.79–3.07 (2H, m), 5.57 (1H, q, $J = 8.2$ Hz), 7.16–7.34 (4H, m), 8.12 (1H, d, $J = 8.3$ Hz), 8.56 (1H, s), 8.65 (1H, d, $J = 1.9$ Hz), 9.15–9.20 (1H, m). MS (ESI/APCI) mass calculated for $[M + H]^+$ ($C_{17}H_{17}N_4O$) requires m/z 293.1, found m/z 292.7. HPLC purity: 100%. mp 160 °C.

N-(4-Methoxybenzyl)-6-methylpyrazolo[1,5-a]pyrimidine-3-carboxamide (9d). The title compound was prepared in 84% yield as a yellow oil from **15b** and 1-(4-methoxyphenyl)methanamine using the procedure analogous to that described for the synthesis of **2**. 1H NMR (400 MHz, $CDCl_3$) δ 2.42 (3H, s), 3.79 (3H, s), 4.65 (2H, d, $J = 5.6$ Hz), 6.88 (2H, d, $J = 8.8$ Hz), 7.33 (2H, d, $J = 8.8$ Hz), 8.12 (1H, s), 8.43 (1H, d, $J = 2.0$ Hz), 8.55 (1H, s), 8.63 (1H, s). MS (ESI/APCI) mass calculated for $[M + H]^+$ ($C_{16}H_{17}N_4O_2$) requires m/z 297.1, found m/z 297.2. HPLC purity: 98.0%.

N-(3-Methoxybenzyl)-6-methylpyrazolo[1,5-a]pyrimidine-3-carboxamide (9e). The title compound was prepared in 90% yield as a colorless oil from **15b** and 2,3-dihydro-1H-inden-1-amine using the procedure analogous to that described for the synthesis of **3e**, except that silica gel was employed in place of basic silica gel in a column chromatographic separation. 1H NMR (300 MHz, DMSO- d_6) δ 2.38 (3H, d, $J = 0.8$ Hz), 3.73 (3H, s), 4.56 (2H, d, $J = 6.1$ Hz), 6.78–6.86 (1H, m), 6.88–6.97 (2H, m), 7.19–7.30 (1H, m), 8.31 (1H, t, $J = 5.9$ Hz), 8.52 (1H, s), 8.71 (1H, d, $J = 1.9$ Hz), 9.14–9.21 (1H, m). MS (ESI/APCI) mass calculated for $[M + H]^+$ ($C_{16}H_{16}N_4O_2$) requires m/z 297.1, found m/z 297.2. HPLC purity: 100%.

***N*-(2-Methoxybenzyl)-6-methylpyrazolo[1,5-*a*]pyrimidine-3-carboxamide (9f).** The title compound was prepared in 69% yield as a white solid from **15b** and (2-methoxyphenyl)methanamine using the procedure analogous to that described for the synthesis of **3c**. ¹H NMR (300 MHz, DMSO-*d*₆) δ 2.38 (3H, d, *J* = 0.8 Hz), 3.88 (3H, s), 4.53 (2H, d, *J* = 6.1 Hz), 6.85–6.94 (1H, m), 7.02 (1H, d, *J* = 8.0 Hz), 7.20–7.31 (2H, m), 8.40 (1H, t, *J* = 5.9 Hz), 8.49 (1H, s), 8.74 (1H, d, *J* = 1.9 Hz), 9.14–9.20 (1H, m). MS (ESI/APCI) mass calculated for [M + H]⁺ (C₁₆H₁₇N₄O₂) requires *m/z* 297.1, found *m/z* 297.1. HPLC purity: 100%. mp 171 °C.

6-Methyl-*N*-(4-(trifluoromethoxy)benzyl)pyrazolo[1,5-*a*]pyrimidine-3-carboxamide (9g). The title compound was prepared in 69% yield as a white solid from **15b** and 1-(4-(trifluoromethoxy)phenyl)methanamine using the procedure analogous to that described for the synthesis of **3e**, except that silica gel was employed in place of basic silica gel in a column chromatographic separation. ¹H NMR (300 MHz, DMSO-*d*₆) δ 2.38 (3H, d, *J* = 0.8 Hz), 4.61 (2H, d, *J* = 6.1 Hz), 7.28–7.37 (2H, m), 7.43–7.51 (2H, m), 8.42 (1H, t, *J* = 6.1 Hz), 8.52 (1H, s), 8.71 (1H, d, *J* = 1.9 Hz), 9.15–9.21 (1H, m). MS (ESI/APCI) mass calculated for [M + H]⁺ (C₁₆H₁₄F₃N₄O₂) requires *m/z* 251.1, found *m/z* 351.1. HPLC purity: 100%. mp 111 °C.

6-Methyl-*N*-(1-(4-(trifluoromethoxy)phenyl)propyl)pyrazolo[1,5-*a*]pyrimidine-3-carboxamide (10). The title compound was prepared in 98% yield as a colorless oil from **15b** and 1-(4-(trifluoromethoxy)phenyl)propan-1-amine using the procedure analogous to that described for the synthesis of **3e**, except that silica gel was employed in place of basic silica gel in a column chromatographic separation. ¹H NMR (300 MHz, DMSO-*d*₆) δ 0.92 (3H, t, *J* = 7.4 Hz), 1.78–1.96 (2H, m), 2.39 (3H, s), 5.04 (1H, q, *J* = 7.2 Hz), 7.27–7.39 (2H, m), 7.44–7.57 (2H, m), 8.28 (1H, d, *J* = 7.9 Hz), 8.47 (1H, s), 8.77 (1H, d, *J* = 2.3 Hz), 9.14–9.23 (1H, m). MS (ESI/APCI) mass calculated for [M + H]⁺ (C₁₈H₁₈F₃N₄O₂) requires *m/z* 379.1, found *m/z* 379.1. HPLC purity: 99.0%.

6-Methyl-*N*-((1*R*)-1-(4-(trifluoromethoxy)phenyl)propyl)pyrazolo[1,5-*a*]pyrimidine-3-carboxamide (10a). **10** (1.07 g, 2.78 mmol) was chirally separated utilizing chiral chromatography with a Chiralpak

AD 50 mm ID × 500 mm L column, mobile phase 100% EtOH, and flow rate 60 mL/min, to afford **10a** (475 mg, tR1), which was recrystallized from hexane/ethyl acetate (5:1) to afford **10a** (339 mg, 0.896 mmol, 32%, 64% theoretical) as a white solid. Analytical HPLC analysis carried out on a 4.6 mm ID × 250 mm L Chiralpak AD column with the same eluent as above at a flow rate of 0.5 mL/min indicated that **10a** was of >99.9% ee. ¹H NMR (300 MHz, DMSO-*d*₆) δ 0.93 (3H, t, *J* = 7.3 Hz), 1.79–1.97 (2H, m), 2.39 (3H, s), 5.04 (1H, q, *J* = 7.3 Hz), 7.27–7.40 (2H, m), 7.45–7.57 (2H, m), 8.29 (1H, d, *J* = 7.9 Hz), 8.48 (1H, s), 8.77 (1H, d, *J* = 1.9 Hz), 9.14–9.23 (1H, m). ¹³C NMR (151 MHz, DMSO-*d*₆) δ 10.50, 14.47, 29.07, 53.01, 104.37, 120.00 (q, *J* = 256.0 Hz, 1C), 120.86, 128.11, 135.10, 142.81, 144.03, 145.06, 146.98 (q, *J* = 1.7 Hz, 1C), 154.57, 160.65. MS (ESI/APCI) mass calculated for [M + H]⁺ (C₁₈H₁₈F₃N₄O₂) requires *m/z* 379.1, found *m/z* 379.1. HPLC purity: 99.7%. Anal. Calcd for C₁₈H₁₇F₃N₄O₂: C, 57.14; H, 4.53; N, 14.81. Found: C, 57.07; H, 4.53; N, 14.74. [α]₂₀^D = -175.5 (*c* = 0.94 in MeOH). mp 106 °C.

6-Methyl-N-((1S)-1-(4-(trifluoromethoxy)phenyl)propyl)pyrazolo[1,5-a]pyrimidine-3-carboxamide (10b). **10** (1.07 g, 2.78 mmol) was chirally separated utilizing chiral chromatography with a Chiralpak AD 50 mm ID × 500 mm L column, mobile phase 100% EtOH, and flow rate 60 mL/min, to afford **10b** (452 mg, tR2), which was recrystallized from hexane/ethyl acetate (5:1) to afford **10b** (230 mg, 0.609 mmol, 22%, 44% theoretical) as a white solid. Analytical HPLC analysis carried out on a 4.6 mm ID × 250 mm L Chiralpak AD column with the same eluent as above at a flow rate of 0.5 mL/min indicated that **10b** was of 99.7% ee. ¹H NMR (300 MHz, DMSO-*d*₆) δ 0.93 (3H, t, *J* = 7.3 Hz), 1.78–1.98 (2H, m), 2.39 (3H, s), 5.04 (1H, q, *J* = 7.3 Hz), 7.27–7.39 (2H, m), 7.44–7.57 (2H, m), 8.29 (1H, d, *J* = 7.9 Hz), 8.48 (1H, s), 8.77 (1H, d, *J* = 1.9 Hz), 9.16–9.23 (1H, m). MS (ESI/APCI) mass calculated for [M + H]⁺ (C₁₈H₁₈F₃N₄O₂) requires *m/z* 379.1, found *m/z* 379.1. HPLC purity: 100%. mp 106 °C. Anal. Calcd for C₁₈H₁₇F₃N₄O₂: C, 57.14; H, 4.53; N, 14.81. Found: C, 57.03; H, 4.55; N, 14.72.

6-Bromo-N-(1-(4-methoxyphenyl)propyl)pyrazolo[1,5-a]pyrimidine-3-carboxamide (11). The title compound was prepared in 83% yield as an off-white solid from **15f** and **21a** using the procedure analogous to that described for the synthesis of **3e**. ¹H NMR (300 MHz, DMSO-*d*₆) δ 0.88 (3H, t, *J* = 7.4 Hz), 1.75–1.92 (2H, m), 3.73 (3H, s), 4.89–5.02 (1H, m), 6.83–6.96 (2H, m), 7.22–7.36 (2H, m), 8.07 (1H, d, *J* = 8.3 Hz), 8.56 (1H, s), 8.93 (1H, d, *J* = 2.3 Hz), 9.79 (1H, d, *J* = 2.3 Hz). MS (ESI/APCI) mass calculated for [M + H]⁺ (C₁₇H₁₈BrN₄O₂) requires *m/z* 389.1, found *m/z* 389.0.

Ethyl 2-Methylpyrazolo[1,5-a]pyrimidine-3-carboxylate (13a). The mixture of **11** (1.04 g, 6.16 mmol) and **12a** (1.21 g, 7.39 mmol) in AcOH (20 mL) was stirred at 70 °C for 16 h. The mixture was concentrated in vacuo and then partitioned between EtOAc and NaHCO₃ aqueous solution. The phases were separated and the aqueous phase was extracted with EtOAc. The combined organic phases were dried over anhydrous Na₂SO₄ and concentrated in vacuo. The residue was purified by column chromatography (basic silica gel, hexane/ethyl acetate, 1:1 to 0:100) to afford **13a** (0.870 g, 4.24 mmol, 69%) as a white solid after trituration with hexane/ethyl acetate (5:1). ¹H NMR (300 MHz, DMSO-*d*₆) δ 1.32 (3H, t, *J* = 7.2 Hz), 2.61 (3H, s), 4.30 (2H, q, *J* = 7.1 Hz), 7.22 (1H, dd, *J* = 6.8, 4.2 Hz), 8.77 (1H, dd, *J* = 4.2, 1.9 Hz), 9.15 (1H, dd, *J* = 7.0, 1.7 Hz).

Ethyl 6-Methylpyrazolo[1,5-a]pyrimidine-3-carboxylate (13b). The title compound was prepared in 87% yield as a white solid from **11** and **12b** using the procedure analogous to that described for the synthesis of **13a**. ¹H NMR (300 MHz, CDCl₃) δ 1.42 (3H, t, *J* = 7.0 Hz), 2.44 (3H, s), 4.44 (2H, q, *J* = 6.9 Hz), 8.51 (1H, s), 8.55 (1H, s), 8.66 (1H, d, *J* = 1.9 Hz).

Ethyl 5-Methylpyrazolo[1,5-a]pyrimidine-3-carboxylate (13c). A mixture of **11** (1.05 g, 6.45 mmol) and **12c** (1.71 g, 12.9 mmol) in toluene (10 mL) was stirred at 100 °C for 16 h and then concentrated in vacuo. The residue was purified by column chromatography (silica gel, hexane/ethyl acetate, 19:1 to 0:100) to afford **13c** (0.898 g, 4.37 mmol, 68%) as a beige solid. ¹H NMR (300 MHz, DMSO-*d*₆) δ 1.31 (3H, t, *J* = 7.0 Hz), 2.62 (3H, s), 4.28 (2H, q, *J* = 7.2 Hz), 7.17 (1H, d, *J* = 7.2 Hz), 8.53 (1H, s), 9.11 (1H, d, *J* = 7.2 Hz).

2-Methylpyrazolo[1,5-a]pyrimidine-3-carboxylic Acid (15a). To a solution of **13a** (866 mg, 4.22 mmol) in THF (20 mL) and MeOH (10 mL) was added 1 M NaOH aqueous solution (12.7 mL, 12.7 mmol). The mixture was stirred at 50 °C for 16 h and then concentrated in vacuo. The residue was suspended in water and 1 M HCl aqueous solution (12.7 mL, 12.7 mmol) was added. The resulting solid was collected by filtration, rinsed with water and dried to afford **15a** (649 mg, 3.66 mmol, 87%) as a white solid. ¹H NMR (300 MHz, DMSO-*d*₆) δ 2.60 (3H, s), 7.19 (1H, dd, *J* = 7.2, 4.2 Hz), 8.73 (1H, dd, *J* = 4.2, 1.5 Hz), 9.14 (1H, dd, *J* = 6.8, 1.9 Hz), 12.26 (1H, brs). MS (ESI/APCI) mass calculated for [M + H]⁺ (C₈H₈N₃O₂) requires *m/z* 178.1, found *m/z* 178.1.

6-Methylpyrazolo[1,5-a]pyrimidine-3-carboxylic Acid (15b). A mixture of **13b** (6.44 g, 31.38 mmol), 2 M NaOH aqueous solution (23.5 mL, 47.1 mmol), THF (20 mL) and MeOH (20 mL) was stirred at 60 °C overnight. The mixture was acidified with 10% citric acid aqueous solution. The resulting precipitate was collected by filtration, washed with water and dried to give **15b** (3.91 g, 22.1 mmol, 70%) as a white solid. ¹H NMR (300 MHz, DMSO-*d*₆) δ 2.37 (3H, s), 8.50 (1H, s), 8.71 (1H, d, *J* = 1.9 Hz), 9.09–9.15 (1H, m), 12.33 (1H, brs). MS (ESI/APCI) mass calculated for [M + H]⁺ (C₈H₈N₃O₂) requires *m/z* 178.1, found *m/z* 178.0.

5-Methylpyrazolo[1,5-a]pyrimidine-3-carboxylic Acid (15c). The title compound was prepared in 84% yield as a beige solid from **13c** using the procedure analogous to that described for the synthesis of **15a**. ¹H NMR (300 MHz, DMSO-*d*₆) δ 2.62 (3H, s), 7.15 (1H, d, *J* = 7.2 Hz), 8.49 (1H, s), 9.10 (1H, d, *J* = 7.2 Hz), 12.27 (1H, brs). MS (ESI/APCI) mass calculated for [M + H]⁺ (C₈H₈N₃O₂) requires *m/z* 178.1, found *m/z* 178.1.

5,7-Dimethylpyrazolo[1,5-a]pyrimidine-3-carboxylic Acid (15d). A mixture of **14b** (502 mg, 3.75 mmol) and **12d** (394 mg, 3.94 mmol) in EtOH (8 mL) and AcOH (8 mL) was stirred at 100 °C for 1.5 h and then concentrated in vacuo. To the residue were added EtOH (4 mL). The resulting solid was collected by filtration, rinsed with EtOH (2 mL) and dried to afford **15d** (487 mg, 2.54 mmol, 68%) as a white solid. ¹H NMR (300 MHz, DMSO-*d*₆) δ 2.58 (3H, s), 2.72 (3H, d, *J* = 0.8 Hz), 7.10 (1H, d, *J* =

0.8 Hz), 8.51 (1H, s), 12.20 (1H, brs). MS (ESI/APCI) mass calculated for $[M + H]^+$ ($C_9H_{10}N_3O_2$) requires m/z 192.1, found m/z 192.1.

6-Chloropyrazolo[1,5-a]pyrimidine-3-carboxylic Acid (15e). To a solution of **11** (1.00 g, 6.45 mmol) in EtOH (15 mL) was added 2 M NaOH aqueous solution (9.67 mL, 19.3 mmol). The mixture was stirred at reflux for 20 h. The mixture was concentrated in vacuo (azeotroped with toluene) to give the crude product **14a**. The residue was suspended in EtOH (2 mL) and AcOH (7 mL), and then **12e** (0.721 g, 6.77 mmol) was added. The mixture was stirred at 80 °C for 2 h and then cooled to rt. Water was then added and the precipitate was filtered by filtration, rinsed with water and EtOH, and dried to afford **15e** (0.809 g, 4.10 mmol, 64%) as a beige solid. 1H NMR (300 MHz, DMSO- d_6) δ 8.61 (1H, s), 8.86 (1H, d, $J = 2.3$ Hz), 9.71 (1H, d, $J = 2.3$ Hz), 12.54 (1H, brs). MS (ESI/APCI) mass calculated for $[M - H]^-$ ($C_7H_3ClN_3O_2$) requires m/z 196.0, found m/z 196.0.

6-Bromopyrazolo[1,5-a]pyrimidine-3-carboxylic Acid (15f). To a solution of **14b** (2.63 g, 19.64 mmol) in EtOH (30 mL) and AcOH (30.0 mL) was added **12f** (3.11 g, 20.6 mmol). The mixture was stirred at 80 °C for 1.5 h and then cooled to rt. The resulting solid was collected by filtration, rinsed with water and dried to afford **15f** (3.58 g, 14.8 mmol, 75%) as a beige solid. 1H NMR (300 MHz, DMSO- d_6) δ 8.58 (1H, s), 8.88 (1H, d, $J = 2.3$ Hz), 9.76 (1H, d, $J = 2.3$ Hz), 12.54 (1H, brs).

N-Methoxy-N-methyl-4-(trifluoromethoxy)benzamide (16). To a solution of **16** (9.96 g, 48.3 mmol) in THF (200 mL) was added oxalyl chloride (5.97 mL, 62.8 mmol), followed by a drop of DMF. The mixture was stirred at rt for 4 h and then concentrated in vacuo (azeotroped with toluene) to afford the corresponding acyl chloride as a pale yellow oil. This was dissolved in DMA (150 mL) and then Et_3N (10.1 mL, 72.5 mmol) and *O,N*-dimethylhydroxylamine hydrochloride (6.13 g, 62.8 mmol) were sequentially added. The mixture was stirred for 16 h and poured into water. The mixture was extracted with EtOAc, washed with water and concentrated in vacuo. The residue was purified by column chromatography (silica gel, hexane/ethyl acetate, 100:0 to 1:1) to afford **17** (3.64 g, 14.6 mmol, 30%)

as a colorless oil. ^1H NMR (300 MHz, $\text{DMSO-}d_6$) δ 3.27 (3H, s), 3.55 (3H, s), 7.44 (2H, dd, $J = 8.9$, 0.9 Hz), 7.69–7.78 (2H, m).

1-(4-(Trifluoromethoxy)phenyl)propan-1-one (18b). To a solution of **17** (3.64 g, 14.6 mmol) in THF (40 mL) at 0 °C was added dropwise EtMgBr (1 M in THF, 21.9 mL, 21.9 mmol). The mixture was stirred at rt for 2 h. LC–MS analysis indicated that the starting material still remained. Therefore, further EtMgBr (1 M in THF, 10.0 mL, 10.0 mmol) was added. The mixture was stirred for another 30 min and then poured into 0.5 M HCl aqueous solution, extracted with EtOAc, dried over anhydrous Na_2SO_4 and concentrated in vacuo. The residue was purified by column chromatography (silica gel, hexane/ethyl acetate, 100:0 to 3:1) to afford **18b** (2.73 g, 12.5 mmol, 86%) as a colorless oil. ^1H NMR (300 MHz, $\text{DMSO-}d_6$) δ 1.09 (3H, t, $J = 7.2$ Hz), 3.07 (2H, q, $J = 7.2$ Hz), 7.44–7.56 (2H, m), 8.02–8.16 (2H, m).

1-(4-Methoxyphenyl)-N-methylpropan-1-amine (19). To a mixture of **18a** (1.50 g, 9.14 mmol) and methylamine (27 wt % in methanol, 2.10 g, 18.3 mmol) in MeOH (20 mL) was added titanium tetraisopropoxide (3.11 g, 11.0 mmol) and the mixture was stirred at rt for 5 h. Then sodium borohydride (0.680 g, 18.3 mmol) was added. After the mixture was stirred overnight, it was diluted with NaOH aqueous solution and filtered. The filtrate was extracted with dichloromethane and the organic layer was washed with saturated aqueous NaCl, dried over anhydrous Na_2SO_4 and concentrated in vacuo. The residue was purified by column chromatography (silica gel, hexane/ethyl acetate, 0:100) to give **19** (0.400 g, 2.23 mmol, 25%) as a yellow oil. ^1H NMR (CDCl_3 , 400 MHz) δ 0.79 (3H, t, $J = 7.6$ Hz), 1.55–1.62 (1H, m), 1.71–1.78 (1H, m), 2.27 (3H, s), 3.29–3.33 (1H, m), 3.81 (3H, s), 6.85–6.88 (2H, m), 7.16–7.19 (2H, m).

1-(4-Methoxyphenyl)propan-1-amine (21a). To a solution of **18a** (23.5 g, 143 mmol) and hydroxylammonium chloride (10.9 g, 157 mmol) in EtOH (300 mL) was added Et_3N (21.9 mL, 157 mmol) at rt. The mixture was refluxed for 3 h and then evaporated under reduced pressure to remove EtOH. The residue was partitioned between EtOAc and water, and the organic layer was washed with

saturated aqueous NaCl, dried over anhydrous Na₂SO₄, and concentrated in vacuo to give the crude product **20a** (26.7 g, 149 mmol, ~quant.) as a white solid, which was subjected to the next reaction without further purification. A mixture of **20a** (12.4 g, 69.2 mmol) and 10% Pd/C (containing 50% water, 8.19 g) in EtOH (300 mL) was hydrogenated under balloon pressure at rt overnight. The catalyst was removed by filtration and the filtrate was concentrated in vacuo. The residue was purified by column chromatography (basic silica gel, 200 g, hexane/ethyl acetate, 9:1 to 1:9) to give **21a** (7.56 g, 45.8 mmol, 66%) as a pale yellow oil. ¹H NMR (300 MHz, DMSO-*d*₆) δ 0.76 (3H, t, *J* = 7.4 Hz), 1.30–1.64 (2H, m), 1.87 (2H, brs), 3.63 (1H, t, *J* = 6.7 Hz), 3.72 (3H, s), 6.74–6.91 (2H, m), 7.15–7.29 (2H, m). MS (ESI/APCI) mass calculated for [M – NH₂]⁺ (C₁₀H₁₃O) requires *m/z* 149.1, found *m/z* 149.2.

1-(4-(Trifluoromethoxy)phenyl)propan-1-amine (21b). The crude product **20b** was prepared in 99% yield as a colorless oil from **18b** using the procedure analogous to that described for the synthesis of **20a**. ¹H NMR (300 MHz, DMSO-*d*₆) δ 1.04 (3H, t, *J* = 7.6 Hz), 2.72 (2H, q, *J* = 7.6 Hz), 7.31–7.44 (2H, m), 7.70–7.82 (2H, m), 11.29 (1H, s). A mixture of **20b** (2.89 g, 12.4 mmol) and 10% Pd/C (containing 50% water, 800 mg) in MeOH (30 mL) was hydrogenated under balloon pressure at rt overnight. The catalyst was removed by filtration and the filtrate was concentrated in vacuo to give the crude product **21b** (2.58 g, 11.8 mmol, 95%) as a colorless oil. This material was taken on to the next reaction without further purification. ¹H NMR (300 MHz, DMSO-*d*₆) δ 0.77 (3H, t, *J* = 7.4 Hz), 1.41–1.68 (2H, m), 2.21 (2H, brs), 3.74 (1H, t, *J* = 6.6 Hz), 7.21–7.34 (2H, m), 7.41–7.52 (2H, m).

1-(4-Methoxyphenyl)propan-1-amine Hydrochloride (22a). A mixture of **20a** (26.7 g, 149 mmol) and 10% Pd/C (containing 50% water, 15.8 g) in MeOH (200 mL) was hydrogenated under balloon pressure at rt overnight. The catalyst was removed by filtration and the filtrate was concentrated in vacuo to give the crude product **21a**. The crude material **21a** was diluted with EtOAc (100 mL) and added 1 M HCl solution in diethyl ether (150 mL). The resulting solid was collected and washed with EtOAc to give **22a** (27.4 g, 136 mmol, 91%) as a white solid. ¹H NMR (300 MHz, DMSO-*d*₆) δ 0.74

(3H, t, $J = 7.4$ Hz), 1.58–2.13 (2H, m), 3.76 (3H, s), 4.04 (1H, dd, $J = 9.5, 5.3$ Hz), 6.84–7.12 (2H, m), 7.29–7.61 (2H, m), 8.44 (3H, brs).

1-(4-(Trifluoromethoxy)phenyl)propan-1-amine Hydrochloride (22b). The crude product **21b** (11.3 g, 51.4 mmol) was dissolved in EtOAc (70 mL) and MeOH (10 mL) and then 4 M HCl solution in EtOAc (40 mL) was added. After 20 min of stirring (no precipitate occurred), the solvent was removed under reduced pressure. To the residual white solid was added Et₂O and the resulting solid was collected by filtration, rinsed with Et₂O and dried to afford **22b** (10.1 g, 39.6 mmol, 67%) as a white solid. ¹H NMR (300 MHz, DMSO-*d*₆) δ 0.76 (3H, t, $J = 7.4$ Hz), 1.70–2.11 (2H, m), 4.20 (1H, dd, $J = 9.1, 5.7$ Hz), 7.39–7.53 (2H, m), 7.61–7.71 (2H, m), 8.63 (3H, brs).

6-Methylpyrazolo[1,5-*a*]pyrimidine-3-carbaldehyde (24). To a solution of **23** (5.91 g, 44.4 mmol) in DMF (50 mL) was added phosphorus oxychloride (12.4 mL, 133 mmol) at 0 °C. The mixture was stirred at rt for 3 h. The mixture was neutralized with 8 M NaOH aqueous solution and extracted with EtOAc/THF (2:1). The organic layer was dried over anhydrous MgSO₄ and was passed through a silica gel pad (eluted with THF). The appropriate fraction was concentrated in vacuo and the obtained solid was collected by filtration, washed with cold EtOAc, and dried to give **24** (5.86 g, 36.4 mmol, 82%) as a yellow solid. ¹H NMR (300 MHz, CDCl₃) δ 2.48 (3H, s), 8.54 (1H, s), 8.60 (1H, s), 8.66 (1H, d, $J = 1.9$ Hz), 10.27 (1H, s). MS (ESI/APCI) mass calculated for [M + H]⁺ (C₈H₈N₃O) requires m/z 162.1, found m/z 162.2.

6-Methylpyrazolo[1,5-*a*]pyrimidine-3-sulfonyl chloride (25). 6-Methylpyrazolo[1,5-*a*]pyrimidine (**23**) (300 mg, 2.25 mmol) was added to chlorosulfonic acid (1.50 mL, 22.5 mmol). The mixture was stirred at 80 °C for 2 h, and then poured into iced water. The precipitate was collected, washed with water, and dried to give **25** (135 mg, 0.583 mmol, 26%) as a white solid. ¹H NMR (300 MHz, CDCl₃) δ 2.53 (3H, d, $J = 1.1$ Hz), 8.52 (1H, s), 8.66 (1H, dd, $J = 2.3, 1.1$ Hz), 8.82 (1H, d, $J = 1.9$ Hz).

Methyl 4-(Hydroxymethyl)pyrazolo[1,5-*a*]pyridine-3-carboxylate (27a). A solution of hydroxylamine-*O*-sulfonic acid (HOSA) (2.07 g, 18.3 mmol) in water (10 mL) was basified with

saturated aqueous NaHCO₃ at 0 °C. To this mixture was added a solution of **26** (1.00 g, 9.16 mmol) in MeOH (10 mL) at the same temperature, and the mixture was heated at 50 °C for 16 h. The mixture was diluted with toluene, and concentrated in vacuo (this protocol was repeated 3 times). The residual solid was suspended in DMF (23 mL), to which methyl propiolate (0.897 mL, 10.1 mmol) and potassium carbonate (3.80 g, 27.5 mmol) were successively added at 0 °C. After vigorous stirring at rt for 2 h, the mixture was filtered by filtration. The filtrate was partitioned between EtOAc and water. The phases were separated and the aqueous phase was extracted with EtOAc. The combined organic phases were washed with water, dried over anhydrous Na₂SO₄, and concentrated in vacuo. The residue was purified by column chromatography (silica gel, hexane/ethyl acetate, 19:1 to 1:4) to afford **27a** (0.556 g, 2.70 mmol, 29%) and methyl 6-(hydroxymethyl)pyrazolo[1,5-*a*]pyridine-3-carboxylate (**27b**) (0.311 g, 1.51 mmol, 16%) as white solids. Data for **27a**: ¹H NMR (300 MHz, DMSO-*d*₆) δ 3.80 (3H, s), 5.04 (2H, d, *J* = 5.7 Hz), 5.37 (1H, t, *J* = 5.7 Hz), 7.10–7.21 (1H, m), 7.65 (1H, dd, *J* = 7.2, 1.1 Hz), 8.44 (1H, s), 8.70–8.78 (1H, m). MS (ESI/APCI) mass calculated for [M + H]⁺ (C₁₀H₁₁N₂O₃) requires *m/z* 207.1, found *m/z* 207.1. Data for **27b**: ¹H NMR (300 MHz, DMSO-*d*₆) δ 3.83 (3H, s), 4.58 (2H, d, *J* = 4.9 Hz), 5.46 (1H, t, *J* = 5.7 Hz), 7.58 (1H, dd, *J* = 9.1, 1.5 Hz), 8.05 (1H, dd, *J* = 9.1, 0.8 Hz), 8.43 (1H, s), 8.67–8.79 (1H, m). MS (ESI/APCI) mass calculated for [M + H]⁺ (C₁₀H₁₁N₂O₃) requires *m/z* 207.1, found *m/z* 207.1.

Methyl 4-Formylpyrazolo[1,5-*a*]pyridine-3-carboxylate (28). To a suspension of **27** (550 mg, 2.67 mmol) in CH₃CN (70 mL) at 0 °C was added portionwise Dess-Martin periodinane (1.36 g, 3.20 mmol). The mixture was stirred at rt for 1.5 h. Further Dess-Martin periodinane (500 mg) was added at rt. Stirring was continued for another 1 h and then NaHCO₃ aqueous solution and solid Na₂S₂O₃ were successively added. After stirring for 20 min, the mixture was extracted with EtOAc, washed with saturated aqueous NaHCO₃ and saturated aqueous NaCl, dried over anhydrous Na₂SO₄, and concentrated in vacuo to afford **28** (545 mg, 2.67 mmol, 100%) as a reddish solid. This was used in the next reaction without further purification. ¹H NMR (300 MHz, DMSO-*d*₆) δ 3.85 (3H, s), 7.29–7.38

(1H, m), 8.06 (1H, dd, $J = 7.6, 1.1$ Hz), 8.64 (1H, s), 9.17 (1H, dd, $J = 6.8, 1.1$ Hz), 10.96 (1H, d, $J = 0.8$ Hz).

Methyl 4-(((1-(4-Methoxyphenyl)propyl)amino)methyl)pyrazolo[1,5-a]pyridine-3-carboxylate (29).

To a mixture of **28** (540 mg, 2.64 mmol), **21a** (612 mg, 3.70 mmol), and acetic acid (0.454 mL, 7.93 mmol) in CH₃CN (25 mL) at 0 °C was added portionwise sodium triacetoxyborohydride (1.18 g, 5.29 mmol). The mixture was stirred at rt for 16 h and then poured into saturated aqueous NaHCO₃. The mixture was extracted with EtOAc, dried over anhydrous Na₂SO₄, and concentrated in vacuo. The residue was purified by column chromatography (basic silica gel, hexane/ethyl acetate, 19:1 to 1:1) to afford **29** (739 mg, 2.09 mmol, 79%) as a colorless oil. ¹H NMR (300 MHz, DMSO-*d*₆) δ 0.68 (3H, t, $J = 7.4$ Hz), 1.36–1.73 (2H, m), 3.31–3.43 (1H, m), 3.73 (3H, s), 3.75 (3H, s), 3.90–4.16 (2H, m), 6.78–6.95 (2H, m), 7.09 (1H, t, $J = 7.0$ Hz), 7.14–7.26 (2H, m), 7.34–7.45 (1H, m), 8.42 (1H, s), 8.65–8.79 (1H, m) (one proton was not observed). MS (ESI/APCI) mass calculated for [M + H]⁺ (C₂₀H₂₄N₃O₃) requires m/z 354.2, found m/z 354.2.

4-(((1-(4-Methoxyphenyl)propyl)amino)methyl)pyrazolo[1,5-a]pyridine-3-carboxylic Acid (30). To a solution of **29** (743 mg, 2.10 mmol) in THF (15 mL) and MeOH (7.5 mL) was added 1 M NaOH aqueous solution (6.31 mL, 6.31 mmol). The mixture was stirred at 50 °C for 30 min and then at 70 °C for 1.5 h. The mixture was acidified with 1 M HCl aqueous solution (12.6 mL, 12.6 mmol) and then evaporated under reduced pressure to remove the organic solvents. The residual aqueous solution was passed through HP20 (DIAIONTM, Mitsubishi Chemical) (eluted with water and then CH₃CN). The acetonitrile fractions containing the desired product was concentrated in vacuo to afford **30** (674 mg, 1.99 mmol, 94%) as a white solid. ¹H NMR (300 MHz, DMSO-*d*₆) δ 0.61–0.77 (3H, m), 1.58–2.05 (2H, m), 3.62–3.93 (5H, m), 3.94–4.09 (1H, m), 6.83–7.03 (3H, m), 7.12 (1H, d, $J = 6.8$ Hz), 7.26–7.43 (2H, m), 8.32 (1H, s), 8.72 (1H, d, $J = 6.8$ Hz), 11.33 (1H, brs) (one proton was not observed). MS (ESI/APCI) mass calculated for [M + H]⁺ (C₁₉H₂₂N₃O₃) requires m/z 340.2, found m/z 340.1 [M + H]⁺.

Enzyme Assay Protocol. *Preparation of human PDE.* Human PDE1A, 3A, 4D2, 5A1, 7B, 8A1, 9A2, and 11A4 enzymes were purchased from BPS Bioscience. Human PDE6AB enzyme was purchased from SB Drug Discovery. Human PDE2A3 full-length gene was transduced into Sf9 cells, and the enzyme was purified by His-tag affinity column and gel filtration. Human PDE10A2 was generated from COS-7 cells that had been transfected with the full-length gene. The enzymes were stored at $-70\text{ }^{\circ}\text{C}$ until use.

PDE2A3 enzyme inhibitory assay. PDE activity was measured using an SPA (Scintillation Proximity Assay) (GE Healthcare). To evaluate the inhibitory activity of a compound, 10 μL of serially diluted compounds were incubated with 20 μL of PDE enzyme (final concentration 0.023 nM) in assay buffer (50 mM HEPES-NaOH, 8.3 mM MgCl_2 , 1.7 mM EGTA, and 0.1% bovine serum albumin (BSA) (pH 7.4)) for 30 min at rt. The final concentration of DMSO in the reaction solution was 1%. Compounds were tested in duplicate in 96-well half-area plates (Corning) or a 384-well OptiPlates (PerkinElmer). We used an 8 concentration serial dilution dose response ranging from 100 μM to 10 pM compound concentrations. To start the reaction, 10 μL of substrate [^3H] cGMP (final concentration 77 nM, PerkinElmer) were added to a total volume of 40 μL . After 60 min at rt, 20 μL of 20 mg/mL yttrium silicate SPA beads containing zinc sulfate were added to terminate the PDE reaction. After allowing to settle for an additional 60 min, the assay plates were counted in a scintillation counter (PerkinElmer) to allow calculation of the inhibition rate. The inhibition rate was calculated based on the 0% control wells with enzyme and DMSO, and the 100% control wells without enzyme. All IC_{50} values were obtained by fitting the results to the following 4 Parameter Logistic Equation:

$$y = A + (B - A) / (1 + (10^{((C - x) * D)}))$$

where A is the minimum y value, B is the maximum y value, C is $\text{Log}(\text{EC}_{50})$ value, and D is the slope factor.

Human PDE enzyme assay. PDE activities were measured using an SPA (GE Healthcare). To evaluate the inhibitory activity, 10 μL of serially diluted compounds were incubated with 20 μL of PDE

enzymes, except for PDE1A, in the following assay buffer: 50 mM HEPES-NaOH, 8.3 mM MgCl₂, 1.7 mM EGTA, and 0.1% BSA (pH 7.4) for 30 min at rt. The PDE1A enzyme assay was performed in the following assay buffer: 50 mM Tris-HCl, 8.3 mM MgCl₂, 0.2 mM CaCl₂, 0.1% BSA, and 30 nM Calmodulin (pH 7.5). The final concentration of DMSO in the assay was 1%, and compounds were tested in duplicate in 96-well half-area plates (Corning). We used an 4 concentration serial dilution dose response ranging from 10 μM to 10 nM compound concentrations. To start the reaction, 10 μL of substrate ([³H] cGMP (final concentration 77 nM, PerkinElmer) for PDE1A, 5A1, 6AB, 9A2, 10A2, and 11A4 or [³H] cAMP (final concentration 14.7 nM, PerkinElmer) for PDE3A, 4D2, 7B, and 8A1) was added for a final assay volume of 40 μL. After 60 min incubation at rt, 20 μL of 20 mg/mL yttrium silicate SPA beads containing zinc sulfate was added to terminate the PDE reaction. After allowing to settle for more than 120 min, the assay plates were counted in a scintillation counter (PerkinElmer) to allow calculation of the inhibition rate.

Estimation of Log *D* at pH 7.4. Log *D*_{7.4}, which is the partition coefficient of the compounds between 1-octanol and aqueous buffer at pH 7.4, was measured using a chromatographic procedure based on a previously published method.⁶⁸ The instruments utilized were a Waters Alliance 2795 HPLC system and a 2996 UV-vis detector (Milford, MA, USA).

In Vitro Metabolic Clearance Assay. In vitro oxidative metabolic studies of the tested compounds were performed using hepatic microsomes obtained from humans, rats or mice. The reaction mixture with a final volume of 0.05 mL consisted of 0.2 mg/mL hepatic microsome in 50 mM KH₂PO₄-K₂HPO₄ phosphate buffer (pH 7.4) and 1 μM test compound. The reaction was initiated by the addition of an NADPH-generating system containing 25 mM MgCl₂, 25 mM glucose 6-phosphate, 2.5 mM β-NADP⁺, and 7.5 unit/mL glucose 6-phosphate dehydrogenase at 20% of the volume of the reaction mixture. After the addition of the NADPH-generating system, the mixture was incubated at 37 °C for 0, 15, and 30 min. The reaction was terminated by adding an equivalent volume of CH₃CN. After the samples were mixed and centrifuged, the supernatant fractions were analyzed using liquid

chromatography tandem mass spectrometry (LC–MS/MS). For metabolic clearance determinations, chromatograms were analyzed for the disappearance rate of the parent compound from the reaction mixtures. All incubations were made in duplicate.

Transcellular Transport Study Using a Transporter-Expression System. Human MDR1-expressing LLC-PK1 cells were cultured as reported previously with minor modifications.¹⁰⁶ The transcellular transport study was performed as reported previously.¹⁰⁷ In brief, the cells were grown for 7 days in an HTS Transwell 96-well permeable support (pore size: 0.4 μm , surface area: 0.143 cm^2) with a polyethylene terephthalate membrane (Corning Life Sciences, Lowell, MA, USA) at a density of 1.125×10^5 cells/well. The cells were preincubated with M199 at 37 °C for 30 min. Subsequently, transcellular transport was initiated by the addition of M199 either to apical compartments (75 μL) or to basolateral compartments (250 μL) containing 10 μM digoxin, 200 μM lucifer yellow as a marker for the monolayer tightness, and 10 μM test compounds, and then terminated by the removal of each assay plate after 2 h. Aliquots (25 μL) from the opposite compartments were mixed with acetonitrile containing alprenolol and diclofenac as internal standards, and then centrifuged. The compound concentrations in the supernatant were measured by LC–MS/MS. The apparent permeability (P_{app}) of test compounds in the receiver wells was determined and the efflux ratio (ER) for the MDR1 membrane permeability test was calculated using the following equation:

$$\text{ER} = P_{\text{app,BtoA}}/P_{\text{app,AtoB}}$$

where $P_{\text{app,AtoB}}$ is the apical-to-basal passive permeability–surface area product and $P_{\text{app,BtoA}}$ is the basal-to-apical passive permeability–surface area product.

Protein Expression and Purification. Human PDE2A catalytic domain (residues 578–919) for crystallographic study was purified from insect cells as a fusion protein with an N-terminal 6 \times histidine tag and adjacent tobacco etch virus (TEV) protease cleavage site. An extra His–Ala sequence was added prior to Ser578 of the PDE2A sequence, based on the previously described structure.¹⁰⁸ The

histidine-tagged PDE2A was expressed in Sf9 insect cells, and the harvested cell pellets were suspended in lysis buffer (50 mM Tris-HCl (pH 8.0), 1 mM DTT, 1 mM EDTA, and 10% glycerol), followed by centrifugation. The supernatant was supplemented with 300 mM NaCl and 20 mM imidazole and loaded onto a nickel–nitrilotriacetic acid (Ni–NTA) Superflow™ cartridge (QIAGEN). The PDE2A bound resin was washed with wash buffer (50 mM Tris-HCl (pH 8.0), 10% glycerol, 300 mM NaCl, and 20 mM imidazole), and eluted with wash buffer containing 250 mM imidazole. The eluted histidine-tagged PDE2A catalytic domain was desalted using a HiPrep 26/10 Desalting column (GE Healthcare) with tris-buffered saline (TBS) (pH 7.4), 0.5 mM DTT, 1 mM EDTA, and 10% glycerol. The histidine-tagged protein was cleaved at the TEV cleavage site by TEV protease treatment. After TEV cleavage, the digested protein was passed through the Ni–NTA Superflow™ cartridge to remove the unwanted histidine-tagged fragments and histidine-tagged TEV proteases, followed by ion exchange chromatography using a MonoQ 10/100 GL column (GE Healthcare) in basal buffer (50 mM Tris-HCl (pH 8.0), 1 mM DTT, and 10% glycerol) with a 0–500 mM NaCl linear gradient. Subsequently, the purified catalytic domain was further treated with HiLoad 26/60 Superdex200 column (GE Healthcare), concentrated by ultrafiltration to 9.5 mg/mL, and stored at –80 °C until use.

Crystallization and Structure Determination. Crystals were obtained using the sitting-drop vapor-diffusion method by mixing 50 nL of protein solution (9.5 mg/mL PDE2A catalytic domain in 1 mM **10a**, TBS (pH 7.4), 0.5 mM DTT, 1 mM EDTA, and 10% glycerol) and 50 nL of reservoir solution containing 0.1 M Tris-HCl (pH 7.5), 410 mM MgCl₂, and 29.3% PEG 3350 at 20 °C. Complex crystals were transferred into liquid nitrogen and stored until data collection. Diffraction data were collected from a single crystal at the Advanced Light Source beamline 5.0.3 (Berkeley, CA) for compounds **10a**, and processed using the program HKL2000.¹⁰⁸ The structures were determined by molecular replacement using MOLREP,¹⁰⁹ utilizing the previously reported coordinate of PDE2A with the PDB accession code 5XKM.¹¹⁰ Subsequently, the structures were refined through an iterative procedure utilizing REFMAC¹¹¹ followed by model building with WinCoot.¹¹² The dictionary files for

the inhibitors were prepared using AFITT (OpenEye Scientific Software). X-ray data collection and refinement statistics for the crystal structure of PDE2A in complex with compound **10a** were summarized in Table 1-7.

Table 1-7. X-ray Data Collection and Refinement Statistics for the Crystal Structure of PDE2A in Complex with Compound **10a**

10a	
Data Collection	
X-ray source	ALS BL5.0.3
Wavelength (Å)	0.97645
Space group	P1
Unit cell dimensions (Å)	a = 72.9, b = 89.8, c = 90.3, α = 107.3, β = 113.9, γ = 89.8
Resolution (Å)	2.20
Unique reflections	100556
Redundancy	1.8
Completeness (%)	96.8 (93.4)
I/ σ (I)	8.5 (1.5)
R _{sym} ^a	0.090 (0.554)
Refinement	
Reflections used	95501
RMS Bonds (Å)	0.006
RMS Angles (°)	0.946
Average B value (Å ²)	28.6
R-value ^b	0.2061
R _{free} ^b	0.2632

^a R_{sym} = $\Sigma h \Sigma j | \langle I(h) \rangle - I(h) | / \Sigma h \Sigma j \langle I(h) \rangle$, where $\langle I(h) \rangle$ is the mean intensity of symmetry-related reflections. ^b R-value = $\Sigma | |F_{obs}| - |F_{calc}| | / \Sigma |F_{obs}|$. R_{free} for 5% of reflections excluded from refinement. Values in parentheses are for the highest resolution shell.

Animal Experiments. The care and use of animals and the experimental protocols were approved by the Experimental Animal Care and Use Committee of Takeda Pharmaceutical Company Limited.

Pharmacokinetic Analysis in Rat or Mouse Cassette Dosing. Compound **10a** was administered intravenously (0.1 mg/kg) or orally (1 mg/kg) by cassette dosing to nonfasted male Crl:CD(SD)(IGS) rats (8W, $n = 3$) or male ICR mice (8W, $n = 3$). The combination for a cassette dosing was determined to avoid combinations of compounds with the same molecular weight. The solution of compounds in dimethylacetamide containing 50% (v/v) 1,3 butanediol at 0.1 mg/mL/kg was administered intravenously to isoflurane-anesthetized mice via femoral vein. The suspension of compounds in 0.5% methyl cellulose with water was used for vehicle (1 mg/kg) and was administered orally by gavage. After administration, blood samples were collected via tail vein by syringes with heparin at 5, 10, 15, 30 min, 1, 2, 4, and 8 h (iv) and 15, 30 min, 1, 2, 4, and 8 h (po), and centrifuged to obtain the plasma fraction. The plasma samples were deproteinized by mixing with acetonitrile followed by centrifugation. The compound concentrations in the supernatant were measured by LC–MS/MS with a standard curve. Pharmacokinetic parameters were calculated by the non-compartmental analysis. The area under the concentration-time curve (AUC) and the area under the first moment curve (AUMC) were calculated using the linear trapezoidal method. The mean residence time (MRT) was calculated as $AUMC/AUC$. The total clearance (CL_{total}) was calculated as $dose_{iv}/AUC_{iv}$. The volume of distribution ($V_{d_{ss}}$) was calculated as $CL_{total} \times MRT_{iv}$. Oral bioavailability (F) was calculated as $(AUC_{po}/dose_{po})/(AUC_{iv}/dose_{iv}) \times 100$.

Brain and Plasma Concentrations in Rats and Mice. Compound **10a** was administered orally to non-fasted rats or mice at 1 mg/kg. Blood and brain samples were collected 2 h or 1 h after oral administration to rats or mice, respectively. The blood samples were centrifuged to obtain the plasma fraction. The brain samples were homogenized in 0.1 M phosphate buffer (pH 7.4) to obtain the brain homogenate. The plasma and brain homogenate samples were deproteinized with CH_3CN containing an internal standard. After centrifugation, the compound concentrations in the supernatant were measured by LC–MS/MS.

Measurement of Cyclic Nucleotide Content in the Mouse Brain. *Animals.* Five-week-old male ICR mice were purchased from CLEA Japan, Inc. (Japan). The mice were housed in groups of 5/cage in a light-controlled room (12 h light/dark cycles with lights on at 07:00). Food and water were provided *ad libitum*. After a one-week acclimation period, the six-week-old mice were used for experiments.

Measurements. Compound **10a** was suspended in 0.5% (w/v) methylcellulose in distilled water, and was administered at 10 mL/kg body weight for mice. Mice were administered orally either vehicle or **10a** (10, 30, or 100 mg/kg) after a habituation period of at least 30 min. A microwave fixation system (Muromachi Kikai, Tokyo, Japan) was used to sacrifice unanesthetized mice by exposure of the head to a microwave beam 30 min after administration of **10a**. Brain tissues were isolated and then homogenized in 0.5 M HCl, followed by centrifugation. Concentration of cyclic nucleotides in the supernatant were measured using cyclic AMP EIA kit or cyclic GMP EIA kit (Cayman Chemical, USA) according to the manufacturer's instructions. Values were calculated as pmol/mg tissue weight.

第 2 章に関する実験

***N*-(1-(4-(Trifluoromethoxy)phenyl)propyl)pyrazolo[1,5-*a*]pyrimidine-3-carboxamide (31)**. A mixture of pyrazolo[1,5-*a*]pyrimidine-3-carboxylic acid (**15**) (26.7 mg, 0.16 mmol), 1-(4-(trifluoromethoxy)phenyl)propan-1-amine hydrochloride (**22b**) (46.0 mg, 0.18 mmol), EDCI·HCl (37.6 mg, 0.20 mmol), HOBt·H₂O (30.1 mg, 0.20 mmol), and Et₃N (0.027 mL, 0.20 mmol) in DMF (1.5 mL) was stirred at rt overnight. The mixture was poured into water and extracted with EtOAc. The organic layer was separated, washed with saturated aqueous NaCl, dried over anhydrous MgSO₄, and concentrated in vacuo. The residue was purified by column chromatography (silica gel, hexane/ethyl acetate, 4:1 to 0:100). The desired fractions were collected and concentrated in vacuo. The resulting solid was triturated with *i*-Pr₂O, collected by filtration, rinsed with *i*-Pr₂O, and dried to give **31** (49.2 mg, 0.135 mmol, 83%) as a white solid. ¹H NMR (300 MHz, DMSO-*d*₆) δ 0.93 (3H, t, *J* = 7.4 Hz), 1.81–1.96 (2H, m), 5.05 (1H, q, *J* = 7.2 Hz), 7.25–7.37 (3H, m), 7.47–7.56 (2H, m), 8.32 (1H, d, *J* = 8.0 Hz), 8.56 (1H, s), 8.86 (1H, dd, *J* = 4.2, 1.9 Hz), 9.29–9.37 (1H, m). MS (ESI/APCI) *m/z* 365.2 [M + H]⁺. HPLC purity: 100%.

2-Oxo-N-(1-(4-(trifluoromethoxy)phenyl)propyl)-2,3-dihydropyrido[2,3-*b*]pyrazine-4(1H)-carboxamide (32). To a solution of **13a** (904 mg, 2.62 mmol) in DMF (15 mL) were added **22b** (736 mg, 2.88 mmol) and Et₃N (1.10 mL, 7.85 mmol). The mixture was stirred at rt for 1 h and then poured into NaHCO₃ aqueous solution. The mixture was extracted with EtOAc, washed with 1 M HCl aqueous solution and saturated aqueous NaCl, dried over anhydrous Na₂SO₄ and concentrated in vacuo. The residue was purified by column chromatography (silica gel, hexane/ethyl acetate, 9:1 to 0:100) to afford **32** (910.6 mg, 2.31 mmol, 88%) as a white solid. ¹H NMR (300 MHz, CDCl₃) δ 0.96 (3H, t, *J* = 7.4 Hz), 1.76–1.96 (2H, m), 4.67 (2H, s), 4.90 (1H, q, *J* = 7.2 Hz), 6.99 (1H, dd, *J* = 7.6, 4.9 Hz), 7.12–7.25 (3H, m), 7.30–7.42 (2H, m), 7.99 (1H, dd, *J* = 5.1, 1.7 Hz), 9.91 (1H, s), 10.46 (1H, d, *J* = 7.2 Hz). MS (ESI/APCI) mass calculated for [M + H]⁺ (C₁₈H₁₈F₃N₄O₃) requires *m/z* 395.1, found *m/z* 395.2. HPLC purity: 98.9%. mp 185 °C.

2-Oxo-N-((1R

or

1S)-1-(4-(trifluoromethoxy)phenyl)propyl)-2,3-dihydropyrido[2,3-b]pyrazine-4(1H)-carboxamide

(32a). Resolution of the enantiomers of **32** was carried out chromatographically using a Chiralpak IC 50 mm ID × 500 mm L column (hexane/ethanol, 400:600) at 60 mL/min. Resolution of **32** (907 mg, 2.30 mmol) provided 439 mg of **32a** as the first eluting enantiomer, which was triturated with hexane/ethyl acetate (5:1) to afford **32a** (416.9 mg, 1.03 mmol, 45%, 89% theoretical) as a pale yellow solid. Analytical HPLC analysis carried out on a 4.6 mm ID × 250 mm L Chiralpak IC column with the same eluent as above at a flow rate of 0.5 mL/min indicated that **32a** was of 99.7% ee. ¹H NMR (300 MHz, DMSO-*d*₆) δ 0.88 (3H, t, *J* = 7.3 Hz), 1.70–1.89 (2H, m), 4.41 (2H, s), 4.81 (1H, q, *J* = 6.9 Hz), 7.10 (1H, dd, *J* = 7.7, 5.1 Hz), 7.25–7.37 (3H, m), 7.38–7.51 (2H, m), 8.02 (1H, dd, *J* = 5.1, 1.7 Hz), 10.34 (1H, d, *J* = 7.5 Hz), 10.82 (1H, brs). MS (ESI/APCI) mass calculated for [M + H]⁺ (C₁₈H₁₈F₃N₄O₃) requires *m/z* 395.1, found *m/z* 395.2. HPLC purity: 97.9%. Anal. Calcd for C₁₈H₁₇F₃N₄O₃: C, 54.82; H, 4.35; N, 14.21. Found: C, 55.01; H, 4.59; N, 14.12.

2-Oxo-N-((1S

or

1R)-1-(4-(trifluoromethoxy)phenyl)propyl)-2,3-dihydropyrido[2,3-b]pyrazine-4(1H)-carboxamide

(32b). Resolution of the enantiomers of **32** was carried out chromatographically using a Chiralpak IC 50 mm ID × 500 mm L column (hexane/ethanol, 400:600) at 60 mL/min. Resolution of **32** (907 mg, 2.30 mmol) provided 429 mg of **32b** as the first eluting enantiomer, which was triturated with hexane/ethyl acetate (5:1) to afford **32b** (399 mg, 1.01 mmol, 44%, 88% theoretical) as a pale yellow solid. Analytical HPLC analysis carried out on a 4.6 mm ID × 250 mm L Chiralpak IC column with the same eluent as above at a flow rate of 0.5 mL/min indicated that **32b** was of >99.9% ee. ¹H NMR (300 MHz, DMSO-*d*₆) δ 0.88 (3H, t, *J* = 7.3 Hz), 1.70–1.90 (2H, m), 4.41 (2H, s), 4.81 (1H, q, *J* = 7.0 Hz), 7.11 (1H, dd, *J* = 7.7, 5.1 Hz), 7.26–7.38 (3H, m), 7.38–7.51 (2H, m), 8.02 (1H, dd, *J* = 4.9, 1.5 Hz), 10.35 (1H, d, *J* = 7.2 Hz), 10.83 (1H, brs). MS (ESI/APCI) mass calculated for [M + H]⁺

(C₁₈H₁₈F₃N₄O₃) requires *m/z* 395.1, found *m/z* 395.1. HPLC purity: 100%. Anal. Calcd for C₁₈H₁₇F₃N₄O₃: C, 54.82; H, 4.35; N, 14.21. Found: C, 54.90; H, 4.50; N, 14.15.

2-Oxo-N-(1-(4-(trifluoromethoxy)phenyl)propyl)-1,2-dihydro-1,5-naphthyridine-4-carboxamide

(33). To a mixture of **49** (372 mg, 1.96 mmol), **22b** (650 mg, 2.54 mmol) and DIEA (1.03 mL, 5.87 mmol) in DMF (15 mL) was added HATU (1.12 g, 2.94 mmol). The mixture was stirred at rt for 2.5 h and then poured into water. The mixture was extracted with EtOAc, washed with water and saturated aqueous NaCl, dried over anhydrous Na₂SO₄ and concentrated in vacuo. The residue was purified by column chromatography (silica gel, hexane/ethyl acetate, 4:1 to 0:100), followed by a second column purification (silica gel, hexane/ethyl acetate, 4:1 to 0:100) to afford **33** (341 mg, 0.871 mmol, 45%) as a white solid after recrystallization from ethyl acetate. ¹H NMR (300 MHz, DMSO-*d*₆) δ 0.95 (3H, t, *J* = 7.4 Hz), 1.78–1.92 (2H, m), 5.03 (1H, q, *J* = 6.9 Hz), 7.08 (1H, s), 7.30–7.40 (2H, m), 7.50–7.58 (2H, m), 7.63 (1H, dd, *J* = 8.5, 4.4 Hz), 7.79 (1H, dd, *J* = 8.3, 1.5 Hz), 8.58 (1H, dd, *J* = 4.5, 1.5 Hz), 10.47 (1H, d, *J* = 8.0 Hz), 12.17 (1H, brs). MS (ESI/APCI) mass calculated for [M + H]⁺ (C₁₉H₁₇F₃N₃O₃) requires *m/z* 392.1, found *m/z* 392.2. HPLC purity: 95.7%.

3-Methyl-N-(1-(4-(trifluoromethoxy)phenyl)propyl)pyrazolo[1,5-b][1,2,4]triazine-8-carboxamide

(34). A mixture of compound **54** (30 mg, containing 50% of **52**), **22b** (46 mg, 0.18 mmol), HOBT (24 mg, 0.18 mmol), EDCI (34 mg, 0.18 mmol), and Et₃N (20 mg, 0.20 mmol) in DMF (3 mL) was stirred at 10–15 °C for 16 h. The mixture was diluted with water (15 mL), extracted with EtOAc (10 mL × 3). The combined organic layer was washed with saturated aqueous NaCl (10 mL), dried over anhydrous Na₂SO₄ and concentrated in vacuo. The residue was purified by preparative HPLC (column: Fuji C18 (25 mm ID × 300 mm L), YMC (20 mm ID × 250 mm L); mobile phase A: 0.05% HCl in water; mobile phase B: 0.05% HCl in acetonitrile; flow rate: 25 mL/min), and most of CH₃CN was removed under reduced pressure. The remaining solvent was removed by lyophilization to give **34** (4 mg, 3% in 2 steps) as a yellow solid. ¹H NMR (400 MHz, DMSO-*d*₆) δ 0.93 (3H, t, *J* = 7.2 Hz), 1.81–1.92 (2H, m), 2.63 (3H, s), 4.97–5.06 (1H, m), 7.32 (2H, d, *J* = 8.0 Hz), 7.52 (2H, d, *J* = 8.8 Hz), 8.14 (1H, d, *J*

= 8.4 Hz), 8.56 (1H, s), 8.81 (1H, s). MS (ESI/APCI) mass calculated for $[M + H]^+$ ($C_{17}H_{17}F_3N_5O_2$) requires m/z 380.1, found m/z 380.2. HPLC purity: 100%.

5-Oxo-N-(1-(4-(trifluoromethoxy)phenyl)propyl)-5,6-dihydro-1,6-naphthyridine-8-carboxamide

(35). A solution of impure **59** (370 mg, 93% LC–MS purity) in TFA (3 mL) was stirred at reflux for 16 h. After cooling to rt, the mixture was concentrated in vacuo. The residue was dissolved in CH_2Cl_2 (20 mL) and the solution was washed with saturated $NaHCO_3$ (20 mL). The organic layer was concentrated in vacuo. The residue was purified by column chromatography (silica gel, petroleum ether/ethyl acetate, 2:1 to 0:100), followed by preparative TLC (EtOAc) to afford **35** (30 mg, 0.0767 mmol, 12% in 2 steps from **58**) as a white solid. 1H NMR (400 MHz, $DMSO-d_6$) δ 0.93 (3H, t, $J = 7.2$ Hz), 1.81–1.94 (2H, m), 5.06 (1H, q, $J = 7.2$ Hz), 7.33 (2H, d, $J = 8.0$ Hz), 7.50 (2H, d, $J = 8.8$ Hz), 7.66 (1H, dd, $J = 8.0, 4.8$ Hz), 8.20 (1H, s), 8.66 (1H, dd, $J = 8.0, 2.0$ Hz), 9.09 (1H, dd, $J = 4.8, 2.0$ Hz), 11.01 (1H, d, $J = 7.6$ Hz), 12.17 (1H, brs). MS (ESI/APCI) m/z 392.0 $[M + H]^+$. mp 185 °C.

3-Oxo-N-(1-(4-(trifluoromethoxy)phenyl)propyl)-3,4-dihydroquinoxaline-1(2H)-carboxamide (**36**).

To a solution of **63h** (313 mg, 1.00 mmol) and **22b** (307 mg, 1.20 mmol) in DMF (10 mL) was added Et_3N (418 μ L, 3.00 mmol) at rt. After being stirred at 80 °C for 24 h, the mixture was quenched with water and extracted with EtOAc. The organic layer was separated, washed with water and saturated aqueous NaCl, dried over anhydrous $MgSO_4$ and concentrated in vacuo. The residue was purified by column chromatography (silica gel, hexane/ethyl acetate, 9:1 to 1:1) to give **36** (281 mg, 0.714 mmol, 72%) as a white solid. 1H NMR (300 MHz, $CDCl_3$) δ 0.88 (3H, t, $J = 7.3$ Hz), 1.69–1.86 (2H, m), 4.30–4.52 (2H, m), 4.81 (1H, q, $J = 7.2$ Hz), 5.39 (1H, d, $J = 7.2$ Hz), 6.91–6.97 (1H, m), 7.07–7.37 (7H, m), 8.02 (1H, brs). MS (ESI/APCI) mass calculated for $[M + H]^+$ ($C_{19}H_{19}F_3N_3O_3$) requires m/z 394.1, found m/z 394.1. HPLC purity: 96.9%. mp 198 °C. Anal. Calcd for $C_{19}H_{18}F_3N_3O_3$: C, 58.01; H, 4.61; N, 10.68. Found: C, 58.17; H, 4.70; N, 10.59.

N-(1-(4-Methoxyphenyl)propyl)-2-oxo-2,3-dihydropyrido[2,3-b]pyrazine-4(1H)-carboxamide (**37a**).

To a solution of **62a** (23.5 mg, 0.160 mmol) and Et_3N (65.9 μ L, 0.470 mmol) in THF (5.0 mL) and

DMA (1.0 mL) was added triphosgene (46.8 mg, 0.160 mmol) at 0 °C. After stirring at 0 °C for 2 h, Et₃N (65.9 μL, 0.470 mmol) and **22a** (159 mg, 0.790 mmol) was added at 0 °C. The mixture was stirred at rt for 2 h and then quenched with water. The mixture was extracted with EtOAc, washed with saturated aqueous NaCl, dried over anhydrous Na₂SO₄ and concentrated in vacuo. The residue was purified by column chromatography (basic silica gel, hexane/ethyl acetate, 1:1 to 0:100) to give **37a** (6.33 mg, 0.019 mmol, 12%) as a white solid after trituration with hexane/*i*-Pr₂O. ¹H NMR (300 MHz, CDCl₃) δ 0.79–1.00 (3H, m), 1.76–1.97 (2H, m), 3.78 (3H, s), 4.68 (2H, s), 4.83 (1H, q, *J* = 7.2 Hz), 6.86 (2H, d, *J* = 8.7 Hz), 6.96 (1H, dd, *J* = 7.7, 5.1 Hz), 7.08–7.37 (3H, m), 7.97 (1H, dd, *J* = 5.1, 1.3 Hz), 9.69 (1H, brs), 10.35 (1H, d, *J* = 7.6 Hz). MS (ESI/APCI) mass calculated for [M – H][–] (C₁₈H₁₉N₄O₃) requires *m/z* 339.2, found *m/z* 339.1. HPLC purity: 99.8%.

2-Oxo-N-(1-(4-(trifluoromethyl)phenyl)propyl)-2,3-dihydropyrido[2,3-*b*]pyrazine-4(1H)-carboxamide (37b). To a solution of **63a** (314 mg, 1.00 mmol) in DMF (10 mL) were added **99g** (223 mg, 1.10 mmol) and Et₃N (0.418 mL, 3.00 mmol). The mixture was stirred at rt for 16 h and then concentrated in vacuo. The residue was diluted with water and extracted with EtOAc. The organic layer was separated, washed with saturated aqueous NaHCO₃, water and saturated aqueous NaCl, dried over anhydrous MgSO₄ and concentrated in vacuo. The residue was purified by column chromatography (silica gel, hexane/ethyl acetate, 9:1 to 3:2) to give **37b** (314 mg, 0.830 mmol, 83%) as a colorless prisms after recrystallized from hexane/ethyl acetate. ¹H NMR (300 MHz, CDCl₃) δ 0.97 (3H, t, *J* = 7.3 Hz), 1.89 (2H, quin, *J* = 7.3 Hz), 4.67 (2H, s), 4.93 (1H, q, *J* = 6.8 Hz), 7.01 (1H, dd, *J* = 7.7, 5.1 Hz), 7.19 (1H, dd, *J* = 7.5, 1.5 Hz), 7.44 (2H, d, *J* = 8.3 Hz), 7.58 (2H, d, *J* = 8.3 Hz), 8.01 (1H, dd, *J* = 4.9, 1.5 Hz), 9.16 (1H, brs), 10.48 (1H, d, *J* = 7.2 Hz). MS (ESI/APCI) mass calculated for [M + H]⁺ (C₁₈H₁₈F₃N₄O₂) requires *m/z* 379.1, found *m/z* 379.2. HPLC purity: 100%. mp 105 °C. Anal. Calcd for C₁₈H₁₇F₃N₄O₂: C, 57.14; H, 4.53; N, 14.81. Found: C, 56.89; H, 4.55; N, 14.74.

N-(1-(4-Cyclopropylphenyl)propyl)-2-oxo-2,3-dihydropyrido[2,3-*b*]pyrazine-4(1H)-carboxamide (37c). The title compound was prepared as a pale yellow solid after recrystallization from hexane/ethyl

acetate in 23% yield from **63a** and **99a** using the procedure analogous to that described for the synthesis of **37b**. ¹H NMR (300 MHz, CDCl₃) δ 0.61–0.70 (2H, m), 0.86–0.98 (5H, m), 1.79–1.95 (3H, m), 4.61–4.75 (2H, m), 4.79–4.90 (1H, m), 6.92–7.06 (3H, m), 7.10–7.24 (3H, m), 7.99 (1H, dd, *J* = 5.1, 1.7 Hz), 8.36–8.67 (1H, m), 10.33 (1H, d, *J* = 7.2 Hz). MS (ESI/APCI) mass calculated for [M + H]⁺ (C₂₀H₂₃N₄O₂) requires *m/z* 351.2, found *m/z* 351.2. HPLC purity: 98.0%.

***N*-(1-(4-(Azetidin-1-yl)phenyl)propyl)-2-oxo-2,3-dihydropyrido[2,3-*b*]pyrazine-4(1H)-carboxamide (37d)**. The title compound was prepared as a colorless prisms after recrystallization from hexane/ethyl acetate in 80% yield from **63a** and **99b** using the procedure analogous to that described for the synthesis of **37b**. ¹H NMR (300 MHz, CDCl₃) δ 0.91 (3H, t, *J* = 7.3 Hz), 1.74–1.96 (2H, m), 2.27–2.39 (2H, m), 3.84 (4H, t, *J* = 7.2 Hz), 4.60–4.72 (2H, m), 4.74–4.85 (1H, m), 6.38–6.45 (2H, m), 6.90–6.99 (1H, m), 7.09–7.21 (3H, m), 7.97 (1H, dd, *J* = 5.1, 1.7 Hz), 8.53 (1H, s), 10.24 (1H, d, *J* = 7.9 Hz). MS (ESI/APCI) mass calculated for [M + H]⁺ (C₂₀H₂₄N₅O₂) requires *m/z* 366.2, found *m/z* 366.2. HPLC purity: 100%. mp 176 °C. Anal. Calcd for C₂₀H₂₃N₅O₂: C, 65.73; H, 6.34; N, 19.16. Found: C, 65.73; H, 6.23; N, 18.93.

***2-Oxo-N*-(1-(3-(trifluoromethoxy)phenyl)propyl)-2,3-dihydropyrido[2,3-*b*]pyrazine-4(1H)-carboxamide (37e)**. To a solution of **63a** (369 mg, 1.17 mmol) and **100c** (335 mg, 1.31 mmol) in DMF (10 mL) was added Et₃N (0.409 mL, 2.94 mmol) at rt. After being stirred for 16 h, the mixture was quenched with water and extracted with EtOAc. The organic layer was separated, washed with water and saturated aqueous NaCl, dried over anhydrous MgSO₄ and concentrated in vacuo. The residue was purified by column chromatography (silica gel, hexane/ethyl acetate, 9:1 to 33:67) to give **37e** (202 mg, 0.512 mmol, 44%) as a white solid after recrystallization from hexane/ethyl acetate. ¹H NMR (300 MHz, CDCl₃) δ 0.96 (3H, t, *J* = 7.3 Hz), 1.82–1.93 (2H, m), 4.68 (2H, s), 4.92 (1H, q, *J* = 6.9 Hz), 7.00 (1H, dd, *J* = 7.5, 4.9 Hz), 7.09 (1H, dd, *J* = 7.9, 1.1 Hz), 7.14–7.20 (2H, m), 7.23–7.29 (1H, m), 7.31–7.39 (1H, m), 8.00 (1H, dd, *J* = 4.9, 1.5 Hz), 8.57–8.77 (1H, m), 10.44 (1H, d, *J* = 7.2 Hz). MS (ESI/APCI) mass calculated for [M + H]⁺ (C₁₈H₁₈F₃N₄O₂) requires *m/z* 395.1, found *m/z* 395.2. HPLC

purity: 99.7%. mp 110 °C. Anal. Calcd for C₁₈H₁₇F₃N₄O₃: C, 54.82; H, 4.35; N, 14.21. Found: C, 54.69; H, 4.37; N, 14.16.

2-Oxo-N-(1-(2-(trifluoromethoxy)phenyl)propyl)-2,3-dihydropyrido[2,3-b]pyrazine-4(1H)-carboxamide (37f). The title compound was prepared as a white solid in 78% yield from **63a** and **100d** using the procedure analogous to that described for the synthesis of **37e**. ¹H NMR (300 MHz, DMSO-*d*₆) δ 0.89 (3H, t, *J* = 7.4 Hz), 1.66–1.91 (2H, m), 4.40 (2H, s), 4.97–5.15 (1H, m), 7.11 (1H, dd, *J* = 7.7, 4.9 Hz), 7.26–7.42 (4H, m), 7.44–7.53 (1H, m), 8.00 (1H, dd, *J* = 5.0, 1.6 Hz), 10.41 (1H, d, *J* = 7.7 Hz), 10.80 (1H, s). MS (ESI/APCI) mass calculated for [M + H]⁺ (C₁₈H₁₈F₃N₄O₂) requires *m/z* 395.1, found *m/z* 395.2. HPLC purity: 99.4%. mp 178 °C. Anal. Calcd for C₁₈H₁₇F₃N₄O₃: C, 54.82; H, 4.35; N, 14.21; F, 14.45. Found: C, 55.00; H, 4.49; N, 14.20; F, 14.21.

N-(1-(3-fluoro-4-(trifluoromethoxy)phenyl)propyl)-2-oxo-2,3-dihydropyrido[2,3-b]pyrazine-4(1H)-carboxamide (37g). The title compound was prepared as a white solid after crystallization from hexane/ethyl acetate in 63% yield from **63a** and **100e** using the procedure analogous to that described for the synthesis of **37e**. ¹H NMR (300 MHz, DMSO-*d*₆) δ 0.77–0.95 (3H, m), 1.81 (2H, quin, *J* = 7.3 Hz), 4.35–4.47 (2H, m), 4.81 (1H, q, *J* = 7.2 Hz), 7.11 (1H, dd, *J* = 7.7, 5.1 Hz), 7.27 (1H, d, *J* = 8.3 Hz), 7.32 (1H, dd, *J* = 7.9, 1.5 Hz), 7.44–7.58 (2H, m), 8.02 (1H, dd, *J* = 4.9, 1.5 Hz), 10.30 (1H, d, *J* = 7.2 Hz), 10.81 (1H, s). MS (ESI/APCI) mass calculated for [M + H]⁺ (C₁₈H₁₇F₄N₄O₃) requires *m/z* 413.1, found *m/z* 413.1. HPLC purity: 100%. mp 154 °C. Anal. Calcd for C₁₈H₁₆F₄N₄O₃: C, 52.43; H, 3.91; N, 13.59. Found: C, 52.48; H, 3.89; N, 13.30.

N-(1-(2-Fluoro-4-(trifluoromethoxy)phenyl)propyl)-2-oxo-2,3-dihydropyrido[2,3-b]pyrazine-4(1H)-carboxamide (37h). The title compound was prepared as a white solid after recrystallization from hexane/ethyl acetate in 87% yield from **63a** and **100f** using the procedure analogous to that described for the synthesis of **37e**. ¹H NMR (300 MHz, DMSO-*d*₆) δ 0.89 (3H, t, *J* = 7.2 Hz), 1.70–1.88 (2H, m), 4.40 (2H, s), 5.00 (1H, q, *J* = 7.4 Hz), 7.11 (1H, dd, *J* = 7.9, 4.9 Hz), 7.22 (1H, d, *J* = 8.7 Hz), 7.27–7.42 (2H, m), 7.49 (1H, t, *J* = 8.5 Hz), 8.02 (1H, dd, *J* = 4.9, 1.9 Hz), 10.43 (1H, d, *J* = 7.5 Hz), 10.81

(1H, s). MS (ESI/APCI) mass calculated for $[M + H]^+$ ($C_{18}H_{17}F_4N_4O_3$) requires m/z 413.1, found m/z 413.2. HPLC purity: 97.2%. mp 173.9–176.3 °C.

***N*-(2-Methoxy-1-(4-(trifluoromethoxy)phenyl)ethyl)-2-oxo-2,3-dihydropyrido[2,3-*b*]pyrazine-4(1H)-carboxamide (38a)**. The title compound was prepared as a white solid after trituration with hexane in 55% yield from **63a** and **99i** using the procedure analogous to that described for the synthesis of **32**. 1H NMR (300 MHz, DMSO- d_6) δ 3.28 (3H, s), 3.55–3.71 (2H, m), 4.33–4.50 (2H, m), 4.99–5.13 (1H, m), 7.11 (1H, dd, $J = 7.9, 4.9$ Hz), 7.27–7.39 (3H, m), 7.42–7.53 (2H, m), 8.00 (1H, dd, $J = 4.9, 1.7$ Hz), 10.51 (1H, d, $J = 7.4$ Hz), 10.83 (1H, brs). MS (ESI/APCI) mass calculated for $[M + H]^+$ ($C_{18}H_{18}F_3N_4O_4$) requires m/z 411.1, found m/z 411.1. HPLC purity: 99.8%. mp 163 °C. Anal. Calcd for $C_{18}H_{17}F_3N_4O_4$: C, 52.69; H, 4.18; N, 13.65. Found: C, 52.83; H, 4.33; N, 13.55.

***N*-(3-Methoxy-1-(4-(trifluoromethoxy)phenyl)propyl)-2-oxo-2,3-dihydropyrido[2,3-*b*]pyrazine-4(1H)-carboxamide (38b)**. The title compound was prepared as a white solid in 25% yield from **63a** and **100h** using the procedure analogous to that described for the synthesis of **37e**. 1H NMR (300 MHz, DMSO- d_6) δ 2.01 (2H, q, $J = 6.0$ Hz), 3.21 (3H, s), 3.25–3.33 (2H, m), 4.29–4.51 (2H, m), 5.01 (1H, q, $J = 6.8$ Hz), 7.11 (1H, dd, $J = 7.9, 4.9$ Hz), 7.26–7.37 (3H, m), 7.39–7.50 (2H, m), 8.02 (1H, dd, $J = 4.9, 1.5$ Hz), 10.31 (1H, d, $J = 7.5$ Hz), 10.81 (1H, brs). MS (ESI/APCI) mass calculated for $[M + H]^+$ ($C_{18}H_{18}F_3N_4O_4$) requires m/z 424.1, found m/z 425.2. HPLC purity: 99.8%. mp 132 °C. Anal. Calcd for $C_{19}H_{19}F_3N_4O_4$: C, 53.77; H, 4.51; N, 13.20; F, 13.43. Found: C, 53.50; H, 4.52; N, 13.02; F, 13.37.

2-Oxo-*N*-(1-(4-(trifluoromethoxy)phenyl)butyl)-2,3-dihydropyrido[2,3-*b*]pyrazine-4(1H)-carboxamide (38c). The title compound was prepared as a white solid after crystallization from hexane/ethyl acetate in 73% yield from **63a** and 1-(4-(trifluoromethoxy)phenyl)butan-1-amine hydrochloride using the procedure analogous to that described for the synthesis of **37e**. 1H NMR (300 MHz, $CDCl_3$) δ 0.86–1.01 (3H, m), 1.23–1.51 (2H, m), 1.68–1.94 (2H, m), 4.58–4.75 (2H, m), 4.96 (1H, q, $J = 7.5$ Hz), 7.00 (1H, dd, $J = 7.7, 5.1$ Hz), 7.10–7.22 (3H, m), 7.31–7.38 (2H, m), 8.00 (1H, dd, $J = 4.9, 1.5$ Hz), 8.99 (1H, s), 10.40 (1H, d, $J = 7.5$ Hz). MS (ESI/APCI) mass calculated for $[M + H]^+$ ($C_{19}H_{20}F_3N_4O_3$)

requires m/z 424.1, found m/z 409.2. HPLC purity: 99.7%. mp 171.7–173.7 °C. Anal. Calcd for $C_{19}H_{19}F_3N_4O_3$: C, 55.88; H, 4.69; N, 13.72. Found: C, 55.94; H, 4.78; N, 13.54.

***N*-(2-Hydroxy-1-(4-(trifluoromethoxy)phenyl)ethyl)-2-oxo-2,3-dihydropyrido[2,3-*b*]pyrazine-4(1H)-carboxamide (38d).** A mixture of *tert*-butyl

(2-hydroxy-1-(4-(trifluoromethoxy)phenyl)ethyl)carbamate (**106**) (52 mg, 0.16 mmol) and 2 M HCl solution in EtOH (2 mL, 4.00 mmol) was stirred at 60 °C for 2 min and then concentrated in vacuo.

To the residue were added DMF (2 mL), Et₃N (0.045 mL, 0.32 mmol), and **63a** (50.9 mg, 0.16 mmol) at rt. The mixture was stirred at rt overnight and then poured into saturated aqueous NaCl. The mixture

was extracted with EtOAc, washed with saturated aqueous NaCl, dried over anhydrous MgSO₄, and concentrated in vacuo. The residue was purified by column chromatography (silica gel, hexane/ethyl

acetate, 1:1 to 0:100), followed by a preparative HPLC purification (column: L-Column2 ODS 20 mm ID × 150 mm L; mobile phase A: 0.1% TFA in water; mobile phase B: 0.1% TFA in acetonitrile; flow

rate: 20 mL/min). The desired fraction was neutralized with saturated aqueous NaHCO₃, concentrated in vacuo to remove most of acetonitrile, and extracted with EtOAc. The organic layer was separated,

dried over anhydrous MgSO₄, and concentrated in vacuo to give **38d** (32.2 mg, 0.081 mmol, 50%) as a white solid. ¹H NMR (300 MHz, DMSO-*d*₆) δ 3.51–3.80 (2H, m), 4.29–4.53 (2H, m), 5.09 (1H, t, *J* =

5.1 Hz), 7.11 (1H, dd, *J* = 7.7, 5.1 Hz), 7.28–7.35 (4H, m), 7.40–7.51 (2H, m), 8.01 (1H, dd, *J* = 4.9, 1.5 Hz), 10.39 (1H, d, *J* = 7.2 Hz), 10.79 (1H, brs). MS (ESI/APCI) mass calculated for [M + H]⁺

(C₁₇H₁₆F₃N₄O₄) requires m/z 397.1, found m/z 397.1. HPLC purity: 98.8%. mp 190 °C.

***N*-(2-Hydroxy-2-methyl-1-(4-(trifluoromethoxy)phenyl)propyl)-2-oxo-2,3-dihydropyrido[2,3-*b*]pyrazine-4(1H)-carboxamide (38e).** The title compound was prepared as a white solid after trituration with

hexane/ethyl acetate in 82% yield from **63a** and **108** using the procedure analogous to that described for the synthesis of **37e**. ¹H NMR (300 MHz, CDCl₃) δ 1.16 (3H, s), 1.37 (3H, s), 1.70 (1H, s), 4.55–

4.76 (2H, m), 4.91 (1H, d, *J* = 8.3 Hz), 7.02 (1H, dd, *J* = 7.9, 4.9 Hz), 7.13–7.22 (3H, m), 7.37–7.46 (2H, m), 8.07 (1H, dd, *J* = 4.9, 1.5 Hz), 8.51 (1H, s), 10.93 (1H, d, *J* = 8.3 Hz). MS (ESI/APCI) mass

calculated for $[M + H]^+$ ($C_{19}H_{20}F_3N_4O_4$) requires m/z 425.1, found m/z 425.1. HPLC purity: 99.5%. mp 164.7–168.5 °C. Anal. Calcd for $C_{19}H_{19}F_3N_4O_4$: C, 53.77; H, 4.51; N, 13.20. Found: C, 53.91; H, 4.66; N, 13.22.

***N*-(2-(Methylsulfonyl)-1-(4-(trifluoromethoxy)phenyl)ethyl)-2-oxo-2,3-dihydropyrido[2,3-*b*]pyrazine-4(1*H*)-carboxamide (38f)**. A mixture of *m*-CPBA (68.7 mg, 0.28 mmol) and **64** (54 mg, 0.13 mmol) in EtOAc (10 mL) was stirred at rt overnight. Then saturated aqueous $Na_2S_2O_3$ was added at rt and the mixture was stirred for 5 min at the same temperature. The mixture was poured into saturated aqueous $NaHCO_3$ and extracted with EtOAc. The organic layer was separated, washed with saturated aqueous $NaHCO_3$ and saturated aqueous $NaCl$, dried over anhydrous $MgSO_4$ and concentrated in vacuo. The resulting solid was triturated from hexane/ethyl acetate to give **38f** (38.2 mg, 0.083 mmol, 66%) as a white solid. 1H NMR (300 MHz, $DMSO-d_6$) δ 2.91 (3H, s), 3.63 (1H, dd, $J = 14.7, 4.5$ Hz), 4.00 (1H, dd, $J = 14.5, 9.2$ Hz), 4.26–4.56 (2H, m), 5.46 (1H, td, $J = 8.5, 3.8$ Hz), 7.11 (1H, dd, $J = 7.9, 4.9$ Hz), 7.30 (1H, dd, $J = 7.9, 1.5$ Hz), 7.33–7.41 (2H, m), 7.53–7.61 (2H, m), 7.98 (1H, dd, $J = 4.9, 1.5$ Hz), 10.62 (1H, d, $J = 7.9$ Hz), 10.82 (1H, s). MS (ESI/APCI) mass calculated for $[M + H]^+$ ($C_{18}H_{18}F_3N_4O_5S$) requires m/z 459.1, found m/z 459.2. HPLC purity: 99.7%. mp 147.2–150.8 °C. Anal. Calcd for $C_{18}H_{17}F_3N_4O_5S$: C, 47.16; H, 3.74; N, 12.22. Found: C, 46.92; H, 3.80; N, 12.00.

***N*-(2-Methoxy-1-(4-(trifluoromethoxy)phenyl)ethyl)-6-methyl-2-oxo-2,3-dihydropyrido[2,3-*b*]pyrazine-4(1*H*)-carboxamide (39a)**. To a suspension of **62c** (118 mg, 0.72 mmol) in THF (20 mL) was added triphosgene (171 mg, 0.58 mmol) at rt. The mixture was stirred at 40 °C under Ar for 1 h. After cooling to rt, the mixture was concentrated in vacuo. The residue was diluted with THF and concentrated in vacuo (this procedure was repeated three times). To a solution of the residue in THF (20 mL) were added **100i** (235 mg, 0.87 mmol) and Et_3N (0.302 mL, 2.16 mmol) at rt. The mixture was stirred at rt for 16 h and then poured into water. The mixture was extracted with EtOAc, dried over anhydrous Na_2SO_4 and concentrated in vacuo. The residue was purified by column chromatography (silica gel, hexane/ethyl acetate, 4:1 to 0:100) to give **39a** (58.3 mg, 0.137 mmol,

19%) as a white solid after crystallization from hexane/ethyl acetate (2:1). ¹H NMR (300 MHz, DMSO-*d*₆) δ 2.42 (3H, s), 3.29 (3H, s), 3.56–3.70 (2H, m), 4.39 (2H, s), 4.97–5.09 (1H, m), 6.96 (1H, d, *J* = 8.3 Hz), 7.22 (1H, d, *J* = 8.0 Hz), 7.27–7.37 (2H, m), 7.42–7.53 (2H, m), 10.72 (1H, s), 10.80 (1H, d, *J* = 7.2 Hz). MS (ESI/APCI) mass calculated for [M + H]⁺ (C₁₉H₂₀F₃N₄O₄) requires *m/z* 425.1, found *m/z* 425.2. HPLC purity: 95.1%. mp 175 °C.

***N*-(2-Methoxy-1-(4-(trifluoromethoxy)phenyl)ethyl)-7-methyl-2-oxo-2,3-dihydropyrido[2,3-*b*]pyrazine-4(1*H*)-carboxamide (39b)**. The title compound was prepared as a pale yellow solid in 96% yield following the general procedure described for preparation of compound **37e**, by using **63d** and **100i**. ¹H NMR (300 MHz, DMSO-*d*₆) δ 2.26 (3H, s), 3.28 (3H, s), 3.56–3.68 (2H, m), 4.32–4.48 (2H, m), 4.99–5.11 (1H, m), 7.14 (1H, d, *J* = 1.5 Hz), 7.27–7.37 (2H, m), 7.41–7.51 (2H, m), 7.85 (1H, d, *J* = 1.3 Hz), 10.38 (1H, d, *J* = 7.4 Hz), 10.78 (1H, brs). MS (ESI/APCI) mass calculated for [M + H]⁺ (C₁₉H₂₀F₃N₄O₄) requires *m/z* 425.1, found *m/z* 425.2. HPLC purity: 99.1%. mp 149 °C.

***N*-(2-Methoxy-1-(4-(trifluoromethoxy)phenyl)ethyl)-8-methyl-2-oxo-2,3-dihydropyrido[2,3-*b*]pyrazine-4(1*H*)-carboxamide (39c)**. To a solution of **63a** (82.5 mg, 0.251 mmol) in DMF (5 mL) were added **100i** (68.3 mg, 0.251 mmol) and Et₃N (0.096 mL, 0.689 mmol). The mixture was stirred at rt for 16 h and then poured into NaHCO₃ aqueous solution. The mixture was extracted with EtOAc, washed with 1 M HCl aqueous solution and saturated aqueous NaCl, dried over anhydrous Na₂SO₄ and concentrated in vacuo. The residue was purified by column chromatography (silica gel, hexane/ethyl acetate, 9:1 to 0:100), followed by a preparative HPLC purification (column: L-Column2 ODS 20 mm ID × 150 mm L; mobile phase A: 0.1% TFA in water; mobile phase B: 0.1% TFA in acetonitrile; flow rate: 20 mL/min). The desired fraction was neutralized with saturated aqueous NaHCO₃, concentrated in vacuo to remove most of acetonitrile, and extracted with EtOAc. The organic layer was separated, dried over anhydrous Na₂SO₄, and concentrated in vacuo to afford **39c** (73.1 mg, 0.172 mmol, 69%) as a white solid. ¹H NMR (300 MHz, DMSO-*d*₆) δ 2.30 (3H, s), 3.27 (3H, s), 3.56–3.68 (2H, m), 4.33–4.49 (2H, m), 5.00–5.10 (1H, m), 7.03 (1H, d, *J* = 5.7 Hz), 7.27–7.36 (2H, m), 7.41–7.51 (2H, m), 7.93

(1H, d, $J = 5.3$ Hz), 10.28 (1H, d, $J = 7.6$ Hz), 10.35 (1H, s). MS (ESI/APCI) mass calculated for $[M + H]^+$ ($C_{19}H_{20}F_3N_4O_4$) requires m/z 425.1, found m/z 425.1. HPLC purity: 99.9%. mp 128 °C.

7-Cyclopropyl-N-(2-methoxy-1-(4-(trifluoromethoxy)phenyl)ethyl)-2-oxo-2,3-dihydropyrido[2,3-b]pyrazine-4(1H)-carboxamide (39d). A mixture of **69** (432 mg, 0.740 mmol) in TFA (2.1 mL) and H₂O (0.236 mL) was stirred at rt for 3.5 h and then concentrated in vacuo. The residue was dissolved in DMF (10 mL) and 8 M NH₃ solution in MeOH (2.0 mL, 16.0 mmol) was added. The mixture was stirred at rt for 1 h and then concentrated in vacuo. The residue was diluted with EtOAc. The solution was washed with water and saturated aqueous NaCl, dried over anhydrous Na₂SO₄ and concentrated in vacuo to give **39d** (279 mg, 0.590 mmol, 80%) as a white solid after trituration with hexane/ethyl acetate (10:1). ¹H NMR (300 MHz, DMSO-*d*₆) δ 0.61–0.71 (2H, m), 0.93–1.05 (2H, m), 1.90–2.03 (1H, m), 3.28 (3H, s), 3.55–3.71 (2H, m), 4.30–4.49 (2H, m), 5.00–5.12 (1H, m), 6.96 (1H, d, $J = 2.3$ Hz), 7.32 (2H, d, $J = 7.9$ Hz), 7.46 (2H, d, $J = 8.7$ Hz), 7.85 (1H, d, $J = 1.9$ Hz), 10.34 (1H, d, $J = 7.5$ Hz), 10.69 (1H, s). MS (ESI/APCI) mass calculated for $[M + H]^+$ ($C_{21}H_{22}F_3N_4O_4$) requires m/z 425.2, found m/z 451.1. HPLC purity: 98.8%. mp 149 °C.

7-Chloro-N-(2-methoxy-1-(4-(trifluoromethoxy)phenyl)ethyl)-2-oxo-2,3-dihydropyrido[2,3-b]pyrazine-4(1H)-carboxamide (39e). To a solution of **57g** (132.4 mg, 0.72 mmol) and Et₃N (305 μL, 2.16 mmol) in THF (6 mL) and DMA (6 mL) was slowly added a solution of triphosgene (214 mg, 0.72 mmol) in THF (3.0 mL) at 0 °C. After stirring at 0 °C for 2 h, a mixture of Et₃N (508 μL, 3.61 mmol) and **100i** (980 mg, 3.61 mmol) in THF (3.0 mL) and DMA (6.0 mL) was added at the same temperature. The mixture was stirred at rt for 3 h and then quenched with water. The phases were separated and the aqueous phase was extracted with EtOAc. The combined organic phases were washed with water and saturated aqueous NaCl, dried over anhydrous Na₂SO₄ and concentrated in vacuo. The residue was purified by column chromatography (silica gel, hexane/ethyl acetate, 99:1 to 3:2) to give **39e** (10.4 mg, 0.023 mmol, 3.2%) as a pale yellow solid after trituration with hexane/ethyl acetate (10:1). ¹H NMR (300 MHz, DMSO-*d*₆) δ 3.29 (3H, s), 3.53–3.71 (2H, m), 4.32–4.52 (2H, m),

4.99–5.12 (1H, m), 7.27–7.38 (3H, m), 7.48 (2H, d, $J = 8.7$ Hz), 8.06 (1H, d, $J = 2.3$ Hz), 10.13 (1H, d, $J = 7.2$ Hz), 10.93 (1H, brs). MS (ESI/APCI) mass calculated for $[M + H]^+$ ($C_{18}H_{17}ClF_3N_4O_4$) requires m/z 445.1, found m/z 445.1. HPLC purity: 96.5%.

7-Methoxy-N-(2-methoxy-1-(4-(trifluoromethoxy)phenyl)ethyl)-2-oxo-2,3-dihydropyrido[2,3-b]pyrazine-4(1H)-carboxamide (39f). A mixture of **70** (395 mg, 0.69 mmol) in TFA (10 mL) and water (1.1 mL) was stirred at rt for 3 h and then concentrated in vacuo. The residue was dissolved in DMF (19 mL) and 8 M NH_3 solution in MeOH (3.73 mL, 29.8 mmol) was added. The mixture was stirred at rt for 2 h and then concentrated in vacuo. The residue was diluted with EtOAc. The solution was washed with water and saturated aqueous NaCl, dried over anhydrous Na_2SO_4 and concentrated in vacuo. The residue was purified by column chromatography (silica gel, hexane/ethyl acetate, 99:1 to 0:100) to give **39f** (203 mg, 0.461 mmol, 67%) as a white solid after trituration with hexane/ethyl acetate (10:1). 1H NMR (300 MHz, $DMSO-d_6$) δ 3.28 (3H, s), 3.54–3.68 (2H, m), 3.83 (3H, s), 4.30–4.51 (2H, m), 4.98–5.12 (1H, m), 6.96 (1H, d, $J = 2.6$ Hz), 7.27–7.37 (2H, m), 7.46 (2H, d, $J = 8.7$ Hz), 7.76 (1H, d, $J = 2.6$ Hz), 10.02 (1H, d, $J = 7.5$ Hz), 10.76 (1H, brs). MS (ESI/APCI) mass calculated for $[M + H]^+$ ($C_{19}H_{20}F_3N_4O_5$) requires m/z 441.1, found m/z 441.2. HPLC purity: 98.7%.

7-Isopropoxy-N-(2-methoxy-1-(4-(trifluoromethoxy)phenyl)ethyl)-2-oxo-2,3-dihydropyrido[2,3-b]pyrazine-4(1H)-carboxamide (39g). A mixture of **71** (90 mg, 0.15 mmol) in TFA (2.13 mL) and water (0.239 mL) was stirred at rt for 3 h. The mixture was concentrated in vacuo. The residue was dissolved in DMF (4 mL) and 8 M NH_3 solution in MeOH (0.808 mL, 6.46 mmol) was added. The mixture was stirred at rt for 2 h and concentrated in vacuo. The residue was diluted with EtOAc. The solution was washed with water and saturated aqueous NaCl, dried over anhydrous Na_2SO_4 and concentrated in vacuo. The residue was purified by column chromatography (silica gel, hexane/ethyl acetate, 99:1 to 0:100) to give **39g** (67.2 mg, 0.143 mmol, 95%) as a white amorphous solid. 1H NMR (300 MHz, $DMSO-d_6$) δ 1.29 (6H, d, $J = 6.0$ Hz), 3.28 (3H, s), 3.52–3.69 (2H, m), 4.28–4.49 (2H, m), 4.60 (1H, dt, $J = 12.1, 6.0$ Hz), 5.04 (1H, d, $J = 7.2$ Hz), 6.94 (1H, d, $J = 2.6$ Hz), 7.27–7.37 (2H, m), 7.46 (2H, d,

$J = 8.7$ Hz), 7.73 (1H, d, $J = 2.6$ Hz), 10.01 (1H, d, $J = 7.2$ Hz), 10.72 (1H, s). MS (ESI/APCI) mass calculated for $[M + H]^+$ ($C_{21}H_{24}F_3N_4O_5$) requires m/z 469.2, found m/z 469.2. HPLC purity: 99.1%.

7-Methoxy-N-((1S)-2-methoxy-1-(4-(trifluoromethoxy)phenyl)ethyl)-2-oxo-2,3-dihydropyrido[2,3-b]pyrazine-4(1H)-carboxamide (40a). (Method A: step **39f** \rightarrow **40a** in Scheme 2-6) Resolution of the enantiomers of **39f** was carried out chromatographically using a Chiralpak IA 20 mm ID \times 250 mm L column (CO_2 /methanol, 43:7) at 50 mL/min. Resolution of **39f** (200 mg, 0.454 mmol) provided 90.0 mg of **40a** as the first eluting enantiomer, which was crystallized from hexane/ethyl acetate to afford **40a** (78.3 mg, 0.178 mmol, 39%, 78% theoretical) as a white solid. Analytical HPLC analysis carried out on a 4.6 mm ID \times 150 mm L Chiralpak IA column (CO_2 /methanol, 41:9) at a flow rate of 4.0 mL/min indicated that **40a** was of 99% ee. 1H NMR (300 MHz, $DMSO-d_6$) δ 3.28 (3H, s), 3.52–3.70 (2H, m), 3.83 (3H, s), 4.26–4.52 (2H, m), 4.97–5.13 (1H, m), 6.96 (1H, d, $J = 2.6$ Hz), 7.32 (2H, d, $J = 8.3$ Hz), 7.46 (2H, d, $J = 8.7$ Hz), 7.76 (1H, d, $J = 2.6$ Hz), 10.02 (1H, d, $J = 7.5$ Hz), 10.77 (1H, brs). MS (ESI/APCI) mass calculated for $[M + H]^+$ ($C_{19}H_{20}F_3N_4O_5$) requires m/z 441.1, found m/z 441.1. HPLC purity: 100%. mp 77.6–78.6 °C. Anal. Calcd for $C_{19}H_{19}N_4O_5F_3 \cdot 0.25H_2O$: C, 51.30; H, 4.42; F, 12.81; N, 12.59. Found: C, 51.58; H, 4.71; F, 12.52; N, 12.41.

7-Methoxy-N-((1S)-2-methoxy-1-(4-(trifluoromethoxy)phenyl)ethyl)-2-oxo-2,3-dihydropyrido[2,3-b]pyrazine-4(1H)-carboxamide (40a). (Method B: step **112** \rightarrow **40a** in Scheme 2-10) To a solution of **112** (179 mg, 1.00 mmol) and 4-nitrophenyl carbonochloridate (242 mg, 1.20 mmol) in THF (10 mL) was added DIEA (262 μ L, 1.50 mmol) at rt. After being stirred at rt for 24 h, the mixture was concentrated in vacuo. To a solution of the residue and **111b** (299 mg, 1.10 mmol) in DMF (10 mL) was added Et_3N (418 μ L, 3.00 mmol) at rt. After being stirred at rt for 24 h, the mixture was quenched with water and extracted with EtOAc. The organic layer was washed with water and saturated aqueous NaCl, dried over $MgSO_4$, and concentrated in vacuo. The residue was purified by column chromatography (silica gel, hexane/ethyl acetate, 4:1 to 1:4) to give **40a** (227 mg, 0.515 mmol, 52%) as a white solid after recrystallization from heptane/acetone. Analytical HPLC analysis carried out on

a 4.6 mm ID × 150 mm L Chiralpak IA column (CO₂/methanol, 41:9) at a flow rate of 4.0 mL/min indicated that **40a** was of >99.9% ee as the first eluting enantiomer. ¹H NMR (300 MHz, CDCl₃) δ 3.40 (3H, s), 3.68 (2H, d, *J* = 4.9 Hz), 3.87 (3H, s), 4.65 (2H, s), 5.12–5.22 (1H, m), 6.80 (1H, d, *J* = 2.6 Hz), 7.13–7.21 (2H, m), 7.37–7.44 (2H, m), 7.71 (1H, d, *J* = 2.6 Hz), 8.90 (1H, s), 10.17 (1H, d, *J* = 7.2 Hz). MS (ESI/APCI) *m/z* 441.1 [M + H]⁺. Anal. Calcd for C₁₉H₁₉N₄O₅F₃: C, 51.82; H, 4.35; N, 12.72. Found: C, 51.65; H, 4.41; N, 12.62.

7-Methoxy-N-((1R)-2-methoxy-1-(4-(trifluoromethoxy)phenyl)ethyl)-2-oxo-2,3-dihydropyrido[2,3-b]pyrazine-4(1H)-carboxamide (40b). Resolution of the enantiomers of **39f** was carried out chromatographically using a Chiralpak IA 20 mm ID × 250 mm L column (CO₂/methanol, 43:7) at 50 mL/min. Resolution of **39f** (200 mg, 0.454 mmol) provided 94.0 mg of **40b** as the second eluting enantiomer, which was crystallized from hexane/ethyl acetate to afford **40b** (60.0 mg, 0.136 mmol, 30%, 60% theoretical) as a white solid. Analytical HPLC analysis carried out on a 4.6 mm ID × 150 mm L Chiralpak IA column (CO₂/methanol, 41:9) at a flow rate of 4.0 mL/min indicated that **40b** was of >99.9% ee. ¹H NMR (300 MHz, DMSO-*d*₆) δ 3.28 (3H, s), 3.53–3.67 (2H, m), 3.83 (3H, s), 4.27–4.51 (2H, m), 4.96–5.16 (1H, m), 6.96 (1H, d, *J* = 3.0 Hz), 7.32 (2H, d, *J* = 8.3 Hz), 7.41–7.54 (2H, m), 7.76 (1H, d, *J* = 2.6 Hz), 10.02 (1H, d, *J* = 7.2 Hz), 10.76 (1H, brs). MS (ESI/APCI) mass calculated for [M + H]⁺ (C₁₉H₂₀F₃N₄O₅) requires *m/z* 441.1, found *m/z* 441.1. HPLC purity: 100%.

7-Methoxy-N-((1S *or*
1R)-2-methoxy-1-(4-(trifluoromethyl)phenyl)ethyl)-2-oxo-2,3-dihydropyrido[2,3-b]pyrazine-4(1H)-carboxamide (41a). Resolution of the enantiomers of **75** was carried out chromatographically using a Chiralpak AD 50 mm ID × 500 mm L column (hexane/ethanol, 3:2) at 80 mL/min. Resolution of **75** (444 mg, 1.05 mmol) provided 210 mg of **41a** as the first eluting enantiomer, which was crystallized from hexane/ethyl acetate to afford **41a** (197 mg, 0.464 mmol, 44%, 88% theoretical) as a white solid. Analytical HPLC analysis carried out on a 4.6 mm ID × 250 mm L Chiralpak AD column (hexane/ethanol, 7:3) at a flow rate of 1.0 mL/min indicated that **41a** was of >99.9% ee. ¹H NMR (300

MHz, DMSO-*d*₆) δ 3.28 (3H, s), 3.61–3.68 (2H, m), 3.83 (3H, s), 4.29–4.50 (2H, m), 5.03–5.16 (1H, m), 6.97 (1H, d, *J* = 2.6 Hz), 7.56 (2H, d, *J* = 8.3 Hz), 7.69 (2H, d, *J* = 8.3 Hz), 7.77 (1H, d, *J* = 2.6 Hz), 10.07 (1H, d, *J* = 7.2 Hz), 10.77 (1H, brs). MS (ESI/APCI) mass calculated for [M + H]⁺ (C₁₉H₂₀F₃N₄O₄) requires *m/z* 425.1, found *m/z* 425.1. HPLC purity: 100%. mp 144 °C.

7-Methoxy-N-((1R

or

1S)-2-methoxy-1-(4-(trifluoromethyl)phenyl)ethyl)-2-oxo-2,3-dihydropyrido[2,3-*b*]pyrazine-4(1H)-carboxamide (41b). Resolution of the enantiomers of **75** was carried out chromatographically using a Chiralpak AD 50 mm ID × 500 mm L column (hexane/ethanol, 3:2) at 80 mL/min. Resolution of **75** (444 mg, 1.05 mmol) provided 210 mg of **41b** as the second eluting enantiomer, which was crystallized from hexane/ethyl acetate to afford **41b** (189 mg, 0.444 mmol, 43%, 85% theoretical) as a white solid. Analytical HPLC analysis carried out on a 4.6 mm ID × 250 mm L Chiralpak AD column (hexane/ethanol, 7:3) at a flow rate of 1.0 mL/min indicated that **41b** was of >99.9% ee. ¹H NMR (300 MHz, DMSO-*d*₆) δ 3.28 (3H, s), 3.61–3.67 (2H, m), 3.83 (3H, s), 4.30–4.50 (2H, m), 5.04–5.16 (1H, m), 6.97 (1H, d, *J* = 2.6 Hz), 7.56 (2H, d, *J* = 8.3 Hz), 7.69 (2H, d, *J* = 8.3 Hz), 7.77 (1H, d, *J* = 2.6 Hz), 10.07 (1H, d, *J* = 7.5 Hz), 10.77 (1H, s). MS (ESI/APCI) mass calculated for [M + H]⁺ (C₁₉H₂₀F₃N₄O₄) requires *m/z* 425.1, found *m/z* 425.1. HPLC purity: 100%. mp 142 °C.

N-((1S)-1-(3-Fluoro-4-(trifluoromethoxy)phenyl)-2-methoxyethyl)-7-methoxy-2-oxo-2,3-dihydropyrido[2,3-*b*]pyrazine-4(1H)-carboxamide (42a). (Method A: step **76** → **42a** in Scheme 2-6) Resolution of the enantiomers of **76** was carried out chromatographically using a Chiralpak AD 50 mm ID × 500 mm L column (hexane/ethanol, 43:7) at 80 mL/min. Resolution of **76** (1.34 g, 2.93 mmol) provided 652 mg of **42a** as the first eluting enantiomer, which was crystallized from hexane/ethyl acetate to afford **42a** (578 mg, 1.26 mmol, 43%, 86% theoretical) as a white solid. Analytical HPLC analysis carried out on a 4.6 mm ID × 250 mm L Chiralpak AD column (hexane/ethanol, 13:7) at a flow rate of 1.0 mL/min indicated that **42a** was of 99.8% ee. ¹H NMR (300 MHz, DMSO-*d*₆) δ 3.29 (3H, s), 3.53–3.72 (2H, m), 3.83 (3H, s), 4.24–4.54 (2H, m), 4.95–5.16 (1H, m), 6.96 (1H, d, *J* = 2.6 Hz), 7.29 (1H,

d, $J = 8.3$ Hz), 7.39–7.61 (2H, m), 7.75 (1H, d, $J = 2.6$ Hz), 10.02 (1H, d, $J = 7.5$ Hz), 10.78 (1H, brs). ^{13}C NMR (151 MHz, DMSO- d_6) δ 45.41, 52.93, 55.99, 58.42, 74.55, 110.38, 115.66 (d, $J = 18.8$ Hz, 1C), 119.97 (q, $J = 257.6$ Hz, 1C), 123.54 (d, $J = 3.3$ Hz, 1C), 123.70, 124.59, 125.82, 133.80 (qd, $J = 1.7, 12.7$ Hz, 1C), 135.07, 143.41 (d, $J = 6.1$ Hz, 1C), 152.10, 153.26 (d, $J = 249.9$ Hz, 1C), 153.75, 165.32. MS (ESI/APCI) mass calculated for $[\text{M} + \text{H}]^+$ ($\text{C}_{19}\text{H}_{20}\text{F}_3\text{N}_4\text{O}_4$) requires m/z 459.1, found m/z 459.2. HPLC purity: 100%. $[\alpha]_{20}^{\text{D}} = -114.5$ ($c = 1.00$ in MeOH). mp 151.2–152.2 °C. Anal. Calcd for $\text{C}_{19}\text{H}_{18}\text{F}_4\text{N}_4\text{O}_5$: C, 49.79; H, 3.96; F, 16.58; N, 12.22. Found: C, 49.84; H, 4.14; F, 16.38; N, 12.12.

N-((1S)-1-(3-Fluoro-4-(trifluoromethoxy)phenyl)-2-methoxyethyl)-7-methoxy-2-oxo-2,3-dihydropyrido[2,3-*b*]pyrazine-4(1H)-carboxamide (42a). (Method B: step **112** \rightarrow **42a** in Scheme 2-11) To a suspension of **112** (2.49 g, 13.90 mmol) and DIEA (7.13 mL, 41.7 mmol) in THF (120 mL) was added portionwise 4-nitrophenyl chloroformate (3.64 g, 18.1 mmol) at 0 °C. The mixture was stirred at rt under N_2 for 3 h and then concentrated in vacuo. To the residue were added *i*-Pr $_2$ O (200 mL) and saturated aqueous NaCl (150 mL) and the mixture was stirred at rt for 20 min. The resulting precipitate was filtered, washed with water and then *i*-Pr $_2$ O, and dried to give 4-nitrophenyl 7-methoxy-2-oxo-2,3-dihydropyrido[2,3-*b*]pyrazine-4(1H)-carboxylate (4.20 g, 12.2 mmol, 88%) as a gray solid. A mixture of 4-nitrophenyl 7-methoxy-2-oxo-2,3-dihydropyrido[2,3-*b*]pyrazine-4(1H)-carboxylate obtained above (4.20 g, 12.2 mmol), DIEA (11.9 mL, 69.5 mmol), **115** (4.43 g, 15.3 mmol) and DMF (130 mL) was stirred at rt for 16 h and concentrated in vacuo. To the residue were added EtOAc (200 mL), THF (100 mL), and NaHCO $_3$ aqueous solution (200 mL). The phases were separated and the aqueous phase was extracted with EtOAc/THF (2:1). The phases were washed with saturated aqueous NaCl, dried over anhydrous Na $_2$ SO $_4$, and concentrated in vacuo. The residue was purified by column chromatography (basic silica gel (200 g), hexane/ethyl acetate, 3:17) to give **42a** (5.01 g, 10.9 mmol, 79%) as a pale yellow solid. To a solution of **42a** (5.00 g, 10.9 mmol) in EtOH (200 mL) was added activated carbon (10 g). After the mixture was stirred at rt for 30 min, the insoluble material was removed by filtration and washed

with acetone several times. The filtrate was concentrated in vacuo. To a solution of the obtained compound (4.17g) in acetone (35 mL) was added dropwise heptane (70 mL) at 52 °C (precipitate occurred) and the mixture was stirred at 52 °C for 1 h. Additional heptane (35 mL) was added dropwise at 52 °C and then gradually cooled to rt. The mixture was stirred overnight, and then stirred at 5 °C for 1 h. The precipitate was collected by filtration, rinsed with acetone/heptane (7:21) to give **42a** (3.15 g, 6.87 mmol, 63%) as a white solid. Analytical HPLC analysis carried out on a 4.6 mm ID × 150 mm L Chiralpak ADH column (hexane/ethanol, 13:7) at a flow rate of 1.0 mL/min indicated that **42a** was of >99.9% ee as the first eluting enantiomer. ¹H NMR (300 MHz, DMSO-*d*₆) δ 3.29 (3H, s), 3.56–3.70 (2H, m), 3.83 (3H, s), 4.30–4.52 (2H, m), 4.95–5.16 (1H, m), 6.96 (1H, d, *J* = 2.6 Hz), 7.29 (1H, d, *J* = 8.3 Hz), 7.43–7.57 (2H, m), 7.75 (1H, d, *J* = 3.0 Hz), 10.02 (1H, d, *J* = 7.2 Hz), 10.78 (1H, brs). MS (ESI/APCI) *m/z* 459.2 [M + H]⁺. HPLC purity: 99.9%.

N-((1*R*)-1-(3-Fluoro-4-(trifluoromethoxy)phenyl)-2-methoxyethyl)-7-methoxy-2-oxo-2,3-dihydropyrido[2,3-*b*]pyrazine-4(1*H*)-carboxamide (**42b**). Resolution of the enantiomers of **76** was carried out chromatographically using a Chiralpak AD 50 mm ID × 500 mm L column (hexane/ethanol, 43:7) at 80 mL/min. Resolution of **76** (1.34 g, 2.93 mmol) provided 680 mg of **42b** as the second eluting enantiomer, which was crystallized from hexane/ethyl acetate to afford **42b** (563 mg, 1.22 mmol, 41%, 83% theoretical) as a white solid. Analytical HPLC analysis carried out on a 4.6 mm ID × 250 mm L Chiralpak AD column (hexane/ethanol, 13:7) at a flow rate of 1.0 mL/min indicated that **42b** was of 99.6% ee. ¹H NMR (300 MHz, DMSO-*d*₆) δ 3.29 (3H, s), 3.53–3.70 (2H, m), 3.83 (3H, s), 4.29–4.51 (2H, m), 4.98–5.12 (1H, m), 6.97 (1H, d, *J* = 3.0 Hz), 7.29 (1H, d, *J* = 8.3 Hz), 7.39–7.59 (2H, m), 7.75 (1H, d, *J* = 2.6 Hz), 10.02 (1H, d, *J* = 7.2 Hz), 10.78 (1H, brs). MS (ESI/APCI) mass calculated for [M + H]⁺ (C₁₉H₂₀F₃N₄O₄) requires *m/z* 459.1, found *m/z* 459.1. HPLC purity: 98.2%. mp 151.2–152.2 °C. Anal. Calcd for C₁₉H₁₈N₄O₃F₄·0.3H₂O: C, 49.21; H, 4.04; F, 16.39; N, 12.08. Found: C, 49.17; H, 4.05; F, 16.20; N, 12.04.

tert-Butyl Ethyl (3-Nitropyridin-2-yl)malonate (44). To a suspension of potassium *tert*-butoxide (26.6 g, 237 mmol) in THF (500 mL) at 60 °C was added dropwise *tert*-butyl ethyl malonate (45 mL, 237 mmol), followed by **43** (25.0 g, 158 mmol) in THF (50 mL). The mixture was refluxed for 3 h. The mixture was concentrated in vacuo and the residue was diluted with 1 M HCl aqueous solution (100 mL). The aqueous solution was extracted with EtOAc and the combined organic phase was washed with saturated aqueous NaCl, dried over anhydrous Na₂SO₄ and concentrated in vacuo to give crude **44** (66.7 g). This was used in the next reaction without further purification. ¹H NMR (400 MHz, CDCl₃) δ 1.30 (3H, t, *J* = 7.2 Hz), 1.49 (9H, s), 4.29–4.33 (2H, m), 5.43 (1H, s), 7.51 (1H, dd, *J* = 8.4, 4.2 Hz), 8.46 (1H, d, *J* = 8.4 Hz), 8.82 (1H, d, *J* = 5.2 Hz).

Ethyl (3-Nitropyridin-2-yl)acetate (45). To a solution of crude **44** (66.7 g) in CH₂Cl₂ (300 mL) was added TFA (100 mL). The mixture was stirred at rt overnight. The mixture was concentrated in vacuo and the residue was diluted with NaHCO₃ aqueous solution (100 mL). The mixture was extracted with EtOAc, washed with saturated aqueous NaCl, dried over anhydrous Na₂SO₄ and concentrated in vacuo to give crude **45** (29.0 g). This was used in the next reaction without further purification. ¹H NMR (400 MHz, CDCl₃) δ 1.26 (3H, t, *J* = 7.2 Hz), 4.20 (2H, q, *J* = 7.2 Hz), 4.33 (2H, s), 7.48 (1H, dd, *J* = 8.0, 1.2 Hz), 8.43 (1H, dd, *J* = 8.4, 1.2 Hz), 8.80 (1H, dd, *J* = 8.4, 1.2 Hz).

Ethyl (3-Aminopyridin-2-yl)acetate (46). A mixture of crude **45** (29.0 g) and 10% Pd/C (containing 50% water, 2.90 g) in EtOH (400 mL) was stirred under 50 psi of H₂ at rt for 3 h. The mixture was filtered through celite and the filtrate was concentrated in vacuo to give crude **46** (25.5 g). This was used in the next reaction without further purification. ¹H NMR (400 MHz, CDCl₃) δ 1.26 (3H, t, *J* = 7.2 Hz), 3.85 (2H, s), 4.17 (2H, q, *J* = 7.2 Hz), 4.32 (2H, br s), 6.99–7.06 (2H, m), 7.99–8.01 (1H, m).

Ethyl (3-((Diethoxyacetyl)amino)pyridin-2-yl)acetate (47). To a mixture of crude **46** (25.5 g, 142 mmol) and 2,2-diethoxyacetic acid (23.0 g, 156 mmol) in DMF (300 mL) was added DIEA (70.3 mL, 425 mmol), followed by HATU (80.7 g, 212 mmol). The mixture was stirred at rt overnight. The mixture was diluted with water and extracted with EtOAc (300 mL × 2). The combined organic phase

was washed with NaHCO₃ aqueous solution and then saturated aqueous NaCl, dried over anhydrous Na₂SO₄ and concentrated in vacuo. The residue was purified by column chromatography (silica gel, petroleum/ethyl acetate, 3:1) to give **47** (26.0 g, 53% in 4 steps from **43**). ¹H NMR (400 MHz, CDCl₃) δ 1.27–1.33 (9H, m), 3.69–3.83 (4H, m), 3.90 (2H, s), 4.20 (2H, q, *J* = 7.2 Hz), 4.97 (1H, s), 7.25–7.28 (1H, m), 8.29–8.35 (2H, m), 9.53 (1H, br s). 2,2-Diethoxylacetic acid was prepared in the following method. To a solution of ethyl 2,2-diethoxyacetate (17.8 g, 101 mmol) in EtOH (50 mL) was added 2 M NaOH aqueous solution (101 mL, 202 mmol). The mixture was stirred at rt for 16 h and then EtOH was removed under reduced pressure. The aqueous phase was extracted with Et₂O. The aqueous phase was acidified with 2 M HCl aqueous solution to pH 3~4, saturated with solid NaCl and extracted with EtOAc. The combined organic phases were dried over anhydrous Na₂SO₄ and concentrated in vacuo to afford 2,2-diethoxyacetic acid (3.37 g, 22.7 mmol, 23%) as a colorless oil. ¹H NMR (300 MHz, DMSO-*d*₆) δ 1.13 (6H, t, *J* = 7.2 Hz), 3.46–3.67 (4H, m), 4.80 (1H, s), 12.92 (1H, brs).

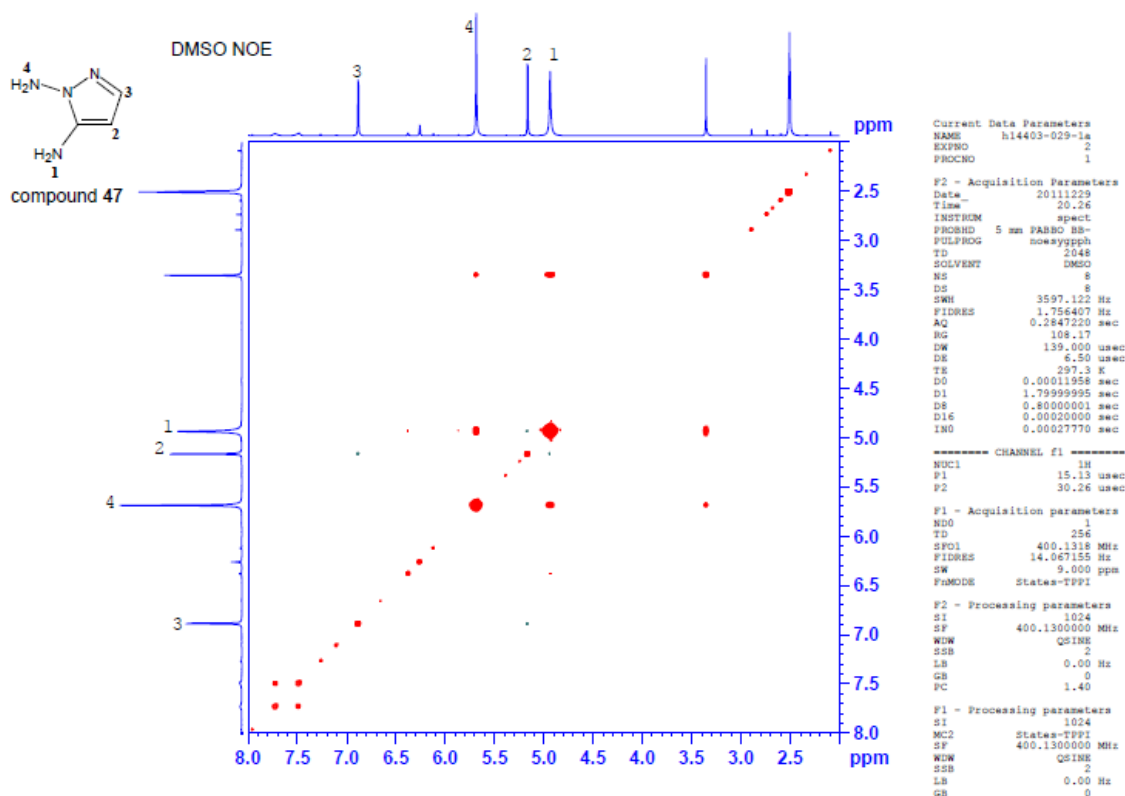
Ethyl 2-Oxo-1,2-dihydro-1,5-naphthyridine-4-carboxylate (48). To a solution of **47** (3.00 g, 9.67 mmol) in TFA (50 mL) was added H₂O (2 mL), followed by 2 drops of I₂ fresh solution (30 mg of I₂ was suspended in TFA (10 mL)). The mixture was heated to 50 °C overnight and then concentrated in vacuo. The residue was dissolved in toluene (50 mL) and piperidine (3 mL). The resulting mixture was refluxed for 6 h, and then concentrated in vacuo. The residue was purified by column chromatography (silica gel, petroleum ether/ethyl acetate, 1:1) to give **48** (550 mg, 26%). ¹H NMR (400 MHz, CDCl₃) δ 1.44 (3H, t, *J* = 7.2 Hz), 4.53 (2H, q, *J* = 7.2 Hz), 7.07 (1H, s), 7.48–7.51 (1H, m), 7.74–7.77 (1H, m), 8.66–8.68 (1H, m), 12.38 (1H, br s).

2-Oxo-1,2-dihydro-1,5-naphthyridine-4-carboxylic Acid (49). To a solution of **48** (70 mg, 0.32 mmol) in EtOH (5 mL) was added 2 M NaOH aqueous solution (4 mL). The mixture was stirred at rt for 2 h. EtOH was removed under reduced pressure and the aqueous phase was acidified to pH ~5 with 1 M HCl aqueous solution. The precipitate was collected by filtration and dried to give **49** (53 mg, 87%) as

a beige solid. ^1H NMR (400 MHz, $\text{DMSO-}d_6$) δ 7.02 (1H, s), 7.64–7.67 (1H, m), 7.80 (1H, d, $J = 8.8$ Hz), 8.55 (1H, d, $J = 4.0$ Hz), 12.26 (1H, d, $J = 10.4$ Hz), 14.86 (1H, br s).

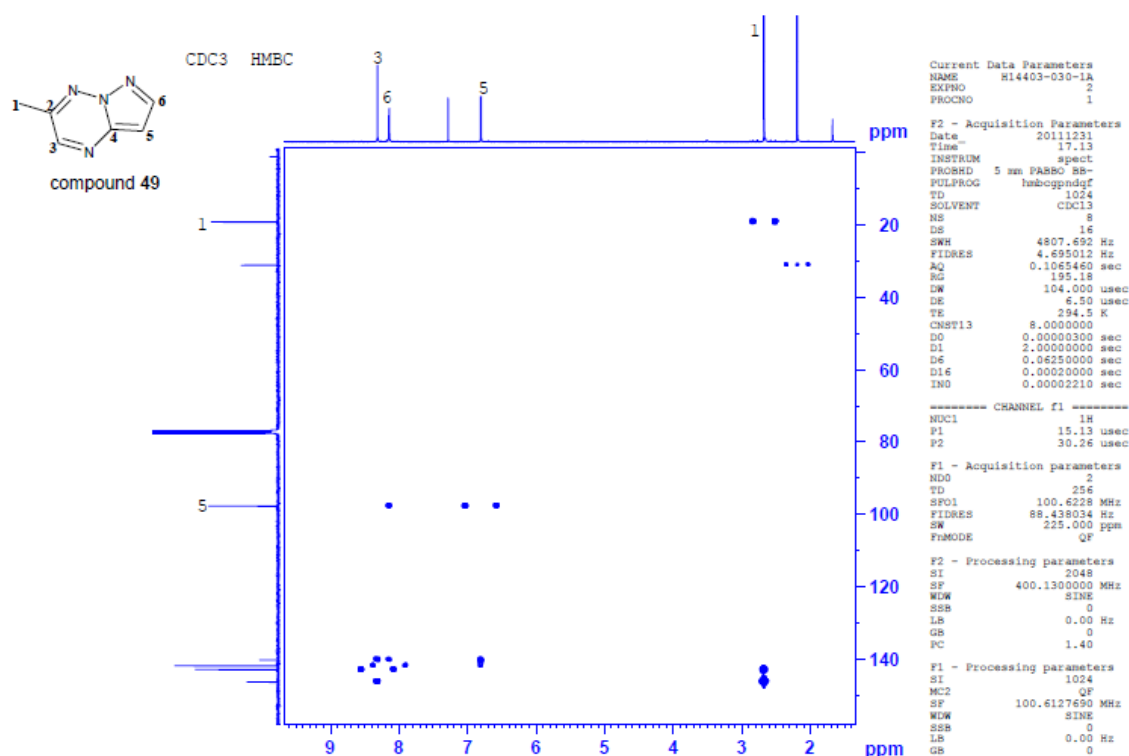
1H-Pyrazole-1,5-diamine (51a). To a vigorously stirred solution of 2H-pyrazol-3-ylamine (**50**) (4.00 g, 48.2 mmol) in DMF (50 mL) cooled in an ice-salt bath was added KOH (20.0 g, 357 mmol). The mixture was stirred at 0 °C for 20 min. Then, HOSA (5.45 g, 48.2 mmol) was added in portions. The mixture was stirred at 10–15 °C for 2 h. The mixture was filtered by a cake of celite and the celite was washed with CH_2Cl_2 (50 mL \times 2). The combined filtrate was concentrated in vacuo. The residue was purified by column chromatography (silica gel, CH_2Cl_2 /methanol, 100:0 to 60:1) to afford **51a** (less polar, 810 mg, 17% yield) as a yellow solid and **51b** (more polar, 520 mg, 11% yield) as a yellow solid. The structures were confirmed by nuclear overhauser effect (NOE) experiments (See below). ^1H NMR for **51a** (400 MHz, $\text{DMSO-}d_6$) δ 4.91 (2H, brs), 5.14 (1H, d, $J = 2.0$ Hz), 5.66 (2H, brs), 6.86 (1H, d, $J = 1.6$ Hz). ^1H NMR for **51b** (400 MHz, $\text{DMSO-}d_6$) δ 4.41 (2H, brs), 5.22 (1H, d, $J = 2.4$ Hz), 5.85 (2H, brs), 7.08 (1H, d, $J = 2.0$ Hz).

NOE Data for 51a



3-Methylpyrazolo[1,5-b][1,2,4]triazine (52). To a solution of 2-oxo-propionaldehyde (40% aqueous solution, 689 mg, 3.83 mmol) in H₂O (4 mL) and concd HCl (0.2 mL) was added **51a** (300 mg, 3.06 mmol) in small portions at 60 °C. The mixture was heated to reflux for 1 h. After cooling to 15 °C, the mixture was basified to pH ~8 with saturated aqueous NaHCO₃ and extracted with CH₂Cl₂ (10 mL × 3). The combined organic layer was dried over anhydrous Na₂SO₄ and concentrated in vacuo. The residue was purified by preparative TLC (CH₂Cl₂/methanol, 10:1) to give **52** (150 mg, 37% yield) as a yellow solid. The structure was confirmed by heteronuclear multiple bond correlation (HMBC) experiments (See below). ¹H NMR (400 MHz, CDCl₃) δ 2.65 (3H, s), 6.79 (1H, d, *J* = 2.4 Hz), 8.12 (1H, d, *J* = 2.8 Hz), 8.30 (1H, s).

HMBC Data for 52



3-Methylpyrazolo[1,5-b][1,2,4]triazine-8-carbaldehyde (53). POCl₃ (800 mg, 5.26 mmol) was added dropwise to DMF (5 mL) at 0 °C under N₂. After 30 min of stirring at 0 °C, a solution of **52** (150 mg, 1.12 mmol) in DMF (3 mL) was added dropwise at the same temperature. The mixture was warmed to 40 °C and stirred for 16 h. After cooling to 10 °C, the mixture was diluted with water (20 mL) and basified to pH ~9 with 1 M NaOH aqueous solution. The mixture was extracted with EtOAc (15 mL × 3). The combined organic layer was washed with saturated aqueous NaCl (15 mL), dried over anhydrous Na₂SO₄, and concentrated in vacuo. The residue was purified by column chromatography (silica gel, petroleum ether/ethyl acetate, 5:1) to give **53** (50 mg, 28% yield) as a yellow solid. ¹H NMR (400 MHz, CDCl₃) δ 2.75 (3H, s), 8.59–8.63 (2H, m), 10.29 (1H, s).

3-Methylpyrazolo[1,5-b][1,2,4]triazine-8-carboxylic acid (54). A mixture of **53** (50 mg, 0.31 mmol), NaClO₂ (140 mg, 1.55 mmol), NaH₂PO₄ (94 mg, 0.78 mmol), and 2-methyl-2-butene (55 mg, 0.78 mmol) in *tert*-BuOH (5 mL) and H₂O (2 mL) was stirred at 30 °C for 16 h. The solvent was removed

under reduced pressure and the residue was diluted with water (10 mL). The mixture was extracted with CH₂Cl₂ (10 mL × 5). The combined organic layer was washed with saturated aqueous NaCl (10 mL), dried over anhydrous Na₂SO₄, and concentrated in vacuo to give **54** (30 mg, containing 50% of **52**) as a yellow solid. ¹H NMR (400 MHz, DMSO-*d*₆) δ 2.57 (3H, s), 8.57 (1H, s), 8.78 (1H, s), 12.73 (1H, brs).

2-(2-Ethoxy-2-oxoethyl)nicotinic Acid (56). Na (2.85 g, 124 mmol) was dissolved in absolute EtOH (100 mL) and the solution was cooled to rt. To the resulting solution were added ethyl acetoacetate (9.66 g, 74.3 mmol), 2-bromonicotinic acid (**55**) (10.0 g, 49.5 mmol), and Cu(OAc)₂ (360 mg, 1.98 mmol). The mixture was stirred at reflux for 16 h. After cooling to rt, the mixture was acidified with AcOH (80 mL) and concentrated in vacuo. The residue was diluted with water (50 mL) and the mixture was extracted with CH₂Cl₂ (50 mL × 5). The extract was concentrated in vacuo. The residue was purified by column chromatography (silica gel, CH₂Cl₂/methanol, 100:0 to 10:1) to afford **56** (5.60 g, 26.8 mmol, 54%) as a yellow solid. ¹H NMR (400 MHz, DMSO-*d*₆) δ 1.16 (3H, t, *J* = 7.2 Hz), 4.06 (2H, q, *J* = 7.2 Hz), 4.17 (2H, s), 7.46 (1H, dd, *J* = 8.0, 4.8 Hz), 8.27 (1H, dd, *J* = 8.0, 2.0 Hz), 8.66 (1H, dd, *J* = 4.8, 2.0 Hz), 13.35 (1H, brs).

(8E or 8Z)-8-((Dimethylamino)methylene)-5H-pyrano[4,3-*b*]pyridine-5,7(8H)-dione (57). To a stirred solution of **56** (700 mg, 3.35 mmol) in DMF (5 mL) was added POCl₃ (0.70 mL, 7.5 mmol) dropwise at 0 °C. The mixture was stirred at 5 °C for 2 h, and then poured into ice/water (20 mL). The mixture was extracted with CH₂Cl₂ (20 mL × 3). The extract was concentrated in vacuo to afford crude **57** (400 mg) as a yellow solid. This was used in the next reaction without further purification. ¹H NMR (400 MHz, CDCl₃) δ 3.37 (3H, s), 3.55 (3H, s), 7.12 (1H, dd, *J* = 8.0, 4.8 Hz), 8.39 (1H, d, *J* = 7.2 Hz), 8.57 (1H, dd, *J* = 4.8, 1.6 Hz), 8.79 (1H, s).

6-(2,4-Dimethoxybenzyl)-5-oxo-5,6-dihydro-1,6-naphthyridine-8-carboxylic Acid (58). To a suspension of crude **57** (400 mg) in DMF (8 mL) were added Et₃N (740 mg, 7.32 mmol) and 2,4-dimethoxybenzylamine (919 mg, 5.50 mmol), and the mixture was stirred at 5 °C for 16 h. The

mixture was poured into ice/water (30 mL) and then acidified with 1 M HCl aqueous solution to pH ~ 1. The precipitate was collected by filtration, washed with water (5 mL), and dried to afford **58** (300 mg, 0.881 mmol, 26% in 2 steps from **56**) as a yellow solid. ¹H NMR (400 MHz, DMSO-*d*₆) δ 3.75 (3H, s), 3.78 (3H, s), 5.16 (2H, s), 6.52 (1H, dd, *J* = 8.4, 2.4 Hz), 6.59 (1H, d, *J* = 2.4 Hz), 7.24 (1H, d, *J* = 8.4 Hz), 7.74 (1H, dd, *J* = 8.0, 4.8 Hz), 8.67 (1H, s), 8.73 (1H, dd, *J* = 8.0, 2.0 Hz), 9.06 (1H, dd, *J* = 4.8, 2.0 Hz).

6-(2,4-Dimethoxybenzyl)-5-oxo-N-(1-(4-(trifluoromethoxy)phenyl)propyl)-5,6-dihydro-1,6-naphthyridine-8-carboxamide (59). A mixture of **58** (300 mg, 0.882 mmol), **22b** (226 mg, 0.882 mmol), EDCI (253 mg, 1.32 mmol), HOBT (178 mg, 1.32 mmol) and Et₃N (268 mg, 2.65 mmol) in DMF (5 mL) was stirred at 5 °C for 16 h and then at 40 °C for 16 h. After cooling to rt, the mixture was poured into water (10 mL) and extracted with CH₂Cl₂ (15 mL × 2). The extract was concentrated in vacuo. The residue was purified by column chromatography (silica gel, petroleum ether/ethyl acetate, 5:1 to 2:1) to afford impure **59** (500 mg, 93% LC–MS purity). 100 mg of impure **59** was further purified by preparative HPLC (column: YMC-pack ODS-A 4.6 mm ID × 150 mm L; mobile phase A: 0.05% HCl in water; mobile phase B: 0.05% HCl in acetonitrile; flow rate: 1.5 mL/min). After most of the solvent was removed under reduced pressure, the residue was lyophilized to afford **59** (27 mg, 0.0467 mmol, 26%) as a yellow solid. The remaining impure **59** (370 mg, 93% LC–MS purity) was used in the next reaction without further purification. ¹H NMR (400 MHz, DMSO-*d*₆) δ 0.92 (3H, t, *J* = 7.2 Hz), 1.82–1.91 (2H, m), 3.74 (3H, s), 3.76 (3H, s), 5.05 (1H, q, *J* = 7.2 Hz), 5.06–5.17 (2H, m), 6.50 (1H, dd, *J* = 8.4, 2.4 Hz), 6.58 (1H, d, *J* = 2.4 Hz), 7.18 (1H, d, *J* = 8.4 Hz), 7.32 (2H, d, *J* = 8.0 Hz), 7.49 (2H, d, *J* = 8.8 Hz), 7.67 (1H, dd, *J* = 8.0, 4.8 Hz), 8.52 (1H, s), 8.69 (1H, dd, *J* = 8.0, 2.0 Hz), 9.09 (1H, dd, *J* = 4.8, 2.0 Hz), 10.99 (1H, d, *J* = 7.6 Hz). MS (ESI/APCI) *m/z* 542.1 [M + H]⁺.

Methyl N-(3-Nitropyridin-2-yl)glycinate (61a). The mixture of **60a** (36.6 g, 231 mmol), methyl glycinate hydrochloride (29 g, 231 mmol), and Et₃N (80 mL, 577 mmol) in DMF (231 mL) was stirred at 90 °C for 3 h. After cooling to rt, the mixture was poured into water. The resulting solid was

collected by filtration, washed with water, and dried to give **61a** (49.8 g, 236 mmol, quantitative yield) as a yellow solid. This was used in the next reaction without further purification. ¹H NMR (300 MHz, CDCl₃) δ 3.80 (3H, s), 4.40 (2H, d, *J* = 5.7 Hz), 6.74 (1H, dd, *J* = 8.3, 4.5 Hz), 8.36–8.55 (3H, m). MS (ESI/APCI) mass calculated for [M + H]⁺ (C₈H₁₀N₃O₄) requires *m/z* 212.1, found *m/z* 212.1.

Methyl N-(4-Methyl-3-nitropyridin-2-yl)glycinate (61b). To a mixture of **60b** (1.51 g, 8.77 mmol) and methyl glycinate hydrochloride (1.16 g, 9.21 mmol) in DMF (12 mL) was added Et₃N (3.06 mL, 21.9 mmol). The mixture was stirred at 80 °C for 16 h. The solvent was evaporated and the residue was diluted with EtOAc. The organic layer was washed with water and saturated aqueous NaCl, dried over anhydrous Na₂SO₄. The solvent was evaporated. The residue was purified by column chromatography (silica gel, hexane/ethyl acetate, 19:1 to 4:1) to give **61b** (0.614 g, 2.73 mmol, 31%) as a yellow solid. ¹H NMR (300 MHz, DMSO-*d*₆) δ 2.39 (3H, s), 3.63 (3H, s), 4.14 (2H, d, *J* = 5.7 Hz), 6.69 (1H, dd, *J* = 4.9, 0.8 Hz), 7.83 (1H, t, *J* = 5.9 Hz), 8.13 (1H, d, *J* = 4.9 Hz). MS (ESI/APCI) mass calculated for [M + H]⁺ (C₉H₁₂N₃O₄) requires *m/z* 226.1, found *m/z* 226.3.

Methyl N-(6-Methyl-3-nitropyridin-2-yl)glycinate (61c). The title compound was prepared in 94% yield as a yellow solid from **60c** and methyl glycinate hydrochloride using the procedure analogous to that described for the synthesis of **61b**. ¹H NMR (300 MHz, DMSO-*d*₆) δ 2.38 (3H, s), 3.66 (3H, s), 4.29 (2H, d, *J* = 6.1 Hz), 6.70 (1H, d, *J* = 8.3 Hz), 8.34 (1H, d, *J* = 8.3 Hz), 8.76 (1H, t, *J* = 5.5 Hz). MS (ESI/APCI) mass calculated for [M + H]⁺ (C₉H₁₂N₃O₄) requires *m/z* 226.1, found *m/z* 226.1.

Methyl N-(5-Methyl-3-nitropyridin-2-yl)glycinate (61d). The title compound was prepared as a yellow solid in 70% yield from **60d** and methyl glycinate hydrochloride using the procedure analogous to that described for the synthesis of **61b**. ¹H NMR (300 MHz, DMSO-*d*₆) δ 2.24 (3H, s), 3.64 (3H, s), 4.28 (2H, d, *J* = 5.7 Hz), 8.27–8.37 (2H, m), 8.60 (1H, t, *J* = 5.7 Hz).

Methyl N-(5-Iodo-3-nitropyridin-2-yl)glycinate (61e). To a solution of **60e** (11.1 g, 39.0 mmol) in EtOH (350 mL) were added methyl glycinate hydrochloride (9.80 g, 78.1 mmol) and Et₃N (13.6 mL, 97.6 mmol) at rt. After being refluxed for 16 h, the reaction mixture was concentrated, and the residue

was quenched with water and extracted with EtOAc. The organic layer was separated, washed with water and saturated aqueous NaCl, dried over anhydrous MgSO₄ and concentrated in vacuo. The residue was crystallized from hexane/ethyl acetate to give **61e** (9.79 g, 29.0 mmol, 74%) as a yellow solid. ¹H NMR (300 MHz, CDCl₃) δ 3.79 (3H, s), 4.36 (2H, d, *J* = 5.5 Hz), 8.43 (1H, brs), 8.53 (1H, d, *J* = 2.1 Hz), 8.70 (1H, d, *J* = 2.1 Hz). MS (ESI/APCI) mass calculated for [M + H]⁺ (C₈H₉IN₃O₄) requires *m/z* 338.0, found *m/z* 337.9.

Methyl N-(5-Bromo-3-nitropyridin-2-yl)glycinate (61f). The title compound was prepared as a dark yellow solid in 82% yield from **60f** and methyl glycinate hydrochloride using the procedure analogous to that described for the synthesis of **61e**. ¹H NMR (300 MHz, CDCl₃) δ 3.80 (3H, s), 4.37 (2H, d, *J* = 5.7 Hz), 8.37–8.51 (2H, m), 8.57 (1H, d, *J* = 2.3 Hz). MS (ESI/APCI) mass calculated for [M + H]⁺ (C₈H₉BrN₃O₄) requires *m/z* 290.0, found *m/z* 290.0.

Methyl 2-((5-Chloro-3-nitropyridin-2-yl)amino)acetate (61g). To a stirred solution of **61f** (400 mg, 1.38 mmol) in NMP (13.8 mL) was added copper(I) chloride (410 mg, 4.14 mmol). The mixture was stirred at 150 °C for 2.5 h under microwave irradiation. The mixture was partitioned between EtOAc and water, and the gray solid was filtered off. The phases of the filtrate were separated and the aqueous phase was extracted with EtOAc. The combined organic phases were washed with water and then saturated aqueous NaCl, dried over anhydrous Na₂SO₄ and concentrated in vacuo. The residue was purified by column chromatography (silica gel, hexane/ethyl acetate, 99:1 to 4:1) to give **61g** (181 mg, 0.737 mmol, 53%) as a yellow solid after trituration with *i*-Pr₂O. The filtrate was concentrated to give the residue. The residue was triturated with hexane/*i*-Pr₂O (5:1) to give **61g** (36.1 mg, 0.147 mmol, 11%) as a yellow solid. ¹H NMR (300 MHz, DMSO-*d*₆) δ 3.65 (3H, s), 4.29 (2H, d, *J* = 5.7 Hz), 8.54 (2H, s), 8.81 (1H, t, *J* = 5.5 Hz). MS (ESI/APCI) mass calculated for [M + H]⁺ (C₈H₉ClN₃O₄) requires *m/z* 246.0, found *m/z* 246.0.

3,4-Dihydropyrido[2,3-*b*]pyrazin-2(1H)-one (62a). A mixture of **61a** (24.1 g, 114 mmol) and 10% Pd/C (containing 50% water, 3.0 g) in EtOH (381 mL) was stirred at rt overnight under H₂. The

catalyst was filtered off and evaporated. A suspension of the residue in EtOH (500 mL) was refluxed for 16 h. After cooling to rt, the solid was collected by filtration, washed with EtOH, and dried to give **62a** (16.8 g, 113 mmol, 99%) as a gray solid. ¹H NMR (300 MHz, DMSO-*d*₆) δ 3.89 (2H, d, *J* = 1.5 Hz), 6.54 (1H, dd, *J* = 7.5, 4.9 Hz), 6.67 (1H, s), 6.91 (1H, dd, *J* = 7.5, 0.8 Hz), 7.59 (1H, dd, *J* = 4.9, 1.5 Hz), 10.34 (1H, brs).

8-Methyl-3,4-dihydropyrido[2,3-*b*]pyrazin-2(1H)-one (62b). A mixture of **61b** (610 mg, 2.71 mmol) and 10% Pd/C (containing 50% water, 500 mg) in EtOH (60 mL) was hydrogenated under balloon pressure at rt for 16 h. The catalyst was removed by filtration and the filtrate was stirred at 80 °C for 8 h. The solvent was removed under reduced pressure. The resulting solid was triturated with hexane/ethyl acetate (1:2) to afford **62b** (258 mg, 1.58 mmol, 58%) as a dark purple solid. ¹H NMR (300 MHz, DMSO-*d*₆) δ 2.14 (3H, s), 3.83 (2H, d, *J* = 1.9 Hz), 6.45 (1H, d, *J* = 5.3 Hz), 6.58 (1H, s), 7.51 (1H, d, *J* = 4.9 Hz), 9.91 (1H, s). MS (ESI/APCI) mass calculated for [M + H]⁺ (C₈H₁₀N₃O) requires *m/z* 164.1, found *m/z* 164.2.

6-Methyl-3,4-dihydropyrido[2,3-*b*]pyrazin-2(1H)-one (62c). A mixture of **61c** (3.08 g, 13.7 mmol) and 10% Pd/C (containing 50% water, 1.5 g) in EtOH (200 mL) was hydrogenated under balloon pressure at rt for 1.5 h. The catalyst was filtered off and the filtrate was stirred at 80 °C for 8 h. EtOH was removed to ~50 mL, to which ethyl acetate/hexane (30 mL/15 mL) were added. The resulting solid was collected by filtration, rinsed with hexane/ethyl acetate (2:1) and dried to afford **62c** (1.911 g, 11.71 mmol, 86%) as a gray solid. ¹H NMR (300 MHz, DMSO-*d*₆) δ 2.20 (3H, s), 3.86 (2H, d, *J* = 1.9 Hz), 6.39 (1H, d, *J* = 7.6 Hz), 6.60 (1H, s), 6.82 (1H, d, *J* = 7.6 Hz), 10.25 (1H, s). MS (ESI/APCI) mass calculated for [M + H]⁺ (C₈H₁₀N₃O) requires *m/z* 164.1, found *m/z* 164.2.

7-Methyl-3,4-dihydropyrido[2,3-*b*]pyrazin-2(1H)-one (62d). A mixture of **61d** (6.99 g, 31.0 mmol) and 10% Pd/C (containing 50% water, 2.0 g) in EtOH (100 mL) was stirred at rt overnight under H₂. The catalyst was filtered off and evaporated. A suspension of the residue in EtOH (100 mL) was refluxed for 5 h and then concentrated to ~1/3 volume in vacuo. To the residue was added *i*-Pr₂O (30

mL) and the precipitate was collected by filtration, rinsed with *i*-Pr₂O and dried to give **62d** (4.56 g, 27.9 mmol, 90%) as a gray solid. ¹H NMR (300 MHz, DMSO-*d*₆) δ 2.09 (3H, s), 3.85 (2H, d, *J* = 1.5 Hz), 6.45 (1H, s), 6.72–6.80 (1H, m), 7.39–7.48 (1H, m), 10.31 (1H, s).

7-Iodo-3,4-dihydropyrido[2,3-*b*]pyrazin-2(1H)-one (62e). A mixture of **61e** (6.0 g, 17.8 mmol) and 5% Pt/C (500 mg) in THF (300 mL) was hydrogenated under balloon pressure at rt overnight. The catalyst was removed by filtration and the filtrate was concentrated in vacuo to give methyl 2-((3-amino-5-iodopyridin-2-yl)amino)acetate as brown oil. This product was subjected to the next reaction without further purification. MS (ESI/APCI) *m/z* 308.0 [M + H]⁺. A solution of methyl 2-((3-amino-5-iodopyridin-2-yl)amino)acetate (5.47 g, 17.8 mmol) in EtOH (200 mL) was refluxed for 16 h. The reaction mixture was concentrated, and the residue was triturated with *i*-Pr₂O to give **62e** (4.48 g, 16.3 mmol, 91%) as a gray solid. ¹H NMR (300 MHz, DMSO-*d*₆) δ 3.93 (2H, d, *J* = 1.5 Hz), 6.96 (1H, br. s), 7.12 (1H, d, *J* = 1.1 Hz), 7.74 (1H, d, *J* = 1.9 Hz), 10.42 (1H, br. s). MS (ESI/APCI) mass calculated for [M + H]⁺ (C₇H₇IN₃O) requires *m/z* 276.0, found *m/z* 276.0.

7-Chloro-3,4-dihydropyrido[2,3-*b*]pyrazin-2(1H)-one (62g). A solution of **61g** (181 mg, 0.74 mmol) in THF (12.5 mL) was hydrogenated over 5% Pt/C (20 mg) at rt for 2 h. The catalyst was filtered off and washed with EtOH, and the filtrate was concentrated in vacuo. The residue was dissolved in EtOH (10 mL), and the mixture was stirred at reflux overnight. Since the starting material remained, 2 M HCl solution in MeOH (1 mL) was added to the mixture, which was stirred at reflux for further 10 min. After the solvent was removed under reduced pressure, the residue was diluted with EtOAc and neutralized with saturated aqueous NaHCO₃. The phases were separated and the aqueous phase was extracted with EtOAc. The combined organic phases were washed with saturated aqueous NaCl, dried over anhydrous Na₂SO₄ and concentrated in vacuo to give **62g** (132 mg, 0.721 mmol, 98%) as a brown solid. This was used in the next reaction without further purification. ¹H NMR (300 MHz, DMSO-*d*₆) δ 3.93 (2H, d, *J* = 1.5 Hz), 6.92 (1H, d, *J* = 2.3 Hz), 6.98 (1H, s), 7.59 (1H, d, *J* = 2.3 Hz), 10.48 (1H, s). MS (ESI/APCI) mass calculated for [M + H]⁺ (C₇H₇ClN₃O) requires *m/z* 184.0, found *m/z* 184.0.

4-Nitrophenyl 2-Oxo-2,3-dihydropyrido[2,3-b]pyrazine-4(1H)-carboxylate (63a). To a solution of **62a** (3.0 g, 20.1 mmol) in DMA (170 mL) and pyridine (30 mL) was added 4-nitrophenyl chloroformate (4.87 g, 24.1 mmol) at rt. After being stirred for 20 h, the mixture was quenched with water and extracted with EtOAc. The organic layer was separated, washed with 1 M HCl aqueous solution, water and saturated aqueous NaCl, dried over anhydrous MgSO₄ and concentrated in vacuo. The residue was crystallized from hexane/ethyl acetate to give **63a** (4.83 g, 15.4 mmol, 76%) as a colorless needle. ¹H NMR (300 MHz, DMSO-*d*₆) δ 4.51 (2H, s), 7.26 (1H, dd, *J* = 7.9, 4.5 Hz), 7.40 (1H, dd, *J* = 7.9, 1.5 Hz), 7.48–7.58 (2H, m), 8.11 (1H, dd, *J* = 4.7, 1.7 Hz), 8.26–8.35 (2H, m). MS (ESI/APCI) mass calculated for [M + H]⁺ (C₁₄H₁₁N₄O₅) requires *m/z* 315.1, found *m/z* 315.1.

4-Nitrophenyl 8-Methyl-2-oxo-2,3-dihydropyrido[2,3-b]pyrazine-4(1H)-carboxylate (63b). To a solution of **62b** (50.5 mg, 0.31 mmol) and DIEA (0.162 mL, 0.93 mmol) in THF (4 mL) was added 4-nitrophenyl chloroformate (81 mg, 0.40 mmol) at 0 °C. After being stirred at rt for 1 h, the mixture was poured into water, extracted with EtOAc, dried over anhydrous Na₂SO₄ and concentrated in vacuo. The resulting solid was triturated with hexane/ethyl acetate (2:1), collected by filtration, rinsed with hexane/ethyl acetate (2:1) and dried to afford **63b** (51.9 mg, 0.158 mmol, 51%) as a tan solid. ¹H NMR (300 MHz, DMSO-*d*₆) δ 2.32 (3H, s), 4.47 (2H, s), 7.15 (1H, d, *J* = 4.9 Hz), 7.48–7.57 (2H, m), 8.01 (1H, d, *J* = 4.9 Hz), 8.26–8.36 (2H, m), 10.52 (1H, s). MS (ESI/APCI) mass calculated for [M + H]⁺ (C₁₅H₁₃N₄O₅) requires *m/z* 329.1, found *m/z* 329.2.

4-Nitrophenyl 7-Methyl-2-oxo-2,3-dihydropyrido[2,3-b]pyrazine-4(1H)-carboxylate (63d). To a solution of **62d** (1 g, 6.13 mmol) in DMA (40 mL) were added 4-nitrophenyl chloroformate (1.48 g, 7.35 mmol) and pyridine (15 mL) at rt. The mixture was stirred at rt for 16 h and then water (ca. 100 mL) was added. The resulting precipitate was collected by filtration, rinsed with water and dried to afford **63d** (1.63 g, 4.97 mmol, 81%) as a beige solid. ¹H NMR (300 MHz, DMSO-*d*₆) δ 2.29 (3H, s), 4.48 (2H, s), 7.20 (1H, d, *J* = 1.3 Hz), 7.45–7.58 (2H, m), 7.95 (1H, d, *J* = 1.3 Hz), 8.21–8.38 (2H, m), 10.85 (1H, s).

4-Nitrophenyl 3-Oxo-3,4-dihydroquinoxaline-1(2H)-carboxylate (63h). To a solution of **62h** (447 mg, 3.02 mmol) in DMA (18 mL) and pyridine (4 mL) was added 4-nitrophenyl chloroformate (730 mg, 3.62 mmol) at rt. After being stirred at 80 °C for 24 h, the mixture was quenched with water at rt and extracted with EtOAc. The organic layer was separated, washed with 1 M HCl aqueous solution, water and saturated aqueous NaCl, dried over anhydrous MgSO₄ and concentrated in vacuo. The residue was crystallized from hexane/ethyl acetate to give **63h** (657 mg, 2.10 mmol, 70%) as a yellow solid. ¹H NMR (300 MHz, DMSO-*d*₆) δ 4.44 (2H, brs), 7.00–7.10 (2H, m), 7.14–7.23 (1H, m), 7.56–7.65 (2H, m), 7.68–7.75 (1H, m), 8.25–8.36 (2H, m), 10.80 (1H, s). MS (ESI/APCI) mass calculated for [M – H][–] (C₁₅H₁₀N₃O₅) requires *m/z* 312.1, found *m/z* 312.1.

N-(2-(Methylsulfonyl)-1-(4-(trifluoromethoxy)phenyl)ethyl)-2-oxo-2,3-dihydropyrido[2,3-*b*]pyrazine-4(1H)-carboxamide (64). The title compound was prepared as a white solid after crystallization from hexane/ethyl acetate in 46% yield from **63a** and **99j** using the procedure analogous to that described for the synthesis of **37b**. ¹H NMR (300 MHz, CDCl₃) δ 2.05 (3H, s), 2.97 (2H, d, *J* = 6.0 Hz), 4.69 (2H, s), 5.24 (1H, q, *J* = 6.4 Hz), 7.01 (1H, dd, *J* = 7.7, 5.1 Hz), 7.12–7.25 (3H, m), 7.34–7.46 (2H, m), 8.03 (1H, dd, *J* = 4.9, 1.5 Hz), 9.55 (1H, brs), 10.76 (1H, d, *J* = 7.2 Hz). MS (ESI/APCI) mass calculated for [M + H]⁺ (C₁₈H₁₈F₃N₄O₃S) requires *m/z* 427.1, found *m/z* 427.1. HPLC purity: 100%. mp 114.5–117.1 °C. Anal. Calcd for C₁₈H₁₇F₃N₄O₃S: C, 50.70; H, 4.02; N, 13.14. Found: C, 50.78; H, 4.18; N, 12.97.

7-Iodo-1-((2-(trimethylsilyl)ethoxy)methyl)-3,4-dihydropyrido[2,3-*b*]pyrazin-2(1H)-one (65). To a stirred solution of **62e** (6.05 g, 22.0 mmol) in DMF (100 mL) and DMSO (150 mL) was added KHMDS (26.4 mL, 26.4 mmol) dropwise at 0 °C under N₂. The mixture was stirred at 0 °C for 20 min and SEMCl (5.74 mL, 30.8 mmol) was added at 0 °C. The mixture was stirred at rt for 3 h and then poured into water. The mixture was extracted with EtOAc, washed with water and saturated aqueous NaCl, dried over anhydrous Na₂SO₄ and concentrated in vacuo. The residue was purified by column chromatography (silica gel, hexane/ethyl acetate, 100:0 to 4:1), followed by a second column

purification (basic silica gel, hexane/ethyl acetate, 100:0 to 4:1) to afford **65** (3.41 g, 8.41 mmol, 38%) as a tan solid. ^1H NMR (300 MHz, $\text{DMSO-}d_6$) δ -0.04 (9H, s), 0.86 (2H, t, $J = 7.7$ Hz), 3.55 (2H, t, $J = 7.7$ Hz), 4.02 (2H, d, $J = 1.5$ Hz), 5.26 (2H, s), 7.08 (1H, s), 7.50 (1H, d, $J = 1.5$ Hz), 7.88 (1H, d, $J = 1.9$ Hz). MS (ESI/APCI) mass calculated for $[\text{M} + \text{H}]^+$ ($\text{C}_{13}\text{H}_{21}\text{IN}_3\text{O}_2\text{Si}$) requires m/z 406.0, found m/z 406.1.

7-Iodo-N-(2-methoxy-1-(4-(trifluoromethoxy)phenyl)ethyl)-2-oxo-1-((2-(trimethylsilyl)ethoxy)methyl)-2,3-dihydropyrido[2,3-b]pyrazine-4(1H)-carboxamide (66). To a stirred solution of **65** (1.11 g, 2.73 mmol) in THF (42 mL) was added a solution of triphosgene (647 mg, 2.18 mmol) in THF (6.3 mL) dropwise at rt under N_2 . The mixture was stirred at 40 °C for 1 h under N_2 and then concentrated in vacuo. The residue was diluted with THF and concentrated in vacuo (this procedure was repeated three times), and suspended in THF (21 mL). The mixture was added dropwise to a mixture of 2-methoxy-1-(4-(trifluoromethoxy)phenyl)ethanamine hydrochloride (889 mg, 3.27 mmol) and Et_3N (1.15 mL, 8.18 mmol) in THF (14 mL) with stirring at rt. The mixture was stirred at 60 °C overnight. The mixture was concentrated in vacuo and the residue was diluted with EtOAc. This solution was washed with water and saturated aqueous NaCl, dried over anhydrous Na_2SO_4 and concentrated in vacuo. The residue was purified by column chromatography (silica gel, hexane/ethyl acetate, 99:1 to 7:3) to give **66** (1.17 g, 1.76 mmol, 64%) as a pale orange solid. ^1H NMR (300 MHz, $\text{DMSO-}d_6$) δ 0.00 (9H, s), 0.91 (2H, t, $J = 7.7$ Hz), 3.34 (3H, s), 3.52–3.76 (4H, m), 4.60 (2H, s), 5.03–5.17 (1H, m), 5.36 (2H, s), 7.37 (2H, d, $J = 8.3$ Hz), 7.52 (2H, d, $J = 8.7$ Hz), 8.01 (1H, d, $J = 1.9$ Hz), 8.39 (1H, d, $J = 1.9$ Hz), 9.96 (1H, d, $J = 7.2$ Hz). MS (ESI/APCI) mass calculated for $[\text{M} + \text{H}]^+$ ($\text{C}_{24}\text{H}_{31}\text{F}_3\text{IN}_4\text{O}_5\text{Si}$) requires m/z 667.1, found m/z 667.1.

7-Iodo-N-(2-methoxy-1-(4-(trifluoromethyl)phenyl)ethyl)-2-oxo-1-((2-(trimethylsilyl)ethoxy)methyl)-2,3-dihydropyrido[2,3-b]pyrazine-4(1H)-carboxamide (67). To a solution of **65** (1.53 g, 3.77 mmol) in THF (60 mL) was added a solution of triphosgene (0.896 g, 3.02 mmol) in THF (8 mL) at rt. After being stirred at 40 °C for 5 h, the mixture was concentrated in vacuo. To a mixture of **100I** (1.16 g,

4.53 mmol) and Et₃N (1.58 mL, 11.3 mmol) in THF (60 mL) was added a solution of the residue obtained above in THF (10 mL) at rt. The mixture was stirred at 60 °C for 16 h, and then quenched with water and extracted with EtOAc. The organic layer was separated, washed with water and saturated aqueous NaCl, dried over anhydrous MgSO₄ and concentrated in vacuo. The residue was purified by column chromatography (basic silica gel, hexane/ethyl acetate, 19:1 to 7:3) to give **67** (2.18 g, 3.35 mmol, 89%) as a pale orange solid. ¹H NMR (300 MHz, CDCl₃) δ 0.00 (9H, s), 0.90–0.99 (2H, m), 3.38 (3H, s), 3.59–3.73 (4H, m), 4.65 (2H, d, *J* = 1.1 Hz), 5.12–5.20 (1H, m), 5.27 (2H, s), 7.42–7.51 (2H, m), 7.53–7.62 (2H, m), 7.95 (1H, d, *J* = 1.9 Hz), 8.25 (1H, d, *J* = 1.9 Hz), 10.15 (1H, d, *J* = 6.8 Hz). MS (ESI/APCI) mass calculated for [M + H]⁺ (C₂₄H₃₁F₃IN₄O₄Si) requires *m/z* 651.1, found *m/z* 651.1.

N-(1-(3-Fluoro-4-(trifluoromethoxy)phenyl)-2-methoxyethyl)-7-iodo-2-oxo-1-((2-(trimethylsilyl)ethoxy)methyl)-2,3-dihydropyrido[2,3-*b*]pyrazine-4(1H)-carboxamide (**68**). To a stirred solution of **65** (3.83 g, 9.45 mmol) in THF (144 mL) was added a solution of triphosgene (2.24 g, 7.56 mmol) in THF (22 mL) dropwise at rt under N₂. The mixture was stirred at 40 °C for 3 h under N₂ and concentrated in vacuo. The residue was diluted with THF and concentrated in vacuo (this procedure was repeated three times), and suspended in THF (72 mL). The mixture was added dropwise to a mixture of **99k** (2.87 g, 11.3 mmol) and Et₃N (2.66 mL, 18.9 mmol) in THF (48 mL) with stirring at rt. The mixture was stirred at 60 °C overnight. The mixture was concentrated in vacuo and the residue was partitioned between EtOAc and water. The phases were separated and the aqueous phase was extracted with EtOAc. The combined organic phases were washed with saturated aqueous NaCl, dried over anhydrous Na₂SO₄ and concentrated in vacuo. The residue was purified by column chromatography (silica gel, hexane/ethyl acetate, 99:1 to 7:3) to give **68** (6.15 g, 8.98 mmol, 95%) as a pale yellow amorphous solid. ¹H NMR (300 MHz, DMSO-*d*₆) δ 0.00 (9H, s), 0.85–0.97 (2H, m), 3.35 (3H, s), 3.59–3.77 (4H, m), 4.60 (2H, s), 5.03–5.18 (1H, m), 5.37 (2H, s), 7.36 (1H, d, *J* = 8.7 Hz), 7.46–7.64 (2H, m), 8.02 (1H, d, *J* = 1.9 Hz), 8.38 (1H, d, *J* = 1.9 Hz), 9.96 (1H, d, *J* = 7.2 Hz).

7-Cyclopropyl-N-(2-methoxy-1-(4-(trifluoromethoxy)phenyl)ethyl)-2-oxo-1-((2-(trimethylsilyl)ethoxy)methyl)-2,3-dihydropyrido[2,3-*b*]pyrazine-4(1*H*)-carboxamide (69). A mixture of **66** (683 mg, 1.03 mmol), cyclopropylboronic acid (176 mg, 2.05 mmol), K₃PO₄ (802 mg, 3.59 mmol), Cy₃P (117 mg, 0.410 mmol), and Pd(OAc)₂ (46.0 mg, 0.210 mmol) was stirred at 100 °C overnight under Ar. The mixture was filtered and the filtrate was washed with water and saturated aqueous NaCl, dried over anhydrous Na₂SO₄ and concentrated in vacuo. The residue was purified by column chromatography (silica gel, hexane/ethyl acetate, 99:1 to 7:3) to give **69** (432 mg, 0.743 mmol, 73%) as a pale yellow solid. ¹H NMR (300 MHz, CDCl₃) δ 0.00 (9H, s), 0.64–0.78 (2H, m), 0.90–0.99 (2H, m), 1.00–1.13 (2H, m), 1.83–1.99 (1H, m), 3.39 (3H, s), 3.59–3.73 (4H, m), 4.65 (2H, d, *J* = 1.1 Hz), 5.17 (1H, d, *J* = 7.5 Hz), 5.29 (2H, s), 7.17 (2H, d, *J* = 7.9 Hz), 7.34–7.45 (3H, m), 7.86 (1H, d, *J* = 1.9 Hz), 10.29 (1H, d, *J* = 7.5 Hz). MS (ESI/APCI) mass calculated for [M + H]⁺ (C₂₇H₃₆F₃IN₄O₅Si) requires *m/z* 581.2, found *m/z* 581.2.

7-Methoxy-N-(2-methoxy-1-(4-(trifluoromethoxy)phenyl)ethyl)-2-oxo-1-((2-(trimethylsilyl)ethoxy)methyl)-2,3-dihydropyrido[2,3-*b*]pyrazine-4(1*H*)-carboxamide (70). A mixture of **66** (900 mg, 1.35 mmol), bis(pinacolato)diboron (707 mg, 2.70 mmol), KOAc (546 mg, 5.40 mmol), and PdCl₂(dppf) (99 mg, 0.14 mmol) in DMF (13.5 mL) was stirred at 80 °C overnight under Ar. The mixture was quenched with water and extracted with EtOAc. The combined organic layer was washed with saturated aqueous NaCl, dried over anhydrous Na₂SO₄ and concentrated in vacuo to afford crude *N*-(2-methoxy-1-(4-(trifluoromethoxy)phenyl)ethyl)-2-oxo-7-(4,4,5,5-tetramethyl-1,3,2-dioxaborolan-2-yl)-1-((2-(trimethylsilyl)ethoxy)methyl)-2,3-dihydropyrido[2,3-*b*]pyrazine-4(1*H*)-carboxamide (1.55 g). This was used in the next reaction without further purification. MS (ESI/APCI) *m/z* 667.4 [M + H]⁺. To a stirred solution of the crude product obtained above (1.55 g) in THF (23 mL) was added 2 M NaOH aqueous solution (4.64 mL, 9.28 mmol) at 0 °C. After 30 min of stirring at 0 °C, hydrogen peroxide (0.813 mL, 9.28 mmol) was added to the mixture. The mixture was stirred at rt for 1.5 h and then quenched with ice-water at rt and extracted with EtOAc. The combined organic layer was washed

with saturated aqueous NaCl and dried over anhydrous Na₂SO₄ and concentrated in vacuo. The residue was purified by column chromatography (silica gel, hexane/ethyl acetate, 99:1 to 1:1) to give 7-hydroxy-*N*-(2-methoxy-1-(4-(trifluoromethoxy)phenyl)ethyl)-2-oxo-1-((2-(trimethylsilyl)ethoxy)methyl)-2,3-dihydropyrido[2,3-*b*]pyrazine-4(1*H*)-carboxamide (0.678 g, 1.22 mmol, 90% in 2 steps from **66**) as a pale yellow oil. ¹H NMR (300 MHz, CDCl₃) δ 0.00 (9H, s), 0.89–1.01 (2H, m), 3.39 (3H, s), 3.60–3.74 (4H, m), 4.65 (2H, s), 5.10–5.20 (1H, m), 5.27 (2H, s), 6.28 (1H, brs), 7.17 (2H, d, *J* = 7.9 Hz), 7.33 (1H, d, *J* = 2.6 Hz), 7.37–7.47 (2H, m), 7.72 (1H, d, *J* = 2.6 Hz), 9.96 (1H, d, *J* = 7.2 Hz). MS (ESI/APCI) mass calculated for [M + H]⁺ (C₂₄H₃₁F₃N₄O₆Si) requires *m/z* 557.2, found *m/z* 557.3.

To a stirred solution of 7-hydroxy-*N*-(2-methoxy-1-(4-(trifluoromethoxy)phenyl)ethyl)-2-oxo-1-((2-(trimethylsilyl)ethoxy)methyl)-2,3-dihydropyrido[2,3-*b*]pyrazine-4(1*H*)-carboxamide (560 mg, 1.01 mmol) in DMF (13 mL) was added K₂CO₃ (140 mg, 1.01 mmol) and methyl iodide (95 μL, 1.51 mmol). The mixture was stirred at rt overnight. The mixture was quenched with water and extracted with EtOAc. The combined organic layer was washed with saturated aqueous NaCl, dried over anhydrous Na₂SO₄ and concentrated in vacuo. The residue was purified by column chromatography (silica gel, hexane/ethyl acetate, 99:1 to 3:2) to give **70** (395 mg, 0.692 mmol, 69%) as a white amorphous solid. ¹H NMR (300 MHz, CDCl₃) δ 0.00 (9H, s), 0.86–1.01 (2H, m), 3.39 (3H, s), 3.58–3.73 (4H, m), 3.90 (3H, s), 4.65 (2H, s), 5.10–5.22 (1H, m), 5.29 (2H, s), 7.17 (2H, d, *J* = 8.3 Hz), 7.31–7.47 (3H, m), 7.75 (1H, d, *J* = 2.6 Hz), 9.98 (1H, d, *J* = 7.2 Hz). MS (ESI/APCI) mass calculated for [M + H]⁺ (C₂₅H₃₄F₃N₄O₆Si) requires *m/z* 571.2, found *m/z* 571.3.

7-Isopropoxy-*N*-(2-methoxy-1-(4-(trifluoromethoxy)phenyl)ethyl)-2-oxo-1-((2-(trimethylsilyl)ethoxy)methyl)-2,3-dihydropyrido[2,3-*b*]pyrazine-4(1*H*)-carboxamide (71). To a stirred solution of 7-hydroxy-*N*-(2-methoxy-1-(4-(trifluoromethoxy)phenyl)ethyl)-2-oxo-1-((2-(trimethylsilyl)ethoxy)methyl)-2,3-dihydropyrido[2,3-*b*]pyrazine-4(1*H*)-carboxamide (102 mg, 0.180 mmol) in DMF (2.4 mL) were added K₂CO₃ (25.6 mg, 0.180 mmol) and 2-iodopropane (28.0 μL, 0.280 mmol). The mixture

was stirred at 70 °C overnight. The mixture was quenched with water and extracted with EtOAc. The combined organic layer was washed with saturated aqueous NaCl, dried over anhydrous Na₂SO₄ and concentrated in vacuo. The residue was purified by column chromatography (silica gel, hexane/ethyl acetate, 99:1 to 7:3) to give **71** (90 mg, 0.150 mmol, 82%) as a colorless oil. ¹H NMR (300 MHz, CDCl₃) δ 0.00 (9H, s), 0.90–1.00 (2H, m), 1.38 (6H, d, *J* = 6.0 Hz), 3.39 (3H, s), 3.61–3.72 (4H, m), 4.56 (1H, dt, *J* = 12.2, 6.2 Hz), 4.65 (2H, s), 5.11–5.21 (1H, m), 5.28 (2H, s), 7.17 (2H, d, *J* = 7.9 Hz), 7.34 (1H, d, *J* = 2.6 Hz), 7.38–7.44 (2H, m), 7.73 (1H, d, *J* = 2.6 Hz), 9.99 (1H, d, *J* = 7.5 Hz). MS (ESI/APCI) mass calculated for [M + H]⁺ (C₂₇H₃₈F₃N₄O₆Si) requires *m/z* 599.2, found *m/z* 599.3.

7-Methoxy-N-(2-methoxy-1-(4-(trifluoromethyl)phenyl)ethyl)-2-oxo-1-((2-(trimethylsilyl)ethoxy)methyl)-2,3-dihydropyrido[2,3-*b*]pyrazine-4(1H)-carboxamide (72). A mixture of **67** (1.19 g, 1.83 mmol), bis(pinacolato)diboron (0.941 g, 3.67 mmol), KOAc (0.742 g, 7.34 mmol), and PdCl₂(dppf) (0.137 g, 0.18 mmol) in DMF (18 mL) was stirred at 80 °C overnight under Ar. The mixture was quenched with water and extracted with EtOAc. The combined organic layer was washed with water and saturated aqueous NaCl, dried over anhydrous Na₂SO₄ and concentrated in vacuo to give crude *N*-(2-methoxy-1-(4-(trifluoromethyl)phenyl)ethyl)-2-oxo-7-(4,4,5,5-tetramethyl-1,3,2-dioxaborolan-2-yl)-1-((2-(trimethylsilyl)ethoxy)methyl)-2,3-dihydropyrido[2,3-*b*]pyrazine-4(1H)-carboxamide (1.19 g). This was used in the next reaction without further purification. MS (ESI/APCI) mass calculated for [M + H]⁺ (C₃₀H₄₃BF₃N₄O₆Si) requires *m/z* 651.3, found *m/z* 651.3. To a stirred solution of the crude product obtained above (1.19 g) in THF (18 mL) was added 2 M NaOH aqueous solution (3.67 mL, 7.34 mmol) at 0 °C. After 30 min of stirring at 0 °C, hydrogen peroxide (0.642 mL, 7.34 mmol) was added to the mixture. The mixture was stirred at rt for 2 h. The mixture was quenched with ice-water and acidified with 1 M HCl aqueous solution, and extracted with EtOAc. The combined organic layer was washed with water and saturated aqueous NaCl, dried over anhydrous Na₂SO₄ and concentrated in vacuo. The residue was purified by column chromatography (silica gel, hexane/ethyl acetate, 99:1 to 1:1) to give

7-hydroxy-*N*-(2-methoxy-1-(4-(trifluoromethyl)phenyl)ethyl)-2-oxo-1-((2-(trimethylsilyl)ethoxy)methyl)-2,3-dihydropyrido[2,3-*b*]pyrazine-4(1*H*)-carboxamide (0.796 g, 1.47 mmol, 80% in 2 steps from **67**) as a pink oil. ¹H NMR (300 MHz, CDCl₃) δ 0.00 (9H, s), 0.87–1.03 (2H, m), 3.39 (3H, s), 3.58–3.75 (4H, m), 4.54–4.76 (2H, m), 5.13–5.23 (1H, m), 5.24–5.34 (2H, m), 7.33 (1H, d, *J* = 2.3 Hz), 7.45–7.54 (2H, m), 7.54–7.63 (2H, m), 7.72 (1H, d, *J* = 2.6 Hz), 10.09 (1H, d, *J* = 7.2 Hz). MS (ESI/APCI) mass calculated for [M + H]⁺ (C₂₄H₃₂F₃N₄O₅Si) requires *m/z* 541.2, found *m/z* 541.2. To a stirred solution of 7-hydroxy-*N*-(2-methoxy-1-(4-(trifluoromethyl)phenyl)ethyl)-2-oxo-1-((2-(trimethylsilyl)ethoxy)methyl)-2,3-dihydropyrido[2,3-*b*]pyrazine-4(1*H*)-carboxamide (796 mg, 1.47 mmol) in DMF (19 mL) was added K₂CO₃ (205 mg, 1.47 mmol) and methyl iodide (139 μL, 2.21 mmol). The mixture was stirred at rt overnight. The mixture was quenched with water and extracted with EtOAc. The combined organic layer was washed with saturated aqueous NaCl, dried over anhydrous Na₂SO₄ and concentrated in vacuo. The residue was purified by column chromatography (silica gel, hexane/ethyl acetate, 99:1 to 11:9) to give **72** (665 mg, 1.20 mmol, 81%) as a white solid. ¹H NMR (300 MHz, CDCl₃) δ 0.00 (9H, s), 0.84–1.01 (2H, m), 3.39 (3H, s), 3.57–3.75 (4H, m), 3.90 (3H, s), 4.65 (2H, s), 5.14–5.24 (1H, m), 5.29 (2H, s), 7.37 (1H, d, *J* = 2.6 Hz), 7.44–7.53 (2H, m), 7.56–7.65 (2H, m), 7.76 (1H, d, *J* = 2.6 Hz), 10.03 (1H, d, *J* = 7.2 Hz). MS (ESI/APCI) mass calculated for [M + H]⁺ (C₂₅H₃₄F₃N₄O₅Si) requires *m/z* 555.2, found *m/z* 555.2.

N-(1-(3-Fluoro-4-(trifluoromethoxy)phenyl)-2-methoxyethyl)-7-methoxy-2-oxo-1-((2-(trimethylsilyl)ethoxy)methyl)-2,3-dihydropyrido[2,3-*b*]pyrazine-4(1*H*)-carboxamide (**73**). A mixture of **68** (6.15 g, 8.98 mmol), bis(pinacolato)diboron (4.61 g, 18.0 mmol), KOAc (3.64 g, 36.0 mmol), and PdCl₂(dppf) (0.657 g, 0.90 mmol) in DMF (90 mL) was stirred at 80 °C overnight under Ar. The mixture was quenched with water and extracted with EtOAc. The combined organic layer was washed with water and saturated aqueous NaCl, dried over anhydrous Na₂SO₄ and concentrated in vacuo to give crude *N*-(1-(3-fluoro-4-(trifluoromethoxy)phenyl)-2-methoxyethyl)-2-oxo-7-(4,4,5,5-tetramethyl-1,3,2-dioxo

borolan-2-yl)-1-((2-(trimethylsilyl)ethoxy)methyl)-2,3-dihydropyrido[2,3-*b*]pyrazine-4(1*H*)-carboxamide. This was used in the next reaction without further purification. MS (ESI/APCI) mass calculated for $[M + H]^+$ ($C_{30}H_{42}BF_4N_4O_7Si$) requires m/z 685.3, found m/z 685.3. To a stirred solution of the crude product obtained above (theoretical amount: 6.15 g, 8.98 mmol) in THF (90 mL) was added 2 M NaOH aqueous solution (18.0 mL, 35.9 mmol) at 0 °C. After 30 min of stirring at 0 °C, hydrogen peroxide (3.15 mL, 35.9 mmol) was added to the mixture. The mixture was stirred at rt for 2 h. The mixture was quenched with ice-water and acidified with 1 M HCl aqueous solution, and extracted with EtOAc. The combined organic layer was washed with water and saturated aqueous NaCl, dried over anhydrous Na_2SO_4 and concentrated in vacuo. The residue was purified by column chromatography (silica gel, hexane/ethyl acetate, 99:1 to 1:1) to give *N*-(1-(3-fluoro-4-(trifluoromethoxy)phenyl)-2-methoxyethyl)-7-hydroxy-2-oxo-1-((2-(trimethylsilyl)ethoxy)methyl)-2,3-dihydropyrido[2,3-*b*]pyrazine-4(1*H*)-carboxamide (4.99 g, 8.69 mmol, 97% in 2 steps from **68**) as a brown oil. 1H NMR (300 MHz, $CDCl_3$) δ 0.00 (9H, s), 0.86–1.02 (2H, m), 3.39 (3H, s), 3.60–3.72 (4H, m), 4.65 (2H, d, $J = 1.1$ Hz), 5.12 (1H, dt, $J = 7.1, 4.7$ Hz), 5.28 (2H, s), 7.08–7.27 (3H, m), 7.35 (1H, d, $J = 2.5$ Hz), 7.72 (1H, d, $J = 2.6$ Hz), 10.03 (1H, d, $J = 7.4$ Hz). MS (ESI/APCI) mass calculated for $[M + H]^+$ ($C_{24}H_{31}F_4N_4O_6Si$) requires m/z 575.2, found m/z 575.2. To a stirred solution of *N*-(1-(3-fluoro-4-(trifluoromethoxy)phenyl)-2-methoxyethyl)-7-hydroxy-2-oxo-1-((2-(trimethylsilyl)ethoxy)methyl)-2,3-dihydropyrido[2,3-*b*]pyrazine-4(1*H*)-carboxamide (8.47 g, 14.7 mmol) in DMF (189 mL) was added K_2CO_3 (2.05 g, 14.7 mmol) and methyl iodide (1.39 mL, 22.1 mmol). The mixture was stirred at rt overnight and then concentrated in vacuo. The residue was partitioned between EtOAc and water. The phases were separated, and the aqueous phase was extracted with EtOAc. The combined organic phases were washed with saturated aqueous NaCl, dried over anhydrous Na_2SO_4 and concentrated in vacuo. The residue was purified by column chromatography (silica gel, hexane/ethyl acetate, 99:1 to 3:2) to give **73** (5.22 g, 8.87 mmol, 60%) as a pale yellow

amorphous solid. ^1H NMR (300 MHz, CDCl_3) δ 0.00 (9H, s), 0.88–1.01 (2H, m), 3.40 (3H, s), 3.58–3.74 (4H, m), 3.90 (3H, s), 4.65 (2H, s), 5.13 (1H, dt, $J = 7.2, 4.7$ Hz), 5.30 (2H, s), 7.11–7.31 (3H, m), 7.33–7.42 (1H, m), 7.76 (1H, d, $J = 2.6$ Hz), 10.01 (1H, d, $J = 7.5$ Hz). MS (ESI/APCI) mass calculated for $[\text{M} + \text{H}]^+$ ($\text{C}_{25}\text{H}_{32}\text{F}_4\text{N}_4\text{O}_6\text{Si}$) requires m/z 589.2, found m/z 589.2.

7-Methoxy-N-(2-methoxy-1-(4-(trifluoromethyl)phenyl)ethyl)-2-oxo-2,3-dihydropyrido[2,3-b]pyrazine-4(1H)-carboxamide (75). A mixture of **72** (665 mg, 1.20 mmol) in TFA (17.3 mL) and water (1.93 mL) was stirred at rt for 1 h and then concentrated in vacuo. The residue was dissolved in DMF (33 mL) and 8 M NH_3 solution in MeOH (6.46 mL, 51.7 mmol) was added. The mixture was stirred at rt for 10 min and concentrated in vacuo. The residue was diluted with EtOAc. The solution was washed with water and saturated aqueous NaCl, dried over anhydrous Na_2SO_4 and concentrated in vacuo to give **75** (474 mg, 1.12 mmol, 93%) as a white solid after trituration with hexane/ethyl acetate (10:1). ^1H NMR (300 MHz, $\text{DMSO}-d_6$) δ 3.28 (3H, s), 3.59–3.68 (2H, m), 3.83 (3H, s), 4.25–4.55 (2H, m), 5.00–5.17 (1H, m), 6.97 (1H, d, $J = 3.0$ Hz), 7.56 (2H, d, $J = 8.3$ Hz), 7.64–7.73 (2H, m), 7.77 (1H, d, $J = 2.6$ Hz), 10.07 (1H, d, $J = 7.5$ Hz), 10.77 (1H, s). MS (ESI/APCI) mass calculated for $[\text{M} + \text{H}]^+$ ($\text{C}_{19}\text{H}_{20}\text{F}_3\text{N}_4\text{O}_4$) requires m/z 425.1, found m/z 425.1.

N-(1-(3-Fluoro-4-(trifluoromethoxy)phenyl)-2-methoxyethyl)-7-methoxy-2-oxo-2,3-dihydropyrido[2,3-b]pyrazine-4(1H)-carboxamide (76). A mixture of **73** (5.22 g, 8.87 mmol) in TFA (128 mL) and water (14.3 mL) was stirred at rt for 1.5 h and then concentrated in vacuo. The residue was dissolved in DMF (243 mL) and 8 M NH_3 solution in MeOH (47.8 mL, 382 mmol) was added. The mixture was stirred at rt for 2 h and concentrated in vacuo. The residue was diluted with EtOAc. The solution was washed with water and saturated aqueous NaCl, dried over anhydrous Na_2SO_4 and concentrated in vacuo to give **76** (3.37 g, 7.36 mmol, 83%) as pale yellow solid after trituration with hexane/ethyl acetate (10:1). ^1H NMR (300 MHz, $\text{DMSO}-d_6$) δ 3.29 (3H, s), 3.63 (2H, tt, $J = 9.6, 4.9$ Hz), 3.83 (3H, s), 4.26–4.52 (2H, m), 4.95–5.15 (1H, m), 6.97 (1H, d, $J = 2.6$ Hz), 7.29 (1H, d, $J = 8.3$ Hz), 7.41–7.60

(2H, m), 7.75 (1H, d, $J = 3.0$ Hz), 10.02 (1H, d, $J = 7.5$ Hz), 10.77 (1H, s). MS (ESI/APCI) mass calculated for $[M + H]^+$ ($C_{19}H_{19}F_4N_4O_5$) requires m/z 459.1, found m/z 459.1.

N-Methoxy-N-methyl-3-(trifluoromethoxy)benzamide (**81**). To a mixture of 3-(trifluoromethoxy)benzoic acid (**78**) (5.00 g, 24.3 mmol), EDCI (7.03 g, 36.6 mmol) and HOBt (4.94 g, 36.6 mmol) in DMF (50 mL) were added *N,O*-dimethylhydroxylamine hydrochloride (2.63 g, 26.7 mmol) and Et_3N (7.36 g, 72.9 mmol). The mixture was stirred at 10 °C for 16 h, and then poured into water (100 mL). The mixture was extracted with EtOAc (150 mL \times 3), washed with saturated aqueous NaCl (400 mL \times 3), dried over anhydrous Na_2SO_4 , and concentrated in vacuo to afford **81** (5.31 g, 21.3 mmol, 88%) as a yellow oil. 1H NMR (400 MHz, $CDCl_3$) δ 3.37 (3H, s), 3.55 (3H, s), 7.28–7.34 (1H, m), 7.45 (1H, t, $J = 8.0$ Hz), 7.57 (1H, s), 7.64 (1H, d, $J = 8.0$ Hz).

N-Methoxy-N-methyl-2-(trifluoromethoxy)benzamide (**82**). To a mixture of 2-(trifluoromethoxy)benzoic acid (**79**) (5.00 g, 24.3 mmol), EDCI (7.03 g, 36.6 mmol) and HOBt (4.94 g, 36.6 mmol) in DMF (50 mL) were added *N,O*-dimethylhydroxylamine hydrochloride (2.63 g, 26.7 mmol) and Et_3N (7.36 g, 72.9 mmol). The mixture was stirred at 10 °C for 16 h, and then poured into water (100 mL). The mixture was extracted with EtOAc (150 mL \times 3), washed with saturated aqueous NaCl (300 mL \times 3), dried over anhydrous Na_2SO_4 , and concentrated in vacuo to afford **82** (5.21 g, 20.9 mmol, 86%) as a colorless oil. 1H NMR (400 MHz, $CDCl_3$) δ 3.36 (3H, s), 3.45 (3H, s), 7.27–7.37 (2H, m), 7.39–7.50 (2H, m).

3-Fluoro-N-methoxy-N-methyl-4-(trifluoromethoxy)benzamide (**83**). A mixture of 3-fluoro-4-(trifluoromethoxy)benzoic acid (**80**) (15.0 g, 66.9 mmol), *N,O*-dimethylhydroxylamine hydrochloride (7.18 g, 73.6 mmol), EDCI·HCl (16.7 g, 87.0 mmol), HOBt·H₂O (13.3 g, 87.0 mmol) and Et_3N (12.1 mL, 87.0 mmol) in DMF (200 mL) was stirred at rt for 64 h. The mixture was quenched with water and extracted with EtOAc. The organic layer was separated, washed with water and saturated aqueous NaCl, dried over anhydrous $MgSO_4$ and concentrated in vacuo. The residue was purified by column chromatography (silica gel, hexane/ethyl acetate, 19:1 to 4:1) to give **83** (17.6 g,

65.7 mmol, 98%) as a colorless oil. ¹H NMR (300 MHz, CDCl₃) δ 3.38 (3H, s), 3.56 (3H, s), 7.30–7.39 (1H, m), 7.52–7.64 (2H, m). MS (ESI/APCI) *m/z* 268.0 [M + H]⁺.

2-Fluoro-4-(trifluoromethoxy)benzonitrile (85). A mixture of dicyanozinc (4.53 g, 38.6 mmol), 1-bromo-2-fluoro-4-(trifluoromethoxy)benzene (**84**) (10.0 g, 38.6 mmol), Pd₂(dba)₃ (1.77 g, 1.93 mmol) and dppf (2.14 g, 3.86 mmol) in DMF (150 mL) was stirred at 100 °C overnight under N₂. The mixture was partitioned between EtOAc and saturated aqueous NaCl. The mixture was filtered through a cake of celite and the filtrate was extracted with EtOAc. The extract was washed with saturated aqueous NaCl, dried over anhydrous MgSO₄, filtered, and concentrated in vacuo. The residue was purified by column chromatography (basic silica gel, hexane/ethyl acetate, 49:1 to 1:1), followed by a second column chromatography purification (silica gel, hexane/ethyl acetate, 49:1 to 7:3) to give **85** (3.39 g, 16.5 mmol, 43%) as an orange oil. ¹H NMR (300 MHz, CDCl₃) δ 7.07–7.18 (2H, m), 7.65–7.76 (1H, m).

1-(4-Cyclopropylphenyl)propan-1-one (86a). A mixture of 1-(4-bromophenyl)propan-1-one (**77**) (1.07 g, 5.00 mmol), cyclopropylboronic acid (558 mg, 6.50 mmol), PdCl₂(dppf) (183 mg, 0.25 mmol) and K₃PO₄ (2.12 g, 10.0 mmol) in DME (15 mL) and water (5 mL) was stirred at 85 °C for 20 h under N₂. The mixture was extracted with EtOAc, washed with saturated aqueous NaCl, dried over anhydrous MgSO₄ and concentrated in vacuo. The residue was purified by column chromatography (silica gel, hexane/ethyl acetate, 9:1 to 7:3) to give **86a** (679 mg, 3.90 mmol, 78%) as a colorless oil. ¹H NMR (300 MHz, CDCl₃) δ 0.73–0.82 (2H, m), 1.01–1.10 (2H, m), 1.21 (3H, t, *J* = 7.2 Hz), 1.94 (1H, tt, *J* = 8.3, 5.0 Hz), 2.97 (2H, q, *J* = 7.2 Hz), 7.08–7.16 (2H, m), 7.82–7.90 (2H, m). MS (ESI/APCI) *m/z* 174.89 [M + H]⁺.

1-(4-(Azetidin-1-yl)phenyl)propan-1-one (86b). A mixture of **77** (639 mg, 3.00 mmol), azetidine (303 μL, 4.50 mmol), Pd₂(dba)₃ (137 mg, 0.15 mmol), xantphos (174 mg, 0.30 mmol) and sodium *tert*-butoxide (432 mg, 4.50 mmol) in toluene (15 mL) was stirred under N₂ at 85 °C for 20 h. The mixture was quenched with water at rt and extracted with EtOAc. The organic layer was separated,

washed with water and saturated aqueous NaCl, dried over anhydrous MgSO₄ and concentrated in vacuo. The residue was purified by column chromatography (silica gel, hexane/ethyl acetate, 19:1 to 4:1) to give **86b** (414 mg, 2.19 mmol, 73%) as a white solid. ¹H NMR (300 MHz, CDCl₃) δ 1.20 (3H, t, *J* = 7.3 Hz), 2.42 (2H, quin, *J* = 7.3 Hz), 2.90 (2H, q, *J* = 7.2 Hz), 3.99 (4H, t, *J* = 7.3 Hz), 6.32–6.39 (2H, m), 7.82–7.90 (2H, m).

1-(3-(Trifluoromethoxy)phenyl)propan-1-one (86c). To a solution of **81** (5.31 g, 21.3 mmol) in THF (50 mL) was added dropwise 3 M EtMgBr solution in Et₂O (14.2 mL, 42.6 mmol) at 0 °C under N₂. The mixture was stirred at 12 °C for 16 h and then poured into saturated aqueous NH₄Cl (50 mL). The mixture was extracted with EtOAc (80 mL × 3). The combined organic layer was dried over anhydrous Na₂SO₄ and concentrated in vacuo. The residue was purified by column chromatography (silica gel, petroleum ether/ethyl acetate, 10:1) to afford **86c** (3.23 g, 14.8 mmol, 69%) as a yellow oil. ¹H NMR (400 MHz, CDCl₃) δ 1.24 (3H, t, *J* = 7.2 Hz), 3.01 (2H, q, *J* = 7.2 Hz), 7.34–7.44 (1H, m), 7.51 (1H, t, *J* = 8.0 Hz), 7.81 (1H, s), 7.85–7.92 (1H, m).

1-(2-(Trifluoromethoxy)phenyl)propan-1-one (86d). To a solution of **82** (5.21 g, 20.9 mmol) in THF (30 mL) was added dropwise 3 M EtMgBr solution in Et₂O (13.9 mL, 41.7 mmol) at 0 °C under N₂. The mixture was stirred at 10 °C for 16 h and then poured into saturated aqueous NH₄Cl (50 mL). The mixture was extracted with EtOAc (100 mL × 3). The combined organic layer was dried over anhydrous Na₂SO₄ and concentrated in vacuo. The residue was purified by column chromatography (silica gel, petroleum ether/ethyl acetate, 10:1) to afford **86d** (3.23 g, yield: 71%) as a yellow oil. ¹H NMR (400 MHz, CDCl₃) δ 1.20 (3H, t, *J* = 7.2 Hz), 2.95 (2H, q, *J* = 7.2 Hz), 7.28–7.33 (1H, m), 7.34–7.41 (1H, m), 7.48–7.55 (1H, m), 7.70 (1H, dd, *J* = 7.6, 2.0 Hz).

1-(3-Fluoro-4-(trifluoromethoxy)phenyl)propan-1-one (86e). To a solution of **83** (5.00 g, 18.7 mmol) in THF (200 mL) at 0 °C was added dropwise 3 M ethylmagnesium bromide solution in Et₂O (7.49 mL, 22.5 mmol). The mixture was stirred at rt for 3 days. The mixture was poured into saturated aqueous NH₄Cl and extracted with EtOAc. The organic layer was separated, washed with saturated

aqueous NaCl, dried over anhydrous MgSO₄ and concentrated in vacuo. The residue was purified by column chromatography (silica gel, hexane/ethyl acetate, 49:1 to 7:3) to give **86e** (2.60 g, 11.0 mmol, 59%) as a pale yellow. ¹H NMR (300 MHz, CDCl₃) δ 1.24 (3H, t, *J* = 7.2 Hz), 2.98 (2H, q, *J* = 7.3 Hz), 7.34–7.49 (1H, m), 7.71–7.88 (2H, m).

1-(2-Fluoro-4-(trifluoromethoxy)phenyl)propan-1-one (86f). To a solution of **85** (3.79 g, 18.5 mmol) in THF (50 mL) at 0 °C was added dropwise 3 M ethylmagnesium bromide solution in Et₂O (7.39 mL, 22.2 mmol). The mixture was stirred at 0 °C for 1 h under N₂. The mixture was poured into saturated aqueous NH₄Cl and extracted with EtOAc. The organic layer was separated, washed with saturated aqueous NaCl, dried over anhydrous MgSO₄ and concentrated in vacuo. The residue was purified by column chromatography (silica gel, hexane/ethyl acetate, 49:1 to 1:1) to give **86f** (1.12 g, 4.75 mmol, 26%) as a yellow oil. ¹H NMR (300 MHz, CDCl₃) δ 1.14–1.24 (3H, m), 3.00 (2H, qd, *J* = 7.2, 3.2 Hz), 6.95–7.05 (1H, m), 7.05–7.13 (1H, m), 7.96 (1H, t, *J* = 8.5 Hz).

3-Methoxy-1-(4-(trifluoromethoxy)phenyl)propan-1-one (86h). To a solution of 1-(4-(trifluoromethoxy)phenyl)prop-2-en-1-one (**89**) (7.92 g, 36.6 mmol) in CH₂Cl₂ (92 mL) was added methanol (1.48 mL, 36.6 mmol) and PdCl₂(CH₃CN)₂ (0.951 g, 3.66 mmol) at 0 °C. The mixture was stirred at rt overnight under Ar and concentrated in vacuo. The residue was purified by column chromatography (silica gel, hexane/ethyl acetate, 100:0 to 17:3) to give **86h** (4.55 g, 18.3 mmol, 50%) as a yellow solid. ¹H NMR (300 MHz, CDCl₃) δ 3.22 (2H, t, *J* = 6.4 Hz), 3.38 (3H, s), 3.82 (2H, t, *J* = 6.4 Hz), 7.22–7.36 (2H, m), 7.97–8.07 (2H, m). MS (ESI/APCI) *m/z* 249.0 [M + H]⁺.

2-Methoxy-1-(4-(trifluoromethoxy)phenyl)ethanone (86i). (Method A: step **92** → **86i**) To a solution of **92** (930 mg, 3.94 mmol) in CH₃CN (20 mL) at 0 °C was added portionwise Dess–Martin periodinane (2.51 g, 5.91 mmol). The mixture was stirred at rt for 1.5 h. NaHCO₃ aqueous solution and Na₂S₂O₃ aqueous solution were sequentially added. After stirring for 15 min, the mixture was extracted with EtOAc, washed with saturated aqueous NaHCO₃, dried over anhydrous Na₂SO₄ and concentrated in vacuo. The residue was purified by column chromatography (silica gel, hexane/ethyl

acetate, 19:1 to 3:2) to afford **86i** (898 mg, 3.83 mmol, 97%) as a colorless oil. ¹H NMR (300 MHz, DMSO-*d*₆) δ 3.36 (3H, s), 4.80 (2H, s), 7.48–7.57 (2H, m), 8.01–8.10 (2H, m).

2-Methoxy-1-(4-(trifluoromethoxy)phenyl)ethanone (86i). (Method B: step **96** → **86i**) To a solution of **96** (9.91 g, 35.0 mmol) in MeOH (250 mL) was added Ag₂CO₃ (12.6 g, 45.5 mmol) and BF₃·OEt₂ (5.96 g, 42.0 mmol) at rt. After being stirred at 50 °C overnight, the mixture was filtered, and the filtrate was concentrated in vacuo. The mixture was diluted with water and extracted with EtOAc. The organic layer was separated, washed with water and saturated aqueous NaCl, dried over anhydrous MgSO₄ and concentrated in vacuo. The residue was purified by column chromatography (silica gel, hexane/ethyl acetate, 100:0 to 4:1) to give **86i** (6.85 g, 29.3 mmol, 84%) as a colorless oil. ¹H NMR (300 MHz, CDCl₃) δ 3.51 (3H, s), 4.67 (2H, s), 7.27–7.35 (2H, m), 7.94–8.07 (2H, m).

2-(Methylsulfanyl)-1-(4-(trifluoromethoxy)phenyl)ethanone (86j). Sodium methanethiolate (1.24 g, 17.7 mmol) was added to a solution of **96** (5.00 g, 17.7 mmol) in THF (150 mL) at 0 °C. The mixture was stirred at rt for 1 h, and then passed through a cake of basic silica gel pad (hexane/ethyl acetate, 10:1). The appropriate fractions were concentrated in vacuo to give **86j** (4.23 g, 16.9 mmol, 96%) as a pale yellow oil. ¹H NMR (300 MHz, CDCl₃) δ 2.14 (3H, s), 3.74 (2H, s), 7.27–7.36 (2H, m), 7.99–8.10 (2H, m).

1-(3-Fluoro-4-(trifluoromethoxy)phenyl)-2-methoxyethanone (86k). To a solution of **95** (4.91 g, 16.3 mmol) in MeOH (150 mL) was added Ag₂CO₃ (5.85 g, 21.2 mmol) at rt. BF₃·OEt₂ (2.48 mL, 19.6 mmol) was added dropwise to the mixture, which was stirred at 60 °C for 2.5 h. The mixture was filtered, and the filtrate was concentrated in vacuo. The residue was purified by column chromatography (silica gel, hexane/ethyl acetate, 19:1 to 4:1) to give **86k** (3.28 g, 13.0 mmol, 80%) as a colorless oil. ¹H NMR (300 MHz, CDCl₃) δ 3.50 (3H, s), 4.63 (2H, s), 7.38–7.46 (1H, m), 7.75–7.87 (2H, m).

2-Methoxy-1-(4-(trifluoromethyl)phenyl)ethanone (86l). To a solution of **97** (2.50 g, 9.36 mmol) in MeOH (50 mL) were added Ag₂CO₃ (2.99 g, 12.2 mmol) and BF₃·OEt₂ (1.42 mL, 11.2 mmol) at rt.

After being stirred at 50 °C for overnight, the mixture was filtered, and the filtrate was concentrated in vacuo. The residue was quenched with water and extracted with EtOAc. The organic layer was separated, washed with water and saturated aqueous NaCl, dried over anhydrous MgSO₄, and concentrated in vacuo. The residue was purified by column chromatography (silica gel, hexane/ethyl acetate, 19:1 to 4:1) to give **86l** (1.84 g, 8.43 mmol, 90%) as a white solid. ¹H NMR (300 MHz, CDCl₃) δ 3.51 (3H, s), 4.70 (2H, s), 7.75 (2H, d, *J* = 8.3 Hz), 8.06 (2H, d, *J* = 7.9 Hz).

1-(4-(Trifluoromethoxy)phenyl)prop-2-en-1-ol (88). To a solution of 4-(trifluoromethoxy)benzaldehyde (**87**) (21.0 g, 110 mmol) in THF (316 mL) at 0 °C was added dropwise 1 M vinylmagnesium bromide solution in THF (133 mL, 133 mmol). The mixture was stirred at 0 °C for 2 h under Ar. The mixture was quenched with saturated aqueous NH₄Cl at 0 °C and extracted with EtOAc. The organic layer was separated, washed with saturated aqueous NaCl, dried over anhydrous MgSO₄ and concentrated in vacuo. The residue was purified by column chromatography (silica gel, hexane/ethyl acetate, 100:0 to 4:1) to give **88** (14.4 g, 66.0 mmol, 60%) as a yellow oil. ¹H NMR (300 MHz, DMSO-*d*₆) δ 5.00–5.15 (2H, m), 5.63 (1H, d, *J* = 4.5 Hz), 5.85–6.03 (1H, m), 7.31 (2H, d, *J* = 8.5 Hz), 7.42–7.48 (2H, m). MS (ESI/APCI) *m/z* 201.0 [M + H – H₂O]⁺.

1-(4-(Trifluoromethoxy)phenyl)prop-2-en-1-one (89). To a solution of **88** (9.8 g, 44.9 mmol) in CH₃CN (150 mL) was added Dess–Martin periodinane (21.0 g, 49.4 mmol) at rt. The mixture was stirred at rt for 1 h. The mixture was evaporated. The residue was purified by column chromatography (silica gel, hexane/ethyl acetate, 100:0 to 17:3) to give **89** (6.47 g, 29.9 mmol, 67%) as a colorless oil. ¹H NMR (300 MHz, CDCl₃) δ 5.98 (1H, dd, *J* = 10.5, 1.5 Hz), 6.46 (1H, dd, *J* = 17.1, 1.7 Hz), 7.13 (1H, dd, *J* = 17.0, 10.5 Hz), 7.31 (2H, d, *J* = 7.9 Hz), 7.98–8.04 (2H, m). MS (ESI/APCI) *m/z* 217.0 [M + H]⁺.

2-(4-(Trifluoromethoxy)phenyl)oxirane (91). To a suspension of 4-(trifluoromethoxy)benzaldehyde (**87**) (5.00 g, 26.3 mmol) in DMSO (35 mL) was added portionwise trimethylsulfoxonium iodide (8.10 g, 36.8 mmol) over 5 min. After H₂ gas evolution ceased, the cloudy solution was treated with a

solution of 4-(trifluoromethoxy)benzaldehyde (5.00 g, 26.3 mmol) in THF (35 mL) over 15 min. After 1 h of stirring, ethanol (1 mL) was slowly added, then the THF and ethanol were removed under reduced pressure. The DMSO solution was poured into water (100 mL) and then extracted with EtOAc. The organic layer was separated, washed with saturated aqueous NaCl, dried over anhydrous Na₂SO₄ and concentrated in vacuo. The residue was purified by column chromatography (silica gel, hexane/ethyl acetate, 100:0 to 7:3) to give **91** (2.44 g, 12.0 mmol, 45%) as a colorless oil. ¹H NMR (300 MHz, CDCl₃) δ 2.76 (1H, dd, *J* = 5.3, 2.7 Hz), 3.16 (1H, dd, *J* = 5.7, 4.2 Hz), 3.87 (1H, dd, *J* = 3.8, 2.7 Hz), 7.14–7.24 (2H, m), 7.27–7.36 (2H, m).

2-Methoxy-1-(4-(trifluoromethoxy)phenyl)ethanol (92). To a solution of **91** (1.00 g, 4.90 mmol) in DMF (5 mL) was added NaOMe (1.32 g, 24.5 mmol) at rt. After being stirred at 60 °C for 2 h, the mixture was partitioned between EtOAc and water, the organic layer was washed with saturated aqueous NaCl, dried over with anhydrous Na₂SO₄, and concentrated in vacuo. The residue was purified by column chromatography (silica gel, hexane/ethyl acetate, 19:1 to 1:9) to give **92** (0.752 g, 3.18 mmol, 65%) as a pale yellow oil. ¹H NMR (300 MHz, CDCl₃) δ 2.92 (1H, br. s.), 3.40 (1H, dd, *J* = 9.8, 8.7 Hz), 3.43 (3H, s), 3.54 (1H, dd, *J* = 9.8, 3.7 Hz), 4.90 (1H, dd, *J* = 8.7, 3.0 Hz), 7.12–7.24 (2H, m), 7.34–7.46 (2H, m).

1-(3-Fluoro-4-(trifluoromethoxy)phenyl)ethanone (93). To a solution of **83** (13.3 g, 49.7 mmol) in THF (250 mL) was added 3 M MeMgBr solution in Et₂O (21.5 mL, 64.6 mmol) at 0 °C. After being stirred at rt for 4 h, the mixture was quenched with 1 M HCl aqueous solution and extracted with EtOAc. The organic layer was separated, washed with water and saturated aqueous NaCl, dried over anhydrous MgSO₄ and concentrated in vacuo. The residue was purified by column chromatography (silica gel, hexane/ethyl acetate, 19:1 to 4:1) to give **93** (10.2 g, 45.9 mmol, 92%) as a colorless oil. ¹H NMR (300 MHz, CDCl₃) δ 2.61 (3H, s), 7.36–7.46 (1H, m), 7.74–7.84 (2H, m).

2-Bromo-1-(3-fluoro-4-(trifluoromethoxy)phenyl)ethanone (95). To a stirred solution of **93** (4.41 g, 19.9 mmol) in AcOH (176 mL) was added Br₂ (1.04 mL, 19.9 mmol). The mixture was stirred at

50 °C for 3 h and then concentrated in vacuo. The mixture was partitioned between EtOAc and NaHCO₃ aqueous solution. The phases were separated and the aqueous phase was extracted with EtOAc. The combined organic phases were washed with saturated aqueous NaCl, dried over anhydrous Na₂SO₄ and concentrated in vacuo. The residue was purified by column chromatography (silica gel, hexane/ethyl acetate, 99:1 to 91:9) to give **95** (4.91 g, 16.3 mmol, 82%) as a pale yellow oil. ¹H NMR (300 MHz, CDCl₃) δ 4.39 (2H, s), 7.36–7.51 (1H, m), 7.77–7.91 (2H, m). MS (ESI/APCI) *m/z* 300.9 [M – H][–].

2-Bromo-1-(4-(trifluoromethoxy)phenyl)ethanone (96). To a solution of **94** (10.0 g, 49.0 mmol) in AcOH (100 mL) was added a solution of Br₂ (2.64 mL, 51.5 mmol) in AcOH (10 mL) at rt. The mixture was stirred at 50 °C for 1 h. The mixture was poured into water and extracted with EtOAc. The organic layer was separated, washed with saturated aqueous NaHCO₃ and saturated aqueous NaCl, dried over anhydrous MgSO₄ and concentrated in vacuo to give **96** (11.3 g, 39.9 mmol, 82%). This was used in the next reaction without further purification. ¹H NMR (300 MHz, CDCl₃) δ 4.42 (2H, s), 7.33 (2H, d, *J* = 7.9 Hz), 8.00–8.11 (2H, m).

1-(4-Cyclopropylphenyl)-N-hydroxypropan-1-imine (98a). To a solution of **86a** (679 mg, 3.90 mmol) and hydroxylammonium chloride (542 mg, 7.79 mmol) in EtOH (40 mL) was added Et₃N (1.09 mL, 7.79 mmol) at rt. After being stirred for 72 h, the mixture was concentrated in vacuo, quenched with water, and extracted with EtOAc. The organic layer was washed with water and saturated aqueous NaCl, dried over anhydrous MgSO₄, and concentrated in vacuo to afford **98a** (738 mg, 3.90 mmol, quantitative yield). This was used in the next reaction without further purification. ¹H NMR (300 MHz, CDCl₃) δ 0.66–0.76 (2H, m), 0.93–1.03 (2H, m), 1.05–1.21 (3H, m), 1.84–1.97 (1H, m), 2.49–2.85 (2H, m), 7.07 (2H, d, *J* = 8.3 Hz), 7.44–7.56 (2H, m), 7.80 (1H, brs). MS (ESI/APCI) *m/z* 190.2 [M + H]⁺.

1-(4-(Azetidin-1-yl)phenyl)-N-hydroxypropan-1-imine (98b). To a solution of **86b** (410 mg, 2.17 mmol) in EtOH (30 mL) were added hydroxylammonium chloride (602 mg, 8.67 mmol) and Et₃N

(1.21 mL, 8.67 mmol) at rt. After being stirred for 20 h, the mixture was concentrated in vacuo, quenched with water, and extracted with EtOAc. The organic layer was washed with saturated aqueous NaCl, dried over anhydrous MgSO₄, and concentrated in vacuo to afford **98b** (443 mg, 2.17 mmol, quantitative yield). This was used in the next reaction without further purification. ¹H NMR (300 MHz, CDCl₃) δ 1.04–1.22 (3H, m), 2.38 (2H, quin, *J* = 7.3 Hz), 2.49–2.82 (2H, m), 3.91 (4H, t, *J* = 7.2 Hz), 6.38–6.47 (2H, m), 7.29–7.53 (3H, m). MS (ESI/APCI) *m/z* 205.1 [M + H]⁺.

1-(3-(Trifluoromethoxy)phenyl)propan-1-one oxime (98c). To a solution of **86c** (3.23 g, 14.8 mmol) in EtOH (20 mL) were added hydroxylammonium chloride (1.23 g, 17.8 mmol) and Et₃N (1.80 g, 17.8 mmol). The mixture was stirred at reflux for 16 h. After cooling to rt, the solvent was removed under reduced pressure. The residue was partitioned between EtOAc (50 mL) and H₂O (50 mL). The aqueous phase was extracted with EtOAc (50 mL × 3). The combined organic layer was dried over anhydrous Na₂SO₄ and concentrated in vacuo to afford **98c** (3.04 g, 13.0 mmol, 88%) as a colorless oil. ¹H NMR (400 MHz, CDCl₃) δ 1.18 (3H, t, *J* = 7.6 Hz), 2.81 (2H, q, *J* = 7.6 Hz), 7.18–7.25 (1H, m), 7.42 (1H, t, *J* = 8.0 Hz), 7.49 (1H, s), 7.51–7.58 (1H, m), 8.44 (1H, brs).

1-(2-(Trifluoromethoxy)phenyl)propan-1-one oxime (98d). To a solution of **86d** (3.23 g, 14.8 mmol) in EtOH (25 mL) were added hydroxylammonium chloride (1.12 g, 16.3 mmol) and Et₃N (1.65 g, 16.3 mmol). The mixture was stirred at reflux for 16 h. After cooling to rt, the mixture was concentrated under reduced pressure to remove EtOH. The residue was partitioned between EtOAc (30 mL) and water (30 mL). The aqueous phase was extracted with EtOAc (30 mL × 3). The combined organic layer was dried over anhydrous Na₂SO₄ and concentrated in vacuo to afford **98d** (2.31 g, 9.91 mmol, 67%) as a colorless oil. ¹H NMR (400 MHz, CDCl₃) δ 1.05 (3H, t, *J* = 7.6 Hz), 2.77 (2H, q, *J* = 7.6 Hz), 7.27–7.35 (2H, m), 7.36–7.44 (2H, m), 8.28 (1H, s).

1-(3-Fluoro-4-(trifluoromethoxy)phenyl)-N-hydroxypropan-1-imine (98e). To a solution of **86e** (2.51 g, 10.6 mmol) in EtOH (35.4 mL) was added hydroxylammonium chloride (0.89 g, 12.8 mmol) and Et₃N (1.78 mL, 12.8 mmol) at rt. The mixture was stirred at rt overnight. The mixture was poured into

water and extracted with EtOAc. The organic layer was separated, washed with saturated aqueous NaCl, dried over anhydrous MgSO₄, and concentrated in vacuo to give **98e** (2.69 g, 10.7 mmol, quantitative yield) as a pale yellow oil. This was used in the next reaction without further purification.

1-(2-Fluoro-4-(trifluoromethoxy)phenyl)-N-hydroxypropan-1-imine (98f). A mixture of **86f** (1.12 g, 4.74 mmol), hydroxylammonium chloride (0.395 g, 5.69 mmol) and Et₃N (0.793 mL, 5.69 mmol) in EtOH (30 mL) was stirred at 80 °C for 3 h. The mixture was poured into saturated aqueous NaCl and extracted with EtOAc. The organic layer was separated, washed with saturated aqueous NaCl, dried over anhydrous MgSO₄ and concentrated in vacuo to give **98f** (1.27 g, 5.06 mmol, quantitative yield) as a yellow oil. ¹H NMR (300 MHz, CDCl₃) δ 1.11 (3H, t, *J* = 7.7 Hz), 2.48–2.85 (1H, m), 6.93–7.14 (2H, m), 7.19–7.53 (1H, m), 7.83–8.53 (1H, m).

N-Hydroxy-1-(4-(trifluoromethyl)phenyl)propan-1-imine (98g). To a solution of **86g** (2.00 g, 9.89 mmol) in EtOH (100 mL) were added hydroxylammonium chloride (1.38 g, 19.8 mmol) and Et₃N (2.76 mL, 19.8 mmol) at rt. After being stirred for 20 h, the mixture was quenched with water and extracted with EtOAc. The organic layer was separated, washed with saturated aqueous NaCl, dried over anhydrous MgSO₄ and concentrated in vacuo to afford **98g** (2.15 g, 9.90 mmol, quantitative yield). The residue was used in the next reaction without further purification. ¹H NMR (300 MHz, CDCl₃) δ 1.06–1.23 (3H, m), 2.54–2.90 (2H, m), 7.47–7.78 (4H, m), 8.14–8.53 (1H, m).

N-Hydroxy-3-methoxy-1-(4-(trifluoromethoxy)phenyl)propan-1-imine (98h). To a solution of **86h** (4.55 g, 18.3 mmol) in EtOH (92 mL) was added hydroxylammonium chloride (1.53 g, 22.0 mmol) and Et₃N (3.07 mL, 22.0 mmol) at rt. The mixture was stirred at 70 °C overnight. The mixture was poured into water at rt and extracted with EtOAc. The organic layer was separated, washed with saturated aqueous NaCl, dried over anhydrous MgSO₄ and concentrated in vacuo to give **98h** (4.70 g, 17.9 mmol, 97%) as a yellow oil. This was used in the next reaction without further purification.

N-Hydroxy-2-methoxy-1-(4-(trifluoromethoxy)phenyl)ethanimine (98i). To a solution of **86i** (898 mg, 3.83 mmol) in EtOH (20 mL) were added hydroxylammonium chloride (320 mg, 4.60 mmol) and

Et₃N (0.641 mL, 4.60 mmol). The mixture was stirred at 80 °C for 4 h and then evaporated under reduced pressure to remove EtOH. The residue was partitioned between EtOAc and water. The phases were separated and the aqueous phase was extracted with EtOAc. The combined organic phases were dried over anhydrous Na₂SO₄ and concentrated in vacuo to afford **98i** (949 mg, 3.81 mmol, 99%) as a colorless oil. This was used in the next reaction without further purification. MS (ESI/APCI) *m/z* 250.1 [M + H]⁺.

N-Hydroxy-2-(methylsulfanyl)-1-(4-(trifluoromethoxy)phenyl)ethanimine (98j). A mixture of **86j** (3.85 g, 15.4 mmol), triethylamine (3.11 g, 30.8 mmol) and hydroxylammonium chloride (1.39 g, 20.0 mmol) in EtOH (100 mL) was stirred at 80 °C for 16 h. The mixture was poured into saturated aqueous NaCl and extracted with EtOAc. The organic layer was separated, washed with saturated aqueous NaCl, dried over anhydrous MgSO₄ and concentrated in vacuo to give **98j** (3.78 g, 14.3 mmol, 93%) as a yellow oil. ¹H NMR (300 MHz, CDCl₃) δ 2.14 (3H, s), 3.83 (2H, s), 7.15–7.39 (2H, m), 7.62–7.87 (2H, m), 8.22 (1H, brs). MS (ESI/APCI) *m/z* 266.0 [M + H]⁺.

1-(3-Fluoro-4-(trifluoromethoxy)phenyl)-N-hydroxy-2-methoxyethanimine (98k). To a solution of **86k** (3.28 g, 13.0 mmol) and hydroxylammonium chloride (1.81 g, 26.0 mmol) in EtOH (150 mL) was added Et₃N (3.63 mL, 26.0 mmol) at rt. After being stirred for 60 h (over weekend), the mixture was concentrated in vacuo, quenched with iced water, and extracted with EtOAc. The organic layer was washed with water and saturated aqueous NaCl, dried over anhydrous MgSO₄, and concentrated in vacuo to afford **98k** (3.26 g, 12.2 mmol, 94%). This was used in the next reaction without further purification. ¹H NMR (300 MHz, CDCl₃) δ 3.33–3.42 (3H, m), 4.25–4.68 (2H, m), 7.27–7.63 (3H, m), 7.68 (1H, s). MS (ESI/APCI) *m/z* 268.1 [M + H]⁺.

N-Hydroxy-2-methoxy-1-(4-(trifluoromethyl)phenyl)ethanimine (98l). To a solution of **86l** (1.84 g, 8.43 mmol) in EtOH (100 mL) were added hydroxylammonium chloride (1.17 g, 16.9 mmol) and Et₃N (2.35 mL, 16.9 mmol) at rt. After being stirred for 4.5 h, the mixture was concentrated, quenched with water, and extracted with EtOAc. The organic layer was washed with saturated aqueous NaCl, dried

over anhydrous MgSO₄, and concentrated in vacuo to afford **98i** (1.97 g, 8.43 mmol, quantitative yield). This was used in the next reaction without further purification. ¹H NMR (300 MHz, CDCl₃) δ 3.33–3.40 (3H, m), 4.29–4.72 (2H, m), 7.58–7.83 (4H, m), 8.01–8.39 (1H, m). MS (ESI/APCI) *m/z* 234.1 [M + H]⁺.

1-(4-Cyclopropylphenyl)propan-1-amine (99a). To a solution of **98a** (738 mg, 3.90 mmol) in THF (40 mL) was added 1 M BH₃·THF solution in THF (7.09 mL, 7.80 mmol) at rt. After being refluxed for 20 h, the mixture was quenched with 1 M HCl aqueous solution at rt and extracted with EtOAc. The organic layer was separated, washed with water and saturated aqueous NaCl, dried over anhydrous MgSO₄ and concentrated in vacuo to afford **99a** (630 mg, 3.60 mmol, 92%). This was used in the next reaction without further purification.

1-(4-(Azetidin-1-yl)phenyl)propan-1-amine (99b). A mixture of **98b** (443 mg, 2.17 mmol) and 10% Pd/C (containing 50% water, 45 mg) in MeOH (15 mL) was hydrogenated under balloon pressure at rt for 20 h. The catalyst was removed by filtration and the filtrate was concentrated in vacuo to give **99b** (410 mg, 2.15 mmol, 99%) as a colorless oil. This was used in the next reaction without further purification. ¹H NMR (300 MHz, CDCl₃) δ 0.85 (3H, t, *J* = 7.3 Hz), 1.61–1.72 (2H, m), 2.28–2.41 (2H, m), 3.70 (1H, t, *J* = 7.0 Hz), 3.86 (4H, t, *J* = 7.2 Hz), 6.38–6.46 (2H, m), 7.11–7.19 (2H, m).

1-(3-(Trifluoromethoxy)phenyl)propan-1-amine Hydrochloride (99c). A mixture of **98c** (1.03 g, 4.21 mmol) and Raney Ni (300 mg) in MeOH (100 mL) was hydrogenated under 50 psi at 50 °C for 4 h. The suspension was filtered through a pad of Celite and the filter cake was washed with MeOH (50 mL × 3). The combined filtrate was concentrated to afford the crude product. The residue was purified by preparative HPLC (column: YMC-pack ODS-A 4.6 mm ID × 150 mm L; mobile phase A: 0.05% HCl in water; mobile phase B: 0.05% HCl in acetonitrile; flow rate: 1.5 mL/min). After most of the solvent was removed under reduced pressure, the residue was lyophilized to afford **100c** (330 mg, 1.29 mmol, 31%) as a yellow solid. ¹H NMR (400MHz, DMSO-*d*₆) δ 0.75 (3H, t, *J* = 7.2 Hz), 1.71–1.85 (1H, m), 1.92–2.05 (1H, m), 4.17–4.28 (1H, m), 7.34–7.42 (1H, m), 7.51–7.61(3H, m), 8.66 (3H, brs).

1-(4-(Trifluoromethyl)phenyl)propan-1-amine (99g). A mixture of crude **98g** (2.15 g, 9.90 mmol) and 20% Pd(OH)₂/C (containing 50% water, 200 mg) in EtOH (100 mL) was hydrogenated under balloon pressure at rt for 5 h. The catalyst was removed by filtration and the filtrate was concentrated in vacuo and purified by column chromatography (basic silica gel, hexane/ethyl acetate, 9:1 to 1:1) to give **99g** (988 mg, 4.86 mmol, 49%) as a colorless oil. ¹H NMR (300 MHz, CDCl₃) δ 0.87 (3H, t, *J* = 7.3 Hz), 1.62–1.77 (2H, m), 3.89 (1H, t, *J* = 6.8 Hz), 7.44 (2H, d, *J* = 7.9 Hz), 7.58 (2H, d, *J* = 7.9 Hz). NH₂ peak was not observed. MS (ESI/APCI) *m/z* 204.1 [M + H]⁺.

2-Methoxy-1-(4-(trifluoromethoxy)phenyl)ethanamine (99i). A mixture of **98i** (948.6 mg, 3.81 mmol) and 10% Pd/C (containing 50% water, 300 mg) in MeOH (20 mL) was hydrogenated under balloon pressure at rt overnight. The catalyst was removed by filtration and the filtrate was concentrated in vacuo to give **99i** (854 mg, 3.63 mmol, 95%) as a white wax-like solid. This was used in the next reaction without further purification. ¹H NMR (300 MHz, DMSO-*d*₆) δ 3.25 (3H, s), 3.29–3.38 (2H, m), 3.98–4.15 (1H, m), 7.25–7.34 (2H, m), 7.47–7.54 (2H, m). MS (ESI/APCI) *m/z* 236.1 [M + H]⁺.

2-(Methylsulfanyl)-1-(4-(trifluoromethoxy)phenyl)ethanamine (99j). A mixture of 1.1 M BH₃·THF solution in THF (5.14 mL, 5.65 mmol) and **98j** (500 mg, 1.88 mmol) in THF (50 mL) was stirred at reflux under N₂ overnight and then 1 M HCl aqueous solution was added. After being stirred at rt for 15 min, the mixture was poured into saturated aqueous NaHCO₃ and extracted with EtOAc. The organic layer was separated, washed with saturated aqueous NaHCO₃ and saturated aqueous NaCl, dried over anhydrous MgSO₄, and concentrated in vacuo to give **99j** (515 mg, 2.05 mmol, quantitative yield) as a colorless oil. This was used to the next reaction without further purification. MS (ESI/APCI) *m/z* 235.0 [M + 1 – NH₃]⁺.

1-(3-Fluoro-4-(trifluoromethoxy)phenyl)-2-methoxyethanamine (99k). A solution of **98k** (3.26 g, 12.2 mmol) in EtOH (60 mL) was treated with 20% Pd(OH)₂/C (containing 50% water, 1 g) under H₂ for 5 h. The catalyst was filtered off and the filtrate was concentrated in vacuo to afford **99k** (2.87 g,

11.3 mmol, 93%) as a white solid. ^1H NMR (300 MHz, CDCl_3) δ 3.32–3.44 (4H, m), 3.43–3.54 (1H, m), 3.56–3.99 (2H, m), 4.19 (1H, brs), 6.99–7.48 (3H, m). MS (ESI/APCI) m/z 254.1 $[\text{M} + \text{H}]^+$.

1-(2-(Trifluoromethoxy)phenyl)propan-1-amine Hydrochloride (100d). A mixture of **98d** (2.31 g, 9.91 mmol) and Raney Ni (1.00 g) in MeOH (100 mL) was hydrogenated under 50 psi at 50 °C for 4 h. The suspension was filtered through a pad of Celite and the filter cake was washed with MeOH (50 mL \times 2). The combined filtrate was concentrated to afford the crude product as a white wax-like solid. The residue was dissolved in EtOAc (70 mL) and MeOH (10 mL). 4 M HCl solution in EtOAc (40 mL, 160 mmol) was added to the above mixture. The mixture was stirred at 15 °C for 2 h and the solvent was removed under reduced pressure. The resulting solid was triturated with MTBE, collected by filtration, rinsed with MTBE (50 mL \times 3), and dried to afford **100d** (1.36 g, 5.32 mmol, 54%) as a white solid. ^1H NMR (400 MHz, $\text{DMSO}-d_6$) δ 0.78 (3H, t, $J = 7.2$ Hz), 1.76–1.89 (1H, m), 1.96–2.10 (1H, m), 4.31–4.41 (1H, m), 7.39–7.48 (1H, m), 7.49–7.59 (2H, m), 7.84 (1H, dd, $J = 6.8, 2.4$ Hz), 8.69 (3H, brs). MS (ESI/APCI) m/z 219.9 $[\text{M} + \text{H}]^+$.

1-(3-Fluoro-4-(trifluoromethoxy)phenyl)propan-1-amine Hydrochloride (100e). A mixture of **98e** (2.69 g, 10.71 mmol) and 10% Pd/C (containing 50% water, 540 mg) in EtOH (36 mL) was hydrogenated under balloon pressure at rt overnight. The catalyst was removed by filtration and the filtrate was concentrated in vacuo. The residue was purified by column chromatography (silica gel, hexane/ethyl acetate, 7:3 to 0:100). The desired fractions were collected and evaporated. To a solution of the residue in EtOAc (10 mL) was added 4 M HCl solution in EtOAc (10 mL, 40 mmol). The mixture was concentrated in vacuo. The resulting solid was triturated with *i*-Pr₂O, collected by filtration, rinsed with *i*-Pr₂O, and dried to give **100e** (1.85 g, 6.76 mmol, 63%) as a white solid. ^1H NMR (300 MHz, $\text{DMSO}-d_6$) δ 0.77 (3H, t, $J = 7.5$ Hz), 1.74–1.92 (1H, m), 1.92–2.12 (1H, m), 4.24 (1H, dd, $J = 9.0, 5.8$ Hz), 7.50 (1H, d, $J = 8.5$ Hz), 7.67 (1H, td, $J = 8.3, 0.9$ Hz), 7.80 (1H, dd, $J = 11.6, 2.0$ Hz), 8.76 (3H, brs).

1-(2-Fluoro-4-(trifluoromethoxy)phenyl)propan-1-amine Hydrochloride (100f). A mixture of **98f** (1.27 g, 5.06 mmol) and 10% Pd/C (containing 50% water, 150 mg) in MeOH (30 mL) was hydrogenated under balloon pressure at rt for 2 days. LC–MS showed no reaction. After the Pd/C was filtered off, Raney nickel (100 mg, 0.85 mmol) was then added to the mixture. The mixture was hydrogenated under balloon pressure at rt for 2 days. LC–MS showed the reaction was slow with most of the starting material remained. After the Raney nickel was filtered off, 20% Pd(OH)₂/C (containing 50% water, 100 mg, 0.71 mmol) was added to the mixture, which was hydrogenated under balloon pressure at rt overnight. The mixture was passed through a cake of celite, and the filtrate was concentrated in vacuo. To the residue was added 4 M HCl solution in EtOAc (5 mL, 20 mmol). The resulting solid was triturated with *i*-Pr₂O at 0 °C, collected by filtration, rinsed with *i*-Pr₂O at 0 °C, and dried to give **100f** (647 mg, 2.36 mmol, 47%) as a white solid. ¹H NMR (300 MHz, DMSO-*d*₆) δ 0.79 (3H, t, *J* = 7.3 Hz), 1.73–1.92 (1H, m), 1.93–2.10 (1H, m), 4.32–4.50 (1H, m), 7.41 (1H, d, *J* = 8.7 Hz), 7.52 (1H, dd, *J* = 10.5, 1.5 Hz), 7.80 (1H, t, *J* = 8.5 Hz), 8.56 (2H, brs). MS (ESI/APCI) *m/z* 221.0 [M + H]⁺.

3-Methoxy-1-(4-(trifluoromethoxy)phenyl)propan-1-amine Hydrochloride (100h). A mixture of **98h** (4.70 g, 17.9 mmol) and 20% Pd(OH)₂/C (containing 50% water, 300 mg) in MeOH (89 mL) was hydrogenated under balloon pressure at rt overnight. The catalyst was removed by filtration and the filtrate was concentrated in vacuo. The residue was purified by column chromatography (silica gel, hexane/ethyl acetate/methanol, 1:1:0 to 0:100:0 to 0:3:2). The desired fractions were collected and evaporated. To the residue was added 4 M HCl solution in EtOAc (15 mL, 60 mmol) at rt. The mixture was stirred at rt for 10 min and concentrated in vacuo. The residue was triturated with hexane/*i*-Pr₂O, collected by filtration, rinsed with hexane/*i*-Pr₂O, and dried to give **100h** (2.40 g, 8.40 mmol, 47%) as a pale yellow solid. ¹H NMR (300 MHz, DMSO-*d*₆) δ 1.92–2.08 (1H, m), 2.26 (1H, d, *J* = 5.3 Hz), 3.05–3.16 (1H, m), 3.18 (3H, s), 3.25–3.36 (1H, m), 4.36 (1H, brs), 7.46 (2H, d, *J* = 8.1 Hz), 7.60–7.72 (2H, m), 8.62 (3H, brs).

2-Methoxy-1-(4-(trifluoromethoxy)phenyl)ethanamine Hydrochloride (100i). To a 4 M HCl solution in EtOAc (100 mL, 400 mmol) was added a solution of **99i** (4.80 g, 20.4 mmol) in EtOAc (10 mL) at rt. After being stirred for 2 h, the mixture was concentrated in vacuo. The resulting solid was triturated with *i*-Pr₂O, collected by filtration, rinsed with *i*-Pr₂O, and dried to afford **100i** (4.20 g, 15.5 mmol, 76%) as a white solid. ¹H NMR (300 MHz, DMSO-*d*₆) δ 3.34 (3H, s), 3.58–3.74 (2H, m), 4.58 (1H, dd, *J* = 6.6, 5.5 Hz), 7.46 (2H, d, *J* = 8.7 Hz), 7.65 (2H, d, *J* = 8.3 Hz), 8.57 (3H, brs). MS (ESI/APCI) *m/z* 236.1 [M + H]⁺.

2-Methoxy-1-(4-(trifluoromethyl)phenyl)ethanamine Hydrochloride (100l). A mixture of **98l** (1.97 g, 8.43 mmol) and 10% Pd/C (containing 50% water, 200 mg) in EtOH (100 mL) was hydrogenated under balloon pressure at rt overnight. The catalyst was removed by filtration and the filtrate was concentrated in vacuo. To a stirred 4 M HCl solution in EtOAc (20 mL, 80 mmol) was added a solution of crude 2-methoxy-1-(4-(trifluoromethyl)phenyl)ethanamine obtained above (1.85 g, 8.43 mmol) in EtOAc (5 mL) at rt. After being stirred for 30 min, the mixture was concentrated in vacuo. The residue was triturated with ethyl acetate, collected by filtration, rinsed with ethyl acetate, and dried to afford **100l** (1.81 g, 7.08 mmol, 84%) as a white solid. ¹H NMR (300 MHz, DMSO-*d*₆) δ 3.26–3.41 (3H, m), 3.59–3.78 (2H, m), 4.58–4.73 (1H, m), 7.66–7.91 (4H, m), 8.69 (3H, brs). MS (ESI/APCI) *m/z* 220.1 [M + H]⁺.

Ethyl Oxo(4-(trifluoromethoxy)phenyl)acetate (102). To a solution of 1-bromo-4-(trifluoromethoxy)benzene (**101**) (10.0 g, 41.5 mmol) in THF (200 mL) at –78 °C was added dropwise 1.6 M butyllithium solution in hexane (31.1 mL, 49.8 mmol). The mixture was stirred at –78 °C for 50 min under N₂. Then, ethyl 2-chloro-2-oxoacetate (6.23 g, 45.6 mmol) was added to the mixture at –78 °C. The mixture was gradually warmed to rt and stirred at the same temperature overnight. The mixture was poured into 1 M HCl aqueous solution at 0 °C and extracted with EtOAc. The organic layer was washed with water and saturated aqueous NaCl, dried over anhydrous MgSO₄, and concentrated in vacuo. The residue was purified by column chromatography (silica gel,

hexane/ethyl acetate, 49:1 to 1:1) to give **102** (2.50 g, 9.54 mmol, 23%) as an orange oil, which contained some impurities. This was used in the next reaction without further purification. ¹H NMR (300 MHz, CDCl₃) δ 1.41–1.47 (3H, m), 4.41–4.51 (2H, m), 7.30–7.40 (2H, m), 8.04–8.19 (2H, m).

Ethyl 2-(Hydroxyimino)-2-(4-(trifluoromethoxy)phenyl)acetate (103). A mixture of Et₃N (1.60 mL, 11.4 mmol), **102** (2.50 g, 9.54 mmol) and hydroxylammonium chloride (0.795 g, 11.4 mmol) in EtOH (100 mL) was stirred at 80 °C overnight. The mixture was poured into saturated aqueous NaCl and extracted with EtOAc. The organic layer was washed with saturated aqueous NaCl, dried over anhydrous MgSO₄, and concentrated in vacuo. The residue was purified by column chromatography (silica gel, hexane/ethyl acetate, 49:1 to 1:1) to give **103** (725 mg, 2.62 mmol, 27%) as a pale yellow solid. ¹H NMR (300 MHz, CDCl₃) δ 1.36 (2H, t, *J* = 7.0 Hz), 1.40 (3H, t, *J* = 7.2 Hz), 4.36 (2H, q, *J* = 7.2 Hz), 4.46 (2H, q, *J* = 7.2 Hz), 7.19–7.33 (4H, m), 7.53–7.64 (4H, m), 8.65 (1H, brs), 9.22 (1H, brs).

Ethyl Amino(4-(trifluoromethoxy)phenyl)acetate (104). A mixture of **103** (720 mg, 2.60 mmol) and 10% Pd/C (containing 50% water, 140 mg) in EtOH (15 mL) was hydrogenated under balloon pressure at rt overnight. The mixture was filtered and the filtrate was concentrated in vacuo to give **104** (590 mg, 2.24 mmol, 86%) as a pale orange solid. ¹H NMR (300 MHz, CDCl₃) δ 1.18–1.28 (3H, m), 2.09 (2H, brs), 3.97–4.37 (2H, m), 4.63 (1H, s), 7.13–7.25 (2H, m), 7.43 (2H, d, *J* = 8.7 Hz). MS (ESI/APCI) *m/z* 264.1 [M + H]⁺.

Ethyl ((tert-Butoxycarbonyl)amino)(4-(trifluoromethoxy)phenyl)acetate (105). A mixture of **104** (590 mg, 2.24 mmol) and Boc₂O (430 mg, 2.47 mmol) in THF (20 mL) was stirred at rt for 2 days. The mixture was concentrated in vacuo to give crude **105** (952 mg, 2.62 mmol, quantitative yield) as a yellow oil. This was used in the next reaction without further purification. ¹H NMR (300 MHz, CDCl₃) δ 1.22 (3H, t, *J* = 7.2 Hz), 1.53 (9H, s), 3.99–4.33 (2H, m), 5.32 (1H, d, *J* = 6.8 Hz), 5.63 (1H, brs), 7.19 (2H, d, *J* = 7.9 Hz), 7.41 (2H, d, *J* = 8.7 Hz).

tert-Butyl (2-Hydroxy-1-(4-(trifluoromethoxy)phenyl)ethyl)carbamate (106). To a suspension of LAH (41.8 mg, 1.10 mmol) in THF (5 mL) at 0 °C was added **105** (100 mg, 0.28 mmol). The mixture was stirred at the same temperature for 30 min and then MgSO₄ and a small amount of H₂O were sequentially added, followed by EtOAc. The mixture was filtered through celite pad and the filtrate was concentrated in vacuo to give **106** (54.8 mg, 0.171 mmol, 62%) as a colorless gum. ¹H NMR (300 MHz, CDCl₃) δ 1.55 (9H, s), 3.71 (1H, brs), 3.86 (2H, brs), 4.79 (1H, brs), 5.28 (1H, brs), 7.11–7.24 (2H, m), 7.29–7.41 (2H, m). MS (ESI/APCI) *m/z* 320.1 [M – H][–].

tert-Butyl (2-Hydroxy-2-methyl-1-(4-(trifluoromethoxy)phenyl)propyl)carbamate (107). To a solution of methylmagnesium bromide (1 M THF solution, 2.20 mL, 2.20 mmol) in THF (5 mL) at 0 °C was added **105** (200 mg, 0.55 mmol). The mixture was stirred at 0 °C for 2 h. The mixture was poured into saturated aqueous NH₄Cl and extracted with EtOAc. The organic layer was separated, washed with saturated aqueous NaCl, dried over anhydrous MgSO₄, and concentrated in vacuo. The residue was purified by column chromatography (silica gel, hexane/ethyl acetate, 9:1 to 1:4) to give **107** (78 mg, 0.224 mmol, 41%) as a pale yellow solid. ¹H NMR (300 MHz, CDCl₃) δ 1.05 (3H, s), 1.36 (3H, s), 1.40 (9H, brs), 1.49 (1H, brs), 4.50 (1H, d, *J* = 5.3 Hz), 5.52 (1H, d, *J* = 5.7 Hz), 7.14–7.23 (2H, m), 7.29–7.38 (2H, m).

1-Amino-2-methyl-1-(4-(trifluoromethoxy)phenyl)propan-2-ol Hydrochloride (108). A mixture of **107** (78 mg, 0.22 mmol) and 4 M HCl solution in EtOA (5 mL, 20 mmol) was stirred at rt for 1 h. The mixture was concentrated in vacuo to give **108** (53.3 mg, 0.187 mmol, 84%) as a pale yellow solid. ¹H NMR (300 MHz, DMSO-*d*₆) δ 0.97 (3H, s), 1.23 (3H, s), 4.23 (1H, s), 5.39 (1H, s), 7.38–7.52 (2H, m), 7.55–7.71 (2H, m), 8.37 (3H, brs). MS (ESI/APCI) *m/z* 250.1 [M + H]⁺.

tert-Butyl (2-Methoxy-1-(4-(trifluoromethoxy)phenyl)ethyl)carbamate (109). To a solution of **99i** (10.8 g, 45.9 mmol) in THF (250 mL) were added Boc₂O (11.7 mL, 50.5 mmol) and Et₃N (7.68 mL, 55.1 mmol) at rt. After being stirred for 20 h, the mixture was quenched with water and extracted with EtOAc. The organic layer was washed with water and saturated aqueous NaCl, dried over anhydrous

MgSO₄, and concentrated in vacuo. The residue was purified by column chromatography (silica gel, hexane/ethyl acetate, 19:1 to 4:1) to give **109** (12.7 g, 37.8 mmol, 82%) as a white solid. ¹H NMR (300 MHz, CDCl₃) δ 1.41 (9H, brs), 3.35 (3H, s), 3.46–3.67 (2H, m), 4.80 (1H, brs), 5.29 (1H, brs), 7.13–7.21 (2H, m), 7.30–7.39 (2H, m).

tert-Butyl ((1R)-2-Methoxy-1-(4-(trifluoromethoxy)phenyl)ethyl)carbamate (110a). Resolution of the enantiomers of **109** was carried out chromatographically using a Chiralpak IC 50 mm ID × 500 mm L column (hexane/ethanol, 93:7) at 85 mL/min. Resolution of **109** (12.7 g, 37.8 mmol) provided **110a** as a white solid (5.84 g, 17.4 mmol, 46%, 92% theoretical) as the first eluting enantiomer. Analytical HPLC analysis carried out on a 4.6 mm ID × 250 mm L Chiralpak IC column (hexane/ethanol, 9:1) at a flow rate of 1.0 mL/min indicated that **110a** was of 99.4% ee. ¹H NMR (300 MHz, CDCl₃) δ 1.41 (9H, brs), 3.35 (3H, s), 3.49–3.67 (2H, m), 4.80 (1H, brs), 5.29 (1H, brs), 7.13–7.21 (2H, m), 7.30–7.38 (2H, m).

tert-Butyl ((1S)-2-Methoxy-1-(4-(trifluoromethoxy)phenyl)ethyl)carbamate (110b). Resolution of the enantiomers of **109** was carried out chromatographically using a Chiralpak IC 50 mm ID × 500 mm L column (hexane/ethanol, 93:7) at 85 mL/min. Resolution of **109** (12.7 g, 37.8 mmol) provided **110b** as a white solid (5.95 g, 17.7 mmol, 47%, 94% theoretical) as the second eluting enantiomer. Analytical HPLC analysis carried out on a 4.6 mm ID × 250 mm L Chiralpak IC column (hexane/ethanol, 9:1) at a flow rate of 1.0 mL/min indicated that **110b** was of 99.8% ee. ¹H NMR (300 MHz, CDCl₃) δ 1.41 (9H, brs), 3.35 (3H, s), 3.49–3.66 (2H, m), 4.81 (1H, brs), 5.29 (1H, brs), 7.13–7.21 (2H, m), 7.30–7.39 (2H, m)..

(1R)-2-Methoxy-1-(4-(trifluoromethoxy)phenyl)ethanamine Hydrochloride (111a). A mixture of **110a** (5.84 g, 17.4 mmol) and 4 M HCl solution in EtOAc (30 mL, 120 mmol) was stirred at rt for 1 h. The mixture was concentrated in vacuo, and the residue was triturated with *i*-Pr₂O, collected by filtration, rinsed with *i*-Pr₂O, and dried to give **111a** (4.52 g, 16.6 mmol, 96%) as a white solid. ¹H

NMR (300 MHz, DMSO-*d*₆) δ 3.33 (3H, s), 3.60–3.77 (2H, m), 4.52–4.61 (1H, m), 7.46 (2H, d, *J* = 8.3 Hz), 7.68 (2H, d, *J* = 8.7 Hz), 8.67 (3H, brs). MS (ESI/APCI) *m/z* 219.0 [M + H – (NH₃)]⁺.

(1S)-2-Methoxy-1-(4-(trifluoromethoxy)phenyl)ethanamine Hydrochloride (111b). A mixture of **110b** (5.95 g, 17.7 mmol) and 4 M HCl solution in EtOAc (30 mL, 120 mmol) was stirred at rt for 1 h. The mixture was concentrated in vacuo, and the residue was triturated with *i*-Pr₂O, collected by filtration, rinsed with *i*-Pr₂O, and dried to give **111b** (4.30 g, 15.8 mmol, 89%) as a white solid. ¹H NMR (300 MHz, DMSO-*d*₆) δ 3.33 (3H, s), 3.60–3.77 (2H, m), 4.52–4.61 (1H, m), 7.46 (2H, d, *J* = 8.3 Hz), 7.68 (2H, d, *J* = 8.7 Hz), 8.67 (3H, brs). MS (ESI/APCI) *m/z* 219.1 [M + H – (NH₃)]⁺.

tert-Butyl (1-(3-Fluoro-4-(trifluoromethoxy)phenyl)-2-methoxyethyl)carbamate (113). To a solution of **99k** (7.47 g, 29.5 mmol) in THF (200 mL) were added Boc₂O (7.53 mL, 32.5 mmol) and Et₃N (6.17 mL, 44.3 mmol) at rt. After being stirred at rt for 16 h, the mixture was quenched with water and extracted with EtOAc. The organic layer was separated, washed with saturated aqueous NaCl, dried over anhydrous MgSO₄, and concentrated in vacuo. The residue was purified by column chromatography (silica gel, hexane/ethyl acetate, 19:1 to 4:1) to give **113** (8.25 g, 23.4 mmol, 79%) as a white solid. ¹H NMR (300 MHz, CDCl₃) δ 1.42 (9H, brs), 3.35 (3H, s), 3.49–3.67 (2H, m), 4.78 (1H, brs), 5.34 (1H, brs), 7.08–7.29 (3H, m). MS (ESI/APCI) *m/z* 254.0 [M + H – (Boc)]⁺.

tert-Butyl ((1S)-1-(3-Fluoro-4-(trifluoromethoxy)phenyl)-2-methoxyethyl)carbamate (114a). Resolution of the enantiomers of **113** was carried out chromatographically using a Chiralpak AD 50 mm ID × 500 mm L column (hexane/ethanol, 19:1) at 80 mL/min. Resolution of **S43** (12.5 g, 35.5 mmol) provided **114a** as a white solid (5.73 g, 16.2 mmol, 46%, 92% theoretical) as the first eluting enantiomer. Analytical HPLC analysis carried out on a 4.6 mm ID × 250 mm L Chiralpak AD column (hexane/ethanol, 19:1) at a flow rate of 1.0 mL/min indicated that **114a** was of >99.9% ee. ¹H NMR (300 MHz, CDCl₃) δ 1.42 (9H, brs), 3.35 (3H, s), 3.49–3.66 (2H, m), 4.77 (1H, brs), 5.34 (1H, brs), 7.07–7.30 (3H, m). MS (ESI/APCI) *m/z* 254.0 [M + H – (Boc)]⁺.

(1S)-1-(3-Fluoro-4-(trifluoromethoxy)phenyl)-2-methoxyethanamine hydrochloride (115). A mixture of **114a** (5.73 g, 16.2 mmol) and 4 M HCl solution in EtOAc (100 mL, 400 mmol) was stirred at rt for 3 h. The mixture was concentrated in vacuo, and the resulting solid was triturated with *i*-Pr₂O, collected by filtration, rinsed with *i*-Pr₂O, and dried to give **115** (4.45 g, 15.4 mmol, 95%) as a white solid. ¹H NMR (300 MHz, DMSO-*d*₆) δ 3.33 (3H, s), 3.61–3.78 (2H, m), 4.55–4.64 (1H, m), 7.47–7.56 (1H, m), 7.64–7.83 (2H, m), 8.74 (3H, brs). MS (ESI/APCI) *m/z* 254.0 [M + H]⁺.

(+)-Di-(*p*-toluoyl)-D-tartaric acid salt of 116 (117). **115** (2.00 g, 6.90 mmol) was suspended in EtOAc and neutralized with saturated aqueous NaHCO₃. The organic phase was dried over anhydrous Na₂SO₄ and concentrated in vacuo to afford **116** (1.74 g, 6.87 mmol, quantitative yield) as a colorless oil. **116** (127 mg, 0.500 mmol) and (2*S*,3*S*)-(+)-di-(*p*-toluoyl)-D-tartaric acid (193 mg, 0.500 mmol) were dissolved in EtOH (200 μl) and water (200 μl) at rt. The mixture was heated to 50 °C and stood overnight to give (2*S*,3*S*)-2,3-bis((4-methylbenzoyl)oxy)butanedioic acid - (1*S*)-1-(3-fluoro-4-(trifluoromethoxy)phenyl)-2-methoxyethanamine (1:1) (**117**) suitable for X-ray crystallography.

Enzyme Assay Protocol. *Preparation of human PDE.* Human PDE1A, 3A, 4D2, 5A1, 7B, 8A1, 9A2, and 11A4 enzymes were purchased from BPS Bioscience. Human PDE6AB enzyme was purchased from SB Drug Discovery. Human PDE2A3 full-length gene was transduced into Sf9, and human PDE2A3 enzyme was purified by His-tag affinity column and gel filtration. Human PDE10A2 was generated from COS-7 cells transfected with the full-length gene. The enzymes were stored at –70 °C until use.

PDE2A3 enzyme inhibitory assay. PDE activity was measured using a SPA (GE Healthcare). To evaluate the inhibitory activity of the compound, 10 μL of serially diluted compounds were reacted with 20 μL of PDE enzyme (final concentration 0.023 nM) in assay buffer (50 mM HEPES-NaOH, 8.3 mM MgCl₂, 1.7 mM EGTA, and 0.1% bovine serum albumin (BSA) (pH 7.4)) for 30 min at rt. The final concentration of DMSO in the reaction solution was 1%. Compounds were tested in duplicate in

96-well half-area plates (Corning) or a 384-well OptiPlate (PerkinElmer). We used an 8 concentration serial dilution dose response ranging from 100 μM to 10 pM compound concentrations. To start the reaction, 10 μL of substrate [^3H] cGMP (final concentration 77 nM, PerkinElmer) was added to a total volume of 40 μL . After reaction for 60 min at rt, 20 μL of 20 mg/mL yttrium SPA beads containing zinc sulfate was added to terminate the PDE reaction. After allowing to settle for an additional 60 min, the assay plates were counted in a scintillation counter (PerkinElmer) to allow calculation of the inhibition rate. The inhibition rate was calculated on the basis of the 0% control wells with enzyme and DMSO, and the 100% control wells without enzyme. All IC_{50} values were obtained by fitting the results to the following 4 Parameter Logistic Equation:

$$y = A + (B - A) / (1 + (10^{((C - x) * D)}))$$

where A is the minimum y value, B is the maximum y value, C is $\text{Log}(\text{EC}_{50})$ value, and D is the slope factor.

Human PDE enzyme assay. PDE activities were measured using a SPA (GE Healthcare). To evaluate the inhibitory activity, 10 μL of serially diluted compounds were incubated with 20 μL of PDE enzymes, except for PDE1A, in the following assay buffer: 50 mM HEPES-NaOH, 8.3 mM MgCl_2 , 1.7 mM EGTA, and 0.1% BSA (pH 7.4) for 30 min at rt. The PDE1A enzyme assay was performed in the following assay buffer: 50 mM Tris-HCl, 8.3 mM MgCl_2 , 0.2 mM CaCl_2 , 0.1% BSA, and 30 nM Calmodulin (pH 7.5). The final concentration of DMSO in the assay was 1%, and compounds were tested in duplicate in 96-well half-area plates (Corning). We used an 4 concentration serial dilution dose response ranging from 10 μM to 10 nM compound concentrations. To start the reaction, 10 μL of substrate ([^3H] cGMP (final concentration 77 nM, PerkinElmer) for PDE1A, 5A1, 6AB, 9A2, 10A2, and 11A4 or [^3H] cAMP (final concentration 14.7 nM, PerkinElmer) for PDE3A, 4D2, 7B, and 8A1) was added for a final assay volume of 40 μL . After 60 min incubation at rt, 20 μL of 20 mg/mL yttrium SPA beads containing zinc sulfate was added to terminate the PDE reaction. After allowing to

settle for more than 120 min, the assay plates were counted in a scintillation counter (PerkinElmer) to allow calculation of the inhibition rate.

Estimation of Log *D* at pH 7.4. Log $D_{7.4}$, which is the partition coefficient of the compounds between 1-octanol and aqueous buffer at pH 7.4, was measured using a chromatographic procedure based on a published method.⁶⁸ The instruments utilized were a Waters Alliance 2795 HPLC system and a 2996 UV–vis detector (Milford, MA, USA).

Transcellular Transport Study Using a Transporter-Expression System. Human MDR1-expressing LLC-PK1 cells were cultured as reported previously with minor modifications.¹⁰⁶ The transcellular transport study was performed as reported previously.¹⁰⁷ In brief, the cells were grown for 7 days in an HTS Transwell 96-well permeable support (pore size: 0.4 μm , surface area: 0.143 cm^2) with a polyethylene terephthalate membrane (Corning Life Sciences, Lowell, MA, USA) at a density of 1.125×10^5 cells/well. The cells were preincubated with M199 at 37 °C for 30 min. Subsequently, transcellular transport was initiated by the addition of M199 either to apical compartments (75 μL) or to the basolateral compartments (250 μL) containing 10 μM digoxin, 200 μM lucifer yellow as a marker for the monolayer tightness, and 10 μM test compounds, and then terminated by the removal of each assay plate after 2 h. The aliquots (25 μL) in the opposite compartments were mixed with acetonitrile containing alprenolol and diclofenac as an internal standard and then centrifuged. The compound concentrations in the supernatant were measured by LC–MS/MS. The apparent permeability (P_{app}) of test compounds in the receiver wells was determined and the efflux ratio (ER) for the MDR1 membrane permeability test was calculated using the following equation: $\text{ER} = P_{\text{app,BtoA}}/P_{\text{app,AtoB}}$ where $P_{\text{app,AtoB}}$ is the apical-to-basal passive permeability–surface area product and $P_{\text{app,BtoA}}$ is the basal-to-apical passive permeability–surface area product.

In Vitro Metabolic Clearance Assay. In vitro oxidative metabolic studies of the test compounds were carried out using hepatic microsomes obtained from humans, rats, or mice. The reaction mixture with

a final volume of 0.05 mL consisted of 0.2 mg/mL hepatic microsomes in 50 mM KH_2PO_4 – K_2HPO_4 phosphate buffer (pH 7.4) and 1 μM test compound. The reaction was initiated by the addition of an NADPH-generating system containing 25 mM MgCl_2 , 25 mM glucose 6-phosphate, 2.5 mM β -NADP⁺, and 7.5 units/mL glucose 6-phosphate dehydrogenase at 20 vol% of the reaction mixture. After addition of the NADPH-generating system, the mixture was incubated at 37 °C for 0, 15, and 30 min. The reaction was terminated by addition of an equivalent volume of acetonitrile. After the samples were mixed and centrifuged, the supernatant fractions were analyzed using LC–MS/MS. For metabolic clearance determinations, chromatograms were analyzed to determine the disappearance of the parent compound from the reaction mixtures. All incubations were carried out in duplicate.

Protein Expression and Purification. The PDE2A catalytic domain (578–919) was cloned into a pFastBac vector, for expression in Sf9 cells, utilizing an N-terminal 6× poly-histidine tag containing a TEV cleavage site. Large-scale production of recombinant protein was carried out in Sf9 cells. The pellet from 10L of baculovirus-infected Sf9 cells was resuspended in 600 mL of lysis buffer containing 25 mM Tris (pH 7.6), 1 M NaCl, 20 mM imidazole, 5% glycerol, and 3 Roche cOmplete Protease Inhibitor tablets. The cell suspension was homogenized with the Polytron PT-3100, centrifuged for 1 h at 13,000 rpm (JA-14 rotor), and the clarified supernatant was brought to 800 mL with lysis buffer before batch binding with 10 mL of Probond Ni resin (Invitrogen) and rolling for 2 h at 4 °C. The beads were collected by low speed centrifugation (3,500 rpm, JS-4.2 rotor), loaded into a gravity column, and washed slowly overnight with 2 L of wash buffer containing 25 mM Tris (pH 7.6), 1 M NaCl, 20 mM imidazole, and 5% glycerol. The following day, the protein was eluted with buffer containing 25 mM Tris (pH 7.9), 50 mM NaCl, 250 mM imidazole, and 10% glycerol. The 1.5 mL sample eluted from the Nickel capture step was brought to 9 mL with Mono Q buffer A containing 25 mM Tris (pH 7.9), and 10% glycerol. After the full sample volume was bound to the Mono Q column, a salt gradient was applied from 0 to ~800 mM NaCl in 40 mL. Fractions corresponding to the unphosphorylated protein (identified by MS with MW = 40178 Da) were pooled for further

purification by size-exclusion chromatography (SEC) on a Superdex 200 column equilibrated in 1XTBS pH 7.4, 0.5 mM DTT, 1 mM EDTA, and 10% glycerol. Peak SEC fractions were collected and concentrated to 12 mg/mL for crystallization.

Crystallization and Structure Determination. Crystals suitable for data collection were first grown in hanging drops using the vapor diffusion method at rt by adding 0.5 μ L of protein solution with 1 mM of IBMX⁵⁹ and 0.5 μ L of reservoir solution (30% PEG 3350, 0.1 M Tris pH 7.5, and 0.2 M MgCl₂). PDE2A IBMX crystals were soaked in a drop containing 5 mM of **42a**, 31% PEG 3350, 0.1 M Tris (pH 7.5), and 0.2 M MgCl₂ for 6 days. Crystals were transferred through a fresh cryo-protected soak drop immediately before being harvested and flash frozen in liquid nitrogen. X-ray diffraction data were collected at ALS beamline 5.0.2 using a Pilatus3 6M (Dectris) detector from a single cryogenically protected crystal (100 K) at a wavelength of 1 Å. The crystals belong to space group C121 and contain three enzyme molecules per asymmetric unit. X-ray diffraction data were reduced using the HKL2000¹⁰⁸ software package. The structure was determined by molecular replacement with PHASER within the CCP4 program suite and refined with REFMAC.¹¹¹ Several cycles of model building using Mifit¹¹³ and refinement using REFMAC were performed to improve the quality of the model. The coordinates and structure factors have been deposited in the PDB with accession code 5VP0.

Animal Experiments. The care and use of animals and the experimental protocols were approved by the Experimental Animal Care and Use Committee of Takeda Pharmaceutical Company Limited.

Pharmacokinetic Analysis in Rat or Mouse Cassette Dosing. Compound **42a** was administered intravenously (0.1 mg/kg) or orally (1 mg/kg) by cassette dosing to nonfasted male CrI:CD(SD)(IGS) rats (8W, $n = 3$) or male ICR mice (8W, $n = 3$). The combination for a cassette dosing was determined to avoid combinations of compounds with the same molecular weight. The solution of compounds in dimethylacetamide containing 50% (v/v) 1,3 butanediol at 0.1 mg/mL/kg was administered intravenously to isoflurane-anesthetized mice via femoral vein. The suspension of compounds in 0.5%

methyl cellulose with water was used for vehicle (1 mg/kg) and was administered orally by gavage. After administration, blood samples were collected via tail vein by syringes with heparin at 5, 10, 15, 30 min, 1, 2, 4, and 8 h (iv) and 15, 30 min, 1, 2, 4, and 8 h (po), and centrifuged to obtain the plasma fraction. The plasma samples were deproteinized by mixing with acetonitrile followed by centrifugation. The compound concentrations in the supernatant were measured by LC–MS/MS with a standard curve. Pharmacokinetic parameters were calculated by the non-compartmental analysis. The area under the concentration-time curve (AUC) and the area under the first moment curve (AUMC) were calculated using the linear trapezoidal method. The mean residence time (MRT) was calculated as $AUMC/AUC$. The total clearance (CL_{total}) was calculated as $dose_{iv}/AUC_{iv}$. The volume of distribution ($V_{d_{ss}}$) was calculated as $CL_{total} \times MRT_{iv}$. Oral bioavailability (F) was calculated as $(AUC_{po}/dose_{po})/(AUC_{iv}/dose_{iv}) \times 100$.

Brain and Plasma Concentration in Rats and Mice. Compound **42a** was suspended in 0.5% (w/v) methylcellulose in distilled water, and was administered at a volume of 2 mL/kg body weight for rats and 10 mL/kg for mice. Seven-week-old male SD rats (Charles River Laboratories Japan, Inc., Yokohama, Japan) and seven-week-old male ICR mice (CLEA Japan Inc., Tokyo, Japan) were euthanized 2 h after oral administration of **42a** (10 mg/kg). Blood was centrifuged and the supernatants were collected as plasma. Brain was homogenized in physiological saline. Concentrations of **42a** were measured in aliquots of rat plasma and tissues, which were mixed well with acetonitrile containing internal standards and then centrifuged. The supernatants were diluted with solvents for LC–MS/MS analysis (mobile phase A: 10 mM ammonium formate/formic acid (100/0.2, v/v), mobile phase B: acetonitrile/formic acid (100/0.2, v/v)). The diluted solutions were injected into an LC–MS/MS (API5000, AB Sciex, Foster City, CA) equipped with a Shimadzu Shim-pack XR-ODS column (2.2 μ m packing particle size, 2.0 mm ID \times 30 mm L) maintained at 50 °C. The chromatographic separation was performed using gradient elution at a flow rate of 0.7 mL/min. The LC time program was as follows: Mobile phase B was held at 5% for 0.2 min, and increased linearly

to 99% in 1.1 min. After maintaining B at 99% for another 0.7 min, it was brought back to 5% in 0.01 min, followed by re-equilibration for 0.59 min. The total cycle time for one injection was 2.6 min. Compound **42a** was detected using multiple reaction monitoring mode and the transition m/z 459.20 → 223.01. AnalystTM software (version 1.4.2) was used for data acquisition and processing.

Measurement of Cyclic Nucleotide Contents in Mouse Brains. *Animals.* Four-week-old male ICR mice were purchased from CLEA Japan, Inc. (Japan). After one week acclimation period, the five-week-old mice were used for the experiment. The mice were housed in groups of 5/cage in a light-controlled room (12 h light/dark cycles with lights on at 07:00). Food and water were provided *ad libitum*.

Measurements. Compound **42a** was suspended in 0.5% (w/v) methylcellulose in distilled water and administered at a volume of 10 mL/kg body weight for mice. Either vehicle or compound **42a** was administered orally to mice after a habituation period of more than 30 min. Compound **42a** was administered at 3 and 10 mg/kg. A microwave fixation system (Muromachi Kikai, Tokyo, Japan) was used to sacrifice unanesthetized mice by exposure of the head to the microwave beam at 60 min after administration of **42a**. Hippocampi were isolated and homogenized in 0.5 mol/L HCl, followed by centrifugation. The cGMP concentration in the supernatant was quantified using a cyclic GMP EIA kit (Cayman Chemical, USA) according to the manufacturer's instructions. Values were expressed as pmol/mg tissue weight.

Compound **42a** was suspended in 0.5% (w/v) methylcellulose in distilled water, and was administered in a volume of 10 mL/kg body weight for mice. Either vehicle or compound **42a** (1, 3, and 10 mg/kg) was administered orally to mice after a habituation period of more than 1 h. A microwave fixation system (Muromachi Kikai, Tokyo, Japan) was used to sacrifice unanesthetized mice by exposure of the head to the microwave beam at 60 min after administration of **42a**. Brain tissues were isolated and homogenized in 0.5 mol/L HCl, followed by centrifugation. The concentration of cyclic nucleotides in

the supernatant was quantified using a cyclic cAMP or GMP EIA kit (Cayman Chemical, USA) according to the manufacturer's instructions. Values were expressed as pmol/mg tissue weight.

Effects of 42a on the Novel Object Recognition Task in Rats. *Animals.* Six-week-old male Long-Evans rats were purchased from Japan SLC Inc. Rats were acclimated for one week prior to the experiment. The rats were housed in groups of 2 or 3/cage in a light-controlled room (12 h light/dark cycles with lights on at 07:00). Food and water were provided *ad libitum*.

Measurements. Compound **42a** was suspended in 0.5% (w/v) methylcellulose in distilled water, and administered at a volume of 2 mL/kg body weight for rats. On day 1, rats were allowed to habituate to the behavioral test room for over 1 h, and then they were allowed to habituate individually to the empty test box (a gray-colored polyvinyl chloride box (40 × 40 × 50 cm)) for 10 min. The test was comprised of two, 3 min trials called the acquisition and retention trials, separated by a 48 h inter-trial interval. On day 2, in the acquisition trial, rats were allowed to explore two identical objects (A1 and A2) for 3 min. Object exploration was defined as rats' licking, sniffing, or touching the object with forelimbs while sniffing. Leaning against the object to look upward and standing or sitting on the object were excluded. The exploration time of rats for each object (A1 and A2) was scored manually. Rats that scored less than 10 s of total exploration time during the acquisition trials were excluded from further study. On day 4, in the retention trial, rats were again allowed to explore a familiar object (A3) and a novel object (B) for 3 min. Exploration times for the familiar and novel objects were manually scored in the same way as in the acquisition trial. Vehicle or **42a** (0.01, 0.1, and 1 mg/kg) was administered orally 2 h prior to the acquisition trial. The novelty discrimination index (NDI) was calculated using the following equation: novel object interaction time/total interaction time × 100 (%). Forty rats were prepared in total, and then one rat treated with 1 mg/kg was excluded because its total exploration time in the acquisition trial was less than 10 s (6.95 s). Numbers of rats treated with vehicle and those treated with 0.01, 0.1, and 1 mg/kg of compound **42a** were 10, 10, 10, and 9, respectively.

Determination of the Absolute Stereochemistry of Amine 111a. The absolute configuration of **111a** was determined by X-ray crystallography.

Crystal data for **111a**: $C_{10}H_{13}F_3NO_2^+ \cdot Cl^- \cdot 0.25C_7H_8$, MW = 294.70; crystal size, $0.20 \times 0.09 \times 0.06$ mm; colorless, block; triclinic, space group $P1$, $a = 7.2413(3)$ Å, $b = 14.4003(6)$ Å, $c = 14.4361(6)$ Å, $\alpha = 105.170(8)^\circ$, $\beta = 103.917(8)^\circ$, $\gamma = 92.350(7)^\circ$, $V = 1401.53(12)$ Å³, $Z = 4$, $D_x = 1.397$ g/cm³, $T = 100$ K, $\mu = 2.736$ mm⁻¹, $\lambda = 1.54187$ Å, $R_1 = 0.051$, $wR_2 = 0.133$, Flack Parameter¹¹⁴ = 0.036(13).

All measurements were made on a Rigaku R-AXIS RAPID-191R diffractometer using graphite monochromated Cu-K α radiation. The structure was solved by direct methods with SHELXS-97¹¹⁵ and was refined using full-matrix least-squares on F^2 with SHELXL-97.¹¹⁵ All non-H atoms were refined with anisotropic displacement parameters.

CCDC 1548480 for compound **111a** contains the supplementary crystallographic data for this paper.

These data can be obtained free of charge from The Cambridge Crystallographic Data Centre via

<http://www.ccdc.cam.ac.uk/Community/Requestastructure/Pages/DataRequest.aspx?>

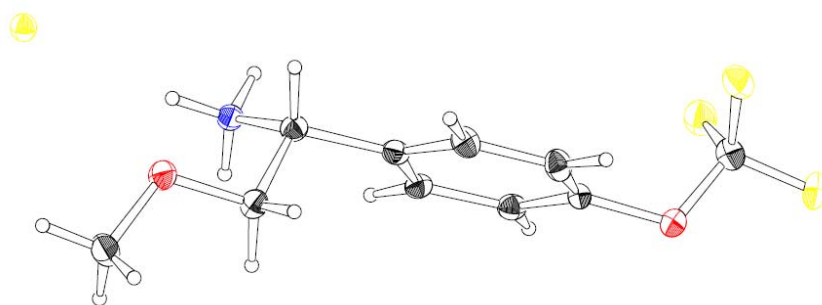


Figure 2-10. ORTEP of **111a**, thermal ellipsoids are drawn at 20% probability.

Determination of the Absolute Stereochemistry of Amine 114a. The absolute configuration of **114a** was determined by X-ray crystallography of its (+)-di-(*p*-toluoyl)-D-tartaric acid salt **117**.

Crystal data for **117**: $C_{10}H_{12}F_4NO_2^+ \cdot C_{20}H_{17}O_8^-$, MW = 639.55; crystal size, $0.20 \times 0.11 \times 0.09$ mm; colorless, block; monoclinic, space group $P2_1$, $a = 7.88545(14)$ Å, $b = 25.3299(5)$ Å, $c = 15.2262(3)$ Å,

$\alpha = \gamma = 90^\circ$, $\beta = 90.330(7)^\circ$, $V = 3041.20(10) \text{ \AA}^3$, $Z = 4$, $D_x = 1.397 \text{ g/cm}^3$, $T = 100 \text{ K}$, $\mu = 1.044 \text{ mm}^{-1}$,
 $\lambda = 1.54187 \text{ \AA}$, $R_1 = 0.060$, $wR_2 = 0.160$, Flack Parameter¹¹⁴ = 0.01(15).

All measurements were made on a Rigaku R-Axis RAPID-191R diffractometer using graphite monochromated Cu-K α radiation. The structure was solved by direct methods with SIR92¹¹⁶ and was refined using full-matrix least-squares on F^2 with SHELXL-97.¹¹⁵ All non-H atoms were refined with anisotropic displacement parameters.

CCDC 1548479 for compound **117** contains the supplementary crystallographic data for this paper.

These data can be obtained free of charge from The Cambridge Crystallographic Data Centre via

<http://www.ccdc.cam.ac.uk/Community/Requestastructure/Pages/DataRequest.aspx?>



Figure 2-11. ORTEP of **117**, thermal ellipsoids are drawn at 20% probability.

第 3 章に関する実験

(S)-N-(2-hydroxy-2-methyl-1-(4-(trifluoromethoxy)phenyl)propyl)pyrazolo[1,5-a]pyrimidine-3-carboxamide (119). A mixture of pyrazolo[1,5-a]pyrimidine-3-carboxylic acid (**15**) (43.8 mg, 0.268 mmol), **130** (84.3 mg, 0.295 mmol), EDCI·HCl (61.7 mg, 0.321 mmol), HOBt·H₂O (49.3 mg, 0.321 mmol), and TEA (0.045 mL, 0.321 mmol) in DMF (1.5 mL) was stirred at rt overnight. The mixture was poured into water and extracted with EtOAc. The organic layer was washed with saturated aqueous NaCl, dried over anhydrous Na₂SO₄ and concentrated in vacuo. The residue was purified by column chromatography (silica gel, hexane/ethyl acetate/methanol, 4:1:0 to 0:100:0 to 0:9:1) to give **119** (43.6 mg, 0.111 mmol, 41%) as a white solid after trituration with *i*-Pr₂O. ¹H NMR (300 MHz, DMSO-*d*₆) δ 1.03 (3H, s), 1.26 (3H, s), 4.87–5.00 (2H, m), 7.24–7.36 (3H, m), 7.46–7.59 (2H, m), 8.52 (1H, s), 8.81–8.95 (2H, m), 9.33 (1H, dd, *J* = 7.0, 1.7 Hz). MS (ESI/APCI) *m/z* 395.0 [M + H]⁺. HPLC purity: 100%. mp 148 °C.

(S)-N-(2-Hydroxy-2-methyl-1-(4-(trifluoromethoxy)phenyl)propyl)-6-methylpyrazolo[1,5-a]pyrimidine-3-carboxamide (120). A mixture of 6-methylpyrazolo[1,5-a]pyrimidine-3-carboxylic acid (**15b**) (53.1 mg, 0.300 mmol), **130** (94.3 mg, 0.330 mmol), EDCI·HCl (69.0 mg, 0.360 mmol), HOBt·H₂O (55.1 mg, 0.360 mmol), and Et₃N (50.2 μL, 0.360 mmol) in DMF (1.5 mL) was stirred at rt overnight. The mixture was poured into water and extracted with EtOAc. The organic layer was washed with saturated aqueous NaCl, dried over anhydrous MgSO₄ and concentrated in vacuo. The residue was purified by column chromatography (basic silica gel, hexane/ethyl acetate, 9:1 to 1:9) to give **120** (107 mg, 0.262 mmol, 87%) as a white solid after trituration with *i*-Pr₂O. ¹H NMR (300 MHz, DMSO-*d*₆) δ 1.02 (3H, s), 1.25 (3H, s), 2.40 (3H, s), 4.89 (1H, s), 4.94 (1H, d, *J* = 8.7 Hz), 7.28 (2H, d, *J* = 7.9 Hz), 7.51 (2H, d, *J* = 8.7 Hz), 8.43 (1H, s), 8.76–8.86 (2H, m), 9.18 (1H, dd, *J* = 1.9, 1.1 Hz). MS (ESI/APCI) *m/z* 409.2 [M + H]⁺. HPLC purity: 100%. mp 208 °C.

N-((1S)-2-Hydroxy-2-methyl-1-(4-(trifluoromethoxy)phenyl)propyl)-5-isopropylpyrazolo[1,5-a]pyrimidine-3-carboxamide (121a). A mixture of **136** (38.6 mg, 0.09 mmol) and 5% Pd/C–ethylenediamine

complex (10 mg) in MeOH (5 mL) was hydrogenated under balloon pressure at rt for 16 h. The catalyst was removed by filtration and the filtrate was concentrated in vacuo. The residue was purified by column chromatography (silica gel, hexane/ethyl acetate, 19:1 to 0:100) to afford **121** (32.1 mg, 0.074 mmol, 83%) as a white amorphous solid. ¹H NMR (300 MHz, DMSO-*d*₆) δ 0.99–1.08 (3H, m), 1.27 (3H, s), 1.41 (3H, d, *J* = 4.5 Hz), 1.43 (3H, d, *J* = 4.5 Hz), 3.20–3.34 (1H, m), 4.81–5.00 (2H, m), 7.22–7.34 (3H, m), 7.48–7.61 (2H, m), 8.44 (1H, s), 9.07 (1H, d, *J* = 8.7 Hz), 9.19 (1H, d, *J* = 7.2 Hz). MS (ESI/APCI) *m/z* 437.1 [M + H]⁺. HPLC purity: 98.9%.

N-((1*S*)-2-Hydroxy-2-methyl-1-(4-(trifluoromethoxy)phenyl)propyl)-5-(tetrahydro-2*H*-pyran-4-yl)pyrazolo[1,5-*a*]pyrimidine-3-carboxamide (**121b**). A mixture of **137** (84.4 mg, 0.177 mmol) and Pd/C (en) (15 mg) in MeOH (10 mL) and THF(dry) (2 mL) was hydrogenated under balloon pressure at rt for 16 h. The catalyst was removed by filtration and the filtrate was concentrated in vacuo. The residue was purified by column chromatography (silica gel, hexane/ethyl acetate, 19:1 to 0:100) to afford **121b** (82.9 mg, 0.173 mmol, 98%) as a white amorphous solid. ¹H NMR (300 MHz, DMSO-*d*₆) δ 1.04 (3H, s), 1.28 (3H, s), 1.86–2.11 (4H, m), 3.13–3.28 (1H, m), 3.45–3.59 (2H, m), 3.97–4.10 (2H, m), 4.88–4.99 (2H, m), 7.24–7.34 (3H, m), 7.50–7.61 (2H, m), 8.45 (1H, s), 9.03 (1H, d, *J* = 8.7 Hz), 9.21 (1H, d, *J* = 7.2 Hz). MS (ESI/APCI) *m/z* 479.1 [M + H]⁺. HPLC purity: 99.6%.

N-((1*S*)-2-Hydroxy-2-methyl-1-(4-(trifluoromethoxy)phenyl)propyl)-5-(pyridin-2-yl)pyrazolo[1,5-*a*]pyrimidine-3-carboxamide (**121c**). A mixture of crude **141** (79.0 mg, 0.329 mmol), **130** (94.0 mg, 0.329 mmol), HATU (163 mg, 0.428 mmol), DIEA (0.172 mL, 0.987 mmol), and DMF (3 mL) was stirred at rt for 12 h. The mixture was diluted with water and extracted with EtOAc. The organic layer was separated, washed with saturated aqueous NaCl, dried over anhydrous Na₂SO₄ and concentrated in vacuo. The residue was purified by column chromatography (basic silica gel, hexane/ethyl acetate, 100:0 to 0:100) to give **121c** (130 mg, 0.276 mmol, 84% (63% yield in 2 steps from **141**)) as a pale yellow amorphous solid. ¹H NMR (300 MHz, CDCl₃) δ 1.21 (3H, s), 1.49 (3H, s), 1.96 (1H, s), 5.14 (1H, d, *J* = 8.3 Hz), 7.14–7.22 (2H, m), 7.44–7.56 (3H, m), 7.88–7.97 (1H, m), 8.26 (1H, d, *J* = 7.4

Hz), 8.64 (1H, s), 8.75–8.88 (3H, m), 9.25 (1H, d, $J = 8.3$ Hz). MS (ESI/APCI) m/z 472.1 $[M + H]^+$. HPLC purity: 97.3%. Anal. Calcd for $C_{23}H_{20}F_3N_5O_3$: C, 58.60; H, 4.28; N, 14.86. Found: C, 58.61; H, 4.51; N, 14.86.

N-((1S)-2-Hydroxy-2-methyl-1-(4-(trifluoromethoxy)phenyl)propyl)-5-(6-methylpyridin-3-yl)pyrazol o[1,5-a]pyrimidine-3-carboxamide (121d). The title compound was prepared as a pale yellow solid after trituration with hexane/ethyl acetate (5:1) in 63% yield from **135** and 2-methyl-5-(4,4,5,5-tetramethyl-1,3,2-dioxaborolan-2-yl)pyridine using the procedure analogous to that described for the synthesis of **137**, except that basic silica gel was employed in a column chromatography purification in place of silica gel. 1H NMR (300 MHz, DMSO- d_6) δ 1.03 (3H, s), 1.33 (3H, s), 2.60 (3H, s), 4.93 (1H, d, $J = 8.3$ Hz), 5.19 (1H, s), 7.23–7.33 (2H, m), 7.48–7.59 (3H, m), 7.98 (1H, d, $J = 7.5$ Hz), 8.50 (1H, s), 8.81 (1H, dd, $J = 8.3, 2.3$ Hz), 9.24 (1H, d, $J = 8.7$ Hz), 9.41 (1H, d, $J = 7.5$ Hz), 9.54 (1H, d, $J = 2.3$ Hz). MS (ESI/APCI) m/z 486.1 $[M + H]^+$. HPLC purity: 100%. mp 237 °C.

N-((1S)-2-Hydroxy-2-methyl-1-(4-(trifluoromethoxy)phenyl)propyl)-5-(2-methylpyridin-4-yl)pyrazol o[1,5-a]pyrimidine-3-carboxamide (121e). A mixture of **135** (130 mg, 0.303 mmol), 2-methyl-4-(4,4,5,5-tetramethyl-1,3,2-dioxaborolan-2-yl)pyridine (100 mg, 0.455 mmol), (Amphos) $_2$ PdCl $_2$ (21.5 mg, 0.0303 mmol), K $_2$ CO $_3$ (62.9 mg, 0.455 mmol), toluene (2 mL) and water (0.2 mL) was heated at 120 °C under microwave irradiation for 2.5 h. After being cooled to rt, the reaction mixture was directly purified by column chromatography (basic silica gel, ethyl acetate/methanol, 100:0 to 19:1) to give **121e** (115 mg, 0.237 mmol, 78%) as an off-white solid after recrystallization from heptane/ethyl acetate. 1H NMR (300 MHz, CDCl $_3$) δ 1.21 (3H, s), 1.50 (3H, s), 1.73 (1H, s), 2.72 (3H, s), 5.13 (1H, d, $J = 8.5$ Hz), 7.13–7.20 (2H, m), 7.46–7.54 (3H, m), 7.91 (1H, dd, $J = 5.1, 1.3$ Hz), 8.09 (1H, s), 8.67 (1H, s), 8.75 (1H, d, $J = 5.3$ Hz), 8.88 (1H, d, $J = 7.4$ Hz), 9.19 (1H, d, $J = 8.3$ Hz). MS (ESI/APCI) m/z 486.1 $[M + H]^+$. HPLC purity: 100%. mp 192 °C. Anal. Calcd for $C_{24}H_{22}F_3N_5O_3$: C, 59.38; H, 4.57; N, 14.43. Found: C, 59.03; H, 4.60; N, 14.24.

5-(1-(Difluoromethyl)-1H-pyrazol-4-yl)-N-((1S)-2-hydroxy-2-methyl-1-(4-(trifluoromethoxy)phenyl)propyl)pyrazolo[1,5-a]pyrimidine-3-carboxamide (121f). The title compound was prepared as a white amorphous solid in 77% yield from **135** and 1-(difluoromethyl)-4-(4,4,5,5-tetramethyl-1,3,2-dioxaborolan-2-yl)-1H-pyrazole using the procedure analogous to that described for the synthesis of **137**, except that the crude material was purified by basic silica gel column chromatography followed by silica gel column chromatography. ¹H NMR (300 MHz, DMSO-*d*₆) δ 1.04 (3H, s), 1.36 (3H, s), 4.89 (1H, d, *J* = 8.3 Hz), 5.28 (1H, s), 7.23–7.35 (2H, m), 7.49–7.59 (2H, m), 7.73 (1H, d, *J* = 7.5 Hz), 7.97 (1H, t, *J* = 59.0 Hz), 8.45 (1H, s), 8.81 (1H, s), 9.29 (1H, s), 9.32–9.42 (2H, m). MS (ESI/APCI) *m/z* 511.1 [M + H]⁺. HPLC purity: 100%.

N-((1S)-2-Hydroxy-2-methyl-1-(4-(trifluoromethoxy)phenyl)propyl)-5-(1H-pyrazol-1-yl)pyrazolo[1,5-a]pyrimidine-3-carboxamide (121g). To a mixture of **135** (126.3 mg, 0.295 mmol) and 1H-pyrazole (24.1 mg, 0.353 mmol) in DMF (4 mL) was added K₂CO₃ (48.8 mg, 0.353 mmol). The mixture was stirred at 90 °C for 30 min and then poured into water. The mixture was extracted with EtOAc, washed with water and saturated aqueous NaCl, dried over anhydrous Na₂SO₄ and concentrated in vacuo. The residue was purified by column chromatography (silica gel, hexane/ethyl acetate, 19:1 to 0:100) to afford **121g** (102 mg, 0.222 mmol, 75%) as a white solid after trituration with hexane/ethyl acetate (5:1). ¹H NMR (300 MHz, DMSO-*d*₆) δ 1.02 (3H, s), 1.36 (3H, s), 4.86 (1H, d, *J* = 8.3 Hz), 5.34 (1H, s), 6.75–6.81 (1H, m), 7.23–7.33 (2H, m), 7.48–7.58 (2H, m), 7.76 (1H, d, *J* = 7.5 Hz), 8.05 (1H, d, *J* = 1.5 Hz), 8.46 (1H, s), 9.02–9.14 (2H, m), 9.37 (1H, d, *J* = 7.5 Hz). MS (ESI/APCI) *m/z* 461.1 [M + H]⁺. HPLC purity: 100%. mp 241 °C.

N-((1S)-2-Hydroxy-2-methyl-1-(4-(trifluoromethoxy)phenyl)propyl)-5-(4-methyl-1H-imidazol-1-yl)pyrazolo[1,5-a]pyrimidine-3-carboxamide (121h). The title compound was prepared as a pale yellow solid after trituration with hexane/ethyl acetate (5:1) in 70% yield from **135** and 4-methyl-1H-imidazole using the procedure analogous to that described for the synthesis of **121g**, except that a preparative HPLC (column: L-Column2 ODS 20 mm ID × 150 mm L; mobile phase A:

0.1% TFA in water; mobile phase B: 0.1% TFA in acetonitrile; flow rate: 20 mL/min) was employed in place of silica gel column chromatography. ¹H NMR (300 MHz, DMSO-*d*₆) δ 1.02 (3H, s), 1.35 (3H, s), 2.24 (3H, s), 4.87 (1H, d, *J* = 8.3 Hz), 5.31 (1H, s), 7.24–7.33 (2H, m), 7.47–7.57 (2H, m), 7.73 (1H, d, *J* = 7.9 Hz), 8.07 (1H, s), 8.45 (1H, s), 8.85 (1H, d, *J* = 0.8 Hz), 9.00 (1H, d, *J* = 8.3 Hz), 9.46 (1H, d, *J* = 7.5 Hz). MS (ESI/APCI) *m/z* 475.1 [M + H]⁺. HPLC purity: 99.2%. mp 130 °C.

(S)-N-(2-Hydroxy-2-methyl-1-(4-(trifluoromethoxy)phenyl)propyl)-5-(4-(trifluoromethyl)-1H-imidazol-1-yl)pyrazolo[1,5-a]pyrimidine-3-carboxamide (121i). The title compound was prepared as a pale yellow solid after trituration with hexane/ethyl acetate (5:1) in 70% yield from **135** and 4-(trifluoromethyl)-1H-imidazole using the procedure analogous to that described for the synthesis of **121g**. ¹H NMR (300 MHz, DMSO-*d*₆) δ 1.02 (3H, s), 1.34 (3H, s), 4.86 (1H, d, *J* = 8.3 Hz), 5.36 (1H, s), 7.23–7.33 (2H, m), 7.47–7.58 (2H, m), 7.89 (1H, d, *J* = 7.5 Hz), 8.53 (1H, s), 8.92–9.02 (2H, m), 9.15 (1H, s), 9.62 (1H, d, *J* = 7.5 Hz). MS (ESI/APCI) *m/z* 529.1 [M + H]⁺. HPLC purity: 100%. mp 220 °C.

N-((1S)-2-Hydroxy-2-methyl-1-(4-(trifluoromethoxy)phenyl)propyl)-5-(4-methyl-1H-1,2,3-triazol-1-yl)pyrazolo[1,5-a]pyrimidine-3-carboxamide (121j). A mixture of **135** (430 mg, 1.00 mmol), 4-methyl-1H-1,2,3-triazole (100 mg, 1.20 mmol) and K₂CO₃ (208 mg, 1.50 mmol) in DMF (4 mL) was stirred at 80 °C for 2 h. The mixture was quenched with water at rt and extracted with EtOAc. The organic layer was separated, washed with water and saturated aqueous NaCl, dried over anhydrous MgSO₄ and concentrated in vacuo (508.7 mg). The residue was purified by using preparative HPLC (column: L-Column2 ODS 20 mm ID × 150 mm L; mobile phase A: 0.1% TFA in water; mobile phase B: 0.1% TFA in acetonitrile; flow rate: 20 mL/min). The first eluting fractions (tR1) were concentrated to dryness, and washed with saturated aqueous NaHCO₃, extracted with EtOAc. The organic layer was separated, washed with water and saturated aqueous NaCl, dried over anhydrous MgSO₄ and concentrated in vacuo. The residue (42.7 mg) was crystallized from hexane/ethyl acetate to give **121j** (34.4 mg, 0.072 mmol, 7.2%) as a white solid. ¹H NMR (300 MHz, DMSO-*d*₆) δ 1.04 (3H, s), 1.37

(3H, s), 2.44 (3H, s), 4.87 (1H, d, $J = 8.3$ Hz), 5.39 (1H, s), 7.23–7.34 (2H, m), 7.48–7.58 (2H, m), 7.93 (1H, d, $J = 7.5$ Hz), 8.55 (1H, s), 8.88 (1H, d, $J = 0.8$ Hz), 9.07 (1H, d, $J = 8.3$ Hz), 9.50 (1H, d, $J = 7.5$ Hz). MS (ESI/APCI) m/z 476.2 $[M + H]^+$. HPLC purity: 99.4%. mp 260 °C.

N-((1S)-2-Hydroxy-2-methyl-1-(4-(trifluoromethoxy)phenyl)propyl)-5-(3-methyl-1H-1,2,4-triazol-1-yl)pyrazolo[1,5-a]pyrimidine-3-carboxamide (121k). The title compound was prepared as a white solid after trituration with *i*-Pr₂O in 35% yield from **135** and 3-methyl-1H-1,2,4-triazole using the procedure analogous to that described for the synthesis of **121g**, except that basic silica gel was employed in a column chromatography purification in place of silica gel. ¹H NMR (300 MHz, DMSO-*d*₆) δ 1.02 (3H, brs), 1.36 (3H, s), 2.47 (3H, brs), 4.86 (1H, d, $J = 8.1$ Hz), 5.43 (1H, s), 7.21–7.35 (2H, m), 7.47–7.59 (2H, m), 7.63 (1H, d, $J = 7.5$ Hz), 8.52 (1H, s), 9.06 (1H, d, $J = 8.1$ Hz), 9.46 (1H, d, $J = 7.5$ Hz), 9.55 (1H, s). MS (ESI/APCI) m/z 476.1 $[M + H]^+$. HPLC purity: 100%.

(S)-N-(2-Hydroxy-2-methyl-1-(4-(trifluoromethoxy)phenyl)propyl)-6-methyl-5-(4-methyl-1H-1,2,3-triazol-1-yl)pyrazolo[1,5-a]pyrimidine-3-carboxamide (122a). To a mixture of **154a** (2.81 g, 10.9 mmol) and **130** (3.26 g, 11.4 mmol) in DMF (250 mL) were added HOBt·H₂O (2.06 g, 13.1 mmol), EDCI·HCl (2.55 g, 13.1 mmol) and TEA (7.65 mL, 54.4 mmol). The mixture was stirred at rt overnight and then quenched with water at rt. The mixture was extracted with EtOAc, washed with saturated aqueous NaHCO₃, water, and then saturated aqueous NaCl, dried over anhydrous Na₂SO₄, and concentrated in vacuo. The residue was purified by column chromatography (silica gel, hexane/ethyl acetate, 100:0 to 3:17) to give **122a** (3.86 g, 7.89 mmol, 73%) as a white solid. ¹H NMR (300 MHz, CDCl₃) δ 1.17 (3H, s), 1.48 (3H, s), 1.74 (1H, s), 2.50 (3H, d, $J = 0.8$ Hz), 2.84 (3H, d, $J = 0.8$ Hz), 5.05 (1H, d, $J = 8.3$ Hz), 7.17 (2H, d, $J = 7.9$ Hz), 7.38–7.48 (2H, m), 8.60 (1H, s), 8.69–8.82 (3H, m). The obtained product (3.86 g, 7.89 mmol) was dissolved in EtOAc (277 mL) at 50–60 °C. To this solution was added hexane (150 mL) at the same temperature and a white solid precipitated. After 2 h of stirring at rt, further hexane (88 mL) was added to the mixture, which was stirred at rt for 10 min. The white precipitate was collected by filtration, washed with hexane/ethyl acetate, and dried to

give **122a** (3.17 g, 6.48 mmol, 82 %) as a white solid. ^1H NMR (300 MHz, CDCl_3) δ 1.17 (3H, s), 1.48 (3H, s), 1.74 (1H, s), 2.50 (3H, d, $J = 0.8$ Hz), 2.84 (3H, d, $J = 0.8$ Hz), 5.05 (1H, d, $J = 8.3$ Hz), 7.17 (2H, d, $J = 8.3$ Hz), 7.39–7.48 (2H, m), 8.60 (1H, s), 8.69–8.83 (3H, m). MS (ESI/APCI) m/z 490.2 [$\text{M} + \text{H}$] $^+$. HPLC purity: 100%. mp 238–239 °C. Anal. Calcd for $\text{C}_{22}\text{H}_{22}\text{F}_3\text{N}_7\text{O}_3$: C, 53.99; H, 4.53; F, 11.64; N, 20.03. Found: C, 53.82; H, 4.42; F, 11.64; N, 19.81.

(S)-N-(2-Hydroxy-2-methyl-1-(4-(trifluoromethoxy)phenyl)propyl)-6-methyl-5-(3-methyl-1H-1,2,4-triazol-1-yl)pyrazolo[1,5-a]pyrimidine-3-carboxamide (122b). To a suspension of **154b** (606 mg, 2.35 mmol) in DMF (12 mL) were added **130** (805 mg, 2.82 mmol), EDCI·HCl (540 mg, 2.82 mmol), HOBt·H₂O (431 mg, 2.82 mmol), and TEA (0.392 mL, 2.82 mmol) at rt. The mixture was stirred at rt for 2 h. The mixture was poured into water and extracted with EtOAc. The organic layer was separated, washed with saturated aqueous NaCl, dried over anhydrous MgSO_4 and concentrated in vacuo. The residue was purified by column chromatography (basic silica gel, hexane/ethyl acetate, 4:1 to 1:9) to give **122b** (858 mg, 1.75 mmol, 75%) as a white solid after recrystallization from *i*-Pr₂O/ethyl acetate. ^1H NMR (300 MHz, $\text{DMSO-}d_6$) δ 1.00 (3H, s), 1.31 (3H, s), 2.46 (3H, s), 2.64 (3H, d, $J = 0.8$ Hz), 4.87 (1H, d, $J = 8.0$ Hz), 5.32 (1H, s), 7.27 (2H, d, $J = 8.0$ Hz), 7.51 (2H, d, $J = 8.7$ Hz), 8.49 (1H, s), 8.85 (1H, d, $J = 8.3$ Hz), 9.46–9.53 (2H, m). ^{13}C NMR (151 MHz, $\text{DMSO-}d_6$) δ 13.81, 16.90, 27.23, 28.42, 59.79, 70.72, 104.48, 112.33, 119.99, 120.00 (q, $J = 256.0$ Hz, 1C), 130.07, 139.82, 140.56, 142.33, 145.40, 146.18, 147.05 (q, $J = 1.7$ Hz, 1C), 148.11, 159.97, 162.02. MS (ESI/APCI) m/z 490.3 [$\text{M} + \text{H}$] $^+$. HPLC purity: 100%. $[\alpha]_{20}^{\text{D}} = -363.2$ ($c = 1.00$ in MeOH). mp 212 °C. Anal. Calcd for $\text{C}_{22}\text{H}_{22}\text{F}_3\text{N}_7\text{O}_3$: C, 53.99; H, 4.53; N, 20.03. Found: C, 54.11; H, 4.50; N, 20.04.

2-Amino-2-(4-(trifluoromethoxy)phenyl)acetic Acid (125). The solution of potassium cyanide (19.4 g, 299 mmol) in water (170 mL) at 50 °C was added dropwise to a solution of 4-trifluoromethoxy benzaldehyde (**123**) (34.1 mL, 239 mmol) and ammonium carbonate (62.0 g, 645 mmol) in EtOH (273 mL) and water (109 mL). The mixture was stirred at 60 °C for 3 h. After cooling to rt, EtOH was removed under reduced pressure. To the mixture was acidified to pH ~1 with concd HCl at 0 °C. The

solid was filtered off and washed with water. To a solution of potassium hydroxide (66.2 g, 1000 mmol) in water (250 mL) was added the product at rt. The mixture was stirred at 90 °C overweekend. After cooling to rt, the mixture was neutralized with concd HCl. The resulting solid was filtered off, washed with water, and dried to give **125** (56.0 g, 238 mmol, 100 %) as a pale yellow solid. This was used in the next reaction without further purification. MS (ESI/APCI) m/z 234.0 $[M - H]^-$.

((tert-Butoxycarbonyl)amino)(4-(trifluoromethoxy)phenyl)acetic Acid (126). To a solution of **125** (56.0 g, 238 mmol) in THF (476 mL) was added Boc_2O (82.9 mL, 357 mmol) and 2 M NaOH aqueous solution (357 mL, 714 mmol) at rt. The mixture was stirred at rt. The mixture was poured into water at rt and extracted with Et_2O . The aqueous layer was acidified to pH ~3 with 1 M HCl aqueous solution at 0 °C and then extracted with EtOAc. The organic layer was washed with saturated aqueous NaCl, dried over anhydrous MgSO_4 and concentrated in vacuo to afford **126** (63.3 g, 189 mmol) as a pale yellow solid. This was subjected to the next reaction without further purification. MS (ESI/APCI) m/z 333.9 $[M - H]^-$.

tert-Butyl (2-Hydroxy-2-methyl-1-(4-(trifluoromethoxy)phenyl)propyl)carbamate (127). To a solution of **126** (63.3 g, 189 mmol) in DMF (378 mL) were added MeI (14.2 mL, 227 mmol) and K_2CO_3 (31.3 g, 227 mmol) at rt. The mixture was stirred at rt for 2 h. The mixture was poured into water at rt and extracted with EtOAc. The organic layer was separated, washed with saturated aqueous NaCl, dried over anhydrous MgSO_4 and concentrated in vacuo. The residue was purified by column chromatography (silica gel, hexane/ethyl acetate, 100:0 to 4:1) to give **127** (38.7 g, 111 mmol, 46 % from **21**) as an off-white solid. ^1H NMR (300 MHz, CDCl_3) δ 1.26–1.53 (9H, m), 3.73 (3H, s), 5.27–5.41 (1H, m), 5.54–5.75 (1H, m), 7.20 (2H, d, $J = 8.3$ Hz), 7.35–7.44 (2H, m). MS (ESI/APCI) m/z 348.1 $[M - H]^-$.

tert-Butyl (2-Hydroxy-2-methyl-1-(4-(trifluoromethoxy)phenyl)propyl)carbamate (128). To a solution of **127** (23.5 g, 67.3 mmol) in THF (336 mL) was added dropwise MeMgBr (269 mL, 269 mmol) at 0 °C. The mixture was stirred at 0 °C under Ar for 1 h. The mixture was quenched with

saturated aqueous NH₄Cl at 0 °C and extracted with EtOAc. The organic layer was separated, washed with saturated aqueous NaCl, dried over anhydrous MgSO₄ and concentrated in vacuo. The residue was purified by column chromatography (silica gel, hexane/ethyl acetate, 19:1 to 2:3) to give **128** (17.9 g, 51.2 mmol, 76 %) as a white solid. ¹H NMR (300 MHz, CDCl₃) δ 1.05 (3H, s), 1.30–1.47 (12H, m), 4.50 (1H, d, *J* = 6.4 Hz), 5.53 (1H, d, *J* = 8.7 Hz), 7.18 (2H, d, *J* = 7.9 Hz), 7.33 (2H, d, *J* = 8.7 Hz). MS (ESI/APCI) *m/z* 348.0 [M – H][–].

tert-Butyl ((1S)-2-Hydroxy-2-methyl-1-(4-(trifluoromethoxy)phenyl)propyl)carbamate (129a).

Resolution of the enantiomers of **128** was carried out chromatographically using a Chiralpak AD 20 mm ID × 250 mm L column (hexane/ethanol, 19:1) at 80 mL/min. Resolution of **128** (22.3 g, 63.8 mmol) provided **129a** as a white solid (10.2 g, 29.1 mmol, 46%, 91% theoretical) as the first eluting enantiomer. Analytical HPLC analysis carried out on a 4.6 mm ID × 250 mm L Chiralpak AD column with the same eluent as above at a flow rate of 1.0 mL/min indicated that **129a** was of >99.9% ee. ¹H NMR (300 MHz, CDCl₃) δ 1.05 (3H, s), 1.36 (3H, s), 1.40 (9H, brs), 1.51 (1H, brs), 4.50 (1H, d, *J* = 7.5 Hz), 5.53 (1H, d, *J* = 8.3 Hz), 7.13–7.23 (2H, m), 7.29–7.39 (2H, m).

(1S)-1-Amino-2-methyl-1-(4-(trifluoromethoxy)phenyl)propan-2-ol Hydrochloride (130).

A mixture of **129a** (10.2 g, 29.3 mmol) and 4 M HCl solution in EtOAc (70.0 mL, 280 mmol) was stirred at rt for 1.5 h. The mixture was concentrated in vacuo and the resulting solid was triturated with hexane/*i*-Pr₂O, collected by filtration, rinsed with hexane/*i*-Pr₂O, and dried to afford **130** (7.00 g, 24.5 mmol, 84 %) as a pale red solid. ¹H NMR (300 MHz, DMSO-*d*₆) δ 0.98 (3H, s), 1.23 (3H, s), 4.23 (1H, brs), 5.39 (1H, s), 7.37–7.48 (2H, m), 7.63 (2H, d, *J* = 8.7 Hz), 8.46 (3H, brs).

Ethyl 5-Hydroxypyrazolo[1,5-*a*]pyrimidine-3-carboxylate (132). To a mixture of ethyl 3-amino-1*H*-pyrazole-4-carboxylate (**131**) (30.0 g, 193 mmol) and ethyl 3-ethoxy-2-propenoate (cis- and trans-mixture, 41.9 mL, 290 mmol) in DMF (387 mL) was added cesium carbonate (113 g, 348 mmol). The mixture was stirred at 100 °C for 2 h, diluted with water and then acidified to pH ~5 with AcOH. The resulting solid was filtered by filtration, washed with water and dried to afford **132** (36.4 g,

176 mmol, 91 %) as a beige solid. ^1H NMR (300 MHz, DMSO- d_6) δ 1.28 (3H, t, $J = 7.1$ Hz), 4.28 (2H, q, $J = 7.1$ Hz), 6.15 (1H, d, $J = 7.9$ Hz), 8.13 (1H, s), 8.57 (1H, d, $J = 7.9$ Hz), 11.73 (1H, brs).

5-Hydroxypyrazolo[1,5-a]pyrimidine-3-carboxylic Acid (133). To a solution of **132** (20.8 g, 100 mmol) in THF (223 mL) and EtOH (111 mL) was added 2 M NaOH aqueous solution (201 mL, 401 mmol). The mixture was stirred at 50 °C overnight. The mixture was evaporated under reduced pressure to remove solvents and then neutralized with 2 M HCl aqueous solution (201 mL, 401 mmol). The resulting solid was collected by filtration, rinsed with water/EtOH and dried to give **133** (17.7 g, 99 mmol, 98 %) as a beige solid. ^1H NMR (300 MHz, DMSO- d_6) δ 6.14 (1H, d, $J = 7.9$ Hz), 8.09 (1H, s), 8.56 (1H, d, $J = 7.9$ Hz).

5-Chloropyrazolo[1,5-a]pyrimidine-3-carbonyl Chloride (134). To cooled (0 °C) POCl₃ (71.0 mL, 762 mmol) were added **133** (5.00 g, 27.9 mmol) and DIEA (16.1 mL, 92.1 mmol). The mixture was stirred at 130 °C for 4 h and then concentrated in vacuo. The residue was diluted with toluene and water at 0 °C, and then extracted with EtOAc. The organic layer was separated, dried over anhydrous Na₂SO₄, filtered through a cake of silica gel pad (eluted with ethyl acetate) and concentrated in vacuo. The resulting solid was triturated with heptane, collected by filtration, washed with heptane and dried to give **134** (4.46 g, 20.7 mmol, 74%) as a beige solid. ^1H NMR (300 MHz, CDCl₃) δ 7.16 (1H, d, $J = 7.2$ Hz), 8.65 (1H, s), 8.70 (1H, d, $J = 7.2$ Hz).

5-Chloro-N-((1S)-2-hydroxy-2-methyl-1-(4-(trifluoromethoxy)phenyl)propyl)pyrazolo[1,5-a]pyrimidine-3-carboxamide (135). To a cooled (0 °C) mixture of **134** (1.48 g, 6.85 mmol) and CH₃CN (30 mL) were added **130** (1.96 g, 6.85 mmol) and DIEA (3.58 mL, 20.6 mmol), and the mixture was stirred at 0 °C to rt for 16 h. The mixture was poured into water and extracted with EtOAc. The organic layer was separated, washed with saturated aqueous NaCl, dried over anhydrous Na₂SO₄, and concentrated in vacuo. The residue was purified by column chromatography (silica gel, hexane/ethyl acetate, 100:0 to 0:100) to give **135** (2.27 g, 5.29 mmol, 77%) as white amorphous solids. ^1H NMR (300 MHz, CDCl₃) δ 1.19 (3H, s), 1.40 (3H, s), 1.88 (1H, s), 5.12 (1H, d, $J = 8.7$ Hz), 6.99 (1H, d, $J = 7.2$ Hz),

7.17–7.23 (2H, m), 7.45–7.53 (2H, m), 8.56 (1H, d, $J = 8.7$ Hz), 8.62 (1H, s), 8.67 (1H, d, $J = 7.2$ Hz). MS (ESI/APCI) m/z 429.1 $[M + H]^+$.

N-((1S)-2-Hydroxy-2-methyl-1-(4-(trifluoromethoxy)phenyl)propyl)-5-(prop-1-en-2-yl)pyrazolo[1,5-a]pyrimidine-3-carboxamide (136). Into a microwave vial equipped with a magnetic stirrer were added **135** (76.1 mg, 0.177 mmol), 4,4,5,5-tetramethyl-2-(prop-1-en-2-yl)-1,3,2-dioxaborolane (46.6 mg, 0.266 mmol), K_2CO_3 (36.8 mg, 0.266 mmol), toluene (4 mL) and water (0.4 mL), followed by $(Amphos)_2PdCl_2$ (12.6 mg, 0.0177 mmol). The reaction vial was flushed with nitrogen, sealed and heated by microwave irradiation at 150 °C for 25 min. The mixture was purified by column chromatography (basic silica gel, hexane/ethyl acetate, 19:1 to 1:4), followed by a second column purification (silica gel, hexane/ethyl acetate, 19:1 to 1:4) to afford **136** (48.8 mg, 0.112 mmol, 63%) as a yellow amorphous solid. 1H NMR (300 MHz, $DMSO-d_6$) δ 1.00 (3H, s), 1.27 (3H, s), 2.37 (3H, s), 4.88–4.98 (2H, m), 5.80 (1H, s), 6.36 (1H, s), 7.24–7.34 (2H, m), 7.49–7.58 (2H, m), 7.65 (1H, d, $J = 7.5$ Hz), 8.45 (1H, s), 9.02 (1H, d, $J = 8.7$ Hz), 9.22 (1H, d, $J = 7.5$ Hz). MS (ESI/APCI) m/z 435.2 $[M + H]^+$.

5-(3,6-Dihydro-2H-pyran-4-yl)-N-((1S)-2-hydroxy-2-methyl-1-(4-(trifluoromethoxy)phenyl)propyl)pyrazolo[1,5-a]pyrimidine-3-carboxamide (137). Into a microwave vial equipped with a magnetic stirrer were added **135** (142 mg, 0.330 mmol), 2-(3,6-dihydro-2H-pyran-4-yl)-4,4,5,5-tetramethyl-1,3,2-dioxaborolane (104 mg, 0.495 mmol), K_2CO_3 (68.5 mg, 0.495 mmol), toluene (4 mL) and water (0.4 mL), followed by $(Amphos)_2PdCl_2$ (23.4 mg, 0.0330 mmol). The reaction vial was flushed with nitrogen, sealed, and heated by microwave irradiation at 150 °C for 25 min. The mixture was purified by column chromatography (silica gel, hexane/ethyl acetate, 19:1 to 1:4) to afford **137** (110 mg, 0.230 mmol, 70%) as a yellow solid. 1H NMR (300 MHz, $DMSO-d_6$) δ 1.00 (3H, s), 1.28 (3H, s), 2.67–2.94 (2H, m), 3.84–3.97 (2H, m), 4.35–4.43 (2H, m), 4.86–5.00 (2H, m), 7.24–7.34 (3H, m), 7.49–7.56 (2H, m), 7.59 (1H, d, $J = 7.5$ Hz), 8.42 (1H, s), 9.06 (1H, d, $J = 8.7$ Hz), 9.20 (1H, d, $J = 7.5$ Hz). MS (ESI/APCI) m/z 477.2 $[M + H]^+$.

Ethyl 5-Chloropyrazolo[1,5-a]pyrimidine-3-carboxylate (138). POCl₃ (30 mL, 322 mmol) was added to **132** (5.54 g, 26.7 mmol) and the mixture was stirred at 100 °C for 16 h. After POCl₃ was removed under reduced pressure, the residue was partitioned between EtOAc and NaHCO₃ aqueous solution. The phases were separated and the aqueous phase was extracted with EtOAc. The combined organic phases were washed with water and saturated aqueous NaCl, dried over anhydrous Na₂SO₄ and concentrated in vacuo. The residue was purified by column chromatography (silica gel, hexane/ethyl acetate, 19:1 to 1:1) to afford **138** (3.69 g, 16.3 mmol, 61%) as a white solid. MS (ESI/APCI) *m/z* 226.1 [M + H]⁺.

Ethyl 5-(Pyridin-2-yl)pyrazolo[1,5-a]pyrimidine-3-carboxylate (140). A mixture of ethyl **138** (300 mg, 1.33 mmol), lithium 4-methyl-1-(pyridin-2-yl)-2,6,7-trioxa-1-borabicyclo[2.2.2]octan-1-uide (**139**) (566 mg, 2.66 mmol), Ph₃P (139 mg, 0.532 mmol), copper(I) iodide (127 mg, 0.665 mmol) and Pd(OAc)₂ (29.9 mg, 0.133 mmol) in DMF (5 mL) was stirred at 80 °C for 2 h under Ar. The mixture was filtered through a cake of basic silica gel pad (eluted with ethyl acetate), followed by a cake of silica gel pad (eluted with ethyl acetate). The appropriate fractions were concentrated in vacuo. The resulting solid was triturated with hot ethyl acetate and insoluble materials were filtered off. After concentration of the filtrate, the residue was purified by column chromatography (basic silica gel, hexane/ethyl acetate, 100:0 to 3:7) to give **140** (309 mg, 1.15 mmol, 87 %) as a pale yellow solid after trituration with *i*-Pr₂O. ¹H NMR (300 MHz, CDCl₃) δ 1.47 (3H, t, *J* = 7.1 Hz), 4.46 (2H, q, *J* = 7.1 Hz), 7.40–7.47 (1H, m), 7.86–7.95 (1H, m), 8.25 (1H, d, *J* = 7.4 Hz), 8.59 (1H, s), 8.71–8.76 (2H, m), 8.80 (1H, d, *J* = 7.4 Hz). MS (ESI/APCI) *m/z* 269.1 [M + H]⁺.

5-(Pyridin-2-yl)pyrazolo[1,5-a]pyrimidine-3-carboxylic Acid (141). A mixture of **140** (117 mg, 0.436 mmol), 4 M NaOH aqueous solution (0.545 mL, 2.18 mmol), THF (3.5 mL) and EtOH (3.5 mL) was stirred at 60 °C for 2 h. After being cooled to 0 °C, the mixture was acidified with 6 M HCl aqueous solution (0.363 mL) and concentrated in vacuo to give crude **141** (79.0 mg, 0.329 mmol, 75%). This was used in the next reaction without further purification.

tert-Butyl 2-cyano-3-(dimethylamino)acrylate (144). A mixture of *tert*-butyl 2-cyanoacetate (**142**) (24.3 g, 172 mmol) and *tert*-butoxy bis(dimethylamino)methane (**143**) (35.5 mL, 172 mmol) was stirred at rt for 30 min. The mixture was evaporated to give **144** as a pale yellow solid. This was used in the next reaction without further purification. ¹H NMR (300 MHz, CDCl₃) δ 1.50 (9H, s), 3.17 (3H, s), 3.36 (3H, s), 7.62 (1H, s).

tert-Butyl 3-Amino-1H-pyrazole-4-carboxylate (145). A mixture of **144** (33.8 g, 172 mmol) and hydrazine monohydrate (8.39 mL, 172 mmol) in MeOH (344 mL) was stirred at 70 °C overnight. After cooling to rt, the mixture was poured into water at rt and extracted with EtOAc. The organic layer was separated, washed with saturated aqueous NaCl, dried over anhydrous MgSO₄ and concentrated in vacuo. The residue was crystallized from *i*-Pr₂O to give **145** (20.0 g, 109 mmol, 64%) as a pale orange solid. ¹H NMR (300 MHz, DMSO-*d*₆) δ 1.47 (9H, s), 4.86–6.14 (2H, m), 7.07–7.92 (1H, m), 11.44–12.34 (1H, m). MS (ESI/APCI) *m/z* 184.1 [M + H]⁺.

Methyl 2,3-Dibromo-2-methylpropanoate (147). To a solution of methyl methacrylate (60.1 g, 600 mmol) in EtOAc (353 mL) at 0 °C was added a solution of bromine (30.7 mL, 600 mmol) in EtOAc (30 mL). The mixture was stirred at rt for 16 h and then saturated aqueous Na₂S₂O₃ was added. The mixture was diluted with water and extracted with EtOAc. The combined organic phases were washed with saturated aqueous NaCl, dried over anhydrous Na₂SO₄ and concentrated in vacuo to afford **147** (152 g, 584 mmol, 97%) as a colorless oil. ¹H NMR (300 MHz, DMSO-*d*₆) δ 1.95 (3H, s), 3.76 (3H, s), 4.08–4.14 (1H, m), 4.16–4.22 (1H, m).

Methyl 3,3-Dimethoxy-2-methylpropanoate (148). A suspension of sodium methoxide (28% MeOH solution, 226 g, 1.17 mol) in MeOH (234 mL) was heated to 70 °C and then a solution of **147** (152 g, 584 mmol) in MeOH (20 mL) was added rapidly. The mixture was stirred at 70 °C for 3 h. After cooling to rt, the mixture was filtered and washed with MeOH, and then the filtrate was concentrated in vacuo. The residue was partitioned between Et₂O and water. The organic layer was washed with water and saturated aqueous NaCl, dried over anhydrous MgSO₄, filtered, and concentrated in vacuo

to give **148** (54.5 g, 336 mmol, 58%) as a pale yellow oil. This was used in the next reaction without further purification. ¹H NMR (300 MHz, CDCl₃) δ 1.17 (3H, d, *J* = 7.2 Hz), 2.71–2.85 (1H, m), 3.35 (3H, s), 3.38 (3H, s), 3.70 (3H, s), 4.50 (1H, d, *J* = 7.6 Hz).

***tert*-Butyl 5-Hydroxy-6-methylpyrazolo[1,5-*a*]pyrimidine-3-carboxylate (149)**. To a mixture of **145** (20.0 g, 109 mmol) and **148** (26.6 g, 164 mmol) in DMF (219 mL) was added cesium carbonate (64.2 g, 197 mmol). The mixture was stirred at 100 °C for 16 h, diluted with water and then acidified to pH ~4 with AcOH. The resulting solid was filtered by filtration, washed with water and dried to afford **149** (22.6 g, 91.8 mmol, 84%) as a white solid. ¹H NMR (300 MHz, DMSO-*d*₆) δ 1.53 (9H, s), 1.96 (3H, d, *J* = 1.1 Hz), 7.97 (1H, s), 8.53 (1H, d, *J* = 1.1 Hz), 11.22 (1H, brs). MS (ESI/APCI) *m/z* 250.1 [M + H]⁺.

***tert*-Butyl 5-Azido-6-methylpyrazolo[1,5-*a*]pyrimidine-3-carboxylate (150)**. To a suspension of **149** (4.99 g, 20.0 mmol) in THF (100 mL) was added DBU (4.52 mL, 30.0 mmol) and DPPA (5.17 mL, 24.0 mmol) at rt. The mixture was stirred at 60 °C under Ar for 3 h. DBU (1.51 mL, 10.0 mmol) and DPPA (1.72 mL, 8.00 mmol) were added thereto. The mixture was stirred at 60 °C under Ar for 2 h. The mixture was poured into water at rt and extracted with a 1:1 mixture of hexane and EtOAc. The organic layer was separated, washed with saturated aqueous NaCl, dried over anhydrous MgSO₄, filtered through a short pad of silica gel, eluted with a 1:1 mixture of hexane and EtOAc, and concentrated in vacuo. The resulting solid was triturated with hexane to give **150** (4.03 g, 14.7 mmol, 74%) as a pale green solid. ¹H NMR (300 MHz, DMSO-*d*₆) δ 1.51–1.65 (9H, m), 2.12–2.55 (3H, m), 8.38–8.49 (1H, m), 8.85–9.11 (1H, m). MS (ESI/APCI) *m/z* 275.1 [M + H]⁺.

***tert*-Butyl 5-Chloro-6-methylpyrazolo[1,5-*a*]pyrimidine-3-carboxylate (152)**. Carbon tetrachloride (9.73 mL, 100 mmol) was added to a solution of PPh₃ (27.1 g, 100 mmol) in 1,2-dichloroethane (223 mL) at rt. The mixture was stirred at the same temperature under N₂ for 30 min. To this mixture was added a suspension of **149** (5.0 g, 20.1 mmol) in 1,2-dichloroethane (111 mL) at rt and the resulting mixture was stirred under N₂ at 75–85 °C for 4.5 h, and then concentrated in vacuo. The residue was

partitioned between EtOAc and water. The phases were separated and the aqueous phase was extracted with EtOAc. The combined organic phases were washed with saturated aqueous NaCl, dried over anhydrous Na₂SO₄, and concentrated in vacuo. The residue was purified by column chromatography (silica gel, hexane/ethyl acetate, 100:0 to 7:3) to give **152** (4.75 g, 17.7 mmol, 88%) as a white solid. ¹H NMR (300 MHz, CDCl₃) δ 1.62 (9H, s), 2.42 (3H, d, *J* = 0.9 Hz), 8.40 (1H, s), 8.52 (1H, d, *J* = 0.9 Hz).

tert-Butyl **6-Methyl-5-(4-methyl-1*H*-1,2,3-triazol-1-yl)pyrazolo[1,5-*a*]pyrimidine-3-carboxylate (153a)**. A mixture of **150** (4.36 g, 15.9 mmol) and **151** (6.07 g, 19.1 mmol) in toluene (79 mL) was stirred at 80 °C for 3 h. To the mixture was added MgCl₂ (4.54 g, 47.7 mmol). After 15 min, to the mixture was added MgCl₂ (3.03 g, 31.8 mmol). The mixture was stirred at 60 °C under Ar for 2 h. The solid was filtered off, washed with hot toluene. The filtrate was evaporated. The residue was purified by column chromatography (silica gel, hexane/ethyl acetate, 19:1 to 9:11) to give **153a** (4.83 g, 15.4 mmol, 97%) as a white solid. ¹H NMR (300 MHz, CDCl₃) δ 1.64 (9H, s), 2.46 (3H, d, *J* = 0.8 Hz), 2.78 (3H, d, *J* = 1.1 Hz), 8.46–8.50 (2H, m), 8.71–8.73 (1H, m). MS (ESI/APCI) *m/z* 315.2 [M + H]⁺.

tert-Butyl **6-Methyl-5-(3-methyl-1*H*-1,2,4-triazol-1-yl)pyrazolo[1,5-*a*]pyrimidine-3-carboxylate (153b)**. To a solution of **152** (1.08 g, 4.03 mmol) in DMF (20 mL) was added 3-methyl-1*H*-1,2,4-triazole (0.469 g, 5.65 mmol) and K₂CO₃ (0.781 g, 5.65 mmol) at rt. The mixture was stirred at rt overnight and warmed to 60 °C for 2 h. After cooling to rt, water was added to the mixture. The solid was collected by filtration, washed with water, and dried to give **153b** (0.870 g, 2.77 mmol, 69%) as a tan solid. ¹H NMR (300 MHz, DMSO-*d*₆) δ 1.56 (9H, s), 2.43 (3H, s), 2.54 (3H, d, *J* = 1.1 Hz), 8.56 (1H, s), 9.10 (1H, s), 9.43 (1H, d, *J* = 1.1 Hz). MS (ESI/APCI) *m/z* 315.2 [M + H]⁺.

6-Methyl-5-(4-methyl-1*H*-1,2,3-triazol-1-yl)pyrazolo[1,5-*a*]pyrimidine-3-carboxylic Acid (154a). To a stirred suspension of **153a** (2.64 g, 8.40 mmol) in CH₃CN (84 mL) was added methanesulfonic acid (2.78 mL, 42.0 mmol) at 0 °C. The mixture was stirred at rt overnight. The starting material remained

on TLC and further methanesulfonic acid (0.555 mL, 8.40 mmol) was added. The mixture was stirred at rt for 1 h and then neutralized with 1 M NaOH aqueous solution at 0 °C. The organic solvent was evaporated under reduced pressure and then diluted with water. The resulting solid was collected by filtration, washed with water and then hexane, and dried to give **154a** (1.98 g, 7.67 mmol, 91%) as a white solid. ¹H NMR (300 MHz, DMSO-*d*₆) δ 2.40 (3H, s), 2.52 (3H, d, *J* = 0.8 Hz), 8.50 (1H, d, *J* = 1.1 Hz), 8.62 (1H, s), 9.50 (1H, d, *J* = 1.1 Hz), 12.52 (1H, brs). MS (ESI/APCI) *m/z* 259.2 [M + H]⁺.

6-Methyl-5-(3-methyl-1H-1,2,4-triazol-1-yl)pyrazolo[1,5-a]pyrimidine-3-carboxylic Acid (154b). To a suspension of **153b** (0.87 g, 2.77 mmol) in CH₃CN (14 mL) was added MsOH (1.26 mL, 19.4 mmol) at 0 °C. After being stirred at rt for 5 h, the mixture was warmed to 60 °C for 30 min. 1 M NaOH aqueous solution (19.4 mL, 19.4 mmol) was added thereto at 0 °C. CH₃CN was evaporated. The solid was collected by filtration, washed with water, dried to give **154b** (0.606 g, 2.35 mmol, 85%) as a tan solid. ¹H NMR (300 MHz, DMSO-*d*₆) δ 2.42 (3H, s), 2.48–2.53 (3H, m), 8.60 (1H, s), 9.09 (1H, s), 9.44 (1H, d, *J* = 1.1 Hz), 12.49 (1H, brs). MS (ESI/APCI) *m/z* 259.1 [M + H]⁺.

(+)-Di-(*p*-toluoyl)-D-tartaric acid salt of 155 (156). (1*S*)-1-amino-2-methyl-1-(4-(trifluoromethoxy)phenyl)propan-2-ol hydrochloride (**130**) (2.00 g, 7.00 mmol) was suspended in EtOAc and neutralized with saturated aqueous NaHCO₃. The organic phase was dried over anhydrous Na₂SO₄ and concentrated in vacuo to afford (1*S*)-1-amino-2-methyl-1-(4-(trifluoromethoxy)phenyl)propan-2-ol (**155**) (1.74 g, 6.98 mmol, quantitative yeild) as a colorless oil. **155** (125 mg, 0.500 mmol) and (2*S*,3*S*)-(+)-di-(*p*-toluoyl)-D-tartaric acid (193 mg, 0.500 mmol) were dissolved in EtOH (500 μl) and water (500 μl) at rt. The mixture was standed at rt overnight to give (2*S*,3*S*)-2,3-bis((4-methylbenzoyl)oxy)butanedioic acid - (1*S*)-1-amino-2-methyl-1-(4-(trifluoromethoxy)phenyl)propan-2-ol (1:1) (**156**) suitable for X-ray crystallography.

Enzyme Assay Protocol. *Preparation of human PDE.* Human PDE1A, 3A, 4D2, 5A1, 7B, 8A1, 9A2, and 11A4 enzymes were purchased from BPS Bioscience. Human PDE6AB enzyme was purchased from SB Drug Discovery. Human PDE2A3 full-length gene was transduced into Sf9 cells, and the enzyme was purified by His-tag affinity column and gel filtration. Human PDE10A2 was generated from COS-7 cells that had been transfected with the full-length gene. The enzymes were stored at $-70\text{ }^{\circ}\text{C}$ until use.

PDE2A3 enzyme inhibitory assay. PDE activity was measured using an SPA (GE Healthcare). To evaluate the inhibitory activity of a compound, 10 μL of serially diluted compounds were incubated with 20 μL of PDE enzyme (final concentration 0.023 nM) in assay buffer (50 mM HEPES-NaOH, 8.3 mM MgCl_2 , 1.7 mM EGTA, and 0.1% bovine serum albumin (BSA) (pH 7.4)) for 30 min at rt. Final concentration of DMSO in the reaction solution was 1%. Compounds were tested in duplicate in 96-well half-area plates (Corning) or 384-well OptiPlates (PerkinElmer). We used an 8 concentration serial dilution dose response ranging from 100 μM to 10 pM compound concentrations. To start the reaction, 10 μL of substrate [^3H] cGMP (final concentration 77 nM, PerkinElmer) were added to a total volume of 40 μL . After 60 min at rt, 20 μL of 20 mg/mL yttrium silicate SPA beads containing zinc sulfate were added to terminate the PDE reaction. After resting undisturbed for an additional 60 min, the assay plates were counted in a scintillation counter (PerkinElmer) to allow calculation of the inhibition rate. Inhibition rate was calculated based on 0% control wells with enzyme and DMSO, and 100% control wells without enzyme. All IC_{50} values were obtained by fitting the results to the following 4 Parameter Logistic Equation:

$$y = A + (B - A) / (1 + (10^{((C - x) * D)}))$$

where A is the minimum y value, B is the maximum y value, C is $\text{Log}(\text{EC}_{50})$ value, and D is the slope factor.

Human PDE enzyme assay. PDE activities were measured using an SPA (GE Healthcare). To evaluate the inhibitory activity, 10 μL of serially diluted compounds were incubated with 20 μL of PDE

enzymes (except for PDE1A) in assay buffer (50 mM HEPES-NaOH, 8.3 mM MgCl₂, 1.7 mM EGTA, and 0.1% BSA (pH 7.4)) for 30 min at rt. The PDE1A enzyme assay was performed in a different assay buffer (50 mM Tris-HCl, 8.3 mM MgCl₂, 0.2 mM CaCl₂, 0.1% BSA, and 30 nM Calmodulin (pH 7.5)). The final concentration of DMSO in the assay was 1%. Compounds were tested in duplicate in 96-well half-area plates (Corning). We used an 4 concentration serial dilution dose response ranging from 10 μM to 10 nM compound concentrations. To start the reaction, 10 μL of substrate ([³H] cGMP (final concentration 77 nM, PerkinElmer) for PDE1A, 5A1, 6AB, 9A2, 10A2, and 11A4 or [³H] cAMP (final concentration 14.7 nM, PerkinElmer) for PDE3A, 4D2, 7B, and 8A1) were added for a final assay volume of 40 μL. After 60 min incubation at rt, 20 μL of 20 mg/mL yttrium silicate SPA beads containing ZnSO₄ were added to terminate the PDE reaction. After resting undisturbed for more than 120 min, the assay plate was counted in a scintillation counter (PerkinElmer) to allow calculation of the inhibition rate.

Transcellular Transport Study Using a Transporter-Expression System. Human MDR1-expressing LLC-PK1 cells were cultured as reported previously with minor modifications.¹⁰⁶ The transcellular transport study was performed as reported previously.¹⁰⁷ In brief, the cells were grown for 7 days in HTS Transwell 96-well permeable support (pore size 0.4 μm, 0.143 cm² surface area) with polyethylene terephthalate membrane (Corning Life Sciences, Lowell, MA, USA) at a density of 1.125×10^5 cells/well. The cells were preincubated with M199 at 37 °C for 30 min. Subsequently, transcellular transport was initiated by the addition of M199 either to apical compartments (75 μL) or to basolateral compartments (250 μL) containing 10 μM digoxin, 200 μM lucifer yellow (as a marker for the tightness of the monolayer), and 10 μM test compounds. The assay was terminated by the removal of each assay plate after 2 h. Aliquots (25 μL) from the opposite compartments were mixed with CH₃CN containing alprenolol and diclofenac as internal standards, and then centrifuged. The compound concentrations in the supernatant were measured by LC-MS/MS. The

apparent permeability (P_{app}) of test compounds in the receiver wells was determined and the efflux ratio (ER) for the MDR1 membrane permeability test was calculated using the following equation:

$$ER = P_{app,BtoA}/P_{app,AtoB}$$

where $P_{app,AtoB}$ is the apical-to-basal passive permeability-surface area product and $P_{app,BtoA}$ is the basal-to-apical passive permeability-surface area product.

Phototoxicity Test. Phototoxicity assay was carried out as described in the OECD guideline No. 432¹¹⁷ with some modifications for a high-throughput screening. BALB/c 3T3 cells were cultured at 37 °C under 5% CO₂ in DMEM supplemented with 10% fetal bovine serum, 50 IU/mL penicillin and 50 mg/mL streptomycin. Cells were seeded at 2.5×10^3 cells/well in 384-well white plates, and cultured in DMEM supplemented with 10% fetal bovine serum, 2 mM L-glutamine, 1 mM sodium pyruvate, 50 IU/mL penicillin, and 50 µg/mL streptomycin for 1 day. Two 384-well plates per test compound (50 µM) in Earle's Balanced Salt Solution (EBSS) supplemented with 1 mM HEPES were preincubated for 1 h. One of the two plates was irradiated (+UV) for 60 min with 1.4–1.7 mW/cm² (5–6 J/cm²), whereas the other plate was kept in the dark (–UV). In both plates the treatment medium was replaced with the culture medium and after another 24 h of culture, the cell viability was determined by measuring the cellular ATP content. The cellular ATP content was measured using the Celltiter-Glo™ assay kit (Promega) following the manufacture's instruction. ATP content was calculated as follows. ATP content (% of control) = (relative light unit (RLU) of test compound/RLU of 1% DMSO) × 100.

Estimation of Log *D* at pH 7.4. Log $D_{7.4}$, which is the partition coefficient of the compounds between 1-octanol and aqueous buffer at pH 7.4, was measured using a chromatographic procedure based on a published method.⁶⁸ The instruments utilized were a Waters Alliance 2795 HPLC system and a 2996 UV–vis detector (Milford, MA, USA).

Thermodynamic Solubility Measurement Using the Shake-Flask Method. The measurement of thermodynamic solubility was carried out as previously described.⁶⁸ Briefly, the drug substances were

weighed into Thomson filter vials (Chrom Tech, Inc., Minnesota, U.S.A.). JP1 (pH 1.2), JP2 (pH 6.8), and JP2-containing 20 mM GCDC were added to the vials. The vials were incubated at 37 °C for 18 h and the resulting suspensions were filtered by compressing the vials. The drug concentration of the filtrates was determined using a UHPLC system.

Powder X-ray Diffraction (PXRD) and Crystallinity Calculation. PXRD patterns were collected using a RINT UltimaIV powder X-ray diffractometer (Rigaku Corp., Tokyo, Japan) according to previously described conditions.⁶⁸ The peak intensities of the crystalline (*I_c*) and non-crystalline (*I_a*) fractions were integrated from the baseline collection according to Herman's method.^{118,119} The crystallinity was calculated using the following equation with an autocrystallinity calculation software (Rigaku, Tokyo, Japan).^{119,120}

$$\text{Crystallinity} = I_c \times 100 / (I_c + I_a) \times 100$$

Protein Expression and Purification. The PDE2A catalytic domain (578–919) was cloned into a pFastBac vector, for expression in Sf9 cells, utilizing an N-terminal 6× poly-histidine tag containing a TEV cleavage site. Large scale production of recombinant protein was carried out in Sf9 cells. The pellet from 10L of baculovirus infected Sf9 cells was resuspended in 600 mL lysis buffer containing 25 mM Tris pH 7.6, 1 M NaCl, 20 mM imidazole, 5% glycerol, and 3 Roche cOmplete Protease Inhibitor tablets. The cell suspension was homogenized with the Polytron PT-3100, centrifuged for 1 h at 13,000 rpm (JA-14 rotor), and the clarified supernatant was brought to 800 mL with lysis buffer before batch binding with 10 mL of Probond Ni resin (Invitrogen) for 2 h at 4 °C, rolling. The beads were collected by low speed centrifugation (3,500 rpm with JS-4.2 rotor), loaded into a gravity column, and washed slowly overnight with 2 L of wash buffer containing 25 mM Tris pH 7.6, 1 M NaCl, 20 mM imidazole, 5% glycerol. The following day the protein was eluted with buffer containing 25 mM Tris pH 7.9, 50 mM NaCl, 250 mM imidazole, 10% glycerol. The 1.5 mL sample eluted from the Nickel capture step was brought to 9 mL with Mono Q buffer A containing 25 mM Tris pH 7.9, and 10% glycerol. After the full sample volume was bound to the Mono Q column, a salt gradient was

applied from 0 M NaCl to ~800 mM NaCl in 40 mL. Fractions corresponding to the unphosphorylated protein (identified by MS with MW = 40178 Da) were pooled for further purification by size-exclusion chromatography on a Superdex 200 column equilibrated in 1XTBS pH 7.4, 0.5 mM DTT, 1 mM EDTA, 10% glycerol. Peak SEC fractions were collected and concentrated to 12 mg/mL for crystallization.

Crystallization and Structure Determination. Crystals suitable for data collection were first grown using the vapor diffusion method in hanging drops at room temperature by adding 0.5 μ L protein solution with 1 mM IBMX⁵⁹ and 0.5 μ L reservoir solution (30% PEG 3350, 0.1 M Tris pH 7.5, and 0.2 M MgCl₂). PDE2A IBMX crystals were soaked in a drop containing 5 mM compound **122b**, 31% PEG 3350, 0.1 M Tris pH 7.5, and 0.2 M MgCl₂ for 3 days. Crystals were transferred through a fresh cryo-protected soak drop immediately before being harvested and flash frozen in liquid nitrogen. X-ray diffraction data was collected at ALS beamline 5.0.2 using a Pilatus3 6M (Dectris) detector from a single cryogenically protected crystal (100K) at a wavelength of 1 Å. The crystals belong to the space group C121 and contain three enzyme molecules per asymmetric unit. X-ray diffraction data was reduced using the HKL2000¹⁰⁸ software package. The structure was determined by molecular replacement with PHASER within the CCP4 program suite and refined with REFMAC.¹¹¹ Several cycles of model building using MIFIT¹¹³ and refinement using REFMAC were performed for improving the quality of the model. The coordinates and structure factors have been deposited in the Protein Data Bank with accession code 5VP1.

Animal Experiments. The care and use of animals and the experimental protocols were approved by the Experimental Animal Care and Use Committee of Takeda Pharmaceutical Company Limited.

Pharmacokinetic Analysis in Rat or Mouse Cassette Dosing. Compound **122b** was administered intravenously (0.1 mg/kg) or orally (1 mg/kg) by cassette dosing to nonfasted male CrI:CD(SD)(IGS) rats (8W, $n = 3$) or male ICR mice (8W, $n = 3$). The combination for a cassette dosing was determined to avoid combinations of compounds with the same molecular weight. The solution of compounds in

dimethylacetamide containing 50% (v/v) 1,3 butanediol at 0.1 mg/mL/kg was administered intravenously to isoflurane-anesthetized mice via femoral vein. The suspension of compounds in 0.5% methyl cellulose with water was used for vehicle (1 mg/kg) and was administered orally by gavage. After administration, blood samples were collected via tail vein by syringes with heparin at 5, 10, 15, 30 min, 1, 2, 4, and 8 h (iv) and 15, 30 min, 1, 2, 4, and 8 h (po), and centrifuged to obtain the plasma fraction. The plasma samples were deproteinized by mixing with acetonitrile followed by centrifugation. The compound concentrations in the supernatant were measured by LC–MS/MS with a standard curve. Pharmacokinetic parameters were calculated by the non-compartmental analysis. The area under the concentration-time curve (AUC) and the area under the first moment curve (AUMC) were calculated using the linear trapezoidal method. The mean residence time (MRT) was calculated as $AUMC/AUC$. The total clearance (CL_{total}) was calculated as $dose_{iv}/AUC_{iv}$. The volume of distribution ($V_{d_{ss}}$) was calculated as $CL_{total} \times MRT_{iv}$. Oral bioavailability (F) was calculated as $(AUC_{po}/dose_{po})/(AUC_{iv}/dose_{iv}) \times 100$.

Brain and Plasma Concentration in Rats. Compound **122b** was administered orally to Long–Evans rats (male, non-fasted, 7-week old) at 10 mg/kg. Blood and whole brain samples were collected 2 h after oral administration. The blood samples were centrifuged to obtain the plasma fraction. The brain samples were homogenized in saline to obtain the brain homogenate. Compound concentrations were measured in aliquots of rat plasma and brain, which were mixed well with acetonitrile containing an internal standard and then centrifuged. The supernatants were diluted with solvents for LC–MS/MS analysis (mobile phase A: 10 mM ammonium formate/formic acid (100/0.2, v/v), mobile phase B: acetonitrile/formic acid (100/0.2, v/v)). The diluted solutions were injected into an LC–MS/MS (API5000, AB Sciex, Foster City, CA) equipped with a Shimadzu Shim-pack XR-ODS column (2.2 μ m packing particle size, 2.0 mm ID \times 30 mm L) maintained at 50°C. The chromatographic separation was performed using gradient elution at a flow rate of 0.7 mL/min. The LC time program was as follows: Mobile phase B was held at 5% for 0.1 min, and increased linearly to 95% in 0.1 min. After

maintaining B at 95% for another 0.8 min, it was decreased to 5% in 0.01 min, followed by re-equilibration for 0.59 min. The total cycle time for one injection was 1.6 min. Compound **122b** was detected using multiple reaction monitoring mode and the transition m/z 490.01 \rightarrow 240.96. AnalystTM software (version 1.4.2) was used for data acquisition and processing.

In Vivo Occupancy Study. In vivo target occupancy study of compound **122b** was conducted using LC–MS/MS. Compound **122b** was suspended in 0.5% (w/v) methylcellulose in distilled water, and PF-05270430¹²¹ was dissolved in dimethylacetamide and 1,3-butanediol (1:1). SD rats were pretreated with vehicle (po, $n = 6$) or compound **122b** (0.3 mg/kg, 1 mg/kg, 3 mg/kg, 10 mg/kg, and 30 mg/kg, po, $n = 4$ in each group) 2 h before sampling. PF-05270430 (0.1 mg/mL/kg) was administered by bolus intravenous injection via lateral tail vein 30 min before sampling. Rats were decapitated, and blood and brain samples (striatum as target tissue and cerebellum as reference tissue) were collected. Brain samples were weighed and saline was added (20% weight/volume), followed by homogenization with Lysing Matrix I beads (MP Biomedicals). Homogenized samples were stored at -30°C until quantification of tracer (PF-05270430) using LC–MS/MS. The supernatants were diluted with solvents for LC–MS/MS analysis (mobile phase A: 10 mM ammonium formate/formic acid (100/0.2, v/v), mobile phase B: acetonitrile/formic acid (100/0.2, v/v)). The diluted solutions were injected into an LC–MS/MS (API5000, AB Sciex, Foster City, CA) equipped with a Shimadzu Shim-pack XR-ODS (2.2 μm packing particle size, 2.0 mm ID \times 30 mm L) maintained at 50°C . The chromatographic separation was performed using gradient elution at a flow rate of 0.7 mL/min. The LC time program was as follows: Mobile phase B was held at 5% for 0.1 min, and increased linearly to 95% in 0.1 min. After maintaining B at 95% for another 0.8 min, it was decreased to 5% in 0.01 min, followed by re-equilibration for 0.59 min. The total cycle time for one injection was 1.6 min. PF-05270430 was detected using multiple reaction monitoring mode and the transition m/z 432 \rightarrow 386. AnalystTM software (version 1.4.2) was used for data acquisition and processing. Specific tracer binding (B_{SP}) in the striatum was represented as the difference between the tracer concentration in

striatum and that in cerebellum. PDE2A occupancy was calculated using the following equation: Occupancy (%) = $(B_{SP,base} - B_{SP,drug})/B_{SP,base} \times 100$, where $B_{SP,base}$ and $B_{SP,drug}$ are the concentrations at baseline (vehicle treatment) and at drug treatment, respectively. Curve fitting of the saturation curve was carried out by nonlinear regression using GraphPad Prism 5.02 (GraphPad Software, Inc., San Diego, CA).

Measurement of Cyclic Nucleotide Contents in Rat Brain. *Animals.* Five-week-old male Long-Evans rats were purchased from Japan SLC, Inc. (Japan). The rats were housed in groups of 3/cage in a light-controlled room (12 h light/dark cycles with lights on at 07:00). Food and water were provided *ad libitum*. After a one week acclimation period, the six-week-old rats were used for experiments.

Measurements. Compound **122b** was suspended in 0.5% (w/v) methylcellulose in distilled water, and was administered in a volume of 2 mL/kg body weight for rats. Rats were administered orally with either vehicle or compound **122b** (1 mg/kg, 3 mg/kg, and 10 mg/kg) after >1 h of habituation. A microwave fixation system (Muromachi Kikai, Tokyo, Japan) was used to sacrifice unanesthetized rats by exposure of the head to the microwave beam at 2 h after administration of **122b**. Brain tissues were isolated and then homogenized in 0.5 mol/L HCl, followed by centrifugation. The concentration of cyclic nucleotides in the supernatant was measured using a cyclic AMP EIA kit or cyclic GMP EIA kit (Cayman Chemical, USA) following the manufacturer's instructions. Values were expressed as pmol/mg tissue weight.

Step-through Passive Avoidance Task. This task was performed as previously described¹²² with some modifications. This experiment was conducted in 7–8-week-old male Long-Evans rats. The apparatus (Brainscience idea, Osaka, Japan) consisted of an illuminated chamber (25 × 10 × 25 cm) connected to a dark chamber (30 × 30 × 30 cm) by a sliding door (8 × 8 cm). On the training day, each animal was subjected to a single pre-training trial 4–6 h before the acquisition trial. The rat was placed in the light chamber, and the sliding door was opened 30 s later. As soon as the rat entered the dark chamber with all four paws, the door was closed. The rat was then allowed to remain in the dark chamber for 30 s

before being returned to its home cage. In the acquisition trial, the rat was placed in the light chamber, and the sliding door was opened. The time required for the rat to enter the dark chamber was then recorded. As soon as the rat entered the dark chamber, the door was closed, and an electric shock (0.5 mA, 3 s) was delivered from the floor grid. The rat was then returned to its home cage. The retention test was conducted 24 h later. The rat was again placed in the light chamber with the sliding door. After 30 s, the door was opened and the latency for the rat to cross over into the dark compartment was recorded. If the animal did not enter the dark chamber within 300 s, the retention test was terminated, and the animal was given a ceiling score of 300 s. Vehicle or compound **122b** (3 mg/kg) was administered po 2 h prior, and saline or MK-801 (0.1 mg/kg) was administered sc 30 min prior to the acquisition trial. The statistical significance of differences between group latency scores was determined by Wilcoxon's test with significance set at $p \leq 0.05$.

Determination of the Absolute Stereochemistry of RHS Amine 155. The absolute configuration of free base of **130** (i.e. **155**) was determined by X-ray crystallography of its (+)-di-(*p*-toluoyl)-D-tartaric acid salt **156**.

Crystal data for **156**: $C_{11}H_{15}F_3NO_2^+ \cdot C_{20}H_{17}O_8^-$, MW = 635.59; crystal size, $0.21 \times 0.13 \times 0.07$ mm; colorless, block; monoclinic, space group *C2*, $a = 25.4050(5)$ Å, $b = 7.84709(14)$ Å, $c = 15.9718(3)$ Å, $\alpha = \gamma = 90^\circ$, $\beta = 95.114(7)^\circ$, $V = 3171.37(11)$ Å³, $Z = 4$, $D_x = 1.331$ g/cm³, $T = 100$ K, $\mu = 0.950$ mm⁻¹, $\lambda = 1.54187$ Å, $R_1 = 0.029$, $wR_2 = 0.077$, Flack Parameter¹¹⁴ = $-0.11(10)$.

All measurements were made on a Rigaku R-AXIS RAPID-191R diffractometer using graphite monochromated Cu-K α radiation. The structure was solved by direct methods with SIR2008¹¹⁶ and was refined using full-matrix least-squares on F^2 with SHELXL-97.¹¹⁵ All non-H atoms were refined with anisotropic displacement parameters.

CCDC 1548481 for compound **156** contains the supplementary crystallographic data for this paper. These data can be obtained free of charge from The Cambridge Crystallographic Data Centre via <http://www.ccdc.cam.ac.uk/Community/Requestastructure/Pages/DataRequest.aspx?>

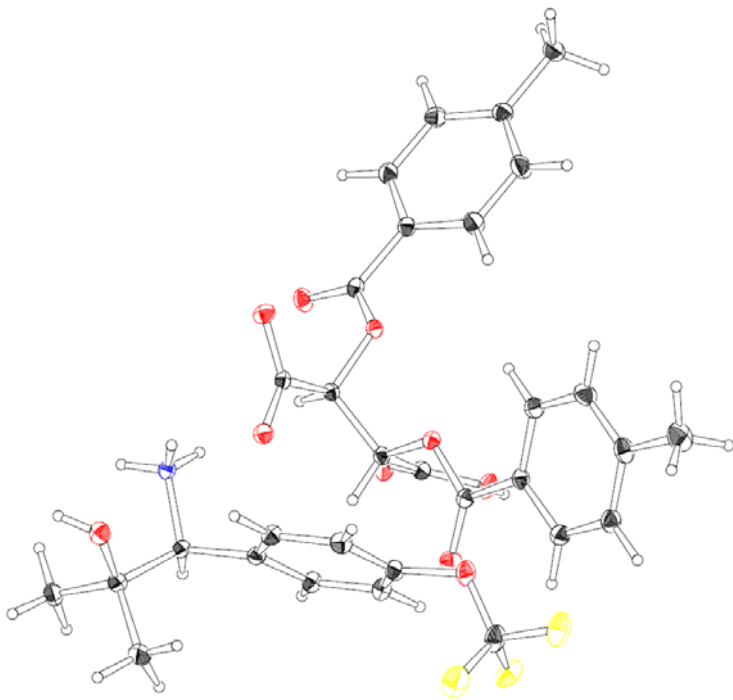


Figure 3-10. ORTEP of **156**, thermal ellipsoids are drawn at 20% probability.

引用文献

1. World Health Organization. WHO, schizophrenia, **2017**.
http://www.who.int/mental_health/management/schizophrenia/en/
2. Health, Labour and Welfare Ministry.
http://www.mhlw.go.jp/kokoro/speciality/detail_into.html
3. Insel, T. R. Rethinking Schizophrenia. *Nature* **2010**, *468*, 187–193.
4. Nishikawa, T. Schizophrenia as a Brain Disease with Postnatal Development-dependent Disturbances. *Folia Pharmacol. Jpn.*, **2006**, *128*, 13.
5. Hashimoto, R.; Yasuda, Y.; Ohi, K.; Fukumoto, M.; Yamamori, H.; Shintani, N.; Hashimoto, H.; Baba, A.; Takeda, M. Translational Research for Mental Disorder — Schizophrenia. *Folia Pharmacol. Jpn.*, **2011**, *137*, 79–82.
6. López-Muñoz, F.; Alamo, C.; Cuenca, E.; Shen, W. W.; Clervoy, P.; Rubio, G. History of the Discovery and Clinical Introduction of Chlorpromazine. *Annals of Clinical Psychiatry* **2005**, *17*, 113–135.
7. Giannini, A. J.; Eighan, M. S.; Loiselle, R. H.; Giannini, M. C. Comparison of Haloperidol and Chlorpromazine in the Treatment of Phencyclidine Psychosis. **1984**, *24*, 202–204.
8. Riedel, M.; Müller, N.; Strassnig, M.; Spellmann, I.; Severus, E.; Hans-Jürgen Möller, H.-J. Quetiapine in the Treatment of Schizophrenia and Related Disorders. *Neuropsychiatr. Dis. Treat.* **2007**, *3*, 219–235.
9. Deeks, E. D.; Keating, G. M. Blonanserin A Review of Its Use in the Management of Schizophrenia. *CNS Drugs* **2010**, *24*, 65–84.
10. Rattehalli, R. D.; Zhao, S.; Li, B. G.; Jayaram, M. B.; Xia, J.; Sampson, S. Risperidone Versus Placebo for Schizophrenia. *Cochrane Database Syst. Rev.* **2016**, *12*, 1–164.

11. Duggan, L.; Fenton, M.; Rathbone, J.; Dardennes, R.; El-Dosoky, A.; Indran, S. Olanzapine for Schizophrenia. *Cochrane Database Syst. Rev.* **2005**, *18*, 1–257.
12. Belgamwar, R. B.; El-Sayeh, H. G. Aripiprazole Versus Placebo for Schizophrenia. *Cochrane Database Syst. Rev.* **2011**, *8*, 1–64.
13. Miyamoto, S.; Miyake, N.; Jarskog, L. F.; Fleischhacker, W. W.; Lieberman, J. A. Pharmacological Treatment of Schizophrenia: A Critical Review of the Pharmacology and Clinical Effects of Current and Future Therapeutic Agents. *Mol. Psychiatry* **2012**, *17*, 1206–1227.
14. Biedermann, F.; Fleischhacker, W. W. Emerging Drugs for Schizophrenia. *Expert Opin. Emerging Drugs* **2011**, *16*, 271–282.
15. Pierre, J. M. Extrapiramidal Symptoms with Atypical Antipsychotics: Incidence, Prevention and Management. *Drug Saf.* **2005**, *28*, 191–208.
16. Krebs, M.; Leopold, K.; Hinzpeter, A.; Schaefer, M. Current Schizophrenia Drugs: Efficacy and Side Effects. *Expert Opin. Pharmacother.* **2006**, *7*, 1005–1016.
17. Janssen, P. A.; Niemegeers, C. J.; Awouters, F.; Schellekens, K. H.; Megens, A. A.; Meert, T. F. Pharmacology of Risperidone (R 64 766), A New Antipsychotic with Serotonin-S₂ and Dopamine-D₂ Antagonistic Properties. *J. Pharmacol. Exp. Ther.* **1988**, *244*, 685–693.
18. Meltzer, H. Y.; Matsubara, S.; Lee, J. C. Classification of Typical and Atypical Antipsychotic Drugs on the Basis of Dopamine D-1, D-2 and Serotonin₂ pK_i Values. *J. Pharmacol. Exp. Ther.* **1989**, *251*, 238–246.
19. Kroeze, W. K.; Hufeisen, S. J.; Popadak, B. A.; Renock, S. M.; Steinberg, S.; Ernsberger, P.; Jayathilake, K.; Meltzer, H. Y.; Roth, B. L. H₁-histamine Receptor Affinity Predicts Short-term Weight Gain for Typical and Atypical Antipsychotic Drugs. *Neuropsychopharmacology* **2003**, *28*, 519–526.
20. Tresguerres, M.; Levin, L. R.; Buck, J. Intracellular cAMP Signaling by Soluble Adenylyl Cyclase. *Kidney Int.* **2011**, *79*, 1277–1288.

21. Lucas, K. A.; Pitari, G. M.; Kazerounian, S.; Ruiz-Stewart, I.; Park, J.; Schulz, S.; Chepenik, K. P.; Waldman, S. A. Guanylyl Cyclases and Signaling by Cyclic GMP. *Pharmacol. Rev.* **2000**, *52*, 375–413.
22. Bender, A. T.; Beavo, J. A. Cyclic Nucleotide Phosphodiesterases: Molecular Regulation to Clinical Use. *Pharmacol. Rev.* **2006**, *58*, 488–520.
23. Beavo, J. A. Cyclic Nucleotide Phosphodiesterases: Functional Implications of Multiple Isoforms. *Phys. Rev.* **1995**, *75*, 725–748.
24. Maurice, D. H.; Ke, H.; Ahmad, F.; Wang, Y.; Chung, J.; Manganiello, V. C. Advances in Targeting Cyclic Nucleotide Phosphodiesterases. *Nat. Rev. Drug Discovery* **2014**, *13*, 290–314.
25. Packer, M.; Carver, J. R.; Rodeheffer, R. J.; Ivanhoe, R. J.; DiBianco, R.; Zeldis, S. M.; Hendrix, G. H.; Bommer, W. J.; Elkayam, U.; Kukin, M. L.; Mallis, G. I.; Sollano, J. A.; Shannon, J.; Tandon, P. K.; DeMets, D. L. Effect of Oral Milrinone on Mortality in Severe Chronic Heart Failure. *N. Engl. J. Med.* **1991**, *325*, 1468–1475.
26. Kanlop, N.; Chattipakorn, S.; Chattipakorn, N. Effects of Cilostazol in the Heart. *J. Cardiovasc. Med.* **2011**, *12*, 88–95.
27. Rabe, K. F. Update on Roflumilast, a Phosphodiesterase 4 Inhibitor for the Treatment of Chronic Obstructive Pulmonary Disease. *Br. J. Pharmacol.* **2011**, *163*, 53–67.
28. Tenor, H.; Hatzelmann, A.; Beume, R.; Lahu, G.; Zech, K.; Bethke, T. D. Pharmacology, Clinical Efficacy, and Tolerability of Phosphodiesterase-4 Inhibitors: Impact of Human Pharmacokinetics. *Handb. Exp. Pharmacol.* **2011**, *204*, 85–119.
29. Fabbri, L. M.; Calverley, P. M.; Izquierdo-Alonso, J. L.; Bundschuh, D. S.; Brose, M.; Martinez, F. J.; Rabe, K. F. Roflumilast in Moderate-to-Severe Chronic Obstructive Pulmonary Disease Treated with Longacting Bronchodilators: Two Randomised Clinical Trials. *Lancet* **2009**, *374*, 695–703.
30. Reed, M.; Crosbie, D. Apremilast in the Treatment of Psoriatic Arthritis: A Perspective Review. *Ther. Adv. Musculoskeletal Dis.* **2017**, *9*, 45–53.

31. Paller, A. S.; Tom, W. L.; Lebwohl, M. G.; Blumenthal, R. L.; Boquniewicz, M.; Call, R. S.; Eichenfield, L. F.; Forsha, D. W.; Rees, W. C.; Simpson, E. L.; Spellman, M. C.; Stein Gold, L. F.; Zaenglein, A. L.; Hughes, M. H.; Zane, L. T.; Hebert, A. A. Efficacy and Safety of Crisaborole Ointment, A Novel, Nonsteroidal Phosphodiesterase 4 (PDE4) Inhibitor for the Topical Treatment of Atopic Dermatitis (AD) in Children and Adults. *J. Am. Acad. Dermatol.* **2016**, *75*, 494–503.
32. Yuan, J.; Zhang, R.; Yang, Z.; Lee, J.; Liu, Y.; Tian, J.; Qin, X.; Ren, Z.; Ding, H.; Chen, Q.; Mao, C.; Tang, J. Comparative Effectiveness and Safety of Oral Phosphodiesterase Type 5 Inhibitors for Erectile Dysfunction: A Systematic Review and Network Meta-Analysis. *Eur. Urol.* **2013**, *63*, 902–912.
33. Archer, S. L.; Michelakis, E. D. Phosphodiesterase Type 5 Inhibitors for Pulmonary Arterial Hypertension. *N. Engl. J. Med.* **2009**, *361*, 1864–1871.
34. Andersson, K. E.; de Groat, W. C.; McVary, K. T.; Lue, T. F.; Maggi, M.; Roehrborn, C. G.; Wyndaele, J. J.; Melby, T.; Viktrup, L. Tadalafil for the Treatment of Lower Urinary Tract Symptoms Secondary to Benign Prostatic Hyperplasia: Pathophysiology and Mechanism(s) of Action. *Neurourol. Urodyn.* **2011**, *30*, 292–301.
35. Menniti, F. S.; Faraci, W. S.; Schmidt, C. J. Phosphodiesterases in the CNS: Targets for Drug Development. *Nat. Rev. Drug Discovery* **2006**, *5*, 660–670.
36. Verhoest, P. R.; Fonseca, K. R.; Hou, X.; Proulx-LaFrance, C.; Corman, M.; Helal, C. J.; Claffey, M. M.; Tuttle, J. B.; Coffman, K. J.; Liu, S.; Nelson, F.; Kleiman, R. J.; Menniti, F. S.; Schmidt, C. J.; Vanase-Frawley, M.; Liras, S. Design and Discovery of 6-[(3*S*,4*S*)-4-Methyl-1-(pyrimidin-2-ylmethyl)pyrrolidin-3-yl]-1-(tetrahydro-2*H*-pyran-4-yl)-1,5-dihydro-4*H*-pyrazolo[3,4-*d*]pyrimidin-4-one (PF-04447943), a Selective Brain Penetrant PDE9A Inhibitor for the Treatment of Cognitive Disorders. *J. Med. Chem.* **2012**, *55*, 9045–9054.
37. Chappie, T. A.; Helal, C. J.; Hou, X. Current Landscape of Phosphodiesterase 10A (PDE10A) Inhibition. *J. Med. Chem.* **2012**, *55*, 7299–7331.

38. Li, P.; Zheng, H.; Zhao, J.; Zhang, L.; Yao, W.; Zhu, H.; Beard, J. D.; Ida, K.; Lane, W.; Snell, G.; Sogabe, S.; Heyser, C. J.; Snyder, G. L.; Hendrick, J. P.; Vanover, K. E.; Davis, R. E.; Wennogle, L. P. Discovery of Potent and Selective Inhibitors of Phosphodiesterase 1 for the Treatment of Cognitive Impairment Associated with Neurodegenerative and Neuropsychiatric Diseases. *J. Med. Chem.* **2016**, *59*, 1149–1164.
39. Lakics, V.; Karran, E. H.; Boess, F. G. Quantitative Comparison of Phosphodiesterase mRNA Distribution in Human Brain and Peripheral Tissues. *Neuropharmacology* **2010**, *59*, 367–374.
40. Stephenson, D. T.; Coskran, T. M.; Wilhelms, M. B.; Adamowicz, W. O.; O'Donnell, M. M.; Muravnick, K. B.; Menniti, F. S.; Kleiman, R. J.; Morton, D. Immunohistochemical Localization of Phosphodiesterase 2A in Multiple Mammalian Species. *J. Histochem. Cytochem.* **2009**, *57*, 933–949.
41. Cote, R. H.; Feng, Q.; Valeriani, B. A. Relative Potency of Various Classes of Phosphodiesterase (PDE) Inhibitors for Rod and Cone Photoreceptor PDE. *Invest. Ophthalmol.* **2003**, *44*, 1524–1527.
42. Young, R. A.; Ward, A. Milrinone. A Preliminary Review of Its Pharmacological Properties and Therapeutic Use. *Drugs* **1988**, *36*, 158–192.
43. Lu, Y.; Kandel, E., R.; Hawkins, R. D. Nitric Oxide Signaling Contributes to Late-Phase LTP and CREB Phosphorylation in the Hippocampus. *J. Neurosci.* **1999**, *19*, 10250–10261.
44. Sanderson, T. M.; Sher, E. The Role of Phosphodiesterases in Hippocampal Synaptic Plasticity. *Neuropharmacology* **2013**, *74*, 86–95.
45. Prickaerts, J.; de Vente, J.; Honig, W.; Steinbusch, H. W. M.; Blokland, A. cGMP, but not cAMP, in Rat Hippocampus Is Involved in Early Stages of Object Memory Consolidation. *Eur. J. Pharmacol.* **2002**, *436*, 83–87.
46. Niewoehner, U.; Schauss, D.; Hendrix, M.; Koenig, G.; Boess, F. G.; van der Staay, F. J.; Schreiber, R.; Schlemmer, K. H.; Grosser, R. Novel Substituted Imidazotriazinones as PDE II-Inhibitors. WO 2002050078, June 27, 2002.

47. Abaarghaz, M.; Biondi, S.; Duranton, J.; Limanton, E.; Mondadori, C.; Wagner, P. Benzo[1,4]diazepin-2-one Derivatives as Phosphodiesterase PDE2 Inhibitors, Preparation and Therapeutic Use Thereof. WO 2005063723, July 14, 2005.
48. Buijnsters, P.; De Angelis, M.; Langlois, X.; Rombouts, F. J. R.; Sanderson, W.; Tresadern, G.; Ritchie, A.; Trabanco, A. A.; VanHoof, G.; Van Roosbroeck, Y.; Andrés, J.-I. Structure-Based Design of a Potent, Selective, and Brain Penetrating PDE2 Inhibitor with Demonstrated Target Engagement. *ACS Med. Chem. Lett.* **2014**, *5*, 1049–1053.
49. Rombouts, F. J. R.; Tresadern, G.; Buijnsters, P.; Langlois, X.; Tovar, F.; Steinbrecher, T. B.; Vanhoof, G.; Somers, M.; Andrés, J.-I.; Trabanco, A. A. Pyrido[4,3-*e*][1,2,4]triazolo[4,3-*a*]pyrazines as Selective, Brain Penetrant Phosphodiesterase 2 (PDE2) Inhibitors. *ACS Med. Chem. Lett.* **2015**, *6*, 282–286.
50. Redrobe, J. P.; Jørgensen, M.; Christoffersen, C. T.; Montezinho L. P.; Bastlund, J. F.; Carnerup, M.; Bundgaard, C.; Lerdrup, L.; Plath, N. In Vitro and In Vivo Characterisation of Lu AF64280, a Novel, Brain Penetrant Phosphodiesterase (PDE) 2A Inhibitor: Potential Relevance to Cognitive Deficits in Schizophrenia. *Psychopharmacology (Berl)* **2014**, *231*, 3151–3167.
51. Helal, C. J. Identification of a Brain Penetrant, Highly Selective Phosphodiesterase 2A Inhibitor for the Treatment of Cognitive Impairment Associated with Schizophrenia (CIAS). 244th ACS National Meeting & Exposition, Philadelphia, PA, USA, August 19–23, 2012.
52. Chappie, T. A.; Humphrey, J. M.; Verhoest, P. R.; Yang, E.; Helal, C. J. Imidazo[5,1-*f*][1,2,4]triazines for the Treatment of Neurological Disorders. WO 2012114222, August 30, 2012.
53. Helal, C. J.; Arnold, E. P.; Boyden, T. L.; Chang, C.; Chappie, T. A.; Fennell, K. F.; Forman, M. D.; Hajos, M.; Harms, J. F.; Hoffman, W. E.; Humphrey, J. M.; Kang, Z.; Kleiman, R. J.; Kormos, B. L.; Lee, C. W.; Lu, J.; Maklad, N.; McDowell, L.; Mente, S.; O'Connor, R. E.; Pandit, J.; Piotrowski, M.; Schmidt, A. W.; Schmidt, C. J.; Ueno, H.; Verhoest, P. R.; Yang, E. X. Application

- of Structure-Based Design and Parallel Chemistry to Identify a Potent, Selective, and Brain Penetrant Phosphodiesterase 2A Inhibitor. *J. Med. Chem.* **2017**, *60*, 5673–5698.
54. Gomez, L.; Massari, M. E.; Vickers, T.; Freestone, G.; Vernier, W.; Ly, K.; Xu, R.; McCarrick, M.; Marrone, T.; Metz, M.; Yan, Y. G.; Yoder, Z. W.; Lemus, R.; Broadbent, N. J.; Barido, R.; Warren, N.; Schmelzer, K.; Neul, D.; Lee, D.; Andersen, C. B.; Sebring, K.; Aertgeerts, K.; Zhou, X.; Tabatabaei, A.; Peters, M.; Breitenbucher, J. G. Design and Synthesis of Novel and Selective Phosphodiesterase 2 (PDE2a) Inhibitors for the Treatment of Memory Disorders. *J. Med. Chem.* **2017**, *60*, 2037–2051.
55. Boess, F. G.; Hendrix, M.; van der Staay, F.-J.; Erb, C.; Schreiber, R.; van Staveren, W.; de Vente, J.; Prickaerts, J.; Blokland, A.; Koenig, G. Inhibition of Phosphodiesterase 2 Increases Neuronal cGMP, Synaptic Plasticity and Memory Performance. *Neuropharmacology* **2004**, *47*, 1081–1092.
56. Rutten, K.; Van Donkelaar, E. L.; Ferrington, L.; Blokland, A.; Bollen, E.; Steinbusch, H. W. M.; Kelly, P. A. T.; Prickaerts, J. H. H. J. Phosphodiesterase Inhibitors Enhance Object Memory Independent of Cerebral Blood Flow and Glucose Utilization in Rats. *Neuropsychopharmacology* **2009**, *34*, 1914–1925.
57. Reneerkens, O. A. H.; Rutten, K.; Bollen, E.; Hage, T.; Blokland, A.; Harry W.M. Steinbusch, H. W. M.; Prickaerts, J. Inhibition of Phosphodiesterase Type 2 or Type 10 Reverses Object Memory Deficits Induced by Scopolamine or MK-801. *Behav. Brain Res.* **2013**, *236*, 16–22.
58. Mahar Doan, K. M.; Humphreys, J. E.; Webster, L. O.; Wring, S. A.; Shampine, L. J.; Serabjit-Singh, C. J.; Adkison, K. K.; Polli, J. W. Passive Permeability and P-glycoprotein-mediated Efflux Differentiate Central Nervous System (CNS) and Non-CNS Marketed Drugs. *J. Pharmacol. Exp. Ther.* **2002**, *303*, 1029–1037.
59. Pandit, J.; Forman, M. D.; Fennell, K. F.; Dillman, K. S.; Menniti, F. S. Mechanism for the Allosteric Regulation of Phosphodiesterase 2A Deduced from the X-ray Structure of a Near Full-Length Construct. *Proc. Natl. Acad. Sci. U.S.A.* **2009**, *106*, 18225–18230.

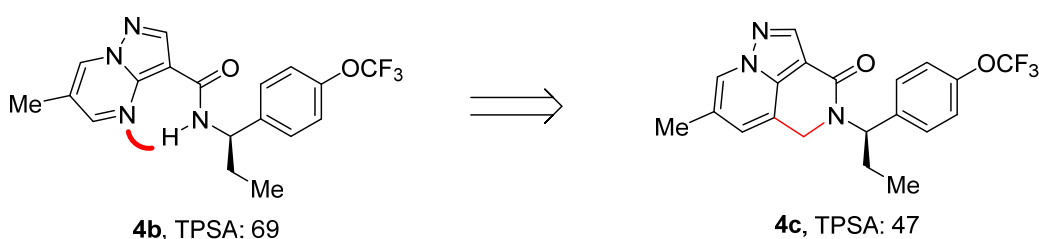
60. Lipinski, C. A.; Lombardo, F.; Dominy, B. W.; Feeney, P. J. Experimental and Computational Approaches to Estimate Solubility and Permeability in Drug Discovery and Development Settings. *Adv. Drug Delivery Rev.* **1997**, *23*, 3–25.
61. Hitchcock, S. A.; Pennington, L. D. Structure–Brain Exposure Relationships. *J. Med. Chem.* **2006**, *49*, 7559–7583.
62. Hitchcock, S. A. Structural Modifications that Alter the P-Glycoprotein Efflux Properties of Compounds. *J. Med. Chem.* **2012**, *55*, 4877–4895.
63. Müller, K.; Faeh, C.; Diederich, F. Fluorine in Pharmaceuticals: Looking beyond Intuition. *Science* **2007**, *317*, 1881–1886.
64. Leroux, F.; Jeschke, P.; Schlosser, M. α -Fluorinated Ethers, Thioethers, and Amines: Anomerically Biased Species. *Chem. Rev.* **2005**, *105*, 827–856.
65. Pierce, A. C.; Sandretto, K. L.; Bemis, G. W. Kinase Inhibitors and the Case for CH \cdots O Hydrogen Bonds in Protein–Ligand Binding. *Proteins: Struct., Funct., Genet.* **2002**, *49*, 567–576.
66. Zhu, J.; Yang, Q.; Dai, D.; Huang, Q. X-ray Crystal Structure of Phosphodiesterase 2 in Complex with a Highly Selective, Nanomolar Inhibitor Reveals a Binding-Induced Pocket Important for Selectivity. *J. Am. Chem. Soc.* **2013**, *135*, 11708–11711.
67. Hopkins, A. L.; Keserü, G. M.; Leeson, P. D.; Rees, D. C.; Reynolds, C. H. The Role of Ligand Efficiency Metrics in Drug Discovery. *Nat. Rev. Drug Discovery* **2014**, *13*, 105–121.
68. Yamamoto, K.; Ikeda, Y. Kinetic Solubility and Lipophilicity Evaluation Connecting Formulation Technology Strategy Perspective. *J. Drug Delivery Sci. Technol.* **2016**, *33*, 13–18.
69. Podzuweit, T.; Nennstiel, P.; Müller, A. Isozyme Selective Inhibition of cGMP-Stimulated Cyclic Nucleotide Phosphodiesterases by Erythro-9-(2-hydroxy-3-nonyl) Adenine. *Cell. Signalling* **1995**, *7*, 733–738.
70. Omori, K.; Kotera, J. Overview of PDEs and Their Regulation. *Circ. Res.* **2007**, *100*, 309–327.

71. Martins, T. J.; Mumby, M. C.; Beavo, J. A. Purification and Characterization of a Cyclic GMP-Stimulated Cyclic Nucleotide Phosphodiesterase from Bovine Tissues. *J. Biol. Chem.* **1982**, *257*, 1973–1979.
72. Miyaura, N.; Suzuki, A. Stereoselective Synthesis of Arylated (*E*)-Alkenes by the Reaction of Alk-1-enylboranes with Aryl Halides in the Presence of Palladium Catalyst. *J. Chem. Soc., Chem. Commun.* **1979**, 866–867.
73. Miyaura, N.; Suzuki, A. Palladium-Catalyzed Cross-Coupling Reactions of Organoboron Compounds. *Chem. Rev.* **1995**, *95*, 2457–2483.
74. Vilsmeier, A.; Haack, A. *Ber. Dtsch. Chem. Ges.* **1927**, *60*, 119–122.
75. Dess, D. B.; Martin, J. C. Readily Accessible 12-I-5 Oxidant for the Conversion of Primary and Secondary Alcohols to Aldehydes and Ketones. *J. Org. Chem.* **1983**, *48*, 4155–4156.
76. Bischoff, E. Potency, Selectivity, and Consequences of Nonselectivity of PDE Inhibition. *Int. J. Impotence Res.* **2004**, *16*, S11–S14.
77. Young, R. A.; Ward, A. Milrinone. A Preliminary Review of Its Pharmacological Properties and Therapeutic Use. *Drugs* **1988**, *36*, 158–192.
78. Cote, R. H.; Feng, Q.; Valeriani, B. A. Relative Potency of Various Classes of Phosphodiesterase (PDE) Inhibitors for Rod and Cone Photoreceptor PDE. *Invest. Ophthalmol.* **2003**, *44*, 1524–1527.
79. Zhang, X.; Feng, Q.; Cote, R. H. Efficacy and Selectivity of Phosphodiesterase-Targeted Drugs in Inhibiting Photoreceptor Phosphodiesterase (PDE6) in Retinal Photoreceptors. *Invest. Ophthalmol. Visual Sci.* **2005**, *46*, 3060–3066.
80. Pissarnitski, D. Phosphodiesterase 5 (PDE5) Inhibitors for the Treatment of Male Erectile Disorder: Attaining Selectivity Versus PDE6. *Med. Res. Rev.* **2006**, *26*, 369–395.
81. Zhang, K. Y.; Card, G. L.; Suzuki, Y.; Artis, D. R.; Fong, D.; Gillette, S.; Hsieh, D.; Neiman, J.; West, B. L.; Zhang, C.; Milburn, M. V.; Kim, S. H.; Schlessinger, J.; Bollag, G. A Glutamine

Switch Mechanism for Nucleotide Selectivity by Phosphodiesterases. *Mol. Cell* **2004**, *15*, 279–286.

82. Zhu, J.; Yang, Q.; Dai, D.; Huang, Q. X-ray Crystal Structure of Phosphodiesterase 2 in Complex with a Highly Selective, Nanomolar Inhibitor Reveals a Binding-Induced Pocket Important for Selectivity. *J. Am. Chem. Soc.* **2013**, *135*, 11708–11711.

83. Compound **4c** was considered as a hypothetical form of **4b**, in which HBA (N4 nitrogen atom of the core) and HBD (NH of the amide) were completely neutralized via the intramolecular hydrogen bond.



84. Wang, H.; Liu, Y.; Hou, J.; Zheng, M.; Robinson, H.; Ke, H. Structural Insight into Substrate Specificity of Phosphodiesterase 10. *Proc. Natl. Acad. Sci. U.S.A.* **2007**, *104*, 5782–5787.

85. Iffland, A.; Kohls, D.; Low, S.; Luan, J.; Zhang, Y.; Kothe, M.; Cao, Q.; Kamath, A. V.; Ding, Y. H.; Ellenberger, T. Structural Determinants for Inhibitor Specificity and Selectivity in PDE2A Using the Wheat Germ In Vitro Translation System. *Biochemistry* **2005**, *44*, 8312–8325.

86. Hughes, J. D.; Blagg, J.; Price, D. A.; Bailey, S.; Decrescenzo, G. A.; Devraj, R. V.; Ellsworth, E.; Fobian, Y. M.; Gibbs, M. E.; Gilles, R. W.; Greene, N.; Huang, E.; Krieger-Burke, T.; Loesel, J.; Wager, T.; Whiteley, L.; Zhang, Y. Physicochemical Drug Properties Associated with In Vivo Toxicological Outcomes. *Bioorg. Med. Chem. Lett.* **2008**, *18*, 4872–4875.

87. Leeson, P. D.; Springthorpe, B. The Influence of Drug-like Concepts on Decision-making in Medicinal Chemistry. *Nature Rev. Drug Discovery* **2007**, *6*, 881–890.

88. Waring, M. J. Lipophilicity in Drug Discovery. *Expert Opin. Drug Discovery* **2010**, *5*, 235–248.

89. Mathiasen, J. R.; DiCamillo, A. Novel Object Recognition in the Rat: A Facile Assay for Cognitive Function. *Curr. Protoc. Pharmacol.* **2010**, 5.59.1–5.59.15.
90. Neill, J. C.; Barnes, S.; Cook, S.; Grayson, B.; Idris, N. F.; McLean, S. L.; Snigdha, S.; Rajagopal, L.; Harte, M. K. Animal Models of Cognitive Dysfunction and Negative Symptoms of Schizophrenia: Focus on NMDA Receptor Antagonism. *Pharmacol. Ther.* **2010**, 128, 419–432.
91. van der Staay, F. J.; Rutten, K.; Erb, C.; Blokland, A. Effects of the Cognition Impairer MK-801 on Learning and Memory in Mice and Rats. *Behav. brain res.* **2011**, 220, 215–229.
92. Nakashima, M.; Imada, H.; Shiraishi, E.; Ito, Y.; Suzuki, N.; Miyamoto, M.; Taniguchi, T.; Iwashita, H. The Phosphodiesterase 2A Inhibitor TAK-915 Ameliorates Cognitive Impairments and Social Withdrawal in N-Methyl-D-aspartate Receptor Antagonist-induced Rat Models of Schizophrenia. *J. Pharmacol. Exp. Ther.* 2018, 365, 179–188.
93. Bal, B. S.; Childers, W. E., Jr.; Pinnick, H. W. Oxidation of α,β -Unsaturated Aldehydes. *Tetrahedron* **1981**, 37, 2091–2096.
94. Ishiyama, T.; Murata, M.; Miyaura, N. Palladium(0)-Catalyzed Cross-Coupling Reaction of Alkoxydiboron with Haloarenes: A Direct Procedure for Arylboronic Esters. *J. Org. Chem.* **1995**, 60, 7508–7510.
95. Surry, D. S.; Buchwald, S. L. Biaryl Phosphane Ligands in Palladium-Catalyzed Amination. *Angew. Chem. Int. Ed.* **2008**, 47, 6338–6361.
96. Hosokawa, T.; Shinohara, T.; Ookawa, Y.; Murahashi, S. Palladium(II)-catalyzed Alkoxylation and Acetoxylation of Alkenes. *Chem. Lett.* **1989**, 18, 2001–2004.
97. Corey, E. J.; Chaykovsky, M. Dimethylsulfoxonium Methylide. *J. Am. Chem. Soc.* **1962**, 84, 867–868.
98. Giordano, C.; Castaldi, G.; Casagrande, F.; Abis, L. Silver Assisted Rearrangement of Primary and Secondary α -Bromo-alkylarylketones. *Tetrahedron Lett.* **1982**, 23, 1385–1386.

99. Stein, K. R.; Scheinfeld, N. S. Drug-induced Photoallergic and Phototoxic Reactions. *Expert Opin. Drug Saf.* **2007**, *6*, 431–443.
100. Peukert, S.; Nunez, J.; He, F.; Dai, M.; Yusuff, N.; DiPesa, A.; Miller-Moslin, K.; Karki, R.; Lagu, B.; Harwell, C.; Zhang, Y.; Bauer, D.; Kelleher, J. F.; Egan, W. A Method for Estimating the Risk of Drug-induced Phototoxicity and Its Application to Smoothened Inhibitors. *Med. Chem. Commun.* **2011**, *2*, 973–976.
101. Ware, E. The Chemistry of the Hydantoins. *Chem. Rev.* **1950**, *46*, 403–470.
102. Yamamoto, Y.; Takizawa, M.; Yu, X.-Q.; Miyaura, N. Palladium-catalyzed Cross-coupling Reaction of Heteroaryltriolborates with Aryl Halides for Synthesis of Biaryls. *Heterocycles* **2010**, *80*, 359–368.
103. Harvey, G. R. The Reactions of Phosphorus Compounds. XII. A New Synthesis of 1,2,3-Triazoles and Diazo Esters from Phosphorus Ylide and Azides. *J. Org. Chem.* **1966**, *31*, 1587–1590.
104. L'abbé, G. Reactions of Vinyl Azides. *Angew. Chem., Int. Ed. Engl.* **1975**, *14*, 775–782.
105. Appel, R. Tertiary Phosphane/Tetrachloromethane, a Versatile Reagent for Chlorination, Dehydration, and P–N Linkage. *Angew. Chem. Int. Ed.* **1975**, *14*, 801–811.
106. Sugimoto, H.; Hirabayashi, H.; Kimura, Y.; Furuta, A.; Amano, N.; Moriwaki, T. Quantitative Investigation of the Impact of P-Glycoprotein Inhibition on Drug Transport across Blood-Brain Barrier in Rats. *Drug Metab. Dispos.* **2011**, *39*, 8–14.
107. Takeuchi, T.; Yoshitomi, S.; Higuchi, T.; Ikemoto, K.; Niwa, S.; Ebihara, T.; Katoh, M.; Yokoi, T.; Asahi, S. Establishment and Characterization of the Transformants Stably-Expressing MDR1 Derived from Various Animal Species in LLC-PK1. *Pharm. Res.* **2006**, *23*, 1460–1472.
108. Otwinowski, Z.; Minor, W. Processing of X-Ray Diffraction Data Collected in Oscillation Mode. *Methods Enzymol.* **1997**, *276*, 307–326.
109. Vagin, A.; Teplyakov, A. MOLREP: an Automated Program for Molecular Replacement. *J. Appl. Crystallogr.* **1997**, *30*, 1022–1025.

110. Iffland, A.; Kohls, D.; Low, S.; Luan, J.; Zhang, Y.; Kothe, M.; Cao, Q.; Kamath, A. V.; Ding, Y. H.; Ellenberger, T. Structural Determinants for Inhibitor Specificity and Selectivity in PDE2A Using the Wheat Germ in Vitro Translation System. *Biochemistry* **2005**, *44*, 8312–8325.
111. Collaborative Computational Project, Number 4. The CCP4 Suite: Programs for Protein Crystallography. *Acta Crystallogr. Sect. D Biol. Crystallogr.* **1994**, *50*, 760–763.
112. Emsley, P.; Lohkamp, B.; Scott, W. G.; Cowtan, K. Features and Development of Coot. *Acta Crystallogr. Sect. D Biol. Crystallogr.* 2010, *66*, 486–501.
113. Smith, B.; Badger, J. *MIFit*, 2010. 10; <https://github.com/mifit/mifit>, June 12, 2010.
114. Flack, H. D. *Acta Cryst. A* **1983**, *39*, 876–881.
115. Sheldrick, G. M. *Acta Cryst. A* **2008**, *64*, 112–122.
116. Altomare, A.; Cascarano, G.; Giacovazzo, C.; Guagliardi, A.; Burla, M.; Polidori, G.; Camalli, M. *J. Appl. Cryst.* **1994**, *27*, 435–436.
117. OECD. OECD Guidelines for the Testing of Chemicals, Section 4: Health Effects (Test No. 432: In Vitro 3T3 NRU Phototoxicity Test). 2004. http://www.oecd-ilibrary.org/environment/test-no-432-in-vitro-3t3-nru-phototoxicity-test_9789264071162-en;jsessionid=3qtfu6logg1hf.x-oecd-live-02 (accessed August 9, 2017).
118. Hermans, P. H.; Weidinger, A. Quantitative X-Ray Investigations on the Crystallinity of Cellulose Fibers. A Background Analysis. *J. Appl. Phys.* **1948**, *19*, 491–506.
119. Ikeda, Y.; Ban, J.; Ishikawa, T.; Hashiguchi, S.; Urayama, S.; Horibe, H. Stability and Stabilization Studies of TAK-599 (Ceftaroline Fosamil), a Novel N-Phosphono Type Prodrug of Anti-methicillin Resistant Staphylococcus aureus Cephalosporin T-91825. *Chem. Pharm. Bull.* **2008**, *56*, 1406–1411.
120. Yamamura, S.; Momose, Y. Quantitative Analysis of Crystalline Pharmaceuticals in Powders and Tablets by A Pattern-fitting Procedure Using X-Ray Powder Diffraction Data. *Int. J. Pharm.* **2001**, *212*, 203–212.

121. Zhang, L.; Villalobos, A.; Beck, E. M.; Bocan, T.; Chappie, T. A.; Chen, L.; Grimwood, S.; Heck, S. D.; Helal, C. J.; Hou, X.; Humphrey, J. M.; Lu, J.; Skaddan, M. B.; McCarthy, T. J.; Verhoest, P. R.; Wager, T. T.; Zasadny, K. Design and Selection Parameters to Accelerate the Discovery of Novel Central Nervous System Positron Emission Tomography (PET) Ligands and Their Application in the Development of a Novel Phosphodiesterase 2A PET Ligand. *J. Med. Chem.* **2013**, *56*, 4568–4579.
122. Miyamoto, M.; Takahashi, H.; Kato, K.; Hirai, K.; Ishihara, Y.; Goto, G. Effects of 3-[1-(Phenylmethyl)-4-piperidiny]-1-(2,3,4,5-tetrahydro-1*H*-1-benzazepin-8-yl)-1-propanone Fumarate (TAK-147), a Novel Acetylcholinesterase Inhibitor, on Impaired Learning and Memory in Animal Models. *J. Pharmacol. Exp. Ther.* **1996**, *277*, 1292–1304.

論文目録

主論文

1. Discovery of an Orally Bioavailable, Brain-Penetrating, In Vivo Active Phosphodiesterase 2A Inhibitor Lead Series for the Treatment of Cognitive Disorders. *J. Med. Chem.* **2017**, *60*, 7658–7676.
2. Discovery of Clinical Candidate *N*-((1*S*)-1-(3-Fluoro-4-(trifluoromethoxy)phenyl)-2-methoxyethyl)-7-methoxy-2-oxo-2,3-dihydroprido[2,3-*b*]pyrazine-4(1*H*)-carboxamide (TAK-915): A Highly Potent, Selective, and Brain-Penetrating Phosphodiesterase 2A Inhibitor for the Treatment of Cognitive Disorders. *J. Med. Chem.* **2017**, *60*, 7677–7702.
3. Discovery of a Novel Series of Pyrazolo[1,5-*a*]pyrimidine-Based Phosphodiesterase 2A Inhibitors Structurally Different from *N*-((1*S*)-1-(3-Fluoro-4-(trifluoromethoxy)phenyl)-2-methoxyethyl)-7-methoxy-2-oxo-2,3-dihydroprido[2,3-*b*]pyrazine-4(1*H*)-carboxamide (TAK-915), for the Treatment of Cognitive Disorders. *Chem. Pharm. Bull.* **2017**, *65*, 1058–1077.

発表

Oral Presentation (March 2018)

255th ACS National Meeting & Exposition (New Orleans, USA)

Discovery of Clinical Candidate TAK-915, A Highly Potent, Selective, and Brain-Penetrating Phosphodiesterase 2A Inhibitor for the Treatment of Cognitive Disorders